Introduction to Quantum Noise, Measurement and Amplification

A.A. Clerk,[1] M.H. Devoret,[2] S.M. Girvin,[3] Florian Marquardt,[4] and R.J. Schoelkopf[2]
[1]*Department of Physics, McGill University, 3600 rue University Montréal, QC Canada H3A 2T8**
[2]*Department of Applied Physics, Yale University PO Box 208284, New Haven, CT 06520-8284*
[3]*Department of Physics, Yale University PO Box 208120, New Haven, CT 06520-8120*
[4]*Department of Physics, Center for NanoScience, and Arnold Sommerfeld Center for Theoretical Physics, Ludwig-Maximilians-Universität München Theresienstr. 37, D-80333 München, Germany*

(Dated: Oct. 26, 2008)

The topic of quantum noise has become extremely timely due to the rise of quantum information physics and the resulting interchange of ideas between the condensed matter and AMO/quantum optics communities. This review gives a pedagogical introduction to the physics of quantum noise and its connections to quantum measurement and quantum amplification. After introducing quantum noise spectra and methods for their detection, we describe the basics of weak continuous measurements. Particular attention is given to treating the standard quantum limit on linear amplifiers and position detectors using a general linear-response framework. We show how this approach relates to the standard Haus-Caves quantum limit for a bosonic amplifier known in quantum optics, and illustrate its application for the case of electrical circuits, including mesoscopic detectors and resonant cavity detectors.

Contents

*Electronic address: clerk@physics.mcgill.ca

I. INTRODUCTION

The physics of classical noise is a topic which is extremely familiar to both physicists and engineers. In the case of electrical circuits, we usually think of noise as an unavoidable nuisance, learning early on that any dissipative circuit element (i.e. a resistor) at finite temperature will inevitably generate Johnson noise. We also know that there are spectrum analyzers that can measure this noise: roughly speaking, these spectrum analyzers consist of a resonant circuit to select a particular frequency of interest, followed by an amplifier and square law detector (e.g. a diode rectifier) which measures the intensity (mean square amplitude) of the signal at that frequency.

Recently, several advances have led to a renewed interest in the quantum mechanical aspects of noise in mesoscopic electrical circuits, detectors and amplifiers. One motivation is that such systems can operate simultaneously at high frequencies and at low temperatures, entering the regime where $\hbar\omega > k_{\rm B}T$. As such, quantum zero-point fluctuations will play a more dominant role in determining their behaviour than the more familiar thermal fluctuations. Recall that in a classical picture, the intensity of Johnson noise from a resistor vanishes linearly with temperature because thermal fluctuations of the charge carriers cease at zero temperature. One knows from quantum mechanics, however, that there are quantum fluctuations even at zero temperature, due to zero-point motion. How do we describe such zero-point fluctuations and their consequences in mesoscopic systems? This question will form a central theme of this review.

Note that zero-point motion is a notion from quantum mechanics that is frequently misunderstood, with even the most basic of questions leading to confusion. One might wonder, for example, whether it is physically possible to use a spectrum analyzer to detect the zero-point motion. As we will discuss extensively, the answer is quite definitely *yes*, if we use a quantum system as our spectrum analyzer. Consider for example a hydrogen atom in the 2p excited state lying 3/4 of a Rydberg above the 1s ground state. We know that this state is unstable and has a lifetime of only about 1 ns before it decays to the ground state and emits an ultraviolet photon. This spontaneous decay is a natural consequence of the zero-point motion of the electromagnetic fields in the vacuum surrounding the atom. In fact, the rate of spontaneous decay gives a simple way in which to *measure* this zero point motion of the vacuum: if one modifies the zero-point noise of the vacuum by, e.g., placing the atom in a resonant cavity, there is a direct change in the atom's decay rate (Haroche and Raimond, 2006; Raimond *et al.*, 2001). We will discuss this more in what follows, as well as provide a thorough discussion of how various different mesoscopic systems can act as spectrum analyzers of

quantum noise.

A second motivation for interest in the quantum noise of mesoscopic systems comes from the relation between quantum noise and quantum measurement. There exists an ever-increasing number of experiments in mesoscopic electronics where one is forced to think about the quantum mechanics of the detection process, and about fundamental quantum limits which constrain the performance of the detector or amplifier used. Noise plays a fundamental role in quantum measurement: quantum noise from the detector acts back on the system being measured to ensure that information about the variable conjugate to the measured variable is destroyed, thus enforcing the Heisenberg uncertainty principle. A direct consequence of this quantum back-action is that a "phase preserving" linear amplifier (i.e. an amplifier which amplifies both quadratures of the input signal by the same amount [1]) necessarily adds a certain minimum amount of noise to the input signal, even if it is otherwise perfect (Caves, 1982; Haus and Mullen, 1962). There are several motivations for understanding in principle, and realizing in practice, amplifiers whose noise reaches this minimum quantum limit. Reaching the quantum limit on continuous position detection has been one of the goals of many recent experiments on quantum electromechanical (Cleland *et al.*, 2002; Etaki *et al.*, 2008; Flowers-Jacobs *et al.*, 2007; Knobel and Cleland, 2003; LaHaye *et al.*, 2004; Naik *et al.*, 2006; Poggio *et al.*, 2008; Regal *et al.*, 2008) and opto-mechanical systems (Arcizet *et al.*, 2006; Schliesser *et al.*, 2008) As we will show, having a near-quantum limited detector would allow one to continuously monitor the quantum zero-point fluctuations of a mechanical resonator. Having a quantum limited detector is also necessary for such tasks as single-spin NMR detection (Rugar *et al.*, 2004), as well as gravitational wave detection (Abramovici *et al.*, 1992). The topic of quantum-limited detection is also directly relevant to recent activity exploring feedback control of quantum systems (Doherty *et al.*, 2000; Geremia *et al.*, 2004; Korotkov, 2001b; Ruskov and Korotkov, 2002); such schemes *necessarily* need a close-to-quantum-limited detector.

In this introductory article, we will discuss both the aforementioned aspects of quantum noise: the description and detection of noise in the quantum regime $\hbar\omega > k_{\rm B}T$, and the relation between quantum noise, quantum measurement and quantum amplification. While some aspects of these topics have been studied in the quantum optics and quantum dissipative systems communities and are the subject of several reviews (Braginsky and Khalili, 1992; Gardiner and Zoller, 2000; Haus, 2000; Weiss, 1999), they are somewhat newer to the mesoscopic physics community; moreover, some of the technical machinery developed in these fields is not directly applicable to the study of quantum noise in mesoscopic systems. Note also that there are many other interesting aspects of quantum noise besides those we discuss in this article; we outline some of these in the last, concluding section of this article.

The remainder of this article is organized as follows. We start in Sec. II by providing a short review of the basic statistical properties of classical noise; we also discuss the key modifications that arise when one includes quantum mechanics. Next, in Sec. III, we discuss the detection of quantum noise using either a two-level system or harmonic oscillator as a quantum spectrum analyzer; we also discuss the physics of other commonly-used noise detection schemes. In Sec. IV we turn to quantum measurements, and give a basic introduction to weak, continuous measurements. To make things concrete, we discuss heuristically measurements of both a qubit and an oscillator using a simple resonant cavity detector, giving an idea of the origin of the quantum limit in each case. Sec. V is devoted to a more rigorous treatment of quantum constraints on noise arising from general quantum linear response theory. In Sec. VI, we give a thorough discussion of quantum limits on amplification and continuous position detection; we also briefly discuss various methods for beating the usual quantum limits on added noise using back-action evasion techniques. We are careful to distinguish two very distinct modes of amplifier operation (the "scattering" versus "op amp" modes); we expand on this in Sec. VII, where we discuss both modes of operation in a simple two-port bosonic amplifier. Importantly, we show that an amplifier can be quantum limited in one mode of operation, but fail to be quantum limited in the other mode of operation. Finally, in Sec. VIII, we highlight a number of practical considerations that one must keep in mind when trying to perform a quantum limited measurement.

In addition to the above, we have supplemented the main text with several pedagogical appendices which cover some basic background topics (e.g. the Wiener-Khinchin theorem; the Caldeira-Leggett formalism for modeling a dissipative circuit element; input-output theory; etc.), as well as more detailed discussions of specific systems (e.g. degenerate and non-degenerate parametric amplifiers, the Mach-Zehnder interferometer as detector, etc.). The appendices devote particular attention to the quantum mechanics of transmission lines and driven electromagnetic cavities, topics which are especially relevant given recent experiments making use of microwave stripline resonators. The discussion of transmission lines also gives a very instructive example of many of the more general principles discussed in the main text. Finally, note that while this article is a review, there is considerable new material presented, especially in our discussion of quantum amplification.

[1] In the literature this is often referred to by the unfortunate name of 'phase insensitive' amplifier. We prefer the term 'phase preserving' to avoid any ambiguity.

TABLE I: Table of symbols and main results.

Symbol	Definition / Result
	General Definitions
$f[\omega]$	Fourier transform of the function or operator $f(t)$, defined via $f[\omega]=\int_{-\infty}^{\infty}dtf(t)e^{i\omega t}$
	(Note that for operators, we use the convention $\hat{f}^\dagger[\omega]=\int_{-\infty}^{\infty}dt\hat{f}^\dagger(t)e^{i\omega t}$, implying $\hat{f}^\dagger[\omega]=\left(\hat{f}[-\omega]\right)^\dagger$)
$\mathcal{S}_{FF}[\omega]$	Classical noise spectral density or power spectrum: $\mathcal{S}_{FF}[\omega]=\int_{-\infty}^{+\infty}dt\,e^{i\omega t}\langle F(t)F(0)\rangle$
$S_{FF}[\omega]$	Quantum noise spectral density: $S_{FF}[\omega]=\int_{-\infty}^{+\infty}dt\,e^{i\omega t}\langle\hat{F}(t)\hat{F}(0)\rangle$
$\bar{S}_{FF}[\omega]$	Symmetrized quantum noise spectral density $\bar{S}_{FF}[\omega]=\frac{1}{2}(S_{FF}[\omega]+S_{FF}[-\omega])=\frac{1}{2}\int_{-\infty}^{+\infty}dt\,e^{i\omega t}\langle\{\hat{F}(t),\hat{F}(0)\}\rangle$
$\chi_{AB}(t)$	General linear response susceptibility describing the response of A to a perturbation which couples to B; in the quantum case, given by the Kubo formula $\chi_{AB}(t)=-\frac{i}{\hbar}\theta(t)\langle[\hat{A}(t),\hat{B}(0)]\rangle$ [Eq. (3.30)]
A	Coupling constant (dimensionless) between measured system and detector/amplifier, e.g. $\hat{V}=AF(t)\hat{\sigma}_x,\hat{V}=A\hat{x}\hat{F}$, or $\hat{V}=A\hat{\sigma}_z\hat{a}^\dagger\hat{a}$
M,Ω	Mass and angular frequency of a mechanical harmonic oscillator.
$x_{\rm ZPF}$	Zero point uncertainty of a mechanical oscillator, $x_{\rm ZPF}=\sqrt{\frac{\hbar}{2M\Omega}}$.
γ_0	Intrinsic damping rate of a mechanical oscillator due to coupling to a bath via $\hat{V}=A\hat{x}\hat{F}$: $\gamma_0=\frac{A^2}{2M\hbar\Omega}(S_{FF}[\Omega]-S_{FF}[-\Omega])$ [Eq. (3.25)]
$\omega_{\rm c}$	Resonant frequency of a cavity
$\kappa,Q_{\rm c}$	Damping, quality factor of a cavity
	Sec. III Quantum spectrum analyzers
$T_{\rm eff}[\omega]$	Effective temperature at a frequency ω for a given quantum noise spectrum, defined via $\frac{S_{FF}[\omega]}{S_{FF}[-\omega]}=\exp\left(\frac{\hbar\omega}{k_{\rm B}T_{\rm eff}[\omega]}\right)$ [Eq. (3.21)]
	Fluctuation-dissipation theorem relating the symmetrized noise spectrum to the dissipative part for an equilibrium bath: $\bar{S}_{FF}[\omega]=\frac{1}{2}\coth(\frac{\hbar\omega}{2k_{\rm B}T})(S_{FF}[\omega]-S_{FF}[-\omega])$ [Eq. (3.34)]
	Sec. IV Quantum Measurements
	Number-phase uncertainty relation for a coherent state: $\Delta N\Delta\theta\geq\frac{1}{2}$ [Eq. (4.8), (G12)]
$\dot{N}$	Photon number flux of a coherent beam
$\delta\theta$	Imprecision noise in the measurement of the phase of a coherent beam
	Fundamental noise constraint for an ideal coherent beam: $S_{\dot{N}\dot{N}}S_{\theta\theta}=\frac{1}{4}$ [Eq. (4.16), (G21)]
$\bar{S}^0_{xx}(\omega)$	symmetrized spectral density of zero-point position fluctuations of a damped harmonic oscillator
$\bar{S}_{xx,\rm tot}(\omega)$	total output noise spectral density (symmetrized) of a linear position detector, referred back to the oscillator
$\bar{S}_{xx,\rm add}(\omega)$	added noise spectral density (symmetrized) of a linear position detector, referred back to the oscillator
	Sec. V: General linear response theory
$\hat{x}$	Input signal
$\hat{F}$	Fluctuating force from the detector, coupling to $\hat{x}$ via $\hat{V}=A\hat{x}\hat{F}$
$\hat{I}$	Detector output signal
	General quantum constraint on the detector output noise, backaction noise and gain: $\bar{S}_{II}[\omega]\bar{S}_{FF}[\omega]-\left\|\bar{S}_{IF}[\omega]\right\|^2\geq\left\|\frac{\hbar\tilde{\chi}_{IF}[\omega]}{2}\right\|^2\left(1+\Delta\left[\frac{\bar{S}_{IF}[\omega]}{\hbar\bar{\lambda}[\omega]/2}\right]\right)$ [Eq. (5.11)] where $\tilde{\chi}_{IF}[\omega]\equiv\chi_{IF}[\omega]-[\chi_{FI}[\omega]]^*$ and $\Delta[z]=(\left\|1+z^2\right\|-\left(1+|z|^2\right))/2$. [Note: $1+\Delta[z]\geq0$ and $\Delta=0$ in most cases of relevance, see discussion around Eq. (5.16)]
α	Complex proportionality constant characterizing a quantum-ideal detector: $\|\alpha\|^2=\bar{S}_{II}/\bar{S}_{FF}$ and $\sin\left(\arg\alpha[\omega]\right)=\frac{\hbar\|\lambda[\omega]\|/2}{\sqrt{\bar{S}_{II}[\omega]\bar{S}_{FF}[\omega]}}$ [Eqs. (5.17,J15)]
$\Gamma_{\rm meas}$	Measurement rate (for a QND qubit measurement) [Eq. 5.23]
Γ_φ	Dephasing rate (due to measurement back-action) [Eqs. (4.44),(5.18)]
	Constraint on weak, continuous QND qubit state detection : $\eta=\frac{\Gamma_{\rm meas}}{\Gamma_\varphi}\leq1$ [Eq. (5.24)]
	Sec. VI: Quantum Limit on Linear Amplifiers and Position Detectors
G	Photon number (power) gain, e.g. in Eq. (6.7b)
	Input-output relation for a bosonic scattering amplifier: $\hat{b}^\dagger=\sqrt{G}\hat{a}^\dagger+\hat{\mathcal{F}}^\dagger$ [Eq.(6.7b)]
$(\Delta a)^2$	Symmetrized field operator uncertainty for the scattering description of a bosonic amplifier: $(\Delta a)^2\equiv\frac{1}{2}\left\langle\{\hat{a},\hat{a}^\dagger\}\right\rangle-\|\langle a\rangle\|^2$

TABLE I: Table of symbols and main results.

Symbol	Definition / Result
	Standard quantum limit for the noise added by a phase-preserving bosonic scattering amplifier in the high-gain limit, $G \gg 1$, where $\langle(\Delta a)^2\rangle_{\rm ZPF} = \frac{1}{2}$: $\frac{(\Delta b)^2}{G} \geq (\Delta a)^2 + \frac{1}{2}$ [Eq. (6.10)]
$G_P[\omega]$	Dimensionless power gain of a linear position detector or voltage amplifier (maximum ratio of the power delivered by the detector output to a load, vs. the power fed into signal source): $G_P[\omega] = \frac{\lvert\chi_{IF}[\omega]\rvert^2}{4{\rm Im}\ \chi_{FF}[\omega]\cdot{\rm Im}\ \chi_{II}[\omega]}$ [Eq. (6.25)] For a quantum-ideal detector, in the high-gain limit: $G_P \simeq \left[\frac{{\rm Im}\ \alpha}{\lvert\alpha\rvert}\frac{4k_{\rm B}T_{\rm eff}}{\hbar\omega}\right]^2$ [Eq. (6.29)]
$\bar{S}_{xx,{\rm eq}}[\omega,T]$	Intrinsic equilibrium noise $\bar{S}_{xx,{\rm eq}}[\omega,T] = \hbar\coth\left(\frac{\hbar\omega}{2k_{\rm B}T}\right)[-{\rm Im}\ \chi_{xx}[\omega]]$ [Eq. (6.31)]
$A_{\rm opt}$	Optimal coupling strength of a linear position detector which minimizes the added noise at frequency ω: $A^4_{\rm opt}[\omega] = \frac{\bar{S}_{II}[\omega]}{\lvert\lambda[\omega]\chi_{xx}[\omega]\rvert^2 S_{FF}[\omega]}$ [Eq. (6.36)]
$\gamma[A_{\rm opt}]$	Detector-induced damping of a quantum-limited linear position detector at optimal coupling, fulfills $\frac{\gamma[A_{\rm opt}]}{\gamma_0+\gamma[A_{\rm opt}]} = \left\lvert\frac{{\rm Im}\ \alpha}{\alpha}\right\rvert\frac{1}{\sqrt{G_P[\Omega]}} = \frac{\hbar\Omega}{4k_{\rm B}T_{\rm eff}} \ll 1$ [Eq. (6.41)]
	Standard quantum limit for the added noise spectral density of a linear position detector (valid at each frequency ω): $S_{xx,{\rm add}}[\omega] \geq \lim_{T\to 0} S_{xx,{\rm eq}}[w,T]$ [Eq. (6.34)]
	Effective increase in oscillator temperature due to coupling to the detector back action, for an ideal detector, with $\hbar\Omega/k_{\rm B} \ll T_{\rm bath} \ll T_{\rm eff}$: $T_{\rm osc} \equiv \frac{\gamma\cdot T_{\rm eff}+\gamma_0\cdot T_{\rm bath}}{\gamma+\gamma_0} \to \frac{\hbar\Omega}{4k_{\rm B}} + T_{\rm bath}$ [Eq. (6.42)]
$Z_{\rm in}, Z_{\rm out}$	Input and output impedances of a linear voltage amplifier
$Z_{\rm s}$	Impedance of signal source attached to input of a voltage amplifier
λ_V	Voltage gain of a linear voltage amplifier
$\tilde{V}(t)$	Voltage noise of a linear voltage amplifier (Proportional to the intrinsic output noise of the generic linear-response detector [Eq. (6.53)])
$\tilde{I}(t)$	Current noise of a linear voltage amplifier (Related to the back-action force noise of the generic linear-response detector [Eqs. (6.52)])
$T_{\rm N}$	Noise temperature of an amplifier [defined in Eq. (6.46)]
$Z_{\rm N}$	Noise impedance of a linear voltage amplifier [Eq. 6.49)]
	Standard quantum limit on the noise temperature of a linear voltage amplifier: $k_{\rm B}T_{\rm N}[\omega] \geq \frac{\hbar\omega}{2}$ [Eq.(6.61)]
	Sec. VII: Bosonic Scattering Description of a Two-Port Amplifier
$\hat{V}_a(\hat{V}_b)$	Voltage at the input (output) of the amplifier Relation to bosonic mode operators: Eq. (7.2a)
$\hat{I}_a(\hat{I}_b)$	Current drawn at the input (leaving the output) of the amplifier Relation to bosonic mode operators: Eq. (7.2b)
λ'_I	Reverse current gain of the amplifier
$s[\omega]$	Input-output 2×2 scattering matrix of the amplifier [Eq. (7.3)] Relation to op-amp parameters $\lambda_V, \lambda'_I, Z_{\rm in}, Z_{\rm out}$: Eqs. (7.7)
$\hat{\tilde{V}}(\hat{\tilde{I}})$	Voltage (current) noise operators of the amplifier
$\hat{\mathcal{F}}_a[\omega]$, $\hat{\mathcal{F}}_b[\omega]$	Input (output) port noise operators in the scattering description [Eq. (7.3)] Relation to op-amp noise operators $\hat{\tilde{V}}, \hat{\tilde{I}}$: Eq. (7.9)

II. BASICS OF CLASSICAL AND QUANTUM NOISE

A. Classical noise correlators

Consider a classical random voltage signal $V(t)$. The signal is characterized by zero mean $\langle V(t)\rangle = 0$, and autocorrelation function

$$G_{VV}(t-t') = \langle V(t)V(t')\rangle \tag{2.1}$$

whose sign and magnitude tells us whether the voltage fluctuations at time t and time t' are correlated, anti-correlated or statistically independent. We assume that the noise process is *stationary* (i.e., the statistical properties are time translation invariant) so that G_{VV} depends only on the time difference. If $V(t)$ is Gaussian distributed, then the mean and autocorrelation completely specify the statistical properties and the probability distribution. We will assume here that the noise is due to the sum of a very large number of fluctuating charges so that by the central limit theorem, it is Gaussian distributed. We also assume that G_{VV} decays (sufficiently rapidly) to zero on some characteristic correlation time scale $\tau_{\rm c}$ which is finite.

The spectral density of the noise as measured by a spectrum analyzer is a measure of the intensity of the signal at different frequencies. In order to understand the spectral density of a random signal, it is useful to define its 'windowed' Fourier transform as follows:

$$V_T[\omega] = \frac{1}{\sqrt{T}} \int_{-T/2}^{+T/2} dt\, e^{i\omega t} V(t), \tag{2.2}$$

where T is the sampling time. In the limit $T \gg \tau_c$ the integral is a sum of a large number $N \approx \frac{T}{\tau_c}$ of random uncorrelated terms. We can think of the value of the integral as the end point of a random walk in the complex plane which starts at the origin. Because the distance traveled will scale with $\sqrt{T}$, our choice of normalization makes the statistical properties of $V[\omega]$ independent of the sampling time T (for sufficiently large T). Notice that $V_T[\omega]$ has the peculiar units of volts$\sqrt{\text{secs}}$ which is usually denoted volts/$\sqrt{\text{Hz}}$.

The spectral density (or 'power spectrum') of the noise is defined to be the ensemble averaged quantity

$$\mathcal{S}_{VV}[\omega] \equiv \lim_{T\to\infty} \langle |V_T[\omega]|^2 \rangle = \lim_{T\to\infty} \langle V_T[\omega] V_T[-\omega] \rangle \tag{2.3}$$

The second equality follows from the fact that the $v(t)$ is real valued. The Wiener-Khinchin theorem (derived in Appendix A) tells us that the spectral density is equal to the Fourier transform of the autocorrelation function

$$\mathcal{S}_{VV}[\omega] = \int_{-\infty}^{+\infty} dt\, e^{i\omega t} G_{VV}(t). \tag{2.4}$$

The inverse transform relates the autocorrelation function to the power spectrum

$$G_{VV}(t) = \int_{-\infty}^{+\infty} \frac{d\omega}{2\pi}\, e^{-i\omega t} \mathcal{S}_{VV}[\omega]. \tag{2.5}$$

We thus see that a short auto-correlation time implies a spectral density which is non-zero over a wide range of frequencies. In the limit of 'white noise'

$$G_{VV}(t) = \sigma^2 \delta(t) \tag{2.6}$$

the spectrum is flat (independent of frequency)

$$\mathcal{S}_{VV}[\omega] = \sigma^2 \tag{2.7}$$

In the opposite limit of a long autocorrelation time, the signal is changing slowly so it can only be made up out of a narrow range of frequencies (not necessarily centered on zero).

Because $V(t)$ is a real-valued classical variable, it naturally follows that $G_{VV}(t)$ is always real. Since $V(t)$ is not a quantum operator, it commutes with its value at other times and thus, $\langle V(t)V(t')\rangle = \langle V(t')V(t)\rangle$. From this it follows that $G_{VV}(t)$ is always symmetric in time and the power spectrum is always symmetric in frequency

$$\mathcal{S}_{VV}[\omega] = \mathcal{S}_{VV}[-\omega]. \tag{2.8}$$

As a prototypical example of these ideas, let us consider a simple harmonic oscillator of mass M and frequency Ω. The oscillator is maintained in equilibrium with a large heat bath at temperature T via some infinitesimal coupling which we will ignore in considering the dynamics. The solution of Hamilton's equations of motion are

$$\begin{aligned} x(t) &= x(0)\cos(\Omega t) + p(0)\frac{1}{M\Omega}\sin(\Omega t) \\ p(t) &= p(0)\cos(\Omega t) - x(0) M\Omega^2 \sin(\Omega t), \end{aligned} \tag{2.9}$$

where $x(0)$ and $p(0)$ are the (random) values of the position and momentum at time $t = 0$. It follows that the position autocorrelation function is

$$\begin{aligned} G_{xx}(t) &= \langle x(t)x(0)\rangle \\ &= \langle x(0)x(0)\rangle \cos(\Omega t) + \langle p(0)x(0)\rangle \frac{1}{M\Omega}\sin(\Omega t). \end{aligned} \tag{2.10}$$

Classically in equilibrium there are no correlations between position and momentum. Hence the second term vanishes. Using the equipartition theorem $\frac{1}{2}M\Omega^2\langle x^2\rangle = \frac{1}{2}k_B T$, we arrive at

$$G_{xx}(t) = \frac{k_B T}{M\Omega^2}\cos(\Omega t) \tag{2.11}$$

which leads to the spectral density

$$\mathcal{S}_{xx}[\omega] = \pi \frac{k_B T}{M\Omega^2}\left[\delta(\omega - \Omega) + \delta(\omega + \Omega)\right] \tag{2.12}$$

which is indeed symmetric in frequency.

B. Square law detectors and classical spectrum analyzers

Now that we understand the basics of classical noise, we can consider how one experimentally measures a classical noise spectral density. With modern high speed digital sampling techniques it is perfectly feasible to directly measure the random noise signal as a function of time and then directly compute the autocorrelation function in Eq. (2.1). This is typically done by first performing an analog-to-digital conversion of the noise signal, and then numerically computing the autocorrelation function. One can then use Eq. (2.4) to calculate the noise spectral density via a numerical Fourier transform. Note that while Eq. (2.4) seems to require an ensemble average, in practice this is not explicitly done. Instead, one uses a sufficiently long averaging time T (i.e. much longer than the correlation time of the noise) such that a single time-average is equivalent to an ensemble average. This approach of measuring a noise spectral density directly from its autocorrelation function is most appropriate for signals at RF frequencies well below 1 MHz.

For microwave signals with frequencies well above 1 GHz, a very different approach is usually taken. Here, the standard route to obtain a noise spectral density involves

first shifting the signal to a lower intermediate frequency via a technique known as heterodyning (we discuss this more in Sec. III.C.3). This intermediate-frequency signal is then sent to a filter which selects a narrow frequency range of interest, the so-called 'resolution bandwidth'. Finally, this filtered signal is sent to a square-law detector (e.g. a diode), and the resulting output is averaged over a certain time-interval (the inverse of the so-called 'video bandwidth'). It is this final output which is then taken to be a measure of the noise spectral density.

It helps to put the above into equations. Ignoring for simplicity the initial heterodyning step, let

$$V_{\rm f}[\omega] = f[\omega]V[\omega] \tag{2.13}$$

be the voltage at the output of the filter and the input of the square law detector. Here, $f[\omega]$ is the (amplitude) transmission coefficient of the filter and $V[\omega]$ is the Fourier transform of the noisy signal we are measuring. From Eq. (2.5) it follows that the output of the square law detector is proportional to

$$\langle I\rangle = \int_{-\infty}^{+\infty} \frac{d\omega}{2\pi} |f[\omega]|^2 \mathcal{S}_{VV}[\omega]. \tag{2.14}$$

Approximating the narrow band filter centered on frequency $\pm\omega_0$ as[2]

$$|f[\omega]|^2 = \delta(\omega-\omega_0) + \delta(\omega+\omega_0) \tag{2.15}$$

we obtain

$$\langle I\rangle = \mathcal{S}_{VV}(-\omega_0) + \mathcal{S}_{VV}(\omega_0) \tag{2.16}$$

showing as expected that the classical square law detector measures the symmetrized noise power.

We thus have two very different basic approaches for the measurement of classical noise spectral densities: for low RF frequencies, one can directly measure the noise autocorrelation, whereas for high microwave frequencies, one uses a filter and a square law detector. For noise signals in intermediate frequency ranges, a combination of different methods is generally used. The whole story becomes even more complicated, as at very high frequencies (e.g. in the far infrared), devices such as the so-called 'Fourier Transform spectrometer' are in fact based on a direct measurement of the equivalent of an autocorrelation function of the signal. In the infrared, visible and ultraviolet, noise spectrometers use gratings followed by a slit acting as a filter.

[2] A linear passive filter performs a convolution $V_{\rm out}(t) = \int_{-\infty}^{+\infty} dt'\, F(t-t')V_{\rm in}(t')$ where F is a real-valued (and causal) function. Hence it follows that $f[\omega]$, which is the Fourier transform of F, obeys $f[-\omega] = f^*[\omega]$ and hence $|f[\omega]|^2$ is symmetric in frequency.

C. Introduction to quantum noise

Based on our review of classical noise, one expects that the study of quantum noise involves spectral densities of the form

$$S_{xx}[\omega] = \int_{-\infty}^{+\infty} dt\, e^{i\omega t}\langle \hat{x}(t)\hat{x}(0)\rangle \tag{2.17}$$

where $\hat{x}$ is a quantum operator (in the Heisenberg representation) and the angular brackets indicate the quantum statistical average evaluated using the quantum density matrix. Note that we will use $\mathcal{S}[\omega]$ throughout this review to denote the spectral density of a classical noise, while $S[\omega]$ will denote a quantum noise spectral density. As a simple example of the important differences from the classical limit, consider the same harmonic oscillator problem as above. The solutions of the Heisenberg equations of motion are the same as for the classical case but with the initial position and momentum replaced by the corresponding quantum operators:

$$\begin{aligned} \hat{x}(t) &= \hat{x}(0)\cos(\Omega t) + \hat{p}(0)\frac{1}{M\Omega}\sin(\Omega t) \\ \hat{p}(t) &= \hat{p}(0)\cos(\Omega t) - \hat{x}(0)M\Omega\sin(\Omega t). \end{aligned} \tag{2.18}$$

Just as before, it follows that the position autocorrelation function is

$$\begin{aligned} G_{xx}(t) &= \langle \hat{x}(t)\hat{x}(0)\rangle \\ &= \langle \hat{x}(0)\hat{x}(0)\rangle\cos(\Omega t) + \langle \hat{p}(0)\hat{x}(0)\rangle\frac{1}{M\Omega}\sin(\Omega t). \end{aligned} \tag{2.19}$$

Classically the second term on the RHS vanishes because in thermal equilibrium the position and momentum are uncorrelated random variables. As we will see shortly below for the quantum case, the symmetrized (sometimes called the 'classical') correlator vanishes in thermal equilibrium

$$\langle \hat{x}\hat{p} + \hat{p}\hat{x}\rangle = 0, \tag{2.20}$$

just as it does classically. Notice however that

$$[\hat{x}(0), \hat{p}(0)] = i\hbar \tag{2.21}$$

which implies that there *must* inevitably be some correlations between position and momentum in the quantum case since $\langle \hat{x}(0)\hat{p}(0)\rangle - \langle \hat{p}(0)\hat{x}(0)\rangle = i\hbar$.

We can evaluate these correlations using the representation of the operators in terms of the harmonic oscillator ladder operators

$$\begin{aligned} \hat{x} &= x_{\rm ZPF}(\hat{a}^\dagger + \hat{a}) \\ \hat{p} &= \frac{i\hbar}{2x_{\rm ZPF}}(\hat{a}^\dagger - \hat{a}) \end{aligned} \tag{2.22}$$

where $x_{\rm ZPF}$ is the RMS zero-point uncertainty of x in the quantum ground state

$$x_{\rm ZPF}^2 \equiv \langle 0|\hat{x}^2|0\rangle = \frac{\hbar}{2M\Omega}. \tag{2.23}$$

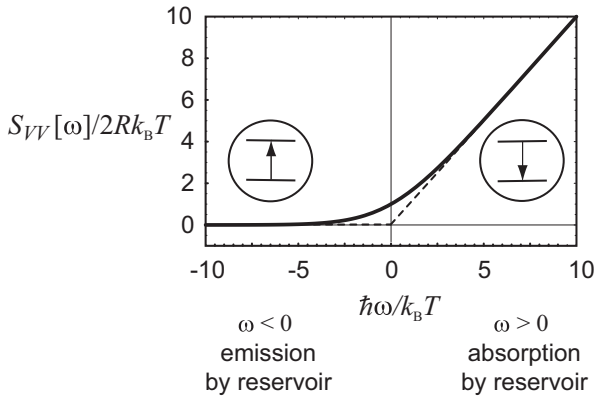

FIG. 1 Quantum noise spectral density of voltage fluctuations across a resistor (resistance R) as a function of frequency at zero temperature (dashed line) and finite temperature (solid line).

For the case of thermal equilibrium, we obtain

$$\begin{aligned} \langle \hat{p}(0)\hat{x}(0)\rangle &= -i\frac{\hbar}{2} \\ \langle \hat{x}(0)\hat{p}(0)\rangle &= +i\frac{\hbar}{2} \end{aligned} \tag{2.24}$$

Not only are the position and momentum correlated, but their correlator is imaginary![3] This means that, despite the fact that the position is an hermitian observable with real eigenvalues, its autocorrelation function is complex and given from Eq. (2.20) by:

$$G_{xx}(t) = x_{\rm ZPF}^2 \left\{ n_{\rm B}(\hbar\Omega) e^{+i\Omega t} + [n_{\rm B}(\hbar\Omega)+1] e^{-i\Omega t} \right\}, \tag{2.25}$$

where $n_{\rm B}$ is the Bose-Einstein occupation factor. The complex nature of the autocorrelation function follows from the fact that the operator $\hat{x}$ does not commute with itself at different times.

Because the correlator is complex it follows that the spectral density is no longer symmetric in frequency

$$\begin{aligned} S_{xx}[\omega] &= 2\pi x_{\rm ZPF}^2 \\ \times\ & \{ n_{\rm B}(\hbar\Omega)\delta(\omega+\Omega) + [n_{\rm B}(\hbar\Omega)+1]\delta(\omega-\Omega) \} \end{aligned} \tag{2.26}$$

The Bose-Einstein factors suggest that the positive frequency part of the spectral density has to do with stimulated emission of energy *into* the oscillator and the negative frequency part of the spectral density has to do with emission of energy *by* the oscillator. That is, the positive frequency part of the spectral density is a measure of the ability of the oscillator to *absorb* energy, while the negative frequency part is a measure of the ability of the oscillator to *emit* energy. Fig. 1 illustrates this for the case of the voltage noise spectral density of a resistor (see Appendix C.3 for more details).

The qualitative picture described above will be confirmed when we consider in detail how it is that quantum spectrum analyzers work. Given that $\hat{x}(t)$ and $\hat{x}(0)$ do not commute, it is not possible to experimentally measure the complex autocorrelation function $G_{xx}(t)$ as the expectation value of some Hermitian observable. Nevertheless we will see below that it is possible to determine its Fourier transform $S_{xx}[\omega]$ for both positive and negative frequencies by means of certain non-equilibrium measurements (Aguado and Kouwenhoven, 2000; Gavish *et al.*, 2000; Lesovik and Loosen, 1997; Schoelkopf *et al.*, 2003).

In closing we note that in the high temperature limit $k_{\rm B}T \gg \hbar\Omega$ we have

$$n_{\rm B}(\hbar\Omega) \sim n_{\rm B}(\hbar\Omega) + 1 \sim \frac{k_{\rm B}T}{\hbar\Omega}. \tag{2.27}$$

Substitution of this approximation into Eq. (2.27) reproduces the classical expression in Eq. (2.12).

The results presented above can be extended to the case of a bath of many harmonic oscillators. As described in Appendix C a resistor can be modeled as an infinite set of harmonic oscillators and from this model the Johnson/Nyquist noise of a resistor can be derived.

III. QUANTUM SPECTRUM ANALYZERS

A. Two-level system as a spectrum analyzer

Consider a quantum system (atom or electrical circuit) which has its two lowest energy levels ϵ_0 and ϵ_1 separated by energy $E_{01} = \hbar\omega_{01}$. We suppose for simplicity that all the other levels are far away in energy and can be ignored. The resulting quantum two-level can be used as a spectrometer of quantum noise (Aguado and Kouwenhoven, 2000; Schoelkopf *et al.*, 2003); we discuss this in detail in what follows.

The states of any two-level system (here after abbreviated TLS) can be mapped onto the states of a fictitious spin-1/2 particle since such a spin also has only two states in its Hilbert space. With spin down representing the ground state ($|g\rangle$) and spin up representing the excited state ($|e\rangle$) [Made sign in front of σ_z consistent with later sections], the Hamiltonian is (taking the zero of energy to be the center of gravity of the two levels)

$$\hat{H}_0 = \frac{\hbar\omega_{01}}{2}\hat{\sigma}_z. \tag{3.1}$$

In keeping with our discussion in the introduction, our goal is to now see how the rate of 'spin-flip' transitions induced by an external noise source can be used to analyze the spectrum of that noise. Suppose for example that there is a noise source with amplitude $f(t)$ which

[3] Notice that this occurs because the product of two non-commuting hermitian operators is not itself an hermitian operator.

can cause transitions via the perturbation[4]

$$\hat{V} = AF(t)\hat{\sigma}_x, \tag{3.2}$$

where A is a coupling constant. The variable $F(t)$ represents the noise source. We can temporarily pretend that F is a classical variable, although its quantum operator properties will be forced upon us very soon. For now, only our two-level spectrum analyzer will be treated quantum mechanically.

We assume that the coupling A is under our control and can be made small enough that the noise can be treated in lowest order perturbation theory. We take the state of the two-level system to be

$$|\psi(t)\rangle = \begin{pmatrix} \alpha_g(t) \\ \alpha_e(t) \end{pmatrix}. \tag{3.3}$$

In the interaction representation, first-order time-dependent perturbation theory gives

$$|\psi_{\rm I}(t)\rangle = |\psi(0)\rangle - \frac{i}{\hbar}\int_0^t d\tau\ \hat{V}(\tau)|\psi(0)\rangle. \tag{3.4}$$

If we initially prepare the two-level system in its ground state, the amplitude to find it in its excited state at time t is from Eq. (3.4)

$$\begin{aligned} \alpha_e &= -\frac{iA}{\hbar}\int_0^t d\tau\ \langle e|\hat{\sigma}_x(\tau)|g\rangle F(\tau), \\ &= -\frac{iA}{\hbar}\int_0^t d\tau\ e^{i\omega_{01}\tau}F(\tau). \end{aligned} \tag{3.5}$$

Since the integrand in Eq. (3.5) is random, α_e is a sum of a large number of random terms; i.e. its value is the endpoint of a random walk in the complex plane (as discussed above in defining the spectral density of classical noise). As a result, for times exceeding the autocorrelation time $\tau_{\rm c}$ of the noise, the integral will not grow linearly with time but rather only as the square root of time, as expected for a random walk. We can now compute the probability

$$p_e(t) \equiv |\alpha_e|^2 = \frac{A^2}{\hbar^2}\int_0^t\int_0^t d\tau_1 d\tau_2\, e^{-i\omega_{01}(\tau_1-\tau_2)}F(\tau_1)F(\tau_2) \tag{3.6}$$

which we expect to grow quadratically for short times $t < \tau_{\rm c}$, but linearly for long times $t > \tau_{\rm c}$. Ensemble averaging the probability over the random noise yields

$$\bar{p}_e(t) = \frac{A^2}{\hbar^2}\int_0^t\int_0^t d\tau_1 d\tau_2\, e^{-i\omega_{01}(\tau_1-\tau_2)}\,\langle F(\tau_1)F(\tau_2)\rangle \tag{3.7}$$

Introducing the noise spectral density

$$S_{FF}(\omega) = \int_{-\infty}^{+\infty} d\tau\, e^{i\omega\tau}\langle F(\tau)F(0)\rangle, \tag{3.8}$$

and utilizing the Fourier transform defined in Eq. (2.2) and the Wiener-Khinchin theorem from Appendix A, we find that the probability to be in the excited state indeed increases *linearly* with time at long times,[5]

$$\bar{p}_e(t) = t\frac{A^2}{\hbar^2}S_{FF}(-\omega_{01}) \tag{3.9}$$

The time derivative of the probability gives the transition rate from ground to excited states

$$\Gamma_\uparrow = \frac{A^2}{\hbar^2}S_{FF}(-\omega_{01}) \tag{3.10}$$

Note that we are taking in this last expression the spectral density on the negative frequency side. If F were a strictly classical noise source, $\langle F(\tau)F(0)\rangle$ would be real, and $S_{FF}(-\omega_{01}) = S_{FF}(+\omega_{01})$. However, because as we discuss below F is actually an operator acting on the environmental degrees of freedom, $\left[\hat{F}(\tau), \hat{F}(0)\right] \neq 0$ and $S_{FF}(-\omega_{01}) \neq S_{FF}(+\omega_{01})$.

Another possible experiment is to prepare the two-level system in its excited state and look at the rate of decay into the ground state. The algebra is identical to that above except that the sign of the frequency is reversed:

$$\Gamma_\downarrow = \frac{A^2}{\hbar^2}S_{FF}(+\omega_{01}). \tag{3.11}$$

We now see that our two-level system does indeed act as a quantum spectrum analyzer for the noise. Operationally, we prepare the system either in its ground state or in its excited state, weakly couple it to the noise source, and after an appropriate interval of time (satisfying the above inequalities) simply measure whether the system is now in its excited state or ground state. Repeating this protocol over and over again, we can find the probability of making a transition, and thereby infer the rate and hence the noise spectral density at positive and negative frequencies. Note that in contrast with a classical spectrum analyzer, we can separate the noise spectral density at positive and negative frequencies from each other since we can separately measure the downward and upward transition rates. Negative frequency noise transfers energy *from the noise source to the spectrometer*. That is,

---

[4] The most general perturbation would also couple to $\hat{\sigma}_y$ but we assume that (as is often, though not always, the case) a spin coordinate system can be chosen so that the perturbation only couples to $\hat{\sigma}_x$. Noise coupled to $\hat{\sigma}_z$ commutes with the Hamiltonian but is nevertheless important in dephasing coherent superpositions of the two states. We will discuss such processes later.

[5] Note that for very long times, where there is a significant depletion of the probability of being in the initial state, first-order perturbation theory becomes invalid. However, for sufficiently small A, there is a wide range of times $\tau_{\rm c} \ll t \ll 1/\Gamma$ for which Eq. 3.9 is valid. Eqs. 3.10 and 3.11 then yield well-defined rates which can be used in a master equation to describe the full dynamics including long times.

it represents energy emitted by the noise source. Positive frequency noise transfers energy *from the spectrometer to the noise source*.[6] Naively one imagines that a spectrometers measures the noise spectrum by extracting a small amount of the signal energy from the noise source and analyzes it. This is *not* the case however. There must be energy flowing in both directions if the noise is to be fully characterized.

We now rigorously treat the quantity $\hat{F}(\tau)$ as a quantum Heisenberg operator which acts in the Hilbert space of the noise source. The previous derivation is unchanged (the ordering of $\hat{F}(\tau_1)\hat{F}(\tau_2)$ having been chosen correctly in anticipation of the quantum treatment), and Eqs. (3.10,3.11) are still valid provided that we interpret the angular brackets in Eq. (3.7,3.8) as representing a quantum expectation value (evaluated in the absence of the coupling to the spectrometer):

$$S_{FF}(\omega) = \int_{-\infty}^{+\infty} d\tau\, e^{i\omega\tau} \sum_{\alpha,\gamma} \rho_{\alpha\alpha}\, \langle\alpha|\hat{F}(\tau)|\gamma\rangle\langle\gamma|\hat{F}(0)|\alpha\rangle. \tag{3.12}$$

Here, we have assumed a stationary situation, where the density matrix ρ of the noise source is diagonal in the energy eigenbasis (in the absence of the coupling to the spectrometer). However, we do not necessarily assume that it is given by the equilibrium expression. This yields the standard quantum mechanical expression for the spectral density:

$$\begin{aligned} S_{FF}(\omega) &= \int_{-\infty}^{+\infty} d\tau\, e^{i\omega\tau} \sum_{\alpha,\gamma} \rho_{\alpha\alpha}\, e^{\frac{i}{\hbar}(\epsilon_\alpha - \epsilon_\gamma)\tau}\, |\langle\alpha|\hat{F}|\gamma\rangle|^2 \\ &= 2\pi\hbar \sum_{\alpha,\gamma} \rho_{\alpha\alpha}\, |\langle\alpha|\hat{F}|\gamma\rangle|^2 \delta(\epsilon_\gamma - \epsilon_\alpha - \hbar\omega) \end{aligned} \tag{3.13}$$

Substituting this expression into Eqs. (3.10,3.11), we derive the familiar Fermi Golden Rule expressions for the two transition rates.

In standard courses, one is not normally taught that the transition rate of a discrete state into a continuum as described by Fermi's Golden Rule can (and indeed should!) be viewed as resulting from the continuum acting as a quantum noise source which causes the amplitudes of the different components of the wave function to undergo random walks. The derivation presented here hopefully provides a motivation for this interpretation. In particular, thinking of the perturbation (i.e. the coupling to the continuum) as quantum noise with a small but finite autocorrelation time (inversely related to the bandwidth of the continuum) neatly explains why the transition probability increases quadratically for very short times, but linearly for very long times. We find this picture to be considerably superior to the tortured arguments about time scales and order of limits invoked in the usual derivation of Fermi's Golden Rule.

It it is important to keep in mind that our expressions for the transition rates are only valid if the autocorrelation time of our noise is much shorter that the typical time we are interested in; this typical time is simply the inverse of the transition rate. The requirement of a short autocorrelation time in turn implies that our noise source must have a large bandwidth (i.e. there must be large number of available photon frequencies in the vacuum) and must not be coupled too strongly to our system. This is true despite the fact that our final expressions for the transition rates only depend on the spectral density at the transition frequency (a consequence of energy conservation).

One standard model for the continuum is an infinite collection of harmonic oscillators. The electromagnetic continuum in the hydrogen atom case mentioned above is a prototypical example. The vacuum electric field noise coupling to the hydrogen atom has an extremely short autocorrelation time because the range of mode frequencies ω_α (over which the dipole matrix element coupling the atom to the mode electric field $\vec{E}_\alpha$ is significant) is extremely large, ranging from many times smaller than the transition frequency to many times larger. Thus, the autocorrelation time of the vacuum electric field noise is considerably less than 10^{-15}s, whereas the decay time of the hydrogen 2p state is about 10^{-9}s. Hence the inequalities needed for the validity of our expressions are very easily satisfied.

To close our discussion of the TLS quantum spectrometer, let us consider the special case where our noise source is in thermodynamic equilibrium. In this case, the transition rates of the TLS *must* obey detailed balance $\Gamma_\downarrow/\Gamma_\uparrow = e^{\beta\hbar\omega_{01}}$ in order to give the correct equilibrium occupancies of the two states of the spectrometer. This in turn implies that the spectral densities obey [7]

$$S_{FF}(+\omega_{01}) = e^{\beta\hbar\omega_{01}} S_{FF}(-\omega_{01}). \tag{3.14}$$

Without the crucial distinction between positive and negative frequencies, and the resulting difference in rates, one would always find that our two level system is completely unpolarized (i.e. there is an equal probability

[6] Unfortunately, there are several conventions in existence for describing the noise spectral density. It is common in engineering contexts to use the phrase 'spectral density' to mean $S_{FF}(+\omega) + S_{FF}[-\omega]$. This is convenient in classical problems where the two are equal. In quantum contexts, one sometimes sees the asymmetric part of the noise $S_{FF}(+\omega) - S_{FF}(-\omega)$ referred to as the 'quantum noise.' We feel it is simpler and clearer to discuss the spectral density for positive and negative frequencies *separately*, since they each have simple physical interpretations and directly relate to measurable quantities. This convention is especially useful in non-equilibrium situations where there is no simple relation between the spectral densities at positive and negative frequencies.

[7] One can of course prove this detailed balance relation rigorously by calculating the quantum noise for a noise source in a thermal state. Consider for example Eq. (2.25) and use the identity $(1 + n_{\rm B})/n_{\rm B} = \exp\beta\hbar\omega$.

to be in either of the two states). Equivalently, a classical noise source (where $S_{FF}(\omega_{01}) = S_{FF}(-\omega_{01})$) corresponds to a noise source whose temperature is much larger than $\hbar\omega_{01}/k_{\rm B}$.

The more general case is where our noise source is *not* in equilibrium; in this case, no general detailed balance relation holds. However, if we are concerned only with a single particular frequency (given say by the transition frequency of our two-level system detector), then it is always possible to *define* an 'effective temperature' for the noise using Eq. (3.14). In NMR language, this effective temperature for the noise will simply be the 'spin temperature' of our TLS spectrometer once it reaches steady state after being coupled to the noise source. We will have more to say about this effective temperature in the sections that follow.

As an aside, we note that a system designed to detect the arrival (or emission) of a photon (say) with very good time resolution *must* necessarily have very poor phase coherence. This can be achieved with a TLS whose state is continuously and strongly measured (Schuster *et al.*, 2005). Because of the strong measurement, we will know immediately when the state of the two-level system changes due to absorption or emission of a photon. On the other hand, the back-action disturbance of the TLS by the measurement (to be discussed in the next section) will cause the two level system to have a very short phase coherence time. As a result, the TLS will have a very broad line width and hence the poor frequency resolution that must necessarily accompany good temporal resolution.

Finally, we also note that a particular realization of a TLS quantum noise spectrometer involving a double quantum dot was discussed by Aguado and Kouwenhoven (2000); here, absorption (but not emission) of energy by the double dot from a noise can lead to a measurable inelastic current. This system was recently realized in experiment (Gustavsson *et al.*, 2007; Onac *et al.*, 2006a). We also note that a more detailed discussion of TLS quantum noise spectrometers can be found in Schoelkopf *et al.* (2003); this work includes a discussion of various different quantum noise sources which can be important in mesoscopic electronic systems, including the back-action quantum noise generated by a single-electron transistor electrometer.

B. Harmonic oscillator as a spectrum analyzer

Let us now consider what happens when we weakly couple a quantum harmonic oscillator to our quantum noise source. Unlike the TLS of the previous subsection, the oscillator has an infinite number of states. However, similar to the TLS, the oscillator still has a well-defined frequency; as a result, we will see that it too may be used as a spectrum analyzer of quantum noise. Moreover, this example will provide us with a new way to view quantum noise, and will demonstrate how the concept of an "effective temperature" of an out-of-equilibrium noise source (introduced above) can be extremely useful.

Our harmonic oscillator is described by the usual Hamiltonian:

$$H_0 = \frac{\hat{p}^2}{2M} + \frac{M\Omega^2\hat{x}^2}{2} = \hbar\Omega\left(\hat{c}^\dagger\hat{c} + \frac{1}{2}\right) \tag{3.15}$$

where $\hat{a}$ is the lowering operator for the oscillator. Our noise source acts as a weak, fluctuating force on the oscillator:

$$\hat{V} = A\hat{x}\hat{F} = A\left[x_{\rm ZPF}(\hat{c} + \hat{c}^\dagger)\right]\hat{F} \tag{3.16}$$

where $\hat{F}$ is the operator describing the fluctuating noise, and A is again a coupling constant. In complete analogy to the previous subsection, noise in $\hat{F}$ at the oscillator frequency Ω can cause transitions between its eigenstates. We again assume both that A is small, and that our noise source has a short autocorrelation time, so we may again use perturbation theory to derive rates for these transitions. There is a rate for increasing the number of quanta in the oscillator by one, taking a state $|n\rangle$ to $|n+1\rangle$:

$$\Gamma_{n\to n+1} = \frac{A^2}{\hbar^2}\left[(n+1)x_{\rm ZPF}^2\right] S_{FF}[-\Omega] \equiv (n+1)\Gamma_\uparrow \tag{3.17}$$

As expected, this rate involves the noise at $-\Omega$, as energy is being *absorbed from* the noise source. The factor in brackets is just the matrix element for the transition, i.e. $|\langle n+1|\hat{x}|n\rangle|^2$. Similarly, there is a rate for decreasing the number of quanta in the oscillator by one:

$$\Gamma_{n\to n-1} = \frac{A^2}{\hbar^2}\left(n x_{\rm ZPF}^2\right) S_{FF}[\Omega] \equiv n\Gamma_\downarrow \tag{3.18}$$

This rate involves the noise at $+\Omega$, as energy is being *emitted to* the noise source.

Given these rates, we may immediately write down a simple master equation which governs the rate of change of the probability $p_n(t)$ that there are n quanta in the oscillator:

$$\begin{aligned}\frac{d}{dt}p_n &= \left[n\Gamma_\uparrow p_{n-1} + (n+1)\Gamma_\downarrow p_{n+1}\right] \\ &- \left[n\Gamma_\downarrow + (n+1)\Gamma_\uparrow\right] p_n\end{aligned} \tag{3.19}$$

The first two terms describe transitions into the state $|n\rangle$ from the states $|n+1\rangle$ and $|n-1\rangle$, and hence increase p_n. In contrast, the last two terms describe transitions out of the state $|n\rangle$ to the states $|n+1\rangle$ and $|n-1\rangle$, and hence decrease p_n.

It is natural to now ask what the stationary state of the oscillator is. By solving Eq. (3.19) for $\frac{d}{dt}p_n = 0$, we find that:

$$p_n = e^{-n\hbar\Omega/(k_{\rm B}T_{\rm eff})}\left(1 - e^{-\hbar\Omega/(k_{\rm B}T_{\rm eff})}\right) \tag{3.20}$$

where

$$k_{\rm B}T_{\rm eff}[\Omega] \equiv \frac{\hbar\Omega}{\log\left[\frac{\Gamma_\downarrow}{\Gamma_\uparrow}\right]} = \frac{\hbar\Omega}{\log\left[\frac{S_{FF}[\Omega]}{S_{FF}[-\Omega]}\right]} \tag{3.21}$$

Eq. (3.20) describes a thermal equilibrium distribution of the oscillator, with an effective oscillator temperature $T_{\rm eff}[\Omega]$ determined by the quantum noise spectrum of $\hat{F}$. This is the same effective temperature that emerged in our discussion of the TLS spectrum analyzer. If our noise source is in equilibrium, we have seen in the previous subsection that $S_{FF}[\omega]$ must obey a condition of detailed balance (Eq. (3.14)); in this case, $T_{\rm eff}$ coincides with the physical temperature of our noise source. In the more general case where the noise source is out-of-equilibrium, $T_{\rm eff}$ only serves to characterize the asymmetry of the quantum noise, and will vary with frequency [8]. Nonetheless, as far as the oscillator is concerned, $T_{\rm eff}$ acts as a real temperature, and determines the form of its distribution.

We can learn more about the quantum noise spectrum of $\hat{F}$ by also looking at the dynamics of the oscillator, as opposed to just its stationary state. In particular, as the average energy $\langle E\rangle$ of the oscillator is just given by:

$$\langle E(t)\rangle = \sum_{n=0}^{\infty} \hbar\Omega \left(n+\frac{1}{2}\right) p_n(t), \tag{3.22}$$

we can use the master equation Eq. (3.19) to derive an equation for its time dependence. One finds straightforwardly:

$$\frac{d}{dt}\langle E\rangle = P - \gamma\langle E\rangle \tag{3.23}$$

where

$$P = \frac{\hbar\Omega}{2}\left(\Gamma_\uparrow + \Gamma_\downarrow\right) = \frac{A^2}{4M}\left[S_{FF}[\Omega] + S_{FF}[-\Omega]\right] \tag{3.24}$$

$$\gamma = \Gamma_\downarrow - \Gamma_\uparrow = \frac{A^2 x_{\rm ZPF}^2}{\hbar^2}\left[S_{FF}[\Omega] - S_{FF}[-\Omega]\right] \tag{3.25}$$

The two terms in Eq. (3.23) describe, respectively, heating and damping of the oscillator by the noise source. The heating effect of the noise is completely analogous to what happens classically: a random force causes the oscillator's momentum to undergo a random walk (i.e. it diffuses), which in turn causes $\langle E\rangle$ to grow linearly in time at rate P. By demanding $d\langle E\rangle/dt = 0$, we find that the combination of damping and heating effects causes the energy to reach a steady state mean value of

$$\langle E\rangle = \frac{P}{\gamma}. \tag{3.26}$$

In the quantum case, we see from Eq. (3.24) that it is the *symmetric-in-frequency* part of the noise spectrum which is responsible for this effect, and which thus plays the role of a classical noise source. This is another reason why the symmetrized quantum noise is often referred to as the "classical" part of the noise.

Note that in the present description the finite ground state energy $\langle E\rangle = \hbar\Omega/2$ of the harmonic oscillator is determined via the balance between the 'heating' by the zero-point fluctuations of the environment (described by the symmetrized correlator at $T = 0$) and the dissipation. It is possible to take an alternative but equally correct viewpoint, where only the deviation $\langle\delta E\rangle = \langle E\rangle - \hbar\Omega/2$ from the ground state energy is considered. Its evolution equation

$$\frac{d}{dt}\langle\delta E\rangle = \langle\delta E\rangle(\Gamma_\uparrow - \Gamma_\downarrow) + \Gamma_\uparrow\hbar\Omega \tag{3.27}$$

only contains a decay term at $T = 0$, leading to $\langle\delta E\rangle \to 0$.

We turn now to the damping term in Eq. (3.23). At first glance, it would appear to be completely quantum in origin, as it involves the *asymmetric-in-frequency* part of the noise. This latter fact is not surprising: damping involves a net absorption of energy by the noise source, and the asymmetric part of the noise directly characterizes the source's tendency to more frequently absorb rather than emit energy via transitions. In contrast, the classical picture of damping is that it results from the random force having a non-zero mean value, i.e.:

$$\langle A\cdot F(t)\rangle = -M\gamma\dot{x}(t) \tag{3.28}$$

Both these pictures of damping are of course rigorously equivalent. In both the classical and quantum cases, we can think of damping as originating from the fact that the noise source changes in response to the oscillator's motion, and hence, so does the average value of F. Quantum mechanically, we can capture this effect by simply doing perturbation theory to calculate the change in $\langle\hat{F}\rangle$ brought on by the coupling $V = A\hat{x}\hat{F}$. Working in the interaction picture, we obtain the standard equations of quantum linear response:

$$\delta\langle A\cdot\hat{F}(t)\rangle = A^2\int dt'\chi_{FF}(t-t')\langle\hat{x}(t')\rangle \tag{3.29}$$

where

$$\chi_{FF}(t) = \frac{-i}{\hbar}\theta(t)\left\langle[\hat{F}(t),\hat{F}(0)]\right\rangle \tag{3.30}$$

Keeping only the part of $\delta\langle F(t)\rangle$ responsible for dissipation (i.e. the part which is in phase with the oscillator velocity and thus out-of-phase with its position), and using the fact that the oscillator motion only involves the frequency Ω, we may write Eq. (3.29) in the familiar form of Eq. (3.28), with:

$$\gamma = \frac{2A^2x_{\rm ZPF}^2}{\hbar}\left[-{\rm Im}\chi_{FF}[\Omega]\right] = \frac{2A^2x_{\rm ZPF}^2}{\hbar}\left[-{\rm Im}\int_{-\infty}^{\infty}dt e^{i\Omega t}\chi_{FF}(t)\right] \tag{3.31}$$

[8] Note that the effective temperature can become negative if the noise source prefers emitting energy versus absorbing it; in the present case, that would lead to an instability.

Remarkably, a straightforward manipulation of Eq. (3.30) for χ_{FF} shows that this expression for γ is *exactly* equivalent to our previous expression, i.e.:

$$\gamma = \frac{2A^2 x_{\rm ZPF}^2}{\hbar}\left[-{\rm Im}\chi_{FF}[\Omega]\right] = \frac{A^2 x_{\rm ZPF}^2}{\hbar^2}\left[S_{FF}[\Omega] - S_{FF}(-\Omega)\right] \tag{3.32}$$

Thus, there are two ways of viewing damping that are both formally and physically equivalent: damping results from the response of the noise source to the oscillator's motion, or equivalently, results from the transfer of energy from the oscillator to the noise source via noise-induced transitions.

Returning to Eqs. (3.24) and (3.25), we see that we now have a new way of looking at quantum noise. The symmetric-in-frequency part of the quantum noise spectrum is analogous to classical noise, and is responsible for heating effects. In contrast, the asymmetric-in-frequency part of the quantum noise spectrum describes the dissipative response of the noise source to whatever system couples to it. We also see that a harmonic oscillator can serve as a spectrum analyzer of quantum noise–if one can measure both the heating rate P (or equivalently, the mean energy $\langle E\rangle$) and the damping rate γ, one can completely characterize the force noise spectrum at both positive and negative frequencies $\pm\Omega$. This idea was recently implemented experimentally by Naik *et al.* (2006), who used a high-Q mechanical resonator to probe both the positive and negative frequency back-action noise produced by a superconducting single-electron transistor.

Before concluding this section, we mention an important consequence of the preceding discussion: it immediately yields the quantum version of the fluctuation-dissipation theorem (Callen and Welton, 1951). As we have seen in the previous section, if our noise source is in equilibrium, the positive and negative frequency parts of the noise spectrum are strictly related to one another by the condition of detailed balance (cf. Eq. (3.14)). This in turn lets us link the classical, symmetric-in-frequency part of the noise to the damping, (i.e. the asymmetric-in-frequency part of the noise). Letting $\beta = 1/(k_{\rm B}T)$, we have:

$$\begin{aligned}
\bar{S}_{FF}[\Omega] &\equiv \frac{S_{FF}[\Omega] + S_{FF}[-\Omega]}{2} \qquad (3.33)\\
&= \frac{1}{2}(1+e^{-\beta\hbar\Omega})S_{FF}[\Omega]\\
&= \frac{1}{2}\frac{(1+e^{-\beta\hbar\Omega})}{(1-e^{-\beta\hbar\Omega})}(1-e^{-\beta\hbar\Omega})S_{FF}[\Omega]\\
&= \frac{1}{2}\coth(\beta\hbar\Omega/2)\left(S_{FF}[\Omega] - S_{FF}[-\Omega]\right)\\
&= \coth(\beta\hbar\Omega/2)\frac{\hbar\Omega M}{A^2}\gamma[\Omega] \qquad (3.34)
\end{aligned}$$

Thus, in equilibrium, the condition that noise-induced transitions obey detailed balance immediately implies that noise and damping are related to one another via the temperature. For $T \gg \hbar\Omega$, we recover the more familiar classical version of the fluctuation dissipation theorem:

$$A^2\bar{S}_{FF}[\Omega] = 2k_{\rm B}TM\gamma \tag{3.35}$$

The derivation here of the fluctuation dissipation theorem is somewhat different than the one usually presented for classical systems; there, it is the requirement that equipartition be obeyed at long times which relates noise and damping at low frequencies Here, the requirement that quantum transition rates obey detailed balance gives us a relation between noise and damping which holds at all frequencies. Further insight into the fluctuation dissipation theorem is provided in Appendix B.3, where we discuss it in the simple but instructive context of a transmission line terminated by an impedance $Z[\omega]$.

C. Practical quantum spectrum analyzers

As we have seen, a 'quantum spectrum analyzer' can in principle be constructed from a two level system (or a harmonic oscillator) in which we can separately measure the up and down transition rates between states differing by some precise energy $\hbar\omega > 0$ given by the frequency of interest. The down transition rate tells us the noise spectral density at frequency $+\omega$ and the up transition rate tells us the noise spectral density at $-\omega$. While we have already discussed experimental implementation of these ideas using two-level systems and oscillators, similar schemes have been implemented in other systems. A number of recent experiments have made use of superconductor-insulator-superconductor junctions (Billangeon *et al.*, 2006; Deblock *et al.*, 2003; Onac *et al.*, 2006b) to measure quantum noise, as the current-voltage characteristics of such junctions are very sensitive to the absorption or emission of energy (so-called photon-assisted transport processes).

In this subsection, we discuss additional methods for the detection of quantum noise. Recall from Sec. II.B that one of the most basic classical noise spectrum analyzers consists of a linear narrow band filter and a square law detector such as a diode. In what follows, we will consider a quantum treatment of such a device where we evade the tricky question of how to model a quantum diode by simply looking at the energy of the filter circuit. We then turn to various noise detection schemes making use of a photomultiplier. We will show that depending on the detection scheme used, one can measure either the symmetrized quantum noise spectral density $\bar{S}[\omega]$, or the non-symmetrized spectral density $S[\omega]$.

1. Filter plus diode

Using the simple treatment we gave of a harmonic oscillator as a quantum spectrum analyzer in Sec. III.B, one can attempt to provide a quantum treatment of the classical 'filter plus diode' spectrum analyzer discussed in Sec. II.B. This approach is due to Lesovik and Loosen

(1997) and Gavish *et al.* (2000). The analysis starts by modeling the spectrum analyzer's resonant filter circuit as a harmonic oscillator of frequency Ω weakly coupled to some equilibrium dissipative bath. The oscillator thus has an intrinsic damping rate $\gamma_0 \ll \Omega$, and is initially at a finite temperature $T_{\rm eq}$. One then drives this damped oscillator (i.e. the filter circuit) with the noisy quantum force $\hat{F}(t)$ whose spectrum at frequency Ω is to be measured.

In the classical 'filter plus diode' spectrum analyzer, the output of the filter circuit was sent to a square law detector, whose time-averaged output was then taken as the measured spectral density. To simplify the analysis, we can instead consider how the noise changes the average energy of the resonant filter circuit, taking this quantity as a proxy for the output of the diode. Sure enough, if we subject the filter circuit to purely classical noise, it would cause the average energy of the circuit $\langle E \rangle$ to increase an amount directly proportional to the classical spectrum $\mathcal{S}_{FF}[\Omega]$. We now consider $\langle E \rangle$ in the case of a quantum noise source, and ask how it relates to the quantum noise spectral density $S_{FF}[\Omega]$.

The quantum case is straightforward to analyze using the approach of Sec. III.B. Unlike the classical case, the noise will both lead to additional fluctuations of the filter circuit *and* increase its damping rate by an amount γ (c.f. Eq. (3.25)). To make things quantitative, we let $n_{\rm eq}$ denote the average number of quanta in the filter circuit prior to coupling to $\hat{F}(t)$, i.e.

$$n_{\rm eq} = \frac{1}{\exp\left(\frac{\hbar\Omega}{k_B T_{\rm eq}}\right) - 1}, \tag{3.36}$$

and let $n_{\rm eff}$ represent the Bose-Einstein factor associated with the effective temperature $T_{\rm eff}[\Omega]$ of the noise source $\hat{F}(t)$,

$$n_{\rm eff} = \frac{1}{\exp\left(\frac{\hbar\Omega}{k_B T_{\rm eff}[\Omega]}\right) - 1}. \tag{3.37}$$

One then finds (Gavish *et al.*, 2000; Lesovik and Loosen, 1997):

$$\Delta\langle E \rangle \;=\; \hbar\Omega \cdot \frac{\gamma}{\gamma_0 + \gamma}(n_{\rm eff} - n_{\rm eq}) \tag{3.38}$$

This equation has an extremely simple interpretation: the first term results from the expected heating effect of the noise, while the second term results from the noise source having increased the circuit's damping by an amount γ. Re-expressing this result in terms of the symmetric and anti-symmetric in frequency parts of the quantum noise spectral density $S_{FF}[\Omega]$, we have:

$$\Delta\langle E \rangle \;=\; \frac{\bar{S}_{FF}(\Omega) - \left(n_{\rm eq} + \frac{1}{2}\right)\left(S_{FF}[\Omega] - S_{FF}[-\Omega]\right)}{2m\left(\gamma_0 + \gamma\right)} \tag{3.39}$$

We see that $\Delta\langle E \rangle$ is in general *not* simply proportional to the symmetrized noise $\bar{S}_{FF}[\Omega]$. Thus, the 'filter plus diode' spectrum analyzer does not simply measure the the symmetrized quantum noise spectral density. We stress that there is nothing particularly quantum about this result. The extra term on the RHS of Eq. (3.39) simply reflects the fact that coupling the noise source to the filter circuit could change the damping of this circuit; this could easily happen in a completely classical setting. As long as this additional damping effect is minimal, the second term in Eq. (3.39) will be minimal, and our spectrum analyzer will (to a good approximation) measure the symmetrized noise. Quantitatively, this requires:

$$n_{\rm eff} \gg n_{\rm eq}. \tag{3.40}$$

We now see where quantum mechanics enters: if the noise to be measured is close to being zero point noise (i.e. $n_{\rm eff} \to 0$), the above condition can never be satisfied, and thus it is *impossible* to ignore the damping effect of the noise source on the filter circuit. In the zero point limit, this damping effect (i.e. second term in Eq. (3.39)) will always be greater than or equal to the expected heating effect of the noise (i.e. first term in Eq. (3.39)).

2. Filter plus photomultiplier

We now turn to quantum spectrum analyzers involving a square law detector we can accurately model– a photomultiplier. As a first example of such a system, consider a photomultiplier with a narrow band filter placed in front of it. The mean photocurrent is then given by

$$\langle I \rangle = \int_{-\infty}^{+\infty} d\omega \, |f[\omega]|^2 r[\omega] S_{\rm VV}[\omega], \tag{3.41}$$

where f is the filter (amplitude) transmission function defined previously and $r[\omega]$ is the response of the photodetector at frequency ω, and $S_{\rm VV}$ represents the electric field spectral density incident upon the photodetector. Naively one thinks of the photomultiplier as a square law detector with the square of the electric field representing the optical power. However, according to the Glauber theory of (ideal) photo-detection (Gardiner and Zoller, 2000; Glauber, 2006; Walls and Milburn, 1994), photocurrent is produced if, and only if, a photon is absorbed by the detector, liberating the initial photoelectron. Glauber describes this in terms of normal ordering of the photon operators in the electric field autocorrelation function. In our language of noise power at positive and negative frequencies, this requirement becomes simply that $r[\omega]$ vanishes for $\omega > 0$. Approximating the narrow band filter centered on frequency $\pm\omega_0$ as in Eq. (2.15), we obtain

$$\langle I \rangle = r[-\omega_0] S_{\rm VV}[-\omega_0] \tag{3.42}$$

which shows that this particular realization of a quantum spectrometer only measures electric field spectral density

at negative frequencies since the photomultiplier never emits energy into the noise source. Also one does not see in the output any 'vacuum noise' and so the output (ideally) vanishes as it should at zero temperature. Of course real photomultipliers suffer from imperfect quantum efficiencies and have non-zero dark current. Note that we have assumed here that there are no additional fluctuations associated with the filter circuit. Our result thus coincides with what we found in the previous subsection for the 'filter plus diode' spectrum analyzer (c.f. Eq. (3.39), in the limit where the filter circuit is initially at zero temperature (i.e. $n_{\rm eq} = 0$).

3. Double sideband heterodyne power spectrum

At RF and microwave frequencies, practical spectrometers often contain heterodyne stages which mix the initial frequency down to a lower IF frequency (possibly in the classical regime). Consider a system with a mixer and local oscillator at frequency $\omega_{\rm LO}$ that mixes both the upper sideband input at $\omega_{\rm u} = \omega_{\rm LO} + \omega_{\rm IF}$ and the lower sideband input at $\omega_{\rm l} = \omega_{\rm LO} - \omega_{\rm IF}$ down to frequency $\omega_{\rm IF}$. This can be achieved by having a Hamiltonian with a 3-wave mixing term which (in the rotating wave approximation) is given by

$$V = \lambda[\hat{a}_{\rm IF}\hat{a}_{\rm l}\hat{a}^\dagger_{\rm LO} + \hat{a}^\dagger_{\rm IF}\hat{a}^\dagger_{\rm l}\hat{a}_{\rm LO}] + \lambda[\hat{a}^\dagger_{\rm IF}\hat{a}_{\rm u}\hat{a}^\dagger_{\rm LO} + \hat{a}_{\rm IF}\hat{a}^\dagger_{\rm u}\hat{a}_{\rm LO}] \tag{3.43}$$

The interpretation of this term is that of a Raman process. Notice that there are two energy conserving processes that can create an IF photon which could then activate the photodetector. First, one can absorb an LO photon and *emit* two photons, one at the IF and one at the lower sideband. The second possibility is to *absorb* an upper sideband photon and create IF and LO photons. Thus we expect from this that the power in the IF channel detected by a photomultiplier would be proportional to the noise power in the following way

$$I \propto S[+\omega_{\rm l}] + S[-\omega_{\rm u}] \tag{3.44}$$

since creation of an IF photon involves the signal source either absorbing a lower sideband photon from the mixer or the signal source emitting an upper sideband photon into the mixer. In the limit of small IF frequency this expression would reduce to the symmetrized noise power

$$I \propto S[+\omega_{\rm LO}] + S[-\omega_{\rm LO}] = 2\bar{S}[\omega_{\rm LO}] \tag{3.45}$$

which is the same as for the 'classical' spectrum analyzer with a square law detector described in Sec. II.B. For equilibrium noise spectral density from a resistance R_0 derived in Appendix C we would then have

$$S_{\rm VV}[\omega] + S_{\rm VV}[-\omega] = 2R_0\hbar|\omega|[2n_{\rm B}(\hbar|\omega|) + 1], \tag{3.46}$$

Assuming our spectrum analyzer has high input impedance so that it does not load the noise source, this voltage spectrum will determine the output signal of the analyzer. This symmetrized quantity does *not* vanish at zero temperature and the output contains the vacuum noise from the input. This vacuum noise has been seen in experiment. (Schoelkopf *et al.*, 1997)

4. Single sideband heterodyne power spectrum

With proper filtering (and large enough IF frequency) one can eliminate one of the two sidebands from the input and hence have only one of the two terms in Eq.(3.44). Thus one can detect either the noise at negative frequencies, or positive frequencies, or both. For example in the driven cavity with moveable mirror discussed in Appendix D, the laser beam can be detuned to the red of the cavity by precisely the cantilever frequency. In the good cavity (resolved sideband) limit, then any photons coming out at the cavity frequency must have come from destroying a cantilever phonon and up converting a laser drive photon to the anti-Stokes sideband which resonates with the cavity. Cantilever position noise at positive frequencies generates Stokes photons but these are so far off resonance from the cavity that they are severely suppressed. Hence the total output power (excluding the laser frequency) measures only the negative frequency cantilever noise. (Note the output electric field at the cavity frequency also contains incoming vacuum noise reflected by the cavity but this does not contribute to the photon number detected by a photomultiplier.) Conversely for blue detuning, any photons must have come from creating a cantilever phonon. This measures the positive frequency cantilever position noise.

IV. QUANTUM MEASUREMENTS

Having introduced both quantum noise and quantum spectrum analyzers, we are now in a position to introduce the general topic of quantum measurements. All practical measurements are affected by noise. Certain quantum measurements remain limited by quantum noise *even though* they use completely ideal apparatus. As we will see, the limiting noise here is associated with the fact that canonically conjugate variables are incompatible observables in quantum mechanics.

The simplest, idealized description of a quantum measurement, introduced by von Neumann (Bohm, 1989; Haroche and Raimond, 2006; von Neumann, 1932; Wheeler and Zurek, 1984), postulates that the measurement process instantaneously collapses the system's quantum state onto one of the eigenstates of the observable to be measured. As a consequence, any initial superposition of these eigenstates is destroyed and the values of observables conjugate to the measured observable are perturbed. This perturbation is an intrinsic feature of quantum mechanics and cannot be avoided in any measurement scheme, be it of the "projection-type" described by von Neumann or rather a weak, continuous measure-

ment to be analyzed further below.

To form a more concrete picture of quantum measurement, we begin by noting that every quantum measurement apparatus consists of a macroscopic 'pointer' coupled to the microscopic system to be measured. (A specific model is discussed in Allahverdyan *et al.* (2001).) This pointer is sufficiently macroscopic that its position can be read out 'classically'. The interaction between the microscopic system and the pointer is arranged so that the two become strongly correlated. One of the simplest possible examples of a quantum measurement is that of the Stern-Gerlach apparatus which measures the projection of the spin of an $S = 1/2$ atom along some chosen direction. What is really measured in the experiment is the final position of the atom on the detector plate. However, the magnetic field gradient in the magnet causes this position to be perfectly correlated ('entangled') with the spin projection so that the latter can be inferred from the former. Suppose for example that the initial state of the atom is a product of a spatial wave function $\xi_0(\vec{r})$ centered on the entrance to the magnet, and a spin state which is the superposition of up and down spins corresponding to the eigenstate of $\hat{\sigma}_x$:

$$|\Psi_0\rangle = \frac{1}{\sqrt{2}} \{|\uparrow\rangle + |\downarrow\rangle\} |\xi_0\rangle. \tag{4.1}$$

After passing through a magnet with field gradient in the z direction, an atom with spin up is deflected upwards and an atom with spin down is deflected downwards. By the linearity of quantum mechanics, an atom in a spin superposition state thus ends up in a superposition of the form

$$|\Psi_1\rangle = \frac{1}{\sqrt{2}} \{|\uparrow\rangle|\xi_+\rangle + |\downarrow\rangle|\xi_-\rangle\}, \tag{4.2}$$

where $\langle\vec{r}|\xi_\pm\rangle = \psi_1(\vec{r} \pm d\hat{z})$ are spatial orbitals peaked in the plane of the detector. The deflection d is determined by the device geometry and the magnetic field gradient. The z-direction position distribution of the particle for each spin component is shown in Fig. 2. If d is sufficiently large compared to the wave packet spread then, given the position of the particle, one can unambiguously determine the distribution from which it came and hence the value of the spin projection of the atom. This is the limit of a strong 'projective' measurement.

In the initial state one has

$$\langle\Psi_0|\hat{\sigma}_x|\Psi_0\rangle = +1, \tag{4.3}$$

but in the final state one has

$$\langle\Psi_1|\hat{\sigma}_x|\Psi_1\rangle = \frac{1}{2} \{\langle\xi_-|\xi_+\rangle + \langle\xi_+|\xi_-\rangle\} \tag{4.4}$$

For sufficiently large d the states $\xi_\pm$ are orthogonal and thus the act of $\hat{\sigma}_z$ measurement destroys the spin coherence

$$\langle\Psi_1|\hat{\sigma}_x|\Psi_1\rangle \to 0. \tag{4.5}$$

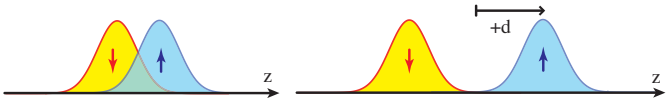

FIG. 2 (Color online) Schematic illustration of position distributions of an atom in the detector plane of a Stern-Gerlach apparatus whose field gradient is in the z direction. For small values of the displacement d (described in the text), there is significant overlap of the distributions and the spin cannot be unambiguously inferred from the position. For large values of d the spin is perfectly entangled with position and can be inferred from the position. This is the limit of strong projective measurement.

This is what we mean by projection or wave function 'collapse'. The result of measurement of the atom position will yield a random and unpredictable value of $\pm\frac{1}{2}$ for the z projection of the spin. This destruction of the coherence in the transverse spin components by a strong measurement of the longitudinal spin component is the first of many examples we will see of the Heisenberg uncertainty principle in action. Measurement of one variable destroys information about its conjugate variable. We will study several examples in which we understand microscopically how it is that the coupling to the measurement apparatus causes the 'back action' quantum noise which destroys our knowledge of the conjugate variable.

In the special case where the eigenstates of the observable we are measuring are also stationary states (i.e. energy eigenstates), measuring the observable a second time would reproduce *exactly* the same measurement result, thus providing a way to confirm the accuracy of the measurement scheme. These optimal kinds of *repeatable* measurements are called "*Quantum Non-Demolition*" (QND) measurements (Braginsky and Khalili, 1992, 1996; Braginsky *et al.*, 1980; Peres, 1993). A simple example would be a sequential pair of Stern-Gerlach devices oriented in the same direction. In the absence of stray magnetic perturbations, the second apparatus would always yield the same answer as the first. The fact that QND measurements are repeatable is of fundamental practical importance in overcoming detector inefficiencies (Gambetta *et al.*, 2007). This point is elaborated in the discussion of reaching the quantum limit in practice in Sec. VIII.

A common confusion is to think that a QND measurement has no effect on the state of the system being measured. While this is true if the initial state is an eigenstate of the observable, it is *not* true in general. Consider again our example of a spin oriented in the x direction. The result of the first $\hat{\sigma}_z$ measurement will be that the state randomly and completely unpredictably collapses onto one of the two z projection eigenstates. However all subsequent measurements using the same orientation for the detectors will always agree with the result of the first measurement. Thus QND measurements may affect the state of the system, but never the value of the observable (once it is determined). Other examples of QND

measurements include: (i) measuring the electromagnetic field energy stored inside a cavity by determining the radiation pressure exerted on a moving piston (Braginsky and Khalili, 1992), (ii) detecting the presence of a photon in a cavity by its effect on the phase of an atom's superposition state (Haroche and Raimond, 2006; Nogues *et al.*, 1999), and (iii) the "dispersive" measurement of a qubit state by its effect on the phase shift of a microwave beam (Blais *et al.*, 2004; Wallraff *et al.*, 2004), which is the first canonical example we will describe below.

In contrast to the above, in non-QND measurements, the back-action of the measurement will affect the observable being studied. The canonical example we will consider below is the position measurement of a harmonic oscillator. Since the position operator does not commute with the Hamiltonian, the QND criterion is not fulfilled. Other examples of non-QND measurements include: (i) photon counting via photo-detectors that absorb the photons, (ii) continuous measurements where the observable does not commute with the Hamiltonian, thus inducing a time-dependence of the measurement result, (iii) measurements that can be repeated only after a time longer than the relaxation (mixing) time of the system.

A. Weak continuous measurements

In discussion "real" quantum measurements, another key notion to introduce is that of *weak, continuous measurements* (Braginsky and Khalili, 1992). Many measurements in practice take an extended time-interval to complete, which is much longer than the "microscopic" time scales (oscillation periods etc.) of the system. The reason may be quite simply that the coupling strength between the detector and the system cannot be made arbitrarily large, and one has to wait for the effect of the system on the detector to accumulate. For example, in our Stern-Gerlach measurement suppose that we are only able to achieve small magnetic field gradients and that consequently, the displacement d cannot be made large compared to the wave packet spread (see Fig. 2). In this case the states $\xi_\pm$ would have non-zero overlap and it would not be possible to reliably distinguish them: we thus would only have a "weak" measurement. However, by cascading together a series of such measurements and taking advantage of the fact that they are QND, we can eventually achieve an unambiguous strong projective measurement. During this process, the overlap of $\xi_\pm$ would gradually fall to zero corresponding to a smooth continuous loss of phase coherence in the transverse spin components. Only in this case of weak continuous measurements does it make sense to define a measurement rate in terms of a rate of gain of information about the variable being measured, and the corresponding dephasing rate, the rate at which information about the conjugate variable is being lost. We will see that these rates are intimately related via the Heisenberg uncertainty principle.

While strong projective measurements are often the ideal, in some cases one may intentionally desire to have a weak continuous measurement which does not drastically perturb the system. For example in doing continuous quantum feedback to control the state of a system, it may be advantageous to continuously monitor both position and momentum of a particle, accepting the fact that since these are incompatible (i.e. non-commuting) variables, we cannot determine them both precisely. There are many practical examples of weak, continuous measurement schemes. These include: (i) charge measurements, where the current through a device (e.g. quantum point contact or single-electron transistor) is modulated by the presence/absence of a nearby charge, and where it is necessary to wait for a sufficiently long time to overcome the shot noise and distinguish between the two current values, (ii) the weak dispersive qubit measurement discussed below, (iii) displacement detection of a nanomechanical beam (e.g. optically or by capacitive coupling to a charge sensor), where one looks at the two quadrature amplitudes of the signal produced at the beam's resonance frequency.

Not surprisingly, quantum noise plays a crucial role in determining the properties of a weak, continuous quantum measurement. For such measurements, noise both determines the back-action effect of the measurement on the measured system, as well as how quickly information is acquired in the measurement process. Previously we saw that a crucial feature of quantum noise is the asymmetry between positive and negative frequencies; we further saw that this corresponds to the difference between absorption and emission events. For measurements, another key aspect of quantum noise will be important: as we will discuss extensively, *quantum mechanics places constraints on the noise of any system capable of acting as a detector or amplifier.* These constraints in turn place restrictions any *weak, continuous* measurement, and lead directly to quantum limits on how well one can make such a measurement.

In the rest of this section, we give an introduction to how one describes a weak, continuous quantum measurement, considering the specific examples of using parametric coupling to a resonant cavity for QND detection of the state of a qubit and the (necessarily non-QND) detection of the position of a harmonic oscillator. In the following section (Sec. V), we derive a very general quantum mechanical constraint on the noise of any system capable of acting as a detector, and show how this constraint *directly* leads to the quantum limit on qubit detection. Finally, in Sec. VI, we will turn to the important but slightly more involved case of a quantum linear amplifier or position detector. We will show that the basic quantum noise constraint derived Sec. V again leads to a quantum limit; here, this limit is on how small one can make the added noise of a linear amplifier.

Before leaving this introductory section, it worth pointing out that the theory of weak continuous measurements is sometimes described in terms of some set

of auxiliary systems which are sequentially momentarily weakly coupled to the system being measured. (See Appendix D.) One then envisions a sequence of projective von Neumann measurements on the auxiliary variables. The weak entanglement between the system of interest and one of the auxiliary variables leads to a kind of partial collapse of the system wave function (more precisely the density matrix) which is described in mathematical terms not by projection operators, but rather by POVMs (positive operator valued measures). We will not use this and the related 'quantum trajectory' language here, but direct the reader to the literature for more information on this important approach. (Brun, 2002; Haroche and Raimond, 2006; Jordan and Korotkov, 2006; Peres, 1993)

B. Measurement with a parametrically coupled resonant cavity

A very simple yet experimentally practical example of a quantum detector consists of a resonant optical or RF cavity parametrically coupled to the system being measured. Changes in the variable being measured (e.g. the state of a qubit or the position of an oscillator) shift the cavity frequency and produce a varying phase shift in the carrier signal reflected from the cavity. This changing phase shift can be converted (via homodyne interferometry) into a changing intensity; this can then be detected using diodes or photomultipliers.

In this subsection, we will analyze weak, continuous measurements made using a parametric cavity detector; this will serve as a good introduction to the more general approaches presented in the rest of this review. The cavity system is an excellent first case to treat both because of its simplicity, and because it is capable of reaching the quantum-limit: it can be used to make a weak, continuous measurement *as well* as is allowed by quantum mechanics. This is true for both the (QND) measurement of the state of a qubit, and the (non-QND) measurement of the position of a harmonic oscillator. Complementary analyses of weak, continuous qubit measurement are given in Makhlin *et al.* (2000, 2001) (using a single-electron transistor) and in Clerk *et al.* (2003); Gurvitz (1997); Korotkov (2001b); Korotkov and Averin (2001); Pilgram and Büttiker (2002) (using a quantum point contact).

In addition to its pedagogical value, the parametric cavity detector is worth examining because of its widespread usage in experiment. One important current realization is a high-Q microwave cavity used to read out the state of a superconducting qubit (Blais *et al.*, 2004; Lupaşcu *et al.*, 2004; Duty *et al.*, 2005; Il'ichev *et al.*, 2003; Izmalkov *et al.*, 2004; Lupaşcu *et al.*, 2005; Schuster *et al.*, 2005; Sillanpää *et al.*, 2005; Wallraff *et al.*, 2004). Another class of examples are optical cavities with a mechanical degree of freedom; here, the cavity can be used for highly sensitive position measurements. Examples of such systems include those where one of the cavity mirrors is mounted on a cantilever (Arcizet *et al.*, 2006; Gigan *et al.*, 2006; Kleckner and Bouwmeester, 2006). Related systems involve a freely suspended mass (Abramovici *et al.*, 1992; Corbitt *et al.*, 2007), an optical cavity with a thin transparent membrane in the middle (Thompson *et al.*, 2008) and, more generally, an elastically deformable whispering gallery mode resonator (Schliesser *et al.*, 2006). Yet another realization of the parametric cavity detector involves a microwave cavity terminated with a DC SQUID, with part of the SQUID loop is a doubly-clamped beam (Blencowe and Buks, 2007); here, the system acts as a position detector.

The cavity uses interference and the *wave* nature of light to convert the input signal to a phase shifted wave. For small phase shifts we have a weak continuous measurement. Interestingly, it is the complementary *particle* nature of light which turns out to be thing which limits the measurement. As we will see, it both limits rate at which we can make a measurement (via photon shot noise in the output beam) and also controls the back action disturbance of the system being measured (due to photon shot noise inside the cavity acting on the system being measured). These two dual aspects are an important part of any weak, continuous quantum measurement; hence, understanding the output noise and back-action noise of detectors will be crucial. The question of reaching the quantum limit in practical measurements will be discussed in Sec. VIII. For now we simply note that, if the secondary amplifiers and detectors are not quiet enough for the output noise to be dominated by photon shot noise and the coupling to the system is not strong enough to see the back action noise, then the measurement cannot be quantum limited.

All of our discussion of measurement imprecision and back action noise in the cavity system will be framed in terms of the number phase uncertainty relation for coherent states, derived in detail in Appendix G. A coherent photon state contains a Poisson distribution of the number of photons. Thus if the mean number of photons is $\bar{N}$, the fluctuations in the number obey

$$(\Delta N)^2 = \bar{N}. \tag{4.6}$$

Coherent states are over complete and states of different phase are not orthogonal to each other. As shown in Appendix G this means that there is an uncertainty in any measurement of the phase given by

$$(\Delta\theta)^2 = \frac{1}{4\bar{N}}. \tag{4.7}$$

(Equivalently, any homodyne measurement of the phase of the beam is subject to photon shot noise which leads to the same phase uncertainty.) Thus coherent states obey the number-phase uncertainty relation

$$\Delta N \Delta\theta = \frac{1}{2} \tag{4.8}$$

analogous to the position momentum uncertainty relation.

We now consider the equivalent of this statement in terms of noise spectral densities associated with the measurement. Consider a continuous photon beam carrying an average photon flux $\overline{\dot{N}}$. As explained in Appendix A, the variance in the number of photons detected grows linearly in time and can be represented in terms of the photon shot noise spectral density

$$(\Delta N)^2 = S_{\dot{N}\dot{N}} t. \tag{4.9}$$

Here, $S_{\dot{N}\dot{N}}$ represents the spectral density of photon-flux fluctuations. It is white, and on a physical level, describes photon shot noise:

$$S_{\dot{N}\dot{N}} = \overline{\dot{N}}. \tag{4.10}$$

In the parametric cavity detector, one needs to readout the phase of the beam reflected from the cavity; it is this phase which contains information on the system being measured. As described in Appendix G, homodyne measurement of this phase is subject to the same photon shot noise fluctuations discussed above. Thus, if the phase of the beam has some nominal small value θ_0, the output signal from the homodyne detector integrated up to time t will be of the form

$$I = \theta_0 t + \int_0^t d\tau\, \delta\theta(\tau) \tag{4.11}$$

where $\delta\theta$ is a noise representing the imprecision in our measurement of θ_0 due to the photon shot noise in the output of the homodyne detector. An unbiased estimate of the phase is

$$\theta = \frac{I}{t}, \tag{4.12}$$

which obeys

$$\langle\theta\rangle = \theta_0 \tag{4.13}$$

and from the results of Appendix A

$$(\Delta\theta)^2 = \frac{S_{\theta\theta}}{t}, \tag{4.14}$$

where $S_{\theta\theta}$ is the spectral density of the $\delta\theta$ white noise associated with the measurement imprecision. Comparison with Eq. (4.7) yields

$$S_{\theta\theta} = \frac{1}{4\overline{\dot{N}}}. \tag{4.15}$$

The larger the photon flux in the beam, the larger is the photon shot noise, but the smaller is the phase noise. We will make repeated use of the fact that the measurement imprecision can be represented in terms of a noise spectral density in this manner.

The results above lead us to the fundamental wave/particle relation for ideal coherent beams

$$S_{\dot{N}\dot{N}} S_{\theta\theta} = \frac{1}{4} \tag{4.16}$$

or in analogy with Eq. (4.8)

$$\sqrt{S_{\dot{N}\dot{N}} S_{\theta\theta}} = \frac{1}{2} \tag{4.17}$$

Before we study the role that these uncertainty relations play in measurements with high Q cavities, let us consider the simplest case of reflecting light from a mirror without a cavity. The phase shift of the beam (having wave vector k) when the mirror moves a distance x is $2kx$. Thus, the uncertainty in the phase measurement corresponds to a position imprecision which can again be represented in terms of a noise spectral density

$$S^{\rm I}_{xx} = \frac{1}{4k^2} S_{\theta\theta}. \tag{4.18}$$

Here the superscript I refers to the fact that this is noise representing imprecision in the measurement, not actual fluctuations in the position. We also need to worry about back action: each photon hitting the mirror transfers a momentum $2\hbar k$ to the mirror, so photon shot noise corresponds to a random back action force noise spectral density

$$S_{FF} = 4\hbar^2 k^2 S_{\dot{N}\dot{N}} \tag{4.19}$$

Multiplying these together we have the central result for the product of the back action force noise and the imprecision

$$S_{FF} S^{\rm I}_{xx} = \hbar^2 S_{\dot{N}\dot{N}} S_{\theta\theta} = \frac{\hbar^2}{4} \tag{4.20}$$

or in analogy with Eq. (4.8)

$$\sqrt{S_{FF} S^{\rm I}_{xx}} = \frac{\hbar}{2}. \tag{4.21}$$

Not surprisingly, the situation considered here is as ideal as possible. Thus, the RHS above is actually a *lower bound* on the product of imprecision and back-action noise for *any* detector; we will prove this rigorously in Sec. V.A. Eq. (4.21) thus represents the quantum-limit on the noise of our detector. As we will see shortly, having a detector with quantum-limited noise is a prerequisite for reaching the quantum limit on various different measurement tasks (e.g. continuous position detection of an oscillator and QND qubit state detection). Note that in general, a given detector will *not* have quantum limited noise: we will devote considerable effort in later sections to determining the necessary conditions to achieve the lower bound of Eq. (4.21) in a general detector.

We now turn to the story of measurement using a high Q cavity which will be very similar to the above, except that we have to take into account the filtering of the noise by the cavity response. As discussed in detail in Appendix D, the cavity is simply described as a single bosonic mode coupled weakly to electromagnetic modes outside the cavity. The Hamiltonian of the system is given by:

$$\hat{H} = H_0 + \hbar\omega_{\rm c}\,(1 + A\hat{z})\,\hat{a}^\dagger\hat{a} + \hat{H}_{\rm envt}. \tag{4.22}$$

Here, H_0 is the unperturbed Hamiltonian of the system whose variable $\hat{z}$ (which is not necessarily a position) is being measured, $\hat{a}$ is the annihilation operator for the cavity mode, and ω_c is the cavity resonance frequency in the absence of the coupling A. We will take both A and $\hat{z}$ to be dimensionless. The term $\hat{H}_{\rm envt}$ describes the electromagnetic modes outside the cavity, and their coupling to the cavity; it is responsible for both driving and damping the cavity mode. The damping is parameterized by rate κ, which tells us how quickly energy leaks out of the cavity; we consider the case of a high quality-factor cavity, where $Q_c \equiv \omega_c/\kappa \gg 1$.

Turning to the interaction term in Eq. (4.22), we see that the parametric coupling strength A determines the change in frequency of the cavity as the system variable $\hat{z}$ changes. We are going to consider two cases, one in which $\hat{z}$ represents the continuously varying position of a harmonic oscillator and one in which it represents the discrete state of a spin-1/2 qubit. In both cases we assume that the dynamics of $\hat{z}$ is slow compared to κ so that the cavity follows the system adiabatically. In this limit the reflected phase shift simply varies slowly in time adiabatically following the instantaneous value of $\hat{z}$. We will also assume that the coupling A is small enough that the phase shifts are always very small and hence the measurement is weak. Many photons will have to pass through the cavity before much information is gained about the value of the phase shift and hence the value of $\hat{z}$.

We first consider the case of a 'one-sided' cavity where only one of the mirrors is semi-transparent, the other being perfectly reflecting (see Fig. 3). In this case, a wave incident on the cavity (say, in a one-dimensional waveguide) will be perfectly reflected, but with a phase shift θ determined by the cavity and the value of $\hat{z}$. As shown in Appendix D, the reflection coefficient at the bare cavity frequency ω_c is simply given by (Walls and Milburn, 1994)

$$r = -\frac{1 + 2iAQ_c\hat{z}}{1 - 2iAQ_c\hat{z}}. \tag{4.23}$$

Note that r has unit magnitude because all photons which are incident are reflected if the cavity is lossless. For weak coupling we can write the reflection phase shift as

$$r = -e^{i\theta} \tag{4.24}$$

with

$$\theta \approx 4Q_cA\hat{z} = (A\omega_c)t_{\rm WD}\hat{z}. \tag{4.25}$$

We see that the scattering phase shift is simply the frequency shift caused by the parametric coupling multiplied by the Wigner delay time (Wigner, 1955)

$$t_{\rm WD} = {\rm Im}\frac{\partial \ln r}{\partial \omega} = \frac{4}{\kappa}. \tag{4.26}$$

Thus the measurement imprecision noise power for a given photon flux $\overline{\dot{N}}$ incident on the cavity is given by

$$S^{\rm I}_{zz} = \frac{1}{(A\omega_c t_{\rm WD})^2} S_{\theta\theta}. \tag{4.27}$$

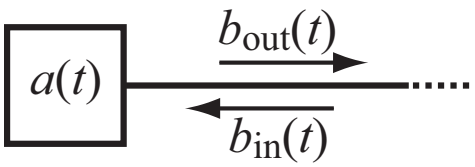

FIG. 3 Schematic of a single-sided resonant cavity with internal mode a, driven by input mode $\hat{b}_{\rm in}$ resulting in the output field $\hat{b}_{\rm out}$.

The random part of the generalized back action force conjugate to $\hat{z}$ is from Eq. (4.22)

$$\hat{F}_z \equiv -\frac{\partial \hat{H}}{\partial \hat{z}} = -A\hbar\omega_c\,\delta\hat{n} \tag{4.28}$$

where, since $\hat{z}$ is dimensionless, $\hat{F}_z$ has units of energy. Here $\delta\hat{n} = \hat{n} - \bar{n} = a^\dagger a - \langle a^\dagger a\rangle$ represents the photon number fluctuations around the mean $\bar{n}$ inside the cavity. The back action force noise spectral density is thus

$$S_{F_zF_z} = (A\hbar\omega_c)^2 S_{nn} \tag{4.29}$$

As shown in Appendix D, the cavity filters the photon shot noise so that at low frequencies $\omega \ll \kappa$ the number fluctuation spectral density is simply

$$S_{nn} = \bar{n}t_{\rm WD}. \tag{4.30}$$

The mean photon number in the cavity (also derived in the Appendix) is

$$\bar{n} = \overline{\dot{N}}t_{\rm WD} \tag{4.31}$$

where again $\overline{\dot{N}}$ the mean photon flux incident on the cavity. From this it follows that

$$S_{nn} = \overline{\dot{N}}t^2_{\rm WD} = S_{\dot{N}\dot{N}}t^2_{\rm WD} \tag{4.32}$$

and

$$S_{F_zF_z} = (A\hbar\omega_c t_{\rm WD})^2 S_{\dot{N}\dot{N}}. \tag{4.33}$$

Combining this with Eq. (4.27) again yields the same result as Eq. (4.21) obtained without the cavity. The parametric cavity detector (used in this way) is thus a quantum-limited detector: it reaches the quantum-limit on its noise spectral densities.

We will now examine how the quantum limit on the noise of our detector directly leads to quantum limits on different measurement tasks. In particular, we will consider the cases of continuous position detection and QND qubit state measurement. For the case of position

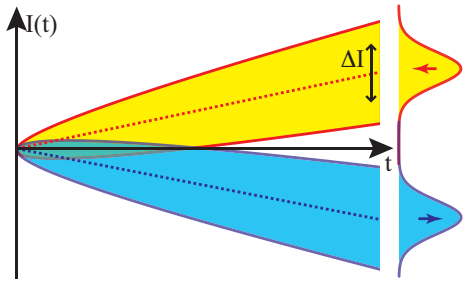

FIG. 4 (Color online) Distribution of the integrated output for the cavity detector, $I(t)$, for the two different qubit states. The separation of the means of the distributions grows linearly in time, while the width of the distributions only grow as the $\sqrt{t}$.

measurements of a mirror, the back action force from the cavity detector is simply the radiation pressure acting on the mirror (enhanced by the multiple reflections inside the cavity when $t_{\rm WD}$ is large). The position measurement case is complicated by the fact that this force will cause changes in the momentum of the mirror. The momentum kicks will in turn increase the position fluctuations over and above the naive measurement imprecision, reflecting the fact that the measurement is non-QND. We will therefore start with the simpler case of QND measurement of the state of a qubit.

1. QND measurement of the state of a qubit using a resonant cavity

Here we specialize to the case where the system operator $\hat{z} = \hat{\sigma}_z$ represents the state of a spin-1/2 quantum bit. Eq. (4.22) becomes

$$\hat{H} = \frac{1}{2}\hbar\omega_{01}\hat{\sigma}_z + +\hbar\omega_{\rm c}\left(1 + A\hat{\sigma}_z\right)\hat{a}^\dagger\hat{a} + \hat{H}_{\rm envt} \qquad (4.34)$$

We see that $\hat{\sigma}_z$ commutes with all terms in the Hamiltonian and is thus a constant of the motion (assuming that $\hat{H}_{\rm envt}$ contains no qubit decay terms so that $T_1 = \infty$) and hence the measurement will be QND. From Eq. (4.25) we see that the two states of the qubit produce phase shifts $\pm\theta_0$ where

$$\theta_0 = A\omega_{\rm c}t_{\rm WD}. \qquad (4.35)$$

As $\theta_0 \ll 1$, it will take many reflected photons before we are able to determine the state of the qubit. This is a direct consequence of the unavoidable photon shot noise in the output of the detector, and is a basic feature of weak measurements– information on the input is only acquired gradually in time.

Let $I(t)$ be the homodyne signal for the wave reflected from the cavity integrated up to time t. Depending on the state of the qubit the mean value of I will be

$$\langle I\rangle = \pm\theta_0 t, \qquad (4.36)$$

and the RMS gaussian fluctuations about the mean will be

$$\Delta I = \sqrt{S_{\theta\theta}t}. \qquad (4.37)$$

As illustrated in Fig. 4 and discussed extensively in Makhlin *et al.* (2001), the integrated signal is drawn from one of two gaussian distributions which are better and better resolved with increasing time (as long as the measurement is QND). The state of the qubit thus becomes ever more reliably determined. The signal energy to noise energy ratio becomes

$$\mathrm{SNR} = \frac{\langle I\rangle^2}{(\Delta I)^2} = \frac{\theta_0^2}{S_{\theta\theta}}t \qquad (4.38)$$

which can be used to define the measurement rate via

$$\Gamma_{\rm meas} \equiv \frac{\mathrm{SNR}}{2} = \frac{\theta_0^2}{2S_{\theta\theta}} = \frac{1}{2S^{\rm I}_{zz}}. \qquad (4.39)$$

There is a certain arbitrariness in the scale factor of 2 in the definition of the measurement rate, but this particular definition is justified on precise information theoretic grounds in Appendix E.

While Eq. (4.34) makes it clear that the state of the qubit modulates the cavity frequency, we can easily rewrite this equation to show that this same interaction term is also responsible for the *back-action* of the measurement (i.e. the disturbance of the qubit state by the measurement process):

$$\hat{H} = \frac{\hbar}{2}\left(\omega_{01} + 2A\omega_{\rm c}\hat{a}^\dagger\hat{a}\right)\hat{\sigma}_z + \hbar\omega_{\rm c}\hat{a}^\dagger\hat{a} + \hat{H}_{\rm envt} \qquad (4.40)$$

We now see that the interaction can also be viewed as providing a 'light shift' (i.e. ac Stark shift) of the qubit splitting frequency (Blais *et al.*, 2004; Schuster *et al.*, 2005) which contains a constant part $2A\bar{n}A\omega_{\rm c}$ plus a randomly fluctuating part

$$\Delta\omega_{01} = 2\hat{F}_z/\hbar \qquad (4.41)$$

which depends on $\hat{n} = \hat{a}^\dagger\hat{a}$, the number of photons in the cavity. During a measurement, $\hat{n}$ will fluctuate around its mean and act as a fluctuating back-action 'force' on the qubit. In the present QND case, noise in $\hat{n} = \hat{a}^\dagger\hat{a}$ cannot cause transitions between the two qubit eigenstates. This is the opposite of the situation considered in Sec. III.A, where we wanted to use the qubit as a spectrometer. Despite the lack of any noise-induced transitions, there still is a back-action here, as noise in $\hat{n}$ causes the effective splitting frequency of the qubit to fluctuate in time. For weak coupling, the resulting phase diffusion leads to measurement-induced dephasing of superpositions in the qubit (Blais *et al.*, 2004; Schuster *et al.*, 2005) according to

$$\left\langle e^{-i\varphi}\right\rangle = \left\langle e^{-i\int_0^t d\tau\,\Delta\omega_{01}(\tau)}\right\rangle. \qquad (4.42)$$

For weak coupling the dephasing rate is slow and thus we are interested in long times t. In this limit the integral

is a sum of a large number of statistically independent terms and thus we can take the accumulated phase to be gaussian distributed. Using the cumulant expansion we then obtain

$$\begin{aligned}\left\langle e^{-i\varphi}\right\rangle &= \exp\left(-\frac{1}{2}\left\langle\left[\int_0^t d\tau\,\Delta\omega_{01}(\tau)\right]^2\right\rangle\right)\\ &= \exp\left(-\frac{2}{\hbar^2}S_{F_zF_z}t\right).\end{aligned}\tag{4.43}$$

Notice that these integrals are precisely of the form that we encountered in the Wiener-Khinchin theorem (see Appendix A). Note also that the noise correlator above is naturally symmetrized– the quantum asymmetry of the noise plays no role for this type of coupling. Thus we identify the dephasing rate

$$\Gamma_\varphi = \frac{2}{\hbar^2}S_{F_zF_z} = 2\theta_0^2 S_{\dot{N}\dot{N}}.\tag{4.44}$$

We may now introduce the fundamental quantum limit for an ideal QND measurement: at best, one can measure as quickly as one dephases. Using Eqs. (4.39) and (4.44), we see that the cavity reaches this quantum limit:

$$\frac{\Gamma_\varphi}{\Gamma_{\rm meas}} = \frac{4}{\hbar^2}S^{\rm I}_{zz}S_{F_zF_z} = 4S_{\dot{N}\dot{N}}S_{\theta\theta} = 1.\tag{4.45}$$

As described earlier, this represents the enforcement of the Heisenberg uncertainty principle. The faster you gain information about one variable, the faster you lose information about the conjugate variable. Note that in general, the ratio $\Gamma_\varphi/\Gamma_{\rm meas}$ will be larger than one, as an arbitrary detector will not reach the quantum limit on its noise spectral densities. Such a non-ideal detector produces excess back-action beyond what is required quantum mechanically; as we shall repeatedly emphasize, this excess back-action is always associated with wasted information.

Before continuing our discussion of the quantum limit, it useful to make an additional remark about dephasing. In addition to the quantum noise point of view presented above, there is a second complementary way in which to understand the origin of measurement induced dephasing (Stern *et al.*, 1990) which is analogous to our description of loss of transverse spin coherence in the Stern-Gerlach experiment in Eq. (4.4). The measurement takes the incident wave, described by a coherent state $|\alpha\rangle$, to a reflected wave described by a (phase shifted) coherent state $|r_\uparrow\cdot\alpha\rangle$ or $|r_\downarrow\cdot\alpha\rangle$, where $r_{\uparrow/\downarrow}$ is the qubit-dependent reflection amplitude given in Eq. (4.23). Considering now the full state of the qubit plus detector, measurement results in:

$$\begin{aligned}\frac{1}{\sqrt{2}}\Big(|\uparrow\rangle+|\downarrow\rangle\Big)\otimes|\alpha\rangle \;\rightarrow\; &\frac{1}{\sqrt{2}}\Big(e^{+i\omega_{01}t/2}|\uparrow\rangle\otimes|r_\uparrow\cdot\alpha\rangle\\ &+\; e^{-i\omega_{01}t/2}|\downarrow\rangle\otimes|r_\downarrow\cdot\alpha\rangle\Big)\end{aligned}\tag{4.46}$$

As $|r_\uparrow\cdot\alpha\rangle \neq |r_\downarrow\cdot\alpha\rangle$, the qubit has become entangled with the detector: the state above cannot be written as a product of a qubit state times a detector state. To assess the coherence of the final qubit state (i.e. the relative phase between $\uparrow$ and $\downarrow$), one looks at the off-diagonal matrix element of the qubit's reduced density matrix:

$$\rho_{\downarrow\uparrow} \equiv \mathrm{Tr}_{\rm\ detector}\langle\downarrow|\psi\rangle\langle\psi|\uparrow\rangle \tag{4.47}$$

$$= \frac{e^{+i\omega_{01}t}}{2}\langle r_\uparrow\cdot\alpha|r_\downarrow\cdot\alpha\rangle \tag{4.48}$$

$$= \frac{e^{+i\omega_{01}t}}{2}\exp\left[-|\alpha|^2\left(1-r_\uparrow^* r_\downarrow\right)\right] \tag{4.49}$$

In Eq. (4.48) we have used the usual expression for the overlap of two coherent states. We see that the measurement reduces the magnitude of $\rho_{\uparrow\downarrow}$: this is dephasing. The amount of dephasing is directly related to the overlap between the different detector states that result when the qubit is up or down; this overlap can be straightforwardly found using Eq. (4.49) and $|\alpha|^2 = \bar{N} = \overline{\dot{N}}t$, where $\bar{N}$ is the mean number of photons that have reflected from the cavity after time t. We have

$$\left|\exp\left[-|\alpha|^2\left(1-r_\uparrow^* r_\downarrow\right)\right]\right| = \exp\left[-2\bar{N}\theta_0^2\right] \equiv \exp\left[-\Gamma_\varphi t\right]\tag{4.50}$$

with the dephasing rate Γ_φ being given by:

$$\Gamma_\varphi = 2\theta_0^2\overline{\dot{N}}\tag{4.51}$$

in complete agreement with the previous result in Eq.(4.44).

In closing, we note that for strong coupling (outside the regime of weak measurements), the light shift per photon can actually exceed the line width of the qubit and the qubit transition spectrum splits into a series of resolved lines which have been observed both via 'quantum revivals' in the time domain (Haroche and Raimond, 2006; Raimond *et al.*, 2001) using Rydberg atom cavity QED, and in the frequency domain (Schuster *et al.*, 2007) using superconducting circuit QED.

2. Quantum limit relation for QND qubit state detection

We now return to the quantum limit relation of Eq. (4.45). We have described the weak, continuous QND measurement of a qubit by a cavity with two rates: $\Gamma_{\rm meas}$, which tells us how quickly information is acquired, and Γ_φ, which tells us how quickly the back-action of the measurement decoheres a superposition. As we saw above, these rates are not completely independent: quantum mechanics enforces the constraint that *the best you can possibly do is measure as quickly as you dephase* (Averin, 2003; Clerk *et al.*, 2003; Devoret and Schoelkopf, 2000; Korotkov and Averin, 2001; Makhlin *et al.*, 2001):

$$\Gamma_{\rm meas} \leq \Gamma_\varphi\tag{4.52}$$

A quantum limited detector (such as the ideal cavity measurement described above) is one which has an equality above; in general, most detectors are very far from

this ideal limit, and dephase the qubit much faster than they acquire information about its state. We will give a rigorous proof of Eq. (4.52) in Sec. V.B; for now, we note that its heuristic origin rests on the fact that both measurement and dephasing rely on the qubit becoming entangled with the detector. Consider again Eq. (4.46), describing the evolution of the qubit-detector system when the qubit is initially in a superposition of $\uparrow$ and $\downarrow$. To say that we have truly measured the qubit, the two detector states $|r_\uparrow \alpha\rangle$ and $|r_\downarrow \alpha\rangle$ need to correspond to different values of the detector output (i.e. phase shift θ in our example); this necessarily implies they are orthogonal. This in turn implies that the qubit is completely dephased: $\rho_{\uparrow\downarrow} = 0$, just as we saw in Eq. (4.5) in the Stern-Gerlach example. Thus, *measurement implies dephasing*. The opposite is not true. The two states $|r_\uparrow \alpha\rangle$ and $|r_\downarrow \alpha\rangle$ could in principle be orthogonal without their corresponding to different values of the detector output (i.e. θ). For example, the qubit may have become entangled with extraneous microscopic degrees of freedom in the detector. Thus, on a heuristic level, the origin of Eq. (4.52) is clear.

Returning to our one-sided cavity system, we see from Eq. (4.45) that the one-sided cavity detector reaches the quantum limit. It is natural to now ask *why* this is the case: is there a general principle in action here which allows the one-sided cavity to reach the quantum limit? The answer is yes: *reaching the quantum limit requires that there is no 'wasted' information in the detector* (Clerk *et al.*, 2003). There should not exist any unmeasured quantity in the detector which could have been probed to learn more about the state of the qubit. In the single-sided cavity detector, information on the state of the qubit is *only* available in (that is, is entirely encoded in) the phase shift of the reflected beam; thus, there is no 'wasted' information, and the detector does indeed reach the quantum limit. This principle of 'no wasted information' is discussed extensively in Clerk *et al.* (2003), and we will expand on it in what follows.

We now consider a simple variant of the single-sided cavity detector which fails to reach the quantum limit precisely due to 'wasted' information. Consider a one-dimensional cavity system where *both* mirrors are slightly transparent. Now, a wave incident at frequency $\omega_{\rm R}$ on one end of the cavity will be partially reflected and partially transmitted; if the initial incident wave is described by a coherent state $|\alpha\rangle$, the scattered state can be described by a tensor product of the reflected wave's state and the transmitted wave's state:

$$|\alpha\rangle \rightarrow |r_\sigma \cdot \alpha\rangle |t_\sigma \cdot \alpha\rangle \tag{4.53}$$

where the qubit-dependent reflection and transmission amplitudes r_σ and t_σ are given by (Walls and Milburn, 1994):

$$t_\downarrow = \frac{1}{1+2iAQ_{\rm c}} \tag{4.54}$$

$$r_\downarrow = \frac{2iQ_{\rm c}A}{1+2iAQ_{\rm c}} \tag{4.55}$$

$$\tag{4.56}$$

with $t_\uparrow = (t_\downarrow)^*$ and $r_\uparrow = (r_\downarrow)^*$. Note that the incident beam is almost perfectly transmitted: $|t_\sigma|^2 = 1 - O(AQ_{\rm c})^2$.

Similar to the one-sided case, the two-sided cavity could be used to make a measurement by monitoring the phase of the transmitted wave. Using the expression for t_σ above, we find that the qubit-dependent transmission phase shift is given by:

$$\tilde{\theta}_{\uparrow/\downarrow} = \pm\tilde{\theta}_0 = \pm 2AQ_{\rm c} \tag{4.57}$$

where again the two signs correspond to the two different qubit eigenstates. The phase shift for transmission is only half as large as in reflection so the Wigner delay time associated with transmission is

$$\tilde{t}_{\rm WD} = \frac{2}{\kappa}. \tag{4.58}$$

Upon making the substitution of $\tilde{t}_{\rm WD}$ for $t_{\rm WD}$, the one-sided cavity Eqs. (4.24-4.29) and Eq. (4.24) remain valid. However the internal cavity photon number shot noise remains fixed so that Eq. (4.30) becomes

$$S_{nn} = 2\bar{n}\tilde{t}_{\rm WD}. \tag{4.59}$$

which means that

$$S_{nn} = 2\overline{\dot{N}}\tilde{t}^2_{\rm WD} = 2S_{\dot{N}\dot{N}}\tilde{t}^2_{\rm WD} \tag{4.60}$$

and

$$S_{F_zF_z} = 2\hbar^2 A^2 \omega_{\rm c}^2 \tilde{t}^2_{\rm WD} S_{\dot{N}\dot{N}}. \tag{4.61}$$

As a result the back action dephasing doubles relative to the measurement rate and we have

$$\frac{\Gamma_{\rm meas}}{\Gamma_\varphi} = 2S_{\dot{N}\dot{N}}S_{\theta\theta} = \frac{1}{2}. \tag{4.62}$$

Thus the two-sided cavity fails to reach the quantum limit by a factor of 2.

Using the entanglement picture, we may again alternatively calculate the amount of dephasing from the overlap between the detector states corresponding to the qubit states $\uparrow$ and $\downarrow$ (cf. Eq. (4.48)). We find:

$$e^{-\Gamma_\varphi t} = \left|\langle t_\uparrow\alpha|t_\downarrow\alpha\rangle\langle r_\uparrow\alpha|r_\downarrow\alpha\rangle\right| \tag{4.63}$$

$$= \exp\left[-|\alpha|^2\left(1-(t_\uparrow)^*t_\downarrow-(r_\uparrow)^*r_\downarrow\right)\right] \tag{4.64}$$

Note that *both* the change in the transmission and reflection amplitudes contribute to the dephasing of the qubit. Using the expressions above, we find:

$$\Gamma_\varphi t = 4(\tilde{\theta}_0)^2|\alpha|^2 = 4(\tilde{\theta}_0)^2\bar{N} = 4(\tilde{\theta}_0)^2\overline{\dot{N}}t = 2\Gamma_{\rm meas}t. \tag{4.65}$$

We thus find that measurement-induced dephasing rate is twice as large as the measurement rate: the two sided cavity misses the quantum limit by a factor of two in agreement with our quantum noise result that the back action noise is doubled.

Why does the two-sided cavity fail to reach the quantum limit? The answer is clear from Eq. (4.64): even though we are not monitoring it, there is information on the state of the qubit available in the phase of the reflected wave. Note from Eq. (4.55) that the magnitude of the reflected wave is weak ($\propto A^2$), but (unlike the transmitted wave) the difference in the reflection phase associated with the two qubit states is large ($\pm\pi/2$). The 'missing information' in the reflected beam makes a direct contribution to the dephasing rate (i.e. the second term in Eq. (4.64)), making it larger than the measurement rate associated with measurement of the transmission phase shift. In fact, there is an equal amount of information in the reflected beam as in the transmitted beam, so the dephasing rate is doubled.

We note in closing that it is often technically easier to work in transmission rather than reflection. One can show however that one may still reach the quantum limit in transmission by using an asymmetric cavity in which the input mirror has much less transmission than the output mirror. Most photons are reflected at the input, but those that enter the cavity will almost certainly be transmitted. The price to be made is that the input carrier power must be increased.

In summary, we see the departure from the quantum limit here can be directly traced to "wasted" information in the detector. This idea holds up for a number of very different systems: in Clerk *et al.* (2003), it was discussed in the context of mesoscopic scattering detectors (i.e. a generalized quantum point-contact detector), while in Appendix H, we consider the role of information in the important case of a Mach-Zehnder-interferometer detector.

3. Measurement of oscillator position using a resonant cavity

In the previous subsections, we studied how a resonant cavity could be used to make a QND measurement of the state of a qubit. We found that the photon shot noise in the output beam limited the precision with which the cavity phase shift could be determined; it thus set the measurement rate. We also found that fluctuations in the cavity photon number produced a random light shift of the qubit's energy splitting, causing dephasing. This example of measurement back action causing dephasing is the simplest possible one because the measurement is QND: the back-action does not affect the observable being measured. The measurement is repeatable precisely because the back action noise only affects the relative phase of the superposition of the two qubit states, but causes no transitions between them.

In this subsection we consider the simplest example of a non-QND measurement, namely the weak continuous measurement of the position of a harmonic oscillator. As a detector, we again use a parametrically-coupled resonant cavity, where the position of the oscillator x changes the frequency of the cavity as per Eq. (4.22) (see, e.g., Tittonen *et al.* (1999)). Similar to the qubit case, for a sufficiently weak coupling the phase shift of the reflected beam from the cavity will depend linearly on the position x of the oscillator (c.f. Eq. (4.25)); by reading out this phase, we may thus measure x. The back action noise is the same as before, namely photon shot noise in the cavity. Now however this represents a random force which changes the momentum of the oscillator. During the subsequent time evolution these random force perturbations will reappear as random fluctuations in the position. Thus the measurement is *not* QND. This will mean that the minimum uncertainty of even an ideal measurement is larger (by exactly a factor of 2) than the 'true' quantum uncertainty of the position (i.e. the ground state uncertainty). We will see later that this is an example of a general principle that a linear 'phase-preserving' amplifier necessarily adds noise, and that the minimum added noise exactly doubles the output noise for the case where the input is vacuum (i.e. zero-point) noise.

In this subsection we will present a highly simplified and heuristic discussion of the standard quantum limit for position measurement which will convey the essential ideas. A more general and complete discussion of the quantum limit on amplifiers and position detectors will be presented in Sec. VI.

Before proceeding, it is worthwhile to make some preliminary points. First, note that we are speaking here of a *weak* continuous measurement of the oscillator position. The measurement is sufficiently weak that the position undergoes many cycles of oscillation before significant information is acquired. Thus we are not talking about the instantaneous position but rather the overall amplitude and phase, or more precisely the two quadrature amplitudes describing the smooth envelope of the motion,

$$\hat{x}(t) = \hat{X}\cos(\Omega t) + \hat{Y}\sin(\Omega t). \tag{4.66}$$

Comparison with Eq. (2.18) shows that the two quadrature amplitudes $\hat{X}$ and $\hat{Y}$ are canonically conjugate and hence do not commute with each other

$$[\hat{X}, \hat{Y}] = \frac{i\hbar}{M\Omega} = 2ix_{\rm ZPF}^2. \tag{4.67}$$

Because the measurement is weak, we are effectively trying to measure two incompatible observables simultaneously. This is also intimately related to the necessity of overall measurement uncertainty mentioned above.

It is also worth emphasizing that the quantum limit on continuous position detection is a very different kind of constraint than that on QND qubit state detection. In the latter case, the quantum limit did not limit the accuracy with which we could measure the state of the qubit. The quantum limit simply set a minimum on the

magnitude of the back-action dephasing; as the measurement is QND, the size of this back-action had no effect on the measurement accuracy. We also found that the precise value of the coupling strength to the detector was not important: if the coupling is made weaker, it takes longer to make the measurement, but since it is QND, this does not matter (assuming the qubit has no intrinsic decay mechanisms). In contrast, for position measurements, back-action does affect the quantity being measured, and thus the quantum limit does indeed place a limit on the accuracy of the measurement. We will also see that in order to achieve the minimum uncertainty (to be defined below), one must adjust the coupling strength to an optimal value. If the coupling is too weak, the phase shift of the cavity is so small that the imprecision of the measurement is dominated by photon shot noise in the output. If the coupling is too strong, the back action noise perturbs the oscillator so strongly that the position uncertainty increases beyond the minimum.

We are now ready to start our heuristic analysis of position detection using a cavity detector; further details and more rigorous formal analysis are presented in Appendix D.3. Consider first the mechanical oscillator we wish to measure. We take it to be a simple harmonic oscillator of natural frequency Ω and mechanical damping rate γ_0. For weak damping, and at zero coupling to the detector, the spectral density of the oscillator's position fluctuations is given by Eq. (2.27) with the delta function replaced by a Lorentzian[9]

$$S_{xx}[\omega] = x_{\rm ZPF}^2 \Bigg\{ n_{\rm B}(\hbar\Omega) \frac{\gamma_0}{(\omega+\Omega)^2 + (\gamma_0/2)^2} + [n_{\rm B}(\hbar\Omega)+1] \frac{\gamma_0}{(\omega-\Omega)^2+(\gamma_0/2)^2} \Bigg\}. \quad (4.68)$$

When we now weakly couple the oscillator to the cavity (as per Eq. (4.22), with $\hat{z} = \hat{x}/x_{\rm ZPF}$) and drive the cavity on resonance, the phase shift θ of the reflected beam will be proportional to x (i.e. $\delta\theta(t) = [d\theta/dx]\cdot x(t)$). As such, the oscillator's position fluctuations will cause additional fluctuations of the phase θ, over and above the intrinsic shot-noise induced phase fluctuations $S_{\theta\theta}$. We consider the usual case where the noise spectrometer being used to measure the noise in θ (i.e. the noise in the homodyne current) measures the symmetric-in-frequency noise spectral density; as such, it is the symmetric-in-frequency position noise that we will detect. In the classical limit $k_{\rm B}T \gg \hbar\Omega$, this is just given by:

$$\bar{S}_{xx}[\omega] \equiv \frac{1}{2}\left(S_{xx}[\omega] + S_{xx}[-\omega]\right) \approx \frac{k_{\rm B}T}{2M\Omega^2} \frac{\gamma_0}{(|\omega|-\Omega)^2 + (\gamma_0/2)^2} \quad (4.69)$$

where as always, we have chosen to define the symmetrized spectral density as the average of the spectral densities at positive and negative frequencies. This is in contrast to the convention used in engineering contexts, where one simply takes the sum of the two spectral densities. If we ignore back-action effects, we expect to see this Lorentzian profile riding on top of the background imprecision noise floor; this is illustrated in Fig. 5.

Note that additional stages of amplification would also add noise, and would thus further augment this background noise floor. If we subtract off this noise floor, the FWHM of the curve will give the damping parameter γ_0, and the area under the experimental curve

$$\int_{-\infty}^{\infty} \frac{d\omega}{2\pi} \bar{S}_{xx}[\omega] = \frac{k_{\rm B}T}{M\Omega^2} \quad (4.70)$$

measures the temperature. What the experimentalist actually plots in making such a curve is the output of the entire detector-plus-following-amplifier chain. Importantly, if the temperature is known, then the area of the measured curve can be used to calibrate the coupling of the detector and the gain of the total overall amplifier chain (see, e.g., Flowers-Jacobs *et al.*, 2007; LaHaye *et al.*, 2004). One can thus make a calibrated plot where the measured output noise is referred back to the oscillator position. Such a plot also calibrates the background noise floor in terms of an effective oscillator temperature: this is related to the detector's "noise temperature" (a quantity to be discussed further in Sec. VI.D).

At zero temperature, Eq. (4.68) yields for the symmetrized noise spectral density

$$\bar{S}^0_{xx}[\omega] = x_{\rm ZPF}^2 \frac{\gamma_0/2}{(|\omega|-\Omega)^2 + (\gamma_0/2)^2}. \quad (4.71)$$

One might expect that one could see this Lorentzian directly in the output noise of the detector (i.e. the θ noise), sitting above the measurement-imprecision noise floor. However, this neglects the effects of measurement back action. From the classical equation of motion

$$\ddot{x} = -\Omega^2 x - \gamma_0 \dot{x} + \frac{F}{M} \quad (4.72)$$

(where $F = F_z$), we expect the response of the oscillator to the back action force F at frequency ω produces an additional displacement

$$\delta x[\omega] = \chi_{xx}[\omega] F[\omega] \quad (4.73)$$

where $\chi_{xx}[\omega]$ is the mechanical susceptibility

$$\chi_{xx}[\omega] \equiv \frac{1}{M} \frac{1}{\Omega^2 - \omega^2 - i\gamma_0\omega}. \quad (4.74)$$

[9] This form is valid only for weak damping because we are assuming that the oscillator frequency is still sharply defined. We have evaluated the Bose-Einstein factor exactly at frequency Ω and we have assumed that the Lorentzian centered at positive (negative) frequency has negligible weight at negative (positive) frequencies.

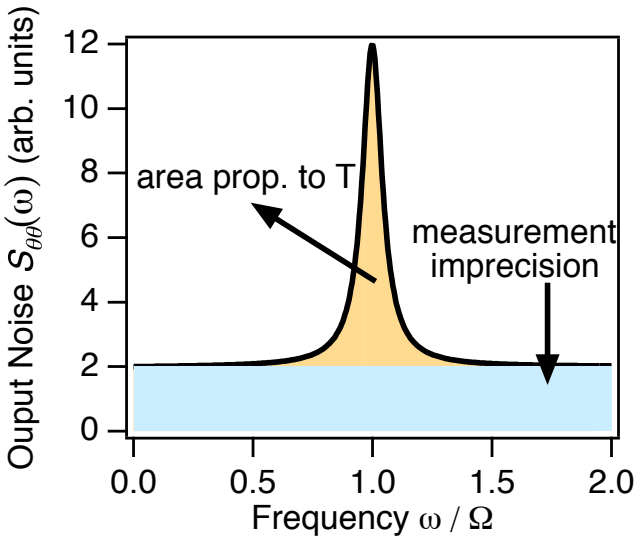

FIG. 5 (Color online) Spectral density of the (symmetrized) output noise $S_{\theta\theta}[\omega]$ of a linear position detector. The oscillator's noise appears as a Lorentzian sitting above a noise floor (i.e. the measurement imprecision). As discussed in the text, the width of the peak is proportional to the oscillator damping rate γ_0, while the area under the peak is proportional to temperature. This latter fact can be used to calibrate the response of the detector.

These extra oscillator fluctuations will show up as additional fluctuations in the output of the detector (i.e. the phase shift θ). For simplicity, let us focus on this noise at the oscillator's resonance frequency Ω. As a result of the detector's back-action, the total measured position noise (i.e. inferred spectral density) at the frequency Ω is given by:

$$\begin{aligned}\bar{S}_{xx,\mathrm{tot}}[\Omega] &= \bar{S}^0_{xx}[\Omega] + \frac{|\chi_{xx}[\Omega]|^2}{2}\left[S_{FF}[+\Omega] + S_{FF}[-\Omega]\right] \\ &+ \frac{1}{2}\left[S^{\mathrm{I}}_{xx}[+\Omega] + S^{\mathrm{I}}_{xx}[-\Omega]\right] \qquad (4.75)\\ &= \bar{S}^0_{xx}[\Omega] + \bar{S}_{xx,\mathrm{add}}[\Omega] \qquad (4.76)\end{aligned}$$

The first term here is just the intrinsic zero-point noise of the oscillator:

$$\bar{S}^0_{xx}[\Omega] = \frac{2x^2_{\mathrm{ZPF}}}{\gamma_0} = \hbar|\chi_{xx}[\Omega]|. \qquad (4.77)$$

The second term $\bar{S}_{xx,\mathrm{add}}$ is the total noise added by the measurement, and includes *both* the measurement imprecision $S^{\mathrm{I}}_{xx} \equiv S^{\mathrm{I}}_{zz}x^2_{\mathrm{ZPF}}$ and the extra fluctuations caused by the back action. We stress that $\bar{S}_{xx,\mathrm{tot}}$ corresponds to a position noise spectral density *inferred* from the output of the detector: one simply scales the spectral density of total output fluctuations $\bar{S}_{\theta\theta,\mathrm{tot}}[\Omega]$ by $(d\theta/dx)^2$.

Implicit in Eq. (4.77) is the assumption that the back action noise and the imprecision noise are uncorrelated and thus add in quadrature. It is not obvious that this is correct, since in the case of position measurement using parametric coupling to a cavity, the back action noise and output shot noise are both caused by the vacuum noise in the beam incident on the cavity. It turns out there are indeed correlations, however the *symmetrized* (i.e. 'classical') correlator $\bar{S}_{\theta F}$ does vanish under the right conditions; we will show this in detail for this particular system in Appendix D and discuss it more generally in Sec. V. Further, Eq. (4.75) assumes that the measurement does not change the damping rate of the oscillator. One can show that this is indeed the case when the cavity is illuminated at its optical resonance, as in this case the back-action force's quantum noise spectral density is symmetric in frequency (see Appendix D). The back-action force thus does not result in any additional measurement-induced damping of the oscillator (c.f. Eq. (3.32)). Note that this is a special situation: for a generic detector, detector back-action will change the total damping of the oscillator (and in fact can heat or cool the oscillator, depending on the setup); we will discuss this further in Sec. VI.D.

Assuming we have a quantum limited detector that obeys Eq. (4.20) (i.e. $S^{\mathrm{I}}_{xx}S_{FF} = \hbar^2/4$) and that the shot noise is symmetric in frequency, the added position noise spectral density at resonance (i.e. second term in Eq. (4.76)) becomes:

$$\bar{S}_{xx,\mathrm{add}}[\Omega] = \left[|\chi[\Omega]|^2 S_{FF} + \frac{\hbar^2}{4}\frac{1}{S_{FF}}\right]. \qquad (4.78)$$

Recall from Eq. (4.33) that the back action noise is proportional to the coupling of the oscillator to the detector and to the intensity of the drive on the cavity. The added position uncertainty noise is plotted in Fig. 6 as a function of S_{FF}. We see that for high drive intensity, the back action noise dominates the position uncertainty, while for low drive intensity, the output shot noise (the last term in the equation above) dominates.

The added noise (and hence the total noise $\bar{S}_{xx,\mathrm{tot}}[\Omega]$) is minimized when S_{FF} is tuned to be equal to $S_{FF,\mathrm{opt}}$, with:

$$S_{FF,\mathrm{opt}} = \frac{\hbar}{2|\chi_{xx}[\Omega]|} = \frac{\hbar}{2}M\Omega\gamma_0. \qquad (4.79)$$

We see that the more heavily damped is the oscillator, the less susceptible it is to back action noise and hence the higher is the optimal coupling. At the optimal point

$$\bar{S}_{xx,\mathrm{add}}[\Omega] = \frac{\hbar}{M\Omega\gamma_0} = \bar{S}^0_{xx}[\Omega] \qquad (4.80)$$

Thus, the spectral density of the added position noise is *exactly* equal to the noise power associated with the oscillator's zero-point fluctuations. This represents a *minimum* value for the added noise of any linear position detector, and is referred to as the standard quantum limit on position detection [CITE]. Note that this limit only involves the added noise of the detector, and thus has

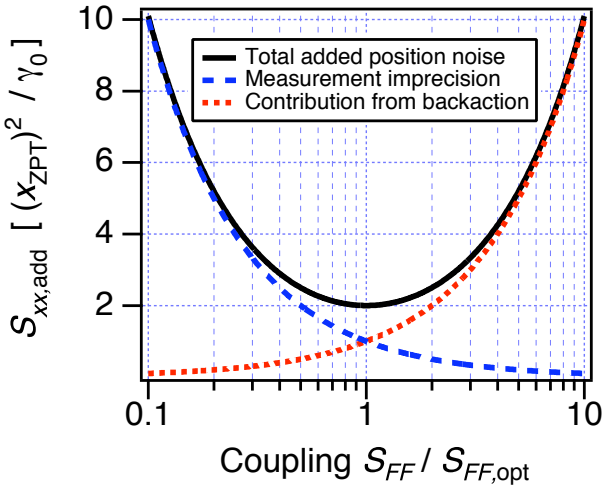

FIG. 6 (Color online) Noise power of the added position noise of a linear position detector, evaluated at the oscillator's resonance frequency ($\bar{S}_{xx,\mathrm{add}}[\Omega]$), as a function of the magnitude of the back-action noise spectral density S_{FF}. S_{FF} is proportional to the oscillator-detector coupling, and in the case of the cavity detector, is also proportional to the power incident on the cavity. The optimal value of S_{FF} is given by $S_{FF,\mathrm{opt}} = \hbar M\Omega\gamma_0/2$ (c.f. Eq. (4.79)). We have assumed that there are no correlations between measurement imprecision noise and back-action noise, as is appropriate for the cavity detector.

nothing to do with the initial temperature of the oscillator. We again emphasize that in order to reach this quantum limit, the detector must be quantum limited: one needs the product $S_{FF}S^{\mathrm{I}}_{xx}$ to be as small as is allowed by quantum mechanics (i.e. $\hbar^2/4$). In addition, the measured output noise must be dominated by the output noise of the cavity, not by the added noise of following amplifier stages. Finally, one must also be able to achieve sufficiently strong coupling to reach the optimum given in Eq. (4.79). Note that at this optimal coupling, the measurement imprecision noise and back-action noise each make equal contributions to the total measured position uncertainty $\bar{S}_{xx,\mathrm{tot}}$. A related, stronger quantum limit refers to the *total* inferred position noise from the measurement, $\bar{S}_{xx,\mathrm{tot}}[\omega]$. It follows from Eq. (4.80) that at resonance, the smallest this can be is *twice* the oscillator's zero point noise:

$$\bar{S}_{xx,\mathrm{tot}}[\Omega] = 2\bar{S}^0_{xx}[\Omega]. \tag{4.81}$$

Half the noise here is from the oscillator itself, half is from the added noise of the detector. Reaching this quantum limit is even more challenging: one needs both to reach the quantum limit on the added noise *and* cool the oscillator to its ground state. Note that recent experiments in quantum nanomechanics have come very close to reaching the quantum limit on the added noise, but have been less close in reaching the limit on the total measured position noise. See Appendix VIII for further discussion of practical issues relevant to reaching the quantum limit. the minimum (symmetrized) noise power (at the resonance frequency) is twice the vacuum value– the added noise from the measurement is precisely equal is the so called 'standard quantum limit' for position measurement uncertainty.

Finally, we emphasize that the optimal value of the coupling derived above was specific to the choice of minimizing the total position noise power at the resonance frequency. If a different frequency had been chosen, the optimal coupling would have been different; one again finds that the minimum possible added noise corresponds to the ground state noise at that frequency. It is useful to ask what the total position noise would be as a function of frequency, assuming that the coupling has been optimized to minimize the noise at the resonance frequency, and that the oscillator is initially in the ground state. From our results above we have

$$\begin{aligned}
&\bar{S}_{xx,\mathrm{tot}}[\omega] \\
&= x^2_{\mathrm{ZPF}}\frac{\gamma_0/2}{(|\omega|-\Omega)^2+(\gamma_0/2)^2} + \frac{\hbar}{2}\left[\frac{|\chi_{xx}[\omega]|^2}{|\chi_{xx}[\Omega]|} + |\chi_{xx}[\Omega]|\right] \\
&\approx \frac{x^2_{\mathrm{ZPF}}}{\gamma_0}\left\{1+3\frac{(\gamma_0/2)^2}{(|\omega|-\Omega)^2+(\gamma_0/2)^2}\right\}
\end{aligned} \tag{4.82}$$

which is plotted in Fig. 7. Assuming that the detector is quantum limited, one sees that the Lorentzian peak rises above the constant background by a factor of three when the coupling is optimized to minimize the total noise power at resonance. This factor of three has a simple interpretation. Recall that if we optimize the coupling to reach the quantum limit at resonance, the total added noise due to the detector (back-action and imprecision) is equal to the oscillator's zero-point noise. For an optimized coupling, back-action and imprecision make equal contributions to the total added noise; this implies that back-action noise heats the oscillator from zero temperature so as to increase its position variance by precisely a factor 3/2. It also implies that the background measurement imprecision has (at resonance) a value equal to 1/2 the oscillator's zero-point noise. This then yields a peak-to-floor ratio of 3. Note the same maximum ratio is obtained when one tries to detect coherent qubit rotations from the noise of a linear detector which is transversely coupled to the qubit (Korotkov and Averin, 2001); this is also a non-QND situation.

In Table II, we give a summary of recent experiments which approach the quantum limit on weak, continuous position detector of a mechanical resonator. Note that in many of these experiments, the effects of detector back-action were not seen. This could either be the result of too low of a detector-oscillator coupling, or due to the presence of excessive thermal noise. As we have shown, the back-action force noise serves to slightly heat the oscillator. If it is already at an elevated temperature due to thermal noise, this additional heating can be very hard to resolve.

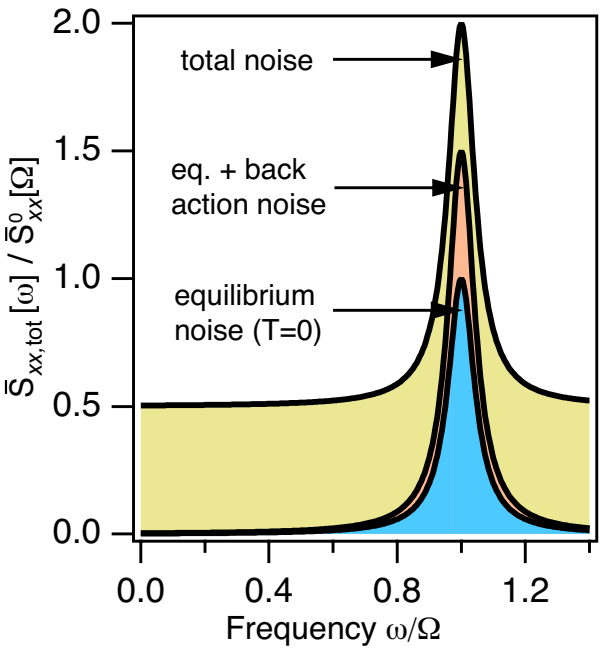

FIG. 7 (Color online) Spectral density of measured position fluctuations of a harmonic oscillator, $\bar{S}_{xx,\mathrm{tot}}[\omega]$, as a function of frequency ω, for a detector which reaches the quantum limit at the oscillator frequency Ω. We have assumed that without the coupling to the detector, the oscillator would be in its ground state. The y-axis has been normalized by the zero-point position-noise spectral density $\bar{S}^0_{xx}[\omega]$, evaluated at $\omega = \Omega$. One clearly sees that the total noise at Ω is twice the zero-point value, and that the peak of the Lorentzian rises a factor of three above the background. This background represents the measurement-imprecision, and is equal to $1/2$ of $\bar{S}^0_{xx}(\Omega)$.

In closing, we stress that this subsection has given only a very rudimentary introduction to the quantum limit on position detection. A complete discussion which treats the important topics of back-action damping, effective temperature, noise cross-correlation and power gain is given in Sec. VI.D.

V. GENERAL LINEAR RESPONSE THEORY

A. Quantum constraints on noise

In the previous section, we introduced the basic language and concepts used to describe weak, continuous quantum measurements. We also gave a heuristic discussion of how quantum constraints on the noise properties of a detector lead to quantum limits on various measurement tasks, focusing on the particular case of a resonant-cavity detector. In this section, we will develop this connection between quantum limits and noise further and in a more general manner. As before, we will emphasize the idea that reaching the quantum limit requires a detector having "quantum-ideal" noise properties. The approach here is different from typical treatments in the quantum optics literature (Gardiner and Zoller, 2000; Haus, 2000), and uses nothing more than features of quantum linear response. Our discussion here will expand upon Clerk (2004); Clerk *et al.* (2003); somewhat similar approaches to quantum measurement are also discussed in Braginsky and Khalili (1992) and Averin (2003).

In this subsection, we will start by heuristically sketching how constraints on noise (similar to Eq. (4.20) for the cavity detector) can emerge directly from the Heisenberg uncertainty principle. We then present a rigorous and general quantum constraint on noise. We introduce both the notion of a generic linear response detector, and the basic quantum constraint on detector noise. In the next subsection (C), we will discuss how this noise constraint leads to the quantum limit on QND state detection of a qubit. The quantum limit on a linear amplifier (or a position detector) is discussed in detail in the next section.

1. Heuristic weak-measurement noise constraints

As we already stressed at the start of Sec. IV.A, there is no fundamental quantum limit on the accuracy with which a given observable can be measured, at least not within the framework of non-relativistic quantum mechanics. For example, one can, in principle, measure the position of a particle to arbitrary accuracy in the course of a projection measurement [10]. However, the situation is different when we specialize to continuous, non-QND measurements. Such a measurement can be envisaged as a series of instantaneous measurements, in the limit where the spacing between the measurements δt is taken to zero. Each measurement in the series has a limited resolution and perturbs the conjugate variables, thereby affecting the subsequent dynamics and measurement results. Let us discuss this briefly for the example of a series of position measurements of a free particle.

After initially measuring the position with an accuracy Δx, the momentum suffers a random perturbation of size $\Delta p \geq \hbar/(2\Delta x)$. Consequently, a second position measurement taking place a time δt later will have an additional uncertainty of size $\delta t(\Delta p/m) \sim \hbar\delta t/(m\Delta x)$. Thus, when trying to obtain a good estimate of the position by averaging several such measurements, it is not optimal to make Δx too small, because otherwise this additional perturbation, called the "back-action" of the measurement device, will become large. The back-action can be described as a random force $\Delta F = \Delta p/\delta t$. A meaningful limit $\delta t \to 0$ is obtained by keeping both $\Delta x^2 \delta t \equiv \bar{S}_{xx}$

[10] In relativistic theory, the possibility of pair production would not allow to have a resolution finer than the Compton wavelength (Berestetskii *et al.*, 1982), but this will be irrelevant for our discussion of detectors in the solid state and quantum optics contexts

TABLE II Synopsis of recent experiments approaching the quantum limit on continuous position detection of a mechanical resonator. The second column corresponds to the best measurement imprecision noise spectral density $\bar{S}^I_{xx}$ achieved in the experiment. All spectral densities are at the oscillator's resonance frequency Ω. As discussed in the text, there is no quantum limit on how small one can make $\bar{S}^I_{xx}$. The third column presents the product of the measured imprecision noise (unless otherwise noted) and measured back-action noises, divided by $\hbar/2$; this quantity must be one to achieve the quantum limit on the added noise.

Experiment	Mechanical frequency [Hz] $\Omega/(2\pi)$	Imprecision noise vs. zero-point noise $\sqrt{\bar{S}^I_{xx}/\bar{S}^0_{xx}[\Omega]}$	Detector Noise Product $\sqrt{\bar{S}^I_{xx}S_{FF}}/(\hbar/2)$
Cleland *et al.* (2002) (quantum point contact)	1.5×10^6	4.2×10^4	back-action not detected
Knobel and Cleland (2003) (single-eletron transistor)	1.2×10^8	1.8×10^2	back-action not detected
LaHaye *et al.* (2004) (single-electron transistor)	2.0×10^7	5.4	back-action not detected
Naik *et al.* (2006) (single-electron transistor) (if $\bar{S}^I_{xx}$ had been limited by SET shot noise)	2.2×10^7	0.33	8.1×10^2 1.5×10^1
Arcizet *et al.* (2006) (optical cavity)	8.1×10^5	19	back-action not detected
Flowers-Jacobs *et al.* (2007) (atomic point-contact)	4.3×10^7	29	1.7×10^3
Regal *et al.* (2008) (microwave cavity)	2.4×10^5	30	back-action not detected
Schliesser *et al.* (2008) (optical cavity)	4.1×10^7	9.9	back-action not detected
Poggio *et al.* (2008) (quantum point contact)	5.2×10^3	63	back-action not detected
Etaki *et al.* (2008) (d.c. SQUID)	2.0×10^6	47	back-action not detected

and $\Delta p^2/\delta t \equiv \bar{S}_{FF}$ fixed. In this limit, the deviations $\delta x(t)$ describing the finite measurement accuracy and the fluctuations of the back-action force F can be described as white noise processes, $\langle \delta x(t)\delta x(0)\rangle = \bar{S}_{xx}\delta(t)$ and $\langle F(t)F(0)\rangle = \bar{S}_{FF}\delta(t)$. The Heisenberg uncertainty relation $\Delta p\Delta x \geq \hbar/2$ then implies $\bar{S}_{xx}\bar{S}_{FF} \geq \hbar^2/4$ (Braginsky and Khalili, 1992). Note this is completely analogous to the relation Eq. (4.20) we derived for the resonant cavity detector using the fundamental number-phase uncertainty relation. In this section, we will derive rigorously more general quantum limit relations on noise spectral densities of this form.

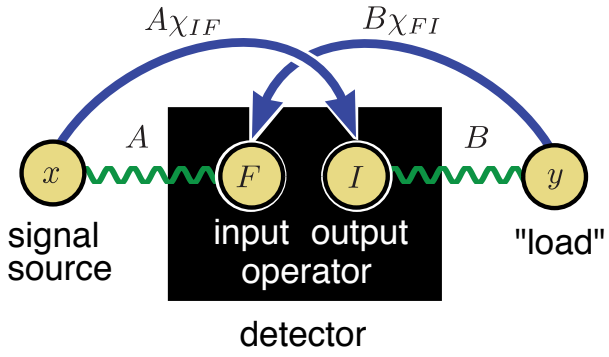

FIG. 8 (Color online) Schematic of a generic linear response detector.

2. Generic linear-response detector

To rigorously discuss the quantum limit, we would like to start with a description of a detector which is as general as possible. To that end, we will think of a detector as some physical system (described by some unspecified Hamiltonian $\hat{H}_{det}$ and some unspecified density matrix $\hat{\rho}_0$) which is time-independent in the absence of coupling to the signal source. The detector has both an input port, characterized by an operator $\hat{F}$, and an output port, characterized by an operator $\hat{I}$ (see Fig. 8). The output operator $\hat{I}$ is simply the quantity which is readout at the output of the detector (e.g., the current in a single-electron transistor, or the phase shift in the cavity detector of the previous section). The input operator $\hat{F}$ is the detector quantity which directly couples to the input signal (e.g., the qubit), and which causes a back-action disturbance of the signal source; in the cavity example of the previous section, we had $\hat{F} = \hat{n}$, the cavity photon number. As we are interested in weak couplings, we will assume a simple bilinear form for the detector-signal interaction Hamiltonian:

$$\hat{H}_{int} = A\hat{x}\hat{F} \tag{5.1}$$

Here, the operator $\hat{x}$ (which is not necessarily a position operator) carries the input signal. Note that because $\hat{x}$ belongs to the signal source, it necessarily commutes with the detector variables $\hat{I}, \hat{F}$.

We will always assume the coupling strength A to be small enough that we can accurately describe the output of the detector using linear response. We thus have:

$$\langle \hat{I}(t)\rangle = \langle \hat{I}\rangle_0 + A\int dt' \chi_{IF}(t-t')\langle \hat{x}(t')\rangle, \tag{5.2}$$

where $\langle \hat{I}\rangle_0$ is the input-independent value of the detector output at zero-coupling, and $\chi_{IF}(t)$ is the linear-response

susceptibility or gain of our detector. Note that in Clerk *et al.* (2003) and Clerk (2004), this gain coefficient is denoted λ. Using standard time-dependent perturbation theory in the coupling $\hat{H}_{int}$, one can easily derive Eq. (5.2), with $\chi_{IF}(t)$ given by a Kubo-like formula:

$$\chi_{IF}(t) = -\frac{i}{\hbar}\theta(t)\left\langle\left[\hat{I}(t),\hat{F}(0)\right]\right\rangle_0 \tag{5.3}$$

Here (and in what follows), the operators $\hat{I}$ and $\hat{F}$ are Heisenberg operators with respect to the detector Hamiltonian, and the subscript 0 indicates an expectation value with respect to the density matrix of the uncoupled detector.

As we have already discussed, there will be unavoidable noise in both the input and output ports of our detector. This noise is subject to quantum mechanical constraints, and its presence is what limits our ability to make a measurement or amplify a signal. We thus need to quantitatively characterize the noise in both these ports. Recall from the discussion in Sec. III.B that it is the symmetric-in-frequency part of a quantum noise spectral density which plays a role akin to classical noise. We will thus want to characterize the *symmetrized* noise correlators of our detector (denoted as always with a bar). Redefining these operators so that their average value is zero at zero coupling (i.e. $\hat{F} \to \hat{F} - \langle\hat{F}\rangle_0$, $\hat{I} \to \hat{I} - \langle\hat{I}\rangle_0$), we have:

$$\bar{S}_{FF}[\omega] \equiv \frac{1}{2}\int_{-\infty}^{\infty} dt e^{i\omega t}\langle\{\hat{F}(t),\hat{F}(0)\}\rangle_0 \tag{5.4a}$$

$$\bar{S}_{II}[\omega] \equiv \frac{1}{2}\int_{-\infty}^{\infty} dt e^{i\omega t}\langle\{\hat{I}(t),\hat{I}(0)\}\rangle_0 \tag{5.4b}$$

$$\bar{S}_{IF}[\omega] \equiv \frac{1}{2}\int_{-\infty}^{\infty} dt e^{i\omega t}\langle\{\hat{I}(t),\hat{F}(0)\}\rangle_0 \tag{5.4c}$$

where $\{,\}$ indicates the anti-commutator, $\bar{S}_{II}$ represents the intrinsic noise in the output of the detector, and $\bar{S}_{FF}$ describes the back-action noise seen by the source of the input signal. In general, there will be some correlation between these two kinds of noise; this is described by the cross-correlator $\bar{S}_{IF}$.

Finally, it will also be useful to introduce the reverse gain χ_{FI} of our detector. This is the response coefficient describing an experiment where we couple our input signal to the *output* port of the detector (i.e. $\hat{H}_{int} = A\hat{x}\hat{I}$), and attempt to observe something at the *input* port (i.e. in $\langle\hat{F}(t)\rangle$). In complete analogy to Eq. (5.2), one would then have:

$$\langle\hat{F}(t)\rangle = \langle\hat{F}\rangle_0 + A\int dt'\chi_{FI}(t-t')\langle\hat{x}(t')\rangle \tag{5.5}$$

with:

$$\chi_{FI}(t) = -\frac{i}{\hbar}\theta(t)\langle\left[\hat{F}(t),\hat{I}(0)\right]\rangle_0 \tag{5.6}$$

Note that in Clerk *et al.* (2003) and Clerk (2004), the reverse gain coefficient χ_{FI} is denoted λ'.

The reverse gain is indeed something we need to worry about (and appears in many standard classical electrical amplifiers such as op amps (Boylestad and Nashelsky, 2006)). To make a measurement of the output operator $\hat{I}$, we must necessarily couple to it in some manner. If $\chi_{FI} \neq 0$, the noise associated with this coupling could in turn lead to additional back-action noise in the operator $\hat{F}$. Even if the reverse gain did nothing but amplify vacuum noise entering the output port, this would heat up the system being measured at the input port and hence produce excess back action. Thus, the ideal situation is to have $\chi_{FI} = 0$, implying a high asymmetry between the input and output of the detector. We note that almost all mesoscopic detectors that have been studied in detail (e.g. single electron transistors and generalized quantum point contacts) have been found to have a vanishing reverse gain: $\chi_{FI} = 0$ (Clerk *et al.*, 2003) [11]. For this reason, we will often assume the ideal situation where $\chi_{FI} = 0$ in what follows.

Before proceeding, it is worth emphasizing that there is a relation between the detector gains χ_{IF} and χ_{FI} and the *unsymmetrized* I-F quantum noise correlator, $S_{IF}[\omega]$. This spectral density, which need not be symmetric in frequency, is defined as:

$$S_{IF}[\omega] = \int_{-\infty}^{\infty} dt e^{i\omega t}\langle\hat{I}(t)\hat{F}(0)\rangle_0 \tag{5.7}$$

Using the definitions, one can easily show that:

$$\bar{S}_{IF}[\omega] = \frac{1}{2}\left[S_{IF}[\omega] + S_{IF}[-\omega]^*\right] \tag{5.8a}$$

$$\chi_{IF}[\omega] - \chi_{FI}[\omega]^* = -\frac{i}{\hbar}\left[S_{IF}[\omega] - S_{IF}[-\omega]^*\right] \tag{5.8b}$$

Thus, while $\bar{S}_{IF}$ represents the classical part of the I-F quantum noise spectral density, the gains χ_{IF}, χ_{FI} are determined by the quantum part of this spectral density. This also demonstrates that though the gains have an explicit factor of $1/\hbar$ in their definitions, they have a well defined $\hbar \to 0$ limit, as the asymmetric-in-frequency part of $S_{IF}[\omega]$ vanishes in this limit.

3. Quantum constraint on noise

Despite having said nothing about the detector's Hamiltonian or state (except that it is time-independent), we can nonetheless derive a very general *quantum* constraint on its noise properties. Note first that for purely classical noise spectral densities, one always has the inequality:

$$\bar{S}_{II}[\omega]\bar{S}_{FF}[\omega] - \left|\bar{S}_{IF}[\omega]\right|^2 \geq 0 \tag{5.9}$$

---

[11] Note that the fact χ_{FI} vanishes for a mesoscopic scattering detector is used directly to define the full counting statistics of current; see Levitov (2003) for a discussion

This simply expresses the fact that the correlation between two different noisy quantities cannot be arbitrarily large; it follows immediately from the Schwartz inequality. In the quantum case, this simple constraint becomes modified. Defining for convenience:

$$\tilde{\chi}_{IF}[\omega] \equiv \chi_{IF}[\omega] - [\chi_{FI}[\omega]]^* \tag{5.10a}$$

$$\Delta[z] = \frac{\left|1+z^2\right| - \left(1+|z|^2\right)}{2}, \tag{5.10b}$$

we will show below that the following quantum noise inequality (involving *symmetrized* noise correlators) is always valid (see also Eq. (6.36) in (Braginsky and Khalili, 1996)):

$$\bar{S}_{II}[\omega]\bar{S}_{FF}[\omega] - \left|\bar{S}_{IF}[\omega]\right|^2 \geq \left|\frac{\hbar\tilde{\chi}_{IF}[\omega]}{2}\right|^2 \left(1 + \Delta\left[\frac{\bar{S}_{IF}[\omega]}{\hbar\tilde{\chi}_{IF}[\omega]/2}\right]\right) \tag{5.11}$$

To interpret this inequality, note that if our detector has no positive feedback, then Re $\chi_{IF} \cdot \chi_{FI} \leq 0$, implying $|\tilde{\chi_{IF}}| \neq 0$. Also note that $1 + \Delta[z] \geq 0$. Eq. (5.11) thus tells us that in general, *if our detector has gain and no positive feedback, it must have a minimum amount of back-action and output noise*; moreover, these two noises cannot be perfectly anti-correlated. Note that in many cases the last term in Eq. (5.11) (involving $\Delta[z]$) is identically zero; we will comment more on this in what follows.

Though Eq. (5.11) may appear reminiscent to the standard fluctuation dissipation theorem, its origin is quite different: in particular, the quantum noise constraint applies irrespective of whether the detector is in equilibrium. Eq. (5.11) instead follows directly from Heisenberg's uncertainty relation applied to the frequency representation of the operators $\hat{I}$ and $\hat{F}$. In its most general form, the Heisenberg uncertainty relation gives a lower bound for the uncertainties of two observables in terms of their commutator and their noise correlator (Gottfried, 1966):

$$(\Delta A)^2(\Delta B)^2 \geq \frac{1}{4}\left\langle\left\{\hat{A},\hat{B}\right\}\right\rangle^2 + \frac{1}{4}\left|\left\langle\left[\hat{A},\hat{B}\right]\right\rangle\right|^2. \tag{5.12}$$

Here we have assumed $\langle\hat{A}\rangle = \langle\hat{B}\rangle = 0$. Let us now choose the Hermitian operators $\hat{A}$ and $\hat{B}$ to be given by the cosine-transforms of $\hat{I}$ and $\hat{F}$, respectively, over a finite time-interval T:

$$\hat{A} \equiv \sqrt{\frac{2}{T}}\int_{-T/2}^{T/2} dt\, \cos(\omega t + \delta)\, \hat{I}(t) \tag{5.13a}$$

$$\hat{B} \equiv \sqrt{\frac{2}{T}}\int_{-T/2}^{T/2} dt\, \cos(\omega t)\, \hat{F}(t) \tag{5.13b}$$

Note that we have phase shifted the transform of $\hat{I}$ relative to that of $\hat{F}$ by a phase δ. In the limit $T \to \infty$ we find, at any finite frequency $\omega \neq 0$:

$$(\Delta A)^2 = \bar{S}_{II}[\omega],\ (\Delta B)^2 = \bar{S}_{FF}[\omega] \tag{5.14a}$$

$$\left\langle\left\{\hat{A},\hat{B}\right\}\right\rangle = 2\mathrm{Re}\, e^{i\delta}\bar{S}_{IF}[\omega] \tag{5.14b}$$

$$\left\langle\left[\hat{A},\hat{B}\right]\right\rangle = \int_{-\infty}^{+\infty} dt\, \cos(\omega t+\delta)\left\langle\left[\hat{I}(t),\hat{F}(0)\right]\right\rangle = i\hbar\mathrm{Re}\,\left[e^{i\delta}\left(\chi_{IF}[\omega] - (\chi_{FI}[\omega])^*\right)\right] \tag{5.14c}$$

In the last line, we have simply made use of the Kubo formula definitions of the gain and reverse gain (cf. Eqs. (5.3) and (5.6)). As a consequence of Eqs. (5.14a)-(5.14c), the Heisenberg uncertainty relation (5.12) directly yields:

$$\bar{S}_{II}[\omega]\bar{S}_{FF}[\omega] \geq \left[\mathrm{Re}\,\left(e^{i\delta}\bar{S}_{IF}[\omega]\right)\right]^2 + \frac{\hbar^2}{4}\left[\mathrm{Re}\, e^{i\delta}\left(\chi_{IF}[\omega] - (\chi_{FI}[\omega])^*\right)\right]^2 \tag{5.15}$$

Maximizing the RHS of this inequality over δ then yields the general quantum noise constraint of Eq. (5.11).

With this derivation, we can now interpret the quantum noise constraint Eq. (5.11) as stating that the *noise at a given frequency* in two observables, $\hat{I}$ and $\hat{F}$, is bounded by the value of their commutator at that frequency. The fact that $\hat{I}$ and $\hat{F}$ do not commute is necessary for the existence of linear response (gain) from the detector, but also means that the noise in both $\hat{I}$ and $\hat{F}$ cannot be arbitrarily small. A more detailed derivation, yielding additional important insights, is described in Appendix J.1.

Given the quantum noise constraint of Eq. (5.11), we can now very naturally define a "quantum-ideal" detector (at a given frequency ω) as one which minimizes the LHS of Eq. (5.11)– a quantum-ideal detector has a minimal amount of noise at frequency ω. We will often be interested in the ideal case where there is no reverse gain (i.e. measuring $\hat{I}$ does not result in additional back-action noise in $\hat{F}$); the condition to have a quantum limited detector thus becomes:

$$\bar{S}_{II}[\omega]\bar{S}_{FF}[\omega] - \left|\bar{S}_{IF}[\omega]\right|^2 = \left|\frac{\hbar\chi_{IF}[\omega]}{2}\right|^2 \left(1 + \Delta\left[\frac{\bar{S}_{IF}[\omega]}{\hbar\chi_{IF}[\omega]/2}\right]\right) \tag{5.16}$$

where $\Delta[z]$ is given in Eq. (5.10b). Again, as we will discuss below, in most cases of interest (e.g. zero frequency and/or large amplifier power gain), the last term on the RHS will vanish. In the following sections, we will demonstrate that the "ideal noise" requirement of Eq. (5.16) is necessary in order to achieve the quantum limit on QND detection of a qubit, or on the added noise of a linear amplifier.

Before leaving our general discussion of the quantum noise constraint, it is worth emphasizing that achieving Eq. (5.16) places a very strong constraint on the properties of the detector. In particular, there must exist a

tight connection between the input and output ports of the detector– in a certain restricted sense, the operators $\hat{I}$ and $\hat{F}$ must be proportional to one another (see Eq. (J13) in Appendix J.1). As is discussed in Appendix J.1, this proportionality immediately tells us that *a quantum-ideal detector cannot be in equilibrium.* The proportionality exhibited by a quantum-ideal detector is parameterized by a single complex valued number $\alpha[\omega]$, whose magnitude is given by:

$$|\alpha[\omega]|^2 \;=\; \bar{S}_{II}[\omega]/\bar{S}_{FF}[\omega] \tag{5.17}$$

While this proportionality requirement may seem purely formal, it does have a simple heuristic interpretation; as is discussed in Clerk *et al.* (2003), it may be viewed as a formal expression of the condition of no 'wasted information' discussed in the previous subsection.

4. Role of noise cross-correlations

We now return to the unwieldy second term in the RHS of the quantum noise constraint of Eq. (5.11). Note that this term is sensitive to the *phase* of the quantity $\bar{S}_{IF}[\omega]/\tilde{\chi}_{IF}$: if this quantity is purely real, then the second term vanishes, as $\Delta[z] = 0$ if z is real (cf. Eq (5.10b)). The result is a simpler looking noise constraint, as found elsewhere in the literature (Averin, 2003; Clerk, 2004; Clerk *et al.*, 2003). This simpler noise constraint is *always* valid in the low-frequency limit $\omega \to 0$, as in this limit χ_{IF}, χ_{FI} and $\bar{S}_{IF}$ must all be real.

The situation is somewhat more delicate at finite frequencies: for finite ω, the quantity $\bar{S}_{IF}[\omega]/\tilde{\chi}_{IF}[\omega]$ need not be purely real. In fact, as the astute reader may have already realized, if this quantity becomes large and purely imaginary, then the RHS of Eq. (5.11) will vanish– in this limit, there is no additional quantum constraint on the noise beyond what already exists classically!

Despite this odd behaviour, there is no need to worry. For simplicity, we again focus on the case of a vanishing reverse gain $\chi_{FI} = 0$. We show in Appendix J.2 that if one wishes to have a quantum limited detector (i.e. equality in Eq. (5.11)) *and* have true amplification, then the ratio $\bar{S}_{IF}[\omega]/\chi_{IF}[\omega]$ *must* also be real. By "true amplification", we mean that the dimensionless *power gain* of the detector must be much larger than one. The power gain is a measure of how much power is provided by the detector at its output compared to how much power is drawn at its input; it will be defined more precisely in Sec. VI.D.3. Thus, even at finite frequency, the last term on the RHS of Eq. (5.11) plays no role if we are interested in a detector which truly amplifies (i.e. has a large power gain). The limit discussed above, where the noise constraint vanishes because $\bar{S}_{IF}/\chi_{IF}$ is imaginary, is of no real interest, as in this limit, our detector has no power gain. Simply put, if our detector performs no amplification, then there need not by any quantum constraint on its noise; see Sec. VI for a more complete discussion of this point.

Finally, an important corollary to the above point is that at the quantum limit, the quantity $\bar{S}_{IF}/\chi_{IF}$ *must be real.* Thus, *at the quantum limit, correlations between the back-action force and the intrinsic output noise fluctuations must have the same phase as the gain* χ_{IF}. As we discuss further in Sec. VI.E , this requirement can also be interpreted in terms of wasted information.

B. Quantum limit on QND detection of a qubit

In Sec. IV.B, we discussed the quantum limit on QND qubit detection in the specific context of a resonant cavity detector. We will now show how the full quantum noise constraint of Eq. (5.11) directly leads to this quantum limit for an arbitrary weakly-coupled detector. Similar to Sec. IV.B, we couple the input operator of our generic linear-response detector to the $\hat{\sigma}_z$ operator of the qubit we wish to measure (i.e. we take $\hat{x} = \hat{\sigma}_z$ in Eq. (5.1)); we also consider the QND regime, where $\hat{\sigma}_z$ commutes with the qubit Hamiltonian. As we saw in Sec. IV.B, the quantum limit in this case involves the inequality $\Gamma_{\rm meas} \leq \Gamma_\varphi$, where $\Gamma_{\rm meas}$ is the measurement rate, and Γ_φ is the back-action dephasing rate. For the latter quantity, we can directly use the results of our calculation for the cavity system, where we found the dephasing rate was set by the zero-frequency noise in the cavity photon number (cf. Eq. 4.44). In complete analogy, the back-action dephasing rate here will be determined by the zero-frequency noise in the input operator $\hat{F}$ of our detector:

$$\Gamma_\varphi = \frac{2A^2}{\hbar^2}\bar{S}_{FF}[0] \tag{5.18}$$

The measurement rate (the rate at which information on the state of qubit is acquired) is also defined in complete analogy to what was done for the cavity detector. We imagine we turn the measurement on at $t = 0$ and start to integrate up the output $I(t)$ of our detector:

$$\hat{m}(t) = \int_0^t dt' \hat{I}(t') \tag{5.19}$$

The probability distribution of the integrated output $\hat{m}(t)$ will depend on the state of the qubit; for long times, we may approximate the distribution corresponding to each qubit state as being gaussian. Noting that we have chosen $\hat{I}$ so that its expectation vanishes at zero coupling, the average value of $\langle \hat{m}(t) \rangle$ corresponding to each qubit state is (in the long time limit of interest):

$$\langle \hat{m}(t) \rangle_\uparrow \;=\; A\chi_{IF}[0]t \tag{5.20a}$$
$$\langle \hat{m}(t) \rangle_\downarrow \;=\; -A\chi_{IF}[0]t \tag{5.20b}$$

The variance of both distributions is, to leading order, independent of the qubit state:

$$\langle \hat{m}^2(t) \rangle_{\uparrow/\downarrow} - \langle \hat{m}(t) \rangle^2_{\uparrow/\downarrow} \equiv \langle\langle \hat{m}^2(t) \rangle\rangle_{\uparrow/\downarrow} = \bar{S}_{II}[0]t \tag{5.21}$$

For the last equality above, we have taken the long-time limit, which results in the variance of $\hat{m}$ being determined completely by the zero-frequency output noise $\bar{S}_{II}[\omega = 0]$ of the detector. The assumption here is that due to the weakness of the measurement, the measurement time (i.e. $1/\Gamma_{\rm meas}$) will be much longer than the autocorrelation time of the detector's noise.

We can now define the measurement rate, in complete analogy to the cavity detector of the previous section (cf. Eq. (4.39)), by how quickly the resolving power of the measurement grows [12]:

$$\frac{1}{4}\frac{\left[\langle\hat{m}(t)\rangle_\uparrow - \langle\hat{m}(t)\rangle_\downarrow\right]^2}{\langle\langle\hat{m}^2(t)\rangle\rangle_\uparrow + \langle\langle\hat{m}^2(t)\rangle\rangle_\downarrow} \equiv \Gamma_{\rm meas} t. \tag{5.22}$$

This yields:

$$\Gamma_{\rm meas} = \frac{A^2\left(\chi_{IF}[0]\right)^2}{2\bar{S}_{II}[0]} \tag{5.23}$$

Putting this all together, we find that the "efficiency" ratio $\eta = \Gamma_{\rm meas}/\Gamma_\varphi$ is given by:

$$\eta \equiv \frac{\Gamma_{\rm meas}}{\Gamma_\varphi} = \frac{\hbar^2\left(\chi_{IF}[0]\right)^2}{4\bar{S}_{II}[0]\bar{S}_{FF}[0]} \tag{5.24}$$

The quantum-limit bound $\eta \leq 1$ thus follows immediately from the quantum noise constraint of Eq. (5.11). Further, achieving the quantum limit for QND detection requires a detector with quantum-ideal noise properties, as defined by Eq. (5.16), as well as a detector with a vanishing noise cross-correlator: $\bar{S}_{IF}[0] = 0$. As discussed in Appendix J.1, achieving this ideal noise condition implies a tight connection between the input and output ports of the detector. This condition also corresponds directly to the idea that reaching the quantum limit requires there to be no unused, "wasted information" in the detector on the state of the qubit (Clerk *et al.*, 2003).

VI. QUANTUM LIMIT ON LINEAR AMPLIFIERS AND POSITION DETECTORS

In the previous section, we established the fundamental quantum constraint on the noise of any system capable of acting as a linear detector; we further showed that this quantum noise constraint directly leads to the "quantum limit" on non-demolition qubit detection using a weakly-coupled detector. In this section, we turn to the more general situation where our detector is a phase-preserving quantum linear amplifier: the input to the detector is described some time-dependent operator $\hat{x}(t)$ which we wish to have amplified at the output of our detector. As we will see, the quantum limit in this case is a limit on how small one can make the noise added by the amplifier to the signal. The discussion in this section both furthers and generalizes the heuristic discussion of position detection using a cavity detector presented in Sec. IV.B.

In this section, we will start by presenting a heuristic discussion of quantum constraints on amplification. We will then demonstrate explicitly how the previously-discussed quantum noise constraint leads directly to the quantum limit on the added noise of a phase-preserving linear amplifier; we will examine both the cases of a generic linear position detector and a generic voltage amplifier, following the approach outlined in Clerk (2004). We will also spend time explicitly connecting the linear response approach we use here to the bosonic scattering formulation of the quantum limit favoured by the quantum optics community (Caves, 1982; Courty *et al.*, 1999; Grassia, 1998; Haus and Mullen, 1962), paying particular attention to the case of two-port scattering amplifier. We will see that there are some important subtleties involved in converting between the two approaches. In particular, there exists a crucial difference between the case where the input signal is tightly coupled to the input of the amplifier (the case usually considered in the quantum optics community), versus the case where, similar to an ideal op-amp, the input signal is only weakly coupled to the input of the amplifier (the case usually considered in the solid state community).

A. Preliminaries on amplification

What exactly does one mean by 'amplification'? As we will see (cf. Sec. VI.D.3), a precise definition requires that the energy provided at the output of the amplifier be much larger than the energy drawn at the input of the amplifier– the "power gain" of the amplifier must be larger than one. For the moment, however, let us work with the cruder definition that amplification involves making some time-dependent signal 'larger'. To set the stage, we will first consider an extremely simple classical analogue of a linear amplifier. Imagine the "signal" we wish to amplify is the coordinate $x(t)$ of a harmonic oscillator; we can write this signal as:

$$x(t) = x(0)\cos(\omega_S t) + \frac{p(0)}{M\omega_S}\sin(\omega_S t) \tag{6.1}$$

Our signal has two quadrature amplitudes, i.e. the amplitude of the cosine and sine components of $x(t)$. To "amplify" this signal, we start at $t = 0$ to parametrically drive the oscillator by changing its frequency ω_S periodically in time: $\omega_S(t) = \omega_0 + \delta\omega\sin(\omega_P t)$, where we assume $\delta\omega \ll \omega_0$. The well-known physical example is a swing whose motion is being excited by effectively changing the length of the pendulum at the right frequency and phase.

[12] The strange looking factor of 1/4 here is purely chosen for convenience; we are defining the measurement rate based on the information theoretic definition given in Appendix E. This factor of four is consistent with the definition used in the cavity system.

For a "pump frequency" ω_P equalling twice the "signal frequency", $\omega_P = 2\omega_S$, the resulting dynamics will lead to an amplification of the initial oscillator position, with the energy provided by the external driving:

$$x(t) = x(0)e^{\lambda t}\cos(\omega_S t) + \frac{p(0)}{M\omega_S}e^{-\lambda t}\sin(\omega_S t) \qquad (6.2)$$

Thus, one of the quadratures is amplified exponentially, at a rate $\lambda = \delta\omega/2$, while the other one decays. In a quantum-mechanical description, this produces a squeezed state out of an initial coherent state. Such a system is called a "degenerate parametric amplifier", and we discuss its quantum dynamics in more detail in Sec. VI.G and in Appendix F. We will see that such an amplifier, which only amplifies a single quadrature, is not required quantum mechanically to add any noise (Braginsky and Khalili, 1992; Caves, 1982; Caves *et al.*, 1980).

Can we now change this parametric amplification scheme slightly in order to make *both* signal quadratures grow with time? It turns out this is impossible, as long as we restrict ourselves to a driven system with a single degree of freedom. The reason in classical mechanics is that Liouville's theorem requires phase space volume to be conserved during motion. In a more formal way, this is related to the conservation of Poisson brackets, or, in quantum mechanics, to the conservation of commutation relations. Nevertheless, it is certainly desirable to have an amplifier that acts equally on both quadratures (a so-called "phase-preserving" or "phase-insensitive" amplifier), since the signal's phase is often not known beforehand. The way around the restriction created by Liouville's theorem is to add more degrees of freedom, such that the phase space volume can expand in both quadratures (i.e. position and momentum) of the interesting signal degree of freedom, while being compressed in other directions. This is achieved most easily by coupling the signal oscillator to another oscillator, the "idler mode". The external driving now modulates the coupling between these oscillators, at a frequency that has to equal the sum of the oscillators' frequencies. The resulting scheme is called a phase-preserving non-degenerate parametric amplifier (see Appendix F).

Crucially, there is a price to pay for the introduction of an extra degree of freedom: there will be noise associated with the "idler" oscillator, and this noise will contribute to the noise in the output of the amplifier. Classically, one could make the noise associate with the "idler" oscillator arbitrarily small by simply cooling it to zero temperature. This is not possible quantum-mechanically; there are always zero-point fluctuations of the idler oscillator to contend with. It is this noise which sets a fundamental quantum limit for the operation of the amplifier. We thus have a heuristic accounting for why there is a quantum-limit on the added noise of a phase-preserving linear amplifier: one needs extra degrees of freedom to amplify both signal quadratures, and such extra degrees of freedom invariably have noise associated with them.

B. Standard Haus-Caves derivation of the quantum limit on a bosonic amplifier

We now make the ideas of the previous subsection more precise by quickly sketching the standard derivation of the quantum limit on the noise added by a phase-preserving amplifier. This derivation is originally due to Haus and Mullen (1962), and was both clarified and extended by Caves (1982); the amplifier quantum limit was also motivated in a slightly different manner by Heffner (1962)[13]. While extremely compact, the Haus-Caves derivation can lead to confusion when improperly applied; we will discuss this in the next subsection, as well as in Sec. VII, where we apply this argument carefully to the important case of a two-port quantum voltage amplifier.

The starting assumption of this derivation is that both the input and output ports of the amplifier can be described by sets of bosonic modes. If we focus on a narrow bandwidth centered on frequency ω, we can describe a classical signal $E(t)$ in terms of a complex number a defining the amplitude and phase of the signal (or equivalently the two quadrature amplitudes) (Haus, 2000; Haus and Mullen, 1962)

$$E(t) \propto i[ae^{-i\omega t} - a^* e^{+i\omega t}]. \qquad (6.3)$$

In the quantum case, the two signal quadratures of $E(t)$ (i.e. the real and imaginary parts of $a(t)$) cannot be measured simultaneously because they are canonically conjugate; this is in complete analogy to a harmonic oscillator (cf. Eq. (4.66)). As a result a, a^* must be elevated to the status of photon ladder operators: $a \to \hat{a}, a^* \to a^\dagger$.

Consider the simplest case, where there is only a single mode at both the input and output, with corresponding annhiliation operators $\hat{a}$ and $\hat{b}$ [14]. It follows that the input signal into the amplifier is described by the expectation value $\langle\hat{a}\rangle$, while the output signal is described by $\langle\hat{b}\rangle$. Correspondingly, the symmetrized noise in both these quantities is described by:

$$(\Delta a)^2 \equiv \frac{1}{2}\left\langle\{\hat{a}, \hat{a}^\dagger\}\right\rangle - |\langle\hat{a}\rangle|^2 \qquad (6.4a)$$

$$(\Delta b)^2 \equiv \frac{1}{2}\left\langle\{\hat{b}, \hat{b}^\dagger\}\right\rangle - \left|\langle\hat{b}\rangle\right|^2 \qquad (6.4b)$$

To derive a quantum limit on the added noise of the amplifier, one uses two simple facts. First, both the input

---

[13] Note that Caves (1982) provides a thorough discussion of why the derivation of the amplifier quantum limit given in Heffner (1962) is not rigorously correct

[14] To relate this to the linear response detector of Sec. V.A, one could naively write $\hat{x}$, the operator carrying the input signal, as, e.g., $\hat{x} = \hat{a} + \hat{a}^\dagger$, and the output operator $\hat{I}$ as, e.g., $\hat{I} = \hat{b} + \hat{b}^\dagger$ (we will discuss how to make this correspondence in more detail in Sec. VII)

and the output operators must satisfy the usual commutation relations:

$$\left[\hat{a}, \hat{a}^\dagger\right] = 1 \tag{6.5a}$$
$$\left[\hat{b}, \hat{b}^\dagger\right] = 1 \tag{6.5b}$$

Second, the linearity of the amplifier and the fact that it is phase preserving (i.e. both signal quadratures are amplified the same way) implies a simple relation between the output operator $\hat{b}$ and the input operator $\hat{a}$:

$$\hat{b} = \sqrt{G}\hat{a} \tag{6.6a}$$
$$\hat{b}^\dagger = \sqrt{G}\hat{a}^\dagger \tag{6.6b}$$

where G is the dimensionless *"photon number gain"* of the amplifier. It is immediately clear however this expression cannot possibly be correct as written because it violates the fundamental bosonic commutation relation $[\hat{b}, \hat{b}^\dagger] = 1$. We are therefore forced to write

$$\hat{b} = \sqrt{G}\hat{a} + \hat{\mathcal{F}} \tag{6.7a}$$
$$\hat{b}^\dagger = \sqrt{G}\hat{a}^\dagger + \hat{\mathcal{F}}^\dagger \tag{6.7b}$$

where $\hat{\mathcal{F}}$ is an operator representing additional noise added by the amplifier. Based on the discussion of the previous subsection, we can anticipate what $\hat{\mathcal{F}}$ represents: it is noise associated with the additional degrees of freedom which must invariably be present in a phase-preserving amplifier.

As $\hat{\mathcal{F}}$ represents noise, it has a vanishing expectation value; in addition, one also assumes that this noise is uncorrelated with the input signal, implying $[\hat{\mathcal{F}}, \hat{a}] = [\hat{\mathcal{F}}, \hat{a}^\dagger] = 0$ and $\langle\hat{\mathcal{F}}\hat{a}\rangle = \langle\hat{\mathcal{F}}\hat{a}^\dagger\rangle = 0$. Insisting that $[\hat{b}, \hat{b}^\dagger] = 1$ thus yields:

$$\left[\hat{\mathcal{F}}, \hat{\mathcal{F}}^\dagger\right] = 1 - G \tag{6.8}$$

The question now becomes how small can we make the noise described by $\hat{\mathcal{F}}$? Using Eqs. (6.7a) and (6.7b), the noise at the amplifier output Δb is given by:

$$\begin{aligned}(\Delta b)^2 &= G(\Delta a)^2 + \frac{1}{2}\left\langle\{\hat{\mathcal{F}}, \hat{\mathcal{F}}^\dagger\}\right\rangle \\ &\geq G(\Delta a)^2 + \frac{1}{2}\left|\left\langle[\hat{\mathcal{F}}, \hat{\mathcal{F}}^\dagger]\right\rangle\right| \\ &\geq G(\Delta a)^2 + \frac{|G-1|}{2}\end{aligned} \tag{6.9}$$

We have used here a standard inequality to bound the expectation of $\{\hat{\mathcal{F}}, \hat{\mathcal{F}}^\dagger\}$. The first term here is simply the amplified noise of the input, while the second term represents the noise added by the amplifier. Note that if there is no amplification (i.e. $G = 1$), there need not be any added noise. However, in the more relevant case of large amplification ($G \gg 1$), the added noise cannot vanish. It is useful to express the noise at the output as an equivalent noise at ("referred to") the input by simply dividing out the photon gain G. Taking the large-G limit, we have:

$$\frac{(\Delta b)^2}{G} \geq (\Delta a)^2 + \frac{1}{2} \tag{6.10}$$

Thus, we have a very simple demonstration that *an amplifier with a large photon gain must add at least half a quantum of noise to the input signal*. Equivalently, the minimum value of the added noise is simply equal to the zero-point noise associated with the input mode; the total output noise (referred to the input) is at least twice the zero point input noise. Note that both these conclusions are identical to what we found (by very different means) in our analysis of the resonant cavity position detector in Sec. IV.B.3.

As we have already discussed, the added noise operator $\mathcal{F}$ is associated with additional degrees of freedom (beyond input and output modes) necessary for phase-preserving amplification. To see this more concretely, note that every linear amplifier is inevitably a *non-linear* system consisting of an energy source and a 'spigot' controlled by the input signal which redirects the energy source partly to the output channel and partly to some other channel(s). Hence there are inevitably other degrees of freedom involved in the amplification process beyond the input and output channels. An explicit example is the quantum parametric amplifier described in more detail in Appendix F. Further insights into amplifier added noise and its connection to the fluctuation-dissipation theorem can be obtained by considering a simple model where a transmission line is terminated by an effective negative impedance; we discuss this model in Appendix B.4.

To see explicitly the role of the additional degrees of freedom, note first that for $G > 1$ the RHS of Eq. (6.8) is negative. Hence the simplest possible form for the added noise is

$$\hat{\mathcal{F}} = \sqrt{G-1}\hat{d}^\dagger \tag{6.11}$$
$$\hat{\mathcal{F}}^\dagger = \sqrt{G-1}\hat{d} \tag{6.12}$$

where $\hat{d}$ and $\hat{d}^\dagger$ represent a single additional mode of the system. This is the minimum number of additional degrees of freedom that must inevitably be involved in the amplification process. Note that for this case, the inequality in Eq. (6.9) is satisfied as an equality, and the added noise takes on its minimum possible value. If instead we had, say, two additional modes (coupled inequivalently):

$$\hat{\mathcal{F}} = \sqrt{G-1}(\cosh\theta\hat{d}_1^\dagger + \sinh\theta\hat{d}_2) \tag{6.13}$$

it is straightforward to show that the added noise is inevitably larger than the minimum. This again can be interpreted in terms of wasted information, as the extra degrees of freedom are not being monitored as part of the measurement process and so information is being lost.

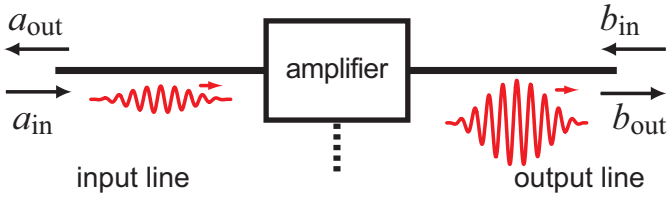

FIG. 9 (Color online) Schematic of a two-port bosonic amplifier. Both the input and outputs of the amplifier are attached to transmission lines. The incoming and outgoing wave amplitudes in the input (output) transmission line are labelled $\hat{a}_{\rm in}, \hat{a}_{\rm out}$ ($\hat{b}_{\rm in}, \hat{b}_{\rm out}$) respectively. The voltages at the end of the two lines ($\hat{V}_a, \hat{V}_b$) are linear combinations of incoming and outgoing wave amplitudes.

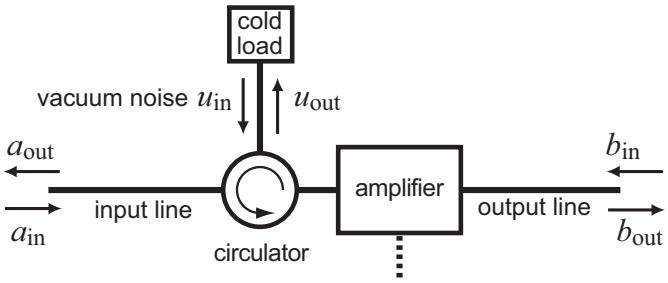

FIG. 10 Illustration of a bosonic two-port amplifier used in the scattering mode of operation. The "signal" is an incoming wave in the input port of the amplifier, and does not depend on what is coming out of the amplifier. This is achieved by connecting the input line to a circulator and a "cold load" (i.e. a zero temperature resistor): all that goes back towards the source of the input signal is vacuum noise.

TABLE III Two different amplifier modes of operation.

Mode	Input Signal $s(t)$	Output Signal $o(t)$
Scattering	$s(t) = a_{\rm in}(t)$ ($a_{\rm in}$ indep. of $a_{\rm out}$)	$o(t) = b_{\rm out}(t)$) ($b_{\rm out}$ indep. of $b_{\rm in}$)
Op-amp	$s(t) = V_a(t)$ ($a_{\rm in}$ depends on $a_{\rm out}$)	$o(t) = V_b(t)$ ($b_{\rm out}$ depends on $b_{\rm in}$)

C. Scattering versus op-amp modes of operation

While extremely elegant and direct, the standard Haus-Caves derivation of the amplifier quantum limit has some puzzling features. Recall that in our heuristic discussion of position detection (Sec. IV.B.3), we saw that a crucial aspect of the quantum limit was the trade-off between back-action noise and measurement imprecision noise. We saw that reaching the quantum limit required both a detector with "ideal" noise, as well as an optimization of the detector-oscillator coupling strength. Somewhat disturbingly, none of these ideas appeared explicitly in the Haus-Caves derivation; this can give the misleading impression that the quantum limit never has anything to do with back-action. A further confusion comes from the fact that many detectors have input and outputs that cannot be described by a set of bosonic modes. How does one apply the above arguments to such systems?

The first step in resolving these seeming inconsistencies is to realize that there are really two different ways in which one can use a given amplifier or detector. In deciding how to couple the input signal (i.e. the signal to be amplified) to the amplifier, and in choosing what quantity to measure, the experimentalist essentially enforces boundary conditions; as we will now show, there are in general two distinct ways in which to do this. For concreteness, consider the situation depicted in Fig. 9: a two-port voltage amplifier where the input and output ports of the amplifier are attached to one-dimensional transmission lines (see App. B for a quick review of quantum transmission lines). Similar to the previous subsection, we focus on a narrow bandwidth signal centered about a frequency ω. At this frequency, there exists both a right-moving and a left-moving wave in each transmission line. We label the corresponding amplitudes in the input (output) line with $a_{\rm in}, a_{\rm out}$ ($b_{\rm in}, b_{\rm out}$), as per Fig. 9. Quantum mechanically, these amplitudes become operators, much in the same way that we treated the mode amplitude a as an operator in the previous subsection. We will analyze this two-port bosonic amplifier in detail in Sec. VII; here, we will only sketch its operation to introduce the two different amplifier operation modes. This will then allow us to understand the subtleties of the Haus-Caves quantum limit derivation.

In the first kind of setup, the experimentalist arranges things so that $a_{\rm in}$, the amplitude of the wave incident on the amplifier's input port, is *precisely* equal to the signal to be amplified (i.e. the input signal), *irrespective* of the amplitude of the wave leaving the input port (i.e. $a_{\rm out}$). Further, the output signal is taken to be the amplitude of the outgoing wave exiting the output of the amplifier (i.e. $\hat{b}_{\rm out}$), again, irrespective of whatever might be entering the output port (see Table III). In this situation, the Haus-Caves description of the quantum limit in the previous subsection is almost directly applicable; we will make this precise in Sec. VII. Back-action is indeed irrelevant, as the prescribed experimental conditions mean that it plays no role. We will call this mode of operation the "scattering mode", as it is most relevant to time-dependent experiments where the experimentalist launches a signal pulse at the amplifier and looks at what exits the output port. One is usually only interested in the scattering mode of operation in cases where the source producing the input signal is matched to the input of the amplifier: only in this case is the input wave $a_{\rm in}$ perfectly transmitted into the amplifier. As we will see in Sec. VII, such a perfect matching requires a relatively strong coupling between the signal source and the input of the amplifier; as such, the amplifier will strongly enhance the damping of the signal source.

The second mode of linear amplifier operation is what we call the "op-amp" mode; this is the mode one usually has in mind when thinking of an amplifier which is weakly coupled to the signal source. The key difference from the "scattering" mode is that here, the input signal *is not* simply the amplitude of a wave incident on the input port of the amplifier; similarly, the output signal *is not* the amplitude of a wave exiting the output port. As such, the Haus-Caves derivation of the quantum limit does not directly apply. For the bosonic amplifier discussed here, the op-amp mode would correspond to using the amplifier as a voltage op-amp. The input signal would thus be the voltage at the end of the input transmission line. Recall from Appendix B that even classically, the voltage at the end of a transmission line involves the amplitude of *both* left and right moving waves, i.e. $V_a(t) \propto \mathrm{Re}\,[a_{\mathrm{in}}(t) + a_{\mathrm{out}}(t)]$. At first, this might seem quite confusing: if the signal source determines $V_a(t)$, does this mean it sets the value of *both* $a_{\mathrm{in}}(t)$ and $a_{\mathrm{out}}(t)$? Doesn't this violate causality? These fears are of course unfounded. The signal source enforces the value of $V_a(t)$ by simply changing $a_{\mathrm{in}}(t)$ in response to the value of $a_{\mathrm{out}}(t)$. While there is no violation of causality, the fact that the signal source is dynamically responding to what comes out of the amplifier's input port implies that back-action is indeed relevant.

The op-amp mode of operation is relevant to the typical situation of weak coupling between the signal source and amplifier input. By weak coupling, we mean that the amplifier does not appreciably change the dissipation of the signal source. This is analogous to the situation in an ideal voltage op-amp, where the amplifier input impedance is much larger than the impedance of the signal source. We stress the op-amp mode and this limit of weak coupling is the relevant situation in most electrical measurements.

Thus, we see that the Haus-Caves formulation of the quantum limit is not directly relevant to amplifiers or detectors operated in the usual op-amp mode of operation. We clearly need some other way to describe quantum amplifiers used in this regime. In the remainder of this section, we will show that the linear-response, quantum noise approach we have been developing provides a convenient and general way to discuss the quantum limit here. The linear response approach will allow us to see (similar to Sec. IV.B.3) that reaching the quantum limit does indeed require a trade-off between back-action and measurement imprecision, and requires use of an amplifier with ideal quantum noise properties (cf. Eq. 5.11). This approach also has the added benefit of being directly applicable to systems where the input and output of the amplifier are not described by bosonic modes [15]. In the next section (Sec. VII), we will return to the scattering description of a two-port voltage amplifier, and show explicitly how an amplifier can be quantum-limited when used in the scattering mode of operation, but miss the quantum limit when used in the op-amp mode of operation.

D. Linear response description of a position detector

In this subsection, we will examine the amplifier quantum limit for a two-port linear amplifier in the usual weak coupling, "op-amp" regime of operation. Our discussion here will make use of the results we have obtained for the noise properties of a generic linear response detector in Sec. V, including the fundamental quantum noise constraint of Eq. (5.11). The approach we use here has the benefits of not being restricted to bosonic systems, and of directly involving noise spectral densities, quantities which can be directly measured in experiment. It provides a rough 'recipe' of what one needs to do in general to reach the quantum limit.

For simplicity, we will start with the concrete problem of continuous position detection of a harmonic oscillator; this will generalize the discussion of Sec. IV.B.3, where we gave a heuristic discussion of weak, continuous position detection using a resonant cavity detector. We now imagine a situation where the generic linear detector introduced in Sec. V.A is weakly coupled at its input to the position $\hat{x}$ of a harmonic oscillator (cf. Eq. (5.1)) [16]. We would like to understand the total output noise of our amplifier in the presence of the oscillator, and, more importantly, how small we can make the amplifier's contribution to this noise. We will discuss the analogous but important quantum limit on the noise temperature of a voltage amplifier in Sec. VI.E. Note that the discussion of a generic position detector presented here is directly applicable to recent experiments with nanoelectromechanical which attempt to reach the quantum limit (Flowers-Jacobs *et al.*, 2007; Knobel and Cleland, 2003; LaHaye *et al.*, 2004; Naik *et al.*, 2006).

1. Detector back-action

We first consider the consequence of noise in the detector input port. As we have already seen in Sec. III.B, the fluctuating back-action force $\hat{F}$ acting on our oscillator will lead to *both* damping and heating of the oscillator. To model the intrinsic (i.e. detector-independent) heating and damping of the oscillator, we will also assume that our oscillator is coupled to an equilibrium heat bath. In

[15] Note that the Haus-Caves derivation for the quantum limit of a scattering amplifier has recently been generalized to the case of fermionic operators (Gavish *et al.*, 2004).

[16] For consistency with previous sections, our coupling Hamiltonian does not have a minus sign. This is different from the convention of Clerk (2004), where the coupling Hamiltonian is written $H_{int} = -A\hat{x} \cdot \hat{F}$.

the weak-coupling limit that we are interested in, one can use lowest-order perturbation theory in the coupling A to describe the effects of the back-action force $\hat{F}$ on the oscillator. While the full quantum theory is somewhat involved (see Appendix J.3), it leads to an extremely simple picture that we can understand even classically. One finds that the oscillator is described by an effective Langevin equation[17]:

$$\begin{aligned} M\ddot{x}(t) &= -M\Omega^2 x(t) - M\gamma_0 \dot{x}(t) + F_0(t) \\ &- MA^2 \int dt' \gamma(t-t')\dot{x}(t') - A \cdot F(t) \end{aligned} \tag{6.14}$$

The position $x(t)$ in the above equation is *not* an operator, but is simply a classical variable whose fluctuations are driven by the fluctuating forces $F(t)$ and $F_0(t)$. Nonetheless, the noise in x calculated from Eq. (6.14) corresponds precisely to $\bar{S}_{xx}[\omega]$, the *symmetrized* quantum mechanical noise in the operator $\hat{x}$ (see Appendix J.3 for the justification of this statement). The fluctuating force exerted by the detector (which represents the heating part of the back-action) is described by $A \cdot F(t)$ in Eq. (6.14); it has zero mean, and a spectral density given by $A^2\bar{S}_{FF}[\omega]$ in Eq. (5.4a). The kernel $\gamma(t)$ describes the damping effect of the detector. It is given by the *asymmetric* part of the detector's quantum noise, as was derived in Sec. III.B (cf. Eq. ((3.32)). Recall that the damping effect of the back-action has a simple origin: the *average* force exerted on the oscillator by the amplifier responds to the motion of the oscillator.

Eq. (6.14) also describes the effects of an equilibrium heat bath at temperature T_0 which models the intrinsic (i.e. detector-independent) damping and heating of the oscillator. γ_0 is the damping arising from this bath, and F_0 is the corresponding fluctuating force. The spectral density of the F_0 noise is determined by γ_0 and T_0 via the fluctuation-dissipation theorem (cf. Eq. (3.34)). T_0 and γ_0 have a simple physical significance: they are the temperature and damping of the oscillator when the coupling to the detector A is set to zero.

To make further progress, we recall from Sec. III.B that even though our detector will in general *not* be in equilibrium, we may nonetheless assign it an effective temperature $T_{\text{eff}}[\omega]$ at each frequency (cf. Eq. (3.21)). In general, this effective temperature is not reflective of some physical temperature in the detector; it also does not correspond to the "noise temperature" of the detector that will be discussed in what follows. The effective temperature of an out-of-equilibrium detector is simply a measure of the asymmetry of the detector's quantum noise. We are often interested in the limit where the internal detector timescales are much faster than the timescales relevant to the oscillator (i.e. $\Omega^{-1}, \gamma^{-1}, \gamma_0^{-1}$). We may then take the $\omega \to 0$ limit in the expression for T_{eff}, yielding:

$$2k_{\text{B}}T_{\text{eff}} \equiv \frac{\bar{S}_{FF}(0)}{M\gamma(0)} \tag{6.15}$$

In this limit, the oscillator position noise calculated from Eq. (6.14) is given by:

$$\bar{S}_{xx}[\omega] = \frac{1}{M} \frac{2(\gamma_0+\gamma)k_{\text{B}}}{(\omega^2-\Omega^2)^2 + \omega^2(\gamma+\gamma_0)^2} \frac{\gamma_0 T + \gamma T_{\text{eff}}}{\gamma_0+\gamma} \tag{6.16}$$

This is exactly what would be expected if the oscillator were *only* attached to an equilibrium Ohmic bath with a damping coefficient $\gamma_\Sigma = \gamma_0 + \gamma$ and temperature $\bar{T} = (\gamma_0 T + \gamma T_{\text{eff}})/\gamma_\Sigma$.

2. Total output noise

The next step in our analysis is to link fluctuations in the position of the oscillator (as determined from Eq. (6.14)) to noise in the output of the detector. As discussed in Sec. IV.B.3, the output noise consists of the intrinsic output noise of the detector (i.e. "measurement imprecision noise") plus the amplified position fluctuations in the position of the oscillator. The latter contains both an intrinsic part and a term due to the response of the oscillator to the back action.

To start, imagine that we can treat both the oscillator position $x(t)$ and the detector output $I(t)$ as classically fluctuating quantities. Using the linearity of the detector's response, we can then write δI_{total}, the fluctuating part of the detector's output, as:

$$\delta I_{\text{total}}[\omega] \;=\; \delta I_0[\omega] + A\chi_{IF}[\omega] \cdot \delta x[\omega] \tag{6.17}$$

The first term (δI_0) describes the intrinsic (oscillator-independent) fluctuations in the detector output, and has a spectral density $\bar{S}_{II}[\omega]$. If we scale this by $|\chi_{IF}|^2$, we have the measurement imprecision noise discussed in Sec. IV.B.3. The second term corresponds to the amplified fluctuations of the oscillator, which are in turn given by solving Eq. (6.14):

$$\begin{aligned} \delta x[\omega] \;&=\; -\left[\frac{1/M}{(\omega^2-\Omega^2) + i\omega\Omega/Q[\omega]}\right](F_0[\omega] - A\cdot F[\omega]) \\ &\equiv\; -\chi_{xx}[\omega](F_0[\omega] - A\cdot F[\omega]) \end{aligned} \tag{6.18}$$

where $Q[\omega] = \Omega/(\gamma_0 + \gamma[\omega])$ is the oscillator quality factor. It follows that the spectral density of the total noise in the detector output is given *classically* by:

$$\begin{aligned} \mathcal{S}_{II,\text{tot}}[\omega] \;&=\; \mathcal{S}_{II}[\omega] \\ &+\; |\chi_{xx}[\omega]\chi_{IF}[\omega]|^2 \left(A^4\mathcal{S}_{FF}[\omega] + A^2\mathcal{S}_{F_0F_0}[\omega]\right) \\ &+\; 2A^2 \text{Re}\;[\chi_{xx}[\omega]\chi_{IF}[\omega]\mathcal{S}_{IF}[\omega]] \end{aligned} \tag{6.19}$$

[17] Note that we have omitted a back-action term in this equation which leads to small renormalizations of the oscillator frequency and mass. These terms are not important for the following discussion, so we have omitted them for clarity; one can consider M and Ω in this equation to be renormalized quantities. See Appendix J.3 for more details.

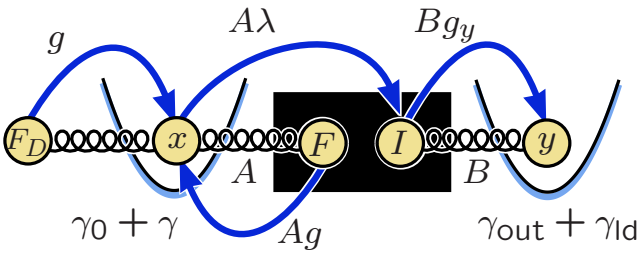

FIG. 11 (Color online) Schematic of a generic linear-response position detector, where a auxiliary oscillator y is driven by the detector output.

Here, $\mathcal{S}_{II}, \mathcal{S}_{FF}$ and $\mathcal{S}_{IF}$ are the (classical) detector noise correlators calculated in the absence of any coupling to the oscillator. Note importantly that we have included the fact that the two kinds of detector noise (in $\hat{I}$ and in $\hat{F}$) may be correlated with one another.

To apply the classically-derived Eq. (6.19) to our quantum detector-plus-oscillator system, we recall from Sec. III.B that symmetrized quantum noise spectral densities play the role of classical noise. The LHS of Eq. (6.19) thus becomes $S_{II,\rm tot}$, the total *symmetrized* quantum-mechanical output noise of the detector, while the RHS will now contain the symmetrized quantum-mechanical detector noise correlators $\bar{S}_{FF}$, $\bar{S}_{II}$ and $\bar{S}_{IF}$, defined as in Eq. (5.4a). Though this may seem rather ad-hoc, one can easily demonstrate that Eq. (6.19) thus interpreted would be quantum-mechanically rigorous *if* the detector correlation functions obeyed Wick's theorem. Thus, quantum corrections to Eq. (6.19) will arise solely from the non-Gaussian nature of the detector noise correlators. We expect from the central limit theorem that such corrections will be small in the relevant limit where ω is much smaller that the typical detector frequency $\sim k_{\rm B}T_{\rm eff}/\hbar$, and neglect these corrections in what follows. Note that the validity of Eq. (6.19) for a specific model of a tunnel junction position detector has been explicitly verified in Clerk and Girvin (2004).

3. Detector power gain

Before proceeding, we need to consider our detector once again in isolation, and return to the fundamental question of what we mean by amplification. To be able to say that our detector truly amplifies the motion of the oscillator, it is not sufficient to simply say the response function χ_{IF} must be large (note that χ_{IF} is not dimensionless!). Instead, true amplification requires that the *power* delivered by the detector to a following amplifier be much larger than the power drawn by the detector at its input– i.e., the detector must have a dimensionless power gain $G_P[\omega]$ much larger than one. If the power gain was not large, we would need to worry about the next stage in the amplification of our signal, and how much noise is added in that process. Having a large power gain means that by the time our signal reaches the following amplifier, it is so large that the added noise of this following amplifier is unimportant. The power gain is analogous to the dimensionless photon number gain G that appears in the standard Haus-Caves description of a bosonic linear amplifier.

To make the above more precise, we start by assuming the simple (and usual) case where there is no reverse gain: $\chi_{FI} = 0$. We will define the power gain $G_P[\omega]$ of our generic position detector in a way that is completely analogous to the power gain of a voltage amplifier [CITE]; alternate and important measures of power gain are discussed in Sec. VIII.B. Imagine we drive the oscillator we are trying to measure with a force $2F_D \cos\omega t$; this will cause the output of our detector $\langle \hat{I}(t) \rangle$ to also oscillate at frequency ω. To optimally detect this signal in the detector output, we further couple the detector output I to a second oscillator with natural frequency ω, mass M, and position y: there is a new coupling term in our Hamiltonian, $H'_{int} = B\hat{I}\cdot\hat{y}$, where B is a coupling strength. The oscillations in $\langle I(t) \rangle$ will now act as a driving force on the auxiliary oscillator y (see Fig 11). We can consider the auxiliary oscillator y as a "load" we are trying to drive with the output of our detector.

To find the power gain, we need to consider both $P_{\rm out}$, the power supplied to the output oscillator y from the detector, and $P_{\rm in}$, the power fed into the input of the amplifier. Consider first $P_{\rm in}$. This is simply the time-averaged power dissipation of the input oscillator x caused by the back-action damping $\gamma[\omega]$. Using a bar to denote a time average, we have:

$$\begin{aligned} P_{\rm in} &\equiv M\gamma[\omega]\cdot\overline{\dot{x}^2} \\ &= M\gamma[\omega]\omega^2|\chi_{xx}[\omega]|^2 F_D^2 \end{aligned} \tag{6.20}$$

The oscillator response function $\chi_{xx}[\omega]$ is defined in Eq. (6.18); note that it depends on both the back-action damping $\gamma[\omega]$ as well as the intrinsic oscillator damping γ_0.

Next, we need to consider the power supplied to the "load" oscillator y at the detector output. This oscillator will have some intrinsic, detector-independent damping $\gamma_{\rm ld}$, as well as a back-action damping $\gamma_{\rm out}$. In the same way that the back-action damping γ of the input oscillator x is determined by the quantum noise in $\hat{F}$ (cf. Eq. (3.30)-(3.32)), the back-action damping of the load oscillator y is determined by the quantum noise in the output operator $\hat{I}$:

$$\begin{aligned} \gamma_{\rm out}[\omega] &= \frac{B^2}{M\omega}\left[-{\rm Im}\ \chi_{II}[\omega]\right] \\ &= \frac{B^2}{M\hbar\omega}\left[\frac{S_{II}[\omega]-S_{II}[-\omega]}{2}\right] \end{aligned} \tag{6.21}$$

where χ_{II} is the linear-response susceptibility which determines how $\langle \hat{I} \rangle$ responds to a perturbation coupling to

$\hat{I}$:

$$\chi_{II}[\omega] = -\frac{i}{\hbar}\int_0^\infty dt \left\langle \left[\hat{I}(t), \hat{I}(0)\right]\right\rangle e^{i\omega t} \qquad (6.22)$$

As the oscillator y is being driven on resonance, the relation between y and I is given by $y[\omega] = \chi_{yy}[\omega]I[\omega]$ with $\chi_{yy}[\omega] = -i[\omega M\gamma_{\rm out}[\omega]]^{-1}$. From conservation of energy, we have that the *net* power flow into the output oscillator from the detector is equal to the power dissipated out of the oscillator through the intrinsic damping $\gamma_{\rm ld}$. We thus have:

$$\begin{aligned} P_{\rm out} &\equiv M\gamma_{\rm ld}\cdot\overline{\dot{y}^2} \\ &= M\gamma_{\rm ld}\omega^2|\chi_{yy}[\omega]|^2\cdot|BA\chi_{IF}\chi_{xx}[\omega]F_D|^2 \\ &= \frac{1}{M}\frac{\gamma_{\rm ld}}{(\gamma_{\rm ld}+\gamma_{\rm out}[\omega])^2}\cdot|BA\chi_{IF}\chi_{xx}[\omega]F_D|^2 \end{aligned} \qquad (6.23)$$

Using the above definitions, we find that the ratio between $P_{\rm out}$ and $P_{\rm in}$ is independent of γ_0, but depends on $\gamma_{\rm ld}$:

$$\frac{P_{\rm out}}{P_{\rm in}} = \frac{1}{M^2\omega^2}\frac{A^2B^2|\chi_{IF}[\omega]|^2}{\gamma_{\rm out}[\omega]\gamma[\omega]}\frac{\gamma_{\rm ld}/\gamma_{\rm out}[\omega]}{(1+\gamma_{\rm ld}/\gamma_{\rm out}[\omega])^2} \qquad (6.24)$$

We now define the detector power gain $G_P[\omega]$ as the value of this ratio maximized over the choice of $\gamma_{\rm ld}$. The maximum occurs for $\gamma_{\rm ld} = \gamma_{\rm out}[\omega]$ (i.e. the load oscillator is "matched" to the output of the detector), resulting in:

$$\begin{aligned} G_P[\omega] &\equiv \max\left[\frac{P_{\rm out}}{P_{\rm in}}\right] \\ &= \frac{1}{4M^2\omega^2}\frac{A^2B^2|\chi_{IF}|^2}{\gamma_{\rm out}\gamma} \\ &= \frac{|\chi_{IF}[\omega]|^2}{4{\rm Im}\ \chi_{FF}[\omega]\cdot{\rm Im}\ \chi_{II}[\omega]} \end{aligned} \qquad (6.25)$$

In the last line, we have used the relation between the damping rates $\gamma[\omega]$ and $\gamma_{\rm out}[\omega]$ and the linear-response susceptibilities $\chi_{FF}[\omega]$ and $\chi_{II}[\omega]$ (c.f. Eqs. (3.31) and (6.21)). We thus find that the power gain is a simple dimensionless ratio formed by the three different response coefficients characterizing the detector, and is independent of the coupling constants A and B. As we will see in subsection VI.E, it is completely analogous to the power gain of a voltage amplifier, which is also determined by three parameters: the voltage gain, the input impedance and the output impedance. Note that there are other important measures of power gain commonly in use in the engineering community: we will comment on these in Sec. VIII.B.

4. Simplifications for a quantum-ideal detector

We now consider the important case where our detector has "ideal" quantum noise (i.e. it satisfies the ideal noise condition of Eq. (5.16)). Fulfilling this condition immediately places some powerful constraints on our detector.

First, note that we have defined in Eq. (6.15) the effective temperature of our detector based on what happens at the input port; this is the effective temperature seen by the oscillator we are trying to measure. We could also consider the effective temperature of the detector as seen at the output (i.e. by the oscillator y used in defining the power gain). This "output" effective temperature is determined by the quantum noise in the output operator $\hat{I}$:

$$k_{\rm B}T_{\rm eff,out}[\omega] \equiv \frac{\hbar\omega}{\log\left(S_{II}[+\omega]/S_{II}[-\omega]\right)} \qquad (6.26)$$

For a general out-of-equilibrium amplifier, $T_{\rm eff,out}$ does not have to be equal to the input effective temperature $T_{\rm eff}$ defined by Eq. (3.21). However, for a quantum-ideal detector, the effective proportionality between input and output operators (cf. Eq. (J13)) immediately yields:

$$T_{\rm eff,out}[\omega] = T_{\rm eff}[\omega] \qquad (6.27)$$

Thus, a detector with quantum-ideal noise necessarily has the same effective temperature at its input and its output. This is all the more remarkable given that a quantum-ideal detector *cannot* be in equilibrium, and thus $T_{\rm eff}$ cannot represent a real physical temperature.

Another important simplification for a quantum-ideal detector is the expression for the power gain. Using the proportionality between input and output operators (cf. Eq. (J13)), one finds:

$$G_P[\omega] = \frac{({\rm Im}\ \alpha)^2\coth^2\left(\frac{\hbar\omega}{2k_{\rm B}T_{\rm eff}}\right) + ({\rm Re}\ \alpha)^2}{|\alpha|^2} \qquad (6.28)$$

where $\alpha[\omega]$ is the parameter characterizing a quantum limited detector in Eq. (5.17); recall that $|\alpha[\omega]|^2$ determines the ratio of S_{II} and S_{FF}. It follows immediately that for a detector with 'ideal noise' to also have a large power gain ($G_P \gg 1$), one absolutely needs $kbT_{\rm eff} \gg \hbar\omega$: *a large power gain implies a large effective detector temperature.* In the large G_P limit, we have

$$G_P \simeq \left[\frac{{\rm Im}\ \alpha}{|\alpha|}\frac{k_{\rm B}T_{\rm eff}}{\hbar\omega/2}\right]^2 \qquad (6.29)$$

Thus, the effective temperature of a quantum-ideal detector does more than just characterize the detector backaction– it also determines the power gain.

Finally, an additional consequence of the large $G_P[\omega]$, large $T_{\rm eff}$ limit is that the gain χ_{IF} and noise cross-correlator $\bar{S}_{IF}$ are in phase: $\bar{S}_{IF}/\chi_{IF}$ is purely real, up to corrections which are small as $\omega/T_{\rm eff}$. This is shown explicitly in Appendix J.2. Thus, we find that *a large power gain detector with ideal quantum noise cannot have significant out-of-phase correlations between its output and input noises.* This last point may be understood in terms

of the idea of wasted information: if there were significant out-of-phase correlations between $\hat{I}$ and $\hat{F}$, it would be possible to improve the performance of the amplifier by using feedback. We will discuss this point more fully in Sec. VII. Note that as $\bar{S}_{IF}/\chi_{IF}$ is real, the last term in the quantum noise constraint of Eq. (5.11) vanishes.

5. Quantum limit on added noise and noise temperature

We now turn to calculating the noise added to our signal (i.e. $\langle \hat{x}(t) \rangle$) by our generic position detector. To characterize this added noise, it is useful to take the total (symmetrized) noise in the output of the detector, and refer it back to the input by dividing out the gain of the detector:

$$\bar{S}_{xx,\mathrm{tot}}[\omega] \equiv \frac{\bar{S}_{II,\mathrm{tot}}[\omega]}{A^2 |\chi_{IF}[\omega]|^2} \tag{6.30}$$

$\bar{S}_{xx,\mathrm{tot}}[\omega]$ is simply the frequency-dependent spectral density of position fluctuations inferred from the output of the detector. It is this quantity which will directly determine the sensitivity of the detector– given a certain detection bandwidth, what is the smallest variation of x that can be resolved? The quantity $\bar{S}_{xx,\mathrm{tot}}[\omega]$ will have contributions both from the intrinsic fluctuations of the input signal, as well as a contribution due to the detector. We first define $\bar{S}_{xx,\mathrm{eq}}[\omega, T]$ to be the symmetrized equilibrium position noise of our damped oscillator (whose damping is $\gamma_0 + \gamma$) at temperature T:

$$\bar{S}_{xx,\mathrm{eq}}[\omega, T] = \hbar \coth\left(\frac{\hbar\omega}{2k_{\mathrm{B}}T}\right) [-\mathrm{Im}\ \chi_{xx}[\omega]] \tag{6.31}$$

where the oscillator susceptibility $\chi_{xx}[\omega]$ is defined in Eq. (6.18). The total inferred position noise may then be written:

$$\bar{S}_{xx,\mathrm{tot}}[\omega] \equiv \left(\frac{\gamma_0}{\gamma_0 + \gamma}\right) \cdot \bar{S}_{xx,\mathrm{eq}}[\omega, T_0] + \bar{S}_{xx,\mathrm{add}}[\omega] \tag{6.32}$$

In the usual case where the detector noise can be approximated as being white, this spectral density will consist of a Lorentzian sitting atop a constant noise floor (c.f. Fig. 7) The first term in Eq. (6.32) represents position noise arising from the fluctuating force $\delta F_0(t)$ associated with the intrinsic (detector-independent) dissipation of the oscillator (c.f. Eq. (6.14)). The prefactor of this term arises because the strength of the intrinsic Langevin force acting on the oscillator is proportional to γ_0, not to $\gamma_0 + \gamma$.

The second term in Eq. (6.32) represents the added position noise due to the detector. It has contributions from both from the detector's intrinsic output noise $\bar{S}_{II}$ as well as from the detector's back-action noise $\bar{S}_{FF}$, and may be written:

$$\bar{S}_{xx,\mathrm{add}}[\omega] = \frac{\bar{S}_{II}}{|\chi_{IF}|^2 A^2} + A^2 |\chi_{xx}[\omega]|^2 \bar{S}_{FF} + \frac{2\mathrm{Re}\left[\chi^*_{IF} \left(\chi_{xx}[\omega]\right)^* \bar{S}_{IF}\right]}{|\chi_{IF}|^2} \tag{6.33}$$

For clarity, we have omitted writing the explicit frequency dependence of the gain χ_{IF} and noise correlators; they should all be evaluated at the frequency ω. Note that the first term on the RHS corresponds to the "measurement imprecision" noise of our detector, $\bar{S}^I_{xx}(\omega)$.

We can now finally address the issue of the quantum limit in our system. As discussed in Sec. VI.C, the Haus-Caves derivation of the quantum limit (c.f. Sec. VI.B) is not directly applicable to the position detector we are describing here; nonetheless, we may use its result to guess what form the quantum limit will take here. The Haus-Caves argument told us that the added noise of a phase-preserving linear amplifier must be at least as large as the zero point noise. We thus anticipate that if our detector has a large power gain, the spectral density of the noise added by the detector (i.e. $\bar{S}_{xx,\mathrm{add}}[\omega]$) must be at least as big as the zero point noise of our damped oscillator:

$$\bar{S}_{xx,\mathrm{add}}[\omega] \geq \lim_{T\to 0} \bar{S}_{xx,\mathrm{eq}}[w, T] = |\hbar \mathrm{Im}\ \chi_{xx}[\omega]| \tag{6.34}$$

We will now show that the bound above is rigorously correct at each frequency ω. Moreover, the approach we take will give us a rough idea of what one needs to do to achieve this quantum limit.

The first step is to examine the dependence of the added noise $\bar{S}_{xx,\mathrm{add}}[\omega]$ (as given by Eq. (6.33)) on the coupling strength A. If we ignore for a moment the detector-dependent damping of the oscillator, the situation is the same as the cavity position detector of Sec. IV.B.3: there is an optimal value of the coupling strength A. For very strong coupling, we will minimize the effects of the intrinsic output noise of the detector (first term in Eq. (6.33)), but the back-action noise will make a large contribution (second term in Eq. (6.33)). Conversely, for very weak couplings we minimize the back-action effect, but make the relative importance of the intrinsic output noise of the detector quite strong. We would thus expect $\bar{S}_{xx,\mathrm{add}}[\omega]$ to attain a minimum value at an optimal choice of coupling $A = A_{\mathrm{opt}}$ where both these terms make equal contributions (see Fig. 6). Defining $\phi[\omega] = \arg \chi_{xx}[\omega]$, we thus have the bound:

$$\bar{S}_{xx,\mathrm{add}}[\omega] \geq 2|\chi_{xx}[\omega]| \left[\sqrt{\frac{\bar{S}_{II}\bar{S}_{FF}}{|\chi_{IF}|^2}} + \frac{\mathrm{Re}\left[\chi^*_{IF} e^{-i\phi[\omega]} \bar{S}_{IF}\right]}{|\chi_{IF}|^2}\right] \tag{6.35}$$

where the minimum value at frequency ω is achieved when:

$$A^2_{\mathrm{opt}} = \sqrt{\frac{\bar{S}_{II}[\omega]}{|\chi_{IF}[\omega]\chi_{xx}[\omega]|^2 \bar{S}_{FF}[\omega]}} \tag{6.36}$$

Using the inequality $X^2 + Y^2 \geq 2|XY|$ we see that this value serves as a lower bound on $\bar{S}_{xx,\mathrm{add}}$ even in the presence of detector-dependent damping. In the case where the detector-dependent damping is negligible, the RHS of Eq. (6.35) is independent of A, and thus Eq. (6.36) can be satisfied by simply tuning the coupling strength A; in

the more general case where there is detector-dependent damping, the RHS is also a function of A (through the response function $\chi_{xx}[\omega]$), and it may no longer be possible to achieve Eq. (6.36) by simply tuning A[18].

While Eq. (6.35) is certainly a bound on the added displacement noise $\bar{S}_{xx,\rm add}[\omega]$, it does not in itself represent the quantum limit. Reaching the quantum limit requires more than simply balancing the detector back-action and intrinsic output noises (i.e. the first two terms in Eq. (6.33)); *one also needs a detector with "quantum-ideal" noise properties, that is a detector which satisfies Eq. (5.16) and thus the proportionality condition of Eq. (J13).* Using the quantum noise constraint of Eq. (5.11) to further bound $\bar{S}_{xx,\rm add}[\omega]$, we obtain:

$$\bar{S}_{xx,\rm add}[\omega] \geq 2\left|\frac{\chi_{xx}[\omega]}{\chi_{IF}}\right| \times \left[\sqrt{\left(\frac{\hbar|\chi_{IF}|}{2}\right)^2\left(1+\Delta\left[\frac{2\bar{S}_{IF}}{\hbar\chi_{IF}}\right]\right)+|\bar{S}_{IF}|^2} + \frac{\mathrm{Re}\,\left[\chi_{IF}^* e^{-i\phi[\omega]}\bar{S}_{IF}\right]}{|\chi_{IF}|}\right] \quad (6.37)$$

where the function $\Delta[z]$ is defined in Eq. (5.10b). The minimum value of $\bar{S}_{xx,\rm add}[\omega]$ in Eq. (6.37) is now achieved when one has *both* an optimal coupling (i.e. Eq. (6.36)) *and* a quantum limited detector, that is one which satisfies Eq. (5.11) as an equality. Note again that *an arbitrary detector will not satisfy this ideal noise condition.*

Next, we consider the relevant case where our detector is a good amplifier and has a power gain $G_P[\omega] \gg 1$ over the width of the oscillator resonance. As we have discussed, this implies that the ratio $\bar{S}_{IF}/\chi_{IF}$ is purely real, up to small $\hbar\omega/(k_{\rm B}T_{\rm eff})$ corrections (see Sec. (V.A.4) and Appendix J.2 for more details). This in turn implies that $\Delta[2\bar{S}_{IF}/\hbar\chi_{IF}] = 0$; we thus have:

$$\bar{S}_{xx,\rm add}[\omega] \geq 2|\chi_{xx}[\omega]|\left[\sqrt{\left(\frac{\hbar}{2}\right)^2+\left(\frac{\bar{S}_{IF}}{\chi_{IF}}\right)^2}+\frac{\cos\left[\phi[\omega]\right]\bar{S}_{IF}}{\chi_{IF}}\right] \quad (6.38)$$

Finally, as there is no further constraint on $\bar{S}_{IF}/\chi_{IF}$ (beyond the fact that it is real), we can minimize the expression over its value. The minimum $\bar{S}_{xx,\rm add}[\omega]$ is achieved for a detector whose cross-correlator satisfies:

$$\left.\frac{\bar{S}_{IF}[\omega]}{\chi_{IF}}\right|_{\rm optimal} = -\frac{\hbar}{2}\cot\phi[\omega], \quad (6.39)$$

with the minimum value being given by:

$$\left.\bar{S}_{xx,\rm add}[\omega]\right|_{min} = \hbar|\mathrm{Im}\;\chi_{xx}[\omega]| = \lim_{T\to 0}\bar{S}_{xx,\rm eq}[\omega,T] \quad (6.40)$$

where $\bar{S}_{xx,\rm eq}[\omega,T]$ is the equilibrium contribution to $\bar{S}_{xx,\rm tot}[\omega]$ defined in Eq. (6.31). Thus, in the limit of a large power gain, we have that *at each frequency, the minimum displacement noise added by the detector is precisely equal to the noise arising from a zero temperature bath.* This conclusion is irrespective of the strength of the intrinsic (detector-independent) oscillator damping.

We have thus derived the amplifier quantum limit (in the context of position detection) for a two-port amplifier used in the "op-amp" mode of operation. Though we reached a conclusion similar to that given by the Haus-Caves approach, the linear-response, quantum noise approach used is quite different. This approach makes explicitly clear what is needed to reach the quantum limit. We find that to reach the quantum-limit on the added displacement noise $\bar{S}_{xx,\rm add}[\omega]$ with a large power gain, one needs:

1. A quantum limited detector, that is a detector which satisfies the "ideal noise" condition of Eq. (5.16), and hence the proportionality condition of Eq. (J13).
2. A coupling A which satisfies Eq. (6.36).
3. A detector cross-correlator $\bar{S}_{IF}$ which satisfies Eq. (6.39).

Note that condition (1) is identical to what is required for quantum-limited detection of a qubit; it is rather demanding, and requires that there is no "wasted" information about the input signal in the detector which is not revealed in the output (Clerk *et al.*, 2003). Also note that $\cot\phi$ changes quickly as a function of frequency across the oscillator resonance, whereas $\bar{S}_{IF}$ will be roughly constant; condition (2) thus implies that it will not be possible to achieve a minimal $\bar{S}_{xx,\rm add}[\omega]$ across the entire oscillator resonance. A more reasonable goal is to optimize $\bar{S}_{xx,\rm add}[\omega]$ at resonance, $\omega = \Omega$. As $\chi_{xx}[\Omega]$ is imaginary, Eq. (6.39) tells us that $\bar{S}_{IF}$ should be zero. Assuming we have a quantum-limited detector with a large power gain ($k_{\rm B}T_{\rm eff} \gg \hbar\Omega$), the remaining condition on the coupling A (Eq. (6.36)) may be written as:

$$\frac{\gamma[A_{\rm opt}]}{\gamma_0+\gamma[A_{\rm opt}]} = \left|\frac{\mathrm{Im}\;\alpha}{\alpha}\right|\frac{1}{2\sqrt{G_P[\Omega]}} = \frac{\hbar\Omega}{4k_{\rm B}T_{\rm eff}} \quad (6.41)$$

As $\gamma[A] \propto A^2$ is the detector-dependent damping of the oscillator, we thus have that *to achieve the quantum-limited value of $\bar{S}_{xx,\rm add}[\Omega]$ with a large power gain, one needs the intrinsic damping of the oscillator to be much larger than the detector-dependent damping.* The detector-dependent damping must be small enough to compensate the large effective temperature of the detector; if the bath temperature satisfies $\hbar\Omega/k_{\rm B} \ll T_{\rm bath} \ll T_{\rm eff}$, Eq. (6.41) implies that at the quantum limit, the temperature of the oscillator will be given by:

$$T_{\rm osc} \equiv \frac{\gamma\cdot T_{\rm eff}+\gamma_0\cdot T_{\rm bath}}{\gamma+\gamma_0} \to \frac{\hbar\Omega}{4k_{\rm B}}+T_{\rm bath} \quad (6.42)$$

[18] Note that in the heuristic discussion of position detection using a resonant cavity detector in Sec. IV.B.3, these concerns did not arise as there was no back-action damping.

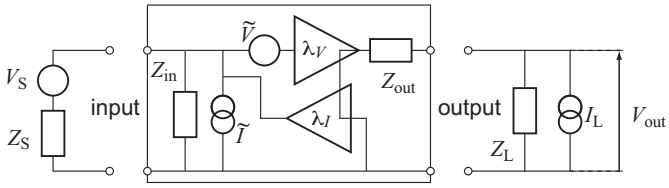

FIG. 12 Schematic of a linear voltage amplifier, including a reverse gain λ_I. $\tilde{V}$ and $\tilde{I}$ represent the standard voltage and current noises of the amplifier, as discussed further in the text. The case with reverse gain is discussed in detail in Sec. VII.

Thus, at the quantum limit and for large $T_{\rm eff}$, the detector raises the oscillator's temperature by $\hbar\Omega/4k_{\rm B}$ [19]. As expected, this additional heating is only *half* the zero-point energy; in contrast, the quantum-limited value of $\bar{S}_{xx,\rm add}[\omega]$ corresponds to the full zero-point result, as it also includes the contribution of the intrinsic output noise of the detector.

Finally, we return to Eq. (6.37); this is the constraint on the added noise $\bar{S}_{xx,\rm add}[\omega]$ *before* we assumed our detector to have a large power gain, and consequently a large $T_{\rm eff}$. Note crucially that *if* we did not require a large power gain, then there need not be *any* added noise. Without the assumption of a large power gain, the ratio $\bar{S}_{IF}/\chi_{IF}$ can be made imaginary with a large magnitude. In this limit, $1+\Delta[2\bar{S}_{IF}/\chi_{IF}] \to 0$: the quantum constraint on the amplifier noises (e.g. the RHS of Eq. (5.11)) vanishes. One can then easily use Eq. (6.37) to show that the added noise $\bar{S}_{xx,\rm add}[\omega]$ can be zero. Thus, similar to the results of Heffner (1962), Haus and Mullen (1962) and Caves (1982), in the limit of unit power gain (i.e. small detector effective temperature), there is no quantum limit on $\bar{S}_{xx,\rm add}$, as perfect anti-correlations between the two kinds of detector noise (i.e. in $\hat{I}$ and $\hat{F}$) are possible. Phrased differently, if our detector does not amplify, then it need not add any noise.

E. Quantum limit on the noise temperature of a voltage amplifier

In this section, we turn our attention to the quantum limit on the added noise of a generic linear voltage amplifier (Devoret and Schoelkopf, 2000). For such amplifiers, the added noise is usually expressed in terms of the "noise temperature" of the amplifier; we will define this concept, and demonstrate that, when appropriately defined, this noise temperature must be bigger than $\hbar\omega/(2k_{\rm B})$, where ω is the signal frequency. Though the voltage amplifier is closely analogous to the position detector treated in the previous section, it is important enough that we will consider it again in some detail. In Sec. VII, we will again discuss a two-port voltage amplifier using a bosonic scattering description similar to that used in formulating the Haus-Caves proof of the amplifier quantum limit; this will allow further insights into what is needed to reach the quantum limit, and how different modes of amplifier operation are not equivalent. We stress that the general treatment presented here can also be applied directly to the system discussed in Sec. VII.

1. Classical description of a voltage amplifier

Let us begin by recalling the standard schematic description of a voltage amplifier, see Figs. 12. The input voltage to be amplified $v_{\rm in}(t)$ is produced by a circuit which has a Thevenin-equivalent impedance $Z_{\rm s}$, the source impedance. We stress that we are considering the "op-amp" mode of amplifier operation, and thus the input signal does not correspond to the amplitude of a wave incident upon the amplifier (see Sec. VI.C). The amplifier itself has an input impedance $Z_{\rm in}$ and an output impedance $Z_{\rm out}$, as well a voltage gain coefficient λ_V: assuming no current is drawn at the output (i.e. $Z_{\rm load}\to\infty$ in Fig. 12), the output voltage $V_{\rm out}(t)$ is simply λ_V times the voltage across the input terminals of the amplifier.

The added noise of the amplifier is standardly represented by two noise sources placed at the amplifier input. There is both a voltage noise source $\tilde{V}(t)$ in series with the input voltage source, and a current noise source $\tilde{I}(t)$ in parallel with input voltage source (Fig. 12). The voltage noise produces a fluctuating voltage $\tilde{V}(t)$ (spectral density $\mathcal{S}_{\tilde{V}\tilde{V}}[\omega]$) which simply adds to the signal voltage at the amplifier input, and is amplified at the output; as such, it is completely analogous to the intrinsic detector output noise $\mathcal{S}_{II}$ of our linear response detector. In contrast, the current noise source of the voltage amplifier represents back-action: this fluctuating current (spectral density $\mathcal{S}_{\tilde{I}\tilde{I}}[\omega]$) flows back across the parallel combination of the source impedance and amplifier input impedance, producing an additional fluctuating voltage at its input. The current noise is thus analogous to the back-action noise $\mathcal{S}_{FF}$ of our generic linear response detector.

Putting the above together, the total voltage at the input terminals of the amplifier is:

$$\begin{aligned} v_{\rm in,tot}(t) &= \frac{Z_{\rm in}}{Z_{\rm in}+Z_{\rm s}}\left[v_{\rm in}(t)+\tilde{V}(t)\right]-\frac{Z_{\rm s}Z_{\rm in}}{Z_{\rm s}+Z_{\rm in}}\tilde{I}(t) \\ &\simeq v_{\rm in}(t)+\tilde{V}(t)-Z_{\rm s}\tilde{I}(t) \end{aligned} \tag{6.43}$$

In the second line, we have taken the usual limit of an ideal voltage amplifier which has an infinite input impedance (i.e. the amplifier draws zero current). The spectral density of the total input voltage fluctuations is thus:

$$\mathcal{S}_{VV,\rm tot}[\omega]=\mathcal{S}_{v_{\rm in}v_{\rm in}}[\omega]+\mathcal{S}_{VV,\rm add}[\omega]. \tag{6.44}$$

[19] If in contrast our oscillator was initially at zero temperature (i.e. $T_{bath}=0$), one finds that the effect of the back-action (at the quantum limit and for $G_P\gg 1$) is to heat the oscillator to a temperature $\hbar\Omega/(k_{\rm B}\ln 5)$.

Here $\mathcal{S}_{v_{\rm in}v_{\rm in}}$ is the spectral density of the voltage fluctuations of the input signal $v_{\rm in}(t)$, and $S_{VV,\rm add}$ is the amplifier's contribution to the total noise at the input:

$$\mathcal{S}_{VV,\rm add}[\omega] = \mathcal{S}_{\tilde{V}\tilde{V}} + |Z_{\rm s}|^2 \mathcal{S}_{\tilde{I}\tilde{I}} - 2{\rm Re}\left[Z_{\rm s}^* \mathcal{S}_{\tilde{V}\tilde{I}}\right] \tag{6.45}$$

For clarity, we have dropped the frequency index for the spectral densities appearing on the RHS of this equation.

It is useful to now consider a narrow bandwidth input signal at a frequency ω, and ask the following question: *if* the signal source was simply an equilibrium resistor at a temperature T_0, how much hotter would it have to be to produce a voltage noise equal to $\mathcal{S}_{VV,\rm tot}[\omega]$? The resulting increase in the source temperature is defined as the noise temperature $T_{\rm N}[\omega]$ of the amplifier and is a convenient measure of the amplifier's added noise. It is standard among engineers to define the noise temperature assuming the initial temperature of the resistor $T_0 \gg \hbar\omega$. One may then use the classical expression for the thermal noise of a resistor, which yields the definition:

$$2{\rm Re}\ Z_{\rm s} \cdot k_{\rm B} T_{\rm N}[\omega] \equiv \mathcal{S}_{VV,\rm tot}[\omega] \tag{6.46}$$

Writing $Z_{\rm s} = |Z_{\rm s}|e^{i\phi}$, we have:

$$2k_{\rm B}T_{\rm N} = \frac{1}{\cos\phi}\left[\frac{\mathcal{S}_{\tilde{V}\tilde{V}}}{|Z_{\rm s}|} + |Z_{\rm s}|\mathcal{S}_{\tilde{I}\tilde{I}} - 2{\rm Re}\ \left(e^{-i\phi}\mathcal{S}_{\tilde{V}\tilde{I}}\right)\right] \tag{6.47}$$

It is clear from this expression that $T_{\rm N}$ will have a minimum as a function of $|Z_{\rm s}|$. For $|Z_{\rm s}|$ too large, the back-action current noise of the amplifier will dominate $T_{\rm N}$, while for $|Z_{\rm s}|$ too small, the voltage noise of the amplifier (i.e. its intrinsic output noise will dominate). The situation is completely analogous to the position detector of the last section; there, we needed to optimize the coupling strength A to balance back-action and intrinsic output noise contributions, and thus minimize the total added noise. Optimizing the source impedance thus yields a completely classical minimum bound on $T_{\rm N}$:

$$k_{\rm B}T_{\rm N} \geq \sqrt{\mathcal{S}_{\tilde{V}\tilde{V}}\mathcal{S}_{\tilde{I}\tilde{I}} - \left[{\rm Im}\ \mathcal{S}_{\tilde{V}\tilde{I}}\right]^2} - {\rm Re}\ \mathcal{S}_{\tilde{V}\tilde{I}} \tag{6.48}$$

where the minimum is achieved for an optimal source impedance which satisfies:

$$|Z_{\rm s}[\omega]|_{\rm opt} = \sqrt{\frac{\mathcal{S}_{\tilde{V}\tilde{V}}[\omega]}{\mathcal{S}_{\tilde{I}\tilde{I}}[\omega]}} \equiv Z_{\rm N} \tag{6.49}$$

$$\sin\phi[\omega]\big|_{\rm opt} = -\frac{{\rm Im}\ \mathcal{S}_{\tilde{V}\tilde{I}}[\omega]}{\sqrt{S_{\tilde{V}\tilde{V}}[\omega]\mathcal{S}_{\tilde{I}\tilde{I}}[\omega]}} \tag{6.50}$$

The above equations define the so-called noise impedance $Z_{\rm N}$. We stress again that the discussion so far in this subsection has been completely classical.

2. Linear response description

It is easy to connect the classical description of a voltage amplifier to the quantum mechanical description of a generic linear response detector; in fact, all that is needed is a "relabeling" of the concepts and quantities we introduced in Sec. VI.D when discussing a linear position detector. Thus, the quantum voltage amplifier will be characterized by both an input operator $\hat{Q}$ and an output operator $\hat{V}_{\rm out}$; these play the role, respectively, of $\hat{F}$ and $\hat{I}$ in the position detector. $\hat{V}_{\rm out}$ represents the output voltage of the amplifier, while $\hat{Q}$ is the operator which couples to the input signal $v_{\rm in}(t)$ via a coupling Hamiltonian:

$$\hat{H}_{int} = v_{\rm in}(t) \cdot \hat{Q} \tag{6.51}$$

In more familiar terms, $\hat{\tilde{I}}_{\rm in} - d\hat{Q}/dt$ represents the current flowing into the amplifier [20]. The voltage gain of our amplifier λ_V will again be given by the Kubo formula of Eq. (5.3), with the substitutions $\hat{F} \to \hat{Q}, \hat{I} \to \hat{V}_{\rm out}$ (we will assume these substitutions throughout this section).

We can now easily relate the fluctuations of the input and output operators to the noise sources used to describe the classical voltage amplifier. As usual, symmetrized quantum noise spectral densities $\bar{S}[\omega]$ will play the role of the classical spectral densities $\mathcal{S}[\omega]$ appearing in the classical description. First, as the operator $\hat{Q}$ represents a back-action force, its fluctuations correspond to the amplifier's current noise $\tilde{I}(t)$:

$$\mathcal{S}_{\tilde{I}\tilde{I}}[\omega] \leftrightarrow \omega^2 \bar{S}_{QQ}[\omega]. \tag{6.52}$$

Similarly, the fluctuations in the operator $\hat{V}_{\rm out}$, when referred back to the amplifier input, will correspond to the voltage noise $\tilde{V}(t)$ discussed above:

$$\mathcal{S}_{\tilde{V}\tilde{V}}[\omega] \leftrightarrow \frac{\bar{S}_{V_{\rm out}V_{\rm out}}[\omega]}{|\lambda_V|^2} \tag{6.53}$$

A similar correspondence holds for the cross-correlator of these noise sources:

$$\mathcal{S}_{\tilde{V}\tilde{I}}[\omega] \leftrightarrow +i\omega\frac{\bar{S}_{V_{\rm out}Q}[\omega]}{\lambda_V} \tag{6.54}$$

To proceed, we need to identify the input and output impedances of the amplifier, and then define its power gain. The first step in this direction is to assume that the output of the amplifier ($\hat{V}_{\rm out}$) is connected to an external circuit via a term:

$$\hat{H}'_{int} = q_{\rm out}(t) \cdot \hat{V}_{\rm out} \tag{6.55}$$

where $\tilde{i}_{\rm out} = dq_{\rm out}/dt$ is the current in the external circuit. We may now identify the input and output

[20] Note that one could have instead written the coupling Hamiltonian in the more traditional form $\hat{H}_{int}(t) = \phi(t) \cdot \hat{\tilde{I}}_{\rm in}$, where $\phi = \int dt' v_{\rm in}(t')$ is the flux associated with the input voltage. The linear response results we obtain are exactly the same. We prefer to work with the charge $\hat{Q}$ in order to be consistent with the rest of the text.

impedances of the amplifier in terms of the damping at the input and output. Using the Kubo formulae for conductance and resistance yields (cf. Eq. (3.32) and Eq. (6.21), with the substitutions $\hat{F} \to \hat{Q}$ and $\hat{I} \to \hat{V}$):

$$1/Z_{\rm in}[\omega] \;=\; i\omega\chi_{QQ}[\omega] \tag{6.56}$$

$$Z_{\rm out}[\omega] \;=\; \frac{\chi_{VV}[\omega]}{-i\omega} \tag{6.57}$$

i.e. $\langle \tilde{I}_{in}\rangle_\omega = \frac{1}{Z_{\rm in}[\omega]} v_{\rm in}[\omega]$ and $\langle V\rangle_\omega = Z_{\rm out}[\omega]\tilde{i}_{\rm out}[\omega]$, where the subscript ω indicates the Fourier transform of a time-dependent expectation value.

We will consider throughout this section the case of no reverse gain, $\chi_{QV_{\rm out}} = 0$. We can define the power gain G_P exactly as we did in Sec. VI.D.3 for a linear position detector. G_P is defined as the ratio of the power delivered to a load attached to the amplifier output divided by the power drawn by the amplifier, maximized over the impedance of the load. One finds:

$$G_P = \frac{|\lambda_V|^2}{4{\rm Re}\ (Z_{\rm out}){\rm Re}\ (1/Z_{\rm in})} \tag{6.58}$$

Expressing this in terms of the linear response coefficients χ_{VV} and χ_{QQ}, we obtain an expression which is completely analogous to Eq. (6.25) for the power gain for a position detector:

$$G_P = \frac{|\lambda_V|^2}{4{\rm Im}\ \chi_{QQ}\cdot {\rm Im}\ \chi_{VV}} \tag{6.59}$$

Finally, we may again define the effective temperature $T_{\rm eff}[\omega]$ of the amplifier via Eq. (3.21), and define a quantum-limited voltage amplifier as one which satisfies the ideal noise condition of Eq. (5.16). For such an amplifier, the power gain will again be determined by the effective temperature via Eq. (6.28).

Turning to the noise, we can again calculate the total symmetrized noise at the output port of the amplifier following the same argument used to the get the output noise of the position detector (cf. Eq. (6.19)). As we did in the classical approach, we will again assume that the input impedance of the amplifier is much larger that source impedance: $Z_{\rm in} \gg Z_{\rm s}$; we will test this assumption for consistency at the end of the calculation. Focusing only on the amplifier contribution to this noise (as opposed to the intrinsic noise of the input signal), and referring this noise back to the amplifier input, we find that the symmetrized quantum noise spectral density describing the added noise of the amplifier, $\bar{S}_{VV,{\rm add}}[\omega]$, satisfies the same equation we found for a classical voltage amplifier, Eq.. (6.45), with each classical spectral density $\mathcal{S}[\omega]$ being replaced by the corresponding symmetrized quantum spectral density $\bar{S}[\omega]$ as per Eqs. (6.52) - (6.54).

It follows that the amplifier noise temperature will again be given by Eq. (6.47), and that the optimal noise temperature (after optimizing over the source impedance) will be given by Eq. (6.48). Whereas classically nothing more could be said, quantum mechanically, we now get a further bound from the quantum noise constraint of Eq. (5.11) and the requirement of a large power gain. The latter requirement tells us that the voltage gain $\lambda_V[\omega]$ and the cross-correlator $\bar{S}_{V_{out}Q}$ must be in phase (cf. Sec. (V.A.4) and Appendix J.2). This in turn means that $\bar{S}_{\tilde{V}\tilde{I}}$ must be purely imaginary. In this case, the quantum noise constraint may be re-written as:

$$\bar{S}_{\tilde{V}\tilde{V}}[\omega]\bar{S}_{\tilde{I}\tilde{I}}[\omega] - \left[{\rm Im}\ \bar{S}_{\tilde{V}\tilde{I}}\right]^2 \geq \left(\frac{\hbar\omega}{2}\right)^2 \tag{6.60}$$

Using these results in Eq. (6.48), we find the ultimate quantum limit on the noise temperature [21]:

$$k_{\rm B}T_{\rm N}[\omega] \geq \frac{\hbar\omega}{2} \tag{6.61}$$

Similar to the case of the position detector, reaching the quantum limit here is *not* simply a matter of tuning the coupling (i.e. tuning the source impedance $Z_{\rm s}$ to match the noise impedance, cf. Eq. (6.49) - (6.50)); one also needs to have a detector with "ideal" quantum noise, that is a detector satisfying Eq. (5.16). As we have repeatedly stressed in this review, this is a condition which is not met by most detectors. It corresponds to the heuristic requirement that there should not be any "wasted" information in the detector.

Finally, we need to test our initial assumption that $|Z_{\rm s}| \ll |Z_{\rm in}|$, taking $|Z_{\rm s}|$ to be equal to its optimal value $Z_{\rm N}$. Using the proportionality condition of Eq. (J13) and the fact that we are in the large power gain limit ($G_P[\omega] \gg 1$), we find:

$$\left|\frac{Z_{\rm N}[\omega]}{{\rm Re}\ Z_{\rm in}[\omega]}\right| = \left|\frac{\alpha}{{\rm Im}\ \alpha}\right| \frac{\hbar\omega}{4k_{\rm B}T_{\rm eff}} = \frac{1}{2\sqrt{G_P[\omega]}} \ll 1 \tag{6.62}$$

It follows that $|Z_{\rm N}| \ll |Z_{\rm in}|$ in the large power gain, large effective temperature regime of interest, thus justifying the form of Eq. (6.45). Eq. (6.62) is analogous to the case of the displacement detector, where we found that reaching the quantum limit on resonance required the detector-dependent damping to be much weaker than the intrinsic damping of the oscillator (cf. Eq. (6.41)).

Thus, similar to the situation of the displacement detector, the linear response approach allows us both to derive rigorously the quantum limit on the noise temperature $T_{\rm N}$ of an amplifier, and to state conditions that must

---

[21] Note that our definition of the noise temperature $T_{\rm N}$ conforms with that of Devoret and Schoelkopf (2000) and most electrical engineering texts, but is slightly different than that of Caves (1982). Caves assumes the source is initially at zero temperature (i.e. $T_0 = 0$), and consequently uses the full quantum expression for its equilibrium noise. In contrast, we have assumed that $k_{\rm B}T_0 \gg \hbar\omega$. The different definition of the noise temperature used by Caves leads to the result $k_{\rm B}T_N \geq \hbar\omega/(\ln 3)$ as opposed to our Eq. (6.61). We stress that the difference between these results has nothing to do with physics, but only with how one defines the noise temperature.

be met to reach this limit. To reach the quantum-limited value of T_N with a large power gain, one needs *both* a tuned source impedance Z_s, *and* an amplifier which possesses ideal noise properties (cf. Eq. (5.16) and Eq. (J13)).

3. Role of noise cross-correlations

Before leaving the topic of a linear voltage amplifier, we pause to note the role of cross-correlations in current and voltage noise in reaching the quantum limit. First, note from Eq. (6.50) that in both the classical and quantum treatments, the noise impedance Z_N of the amplifier will have a reactive part (i.e. Im $Z_N \neq 0$) if there are out-of-phase correlations between the amplifier's current and voltage noises (i.e. if Im $S_{VI} \neq 0$). Thus, if such correlations exist, it will not be possible to minimize the noise temperature (and hence, reach the quantum limit), if one uses a purely real source impedance Z_s.

More significantly, note that the final classical expression for the noise temperature T_N explicitly involves the real part of the S_{VI} correlator (cf. Eq. (6.48)). In contrast, we have shown that in the quantum case, Re $\bar{S}_{VI}$ *must* be zero if one wishes to reach the quantum limit while having a large power gain (cf. Appendix J.2); as such, this quantity does not appear in the final expression for the minimal T_N. It also follows that *to reach the quantum limit while having a large power gain, an amplifier cannot have significant in-phase correlations between its current and voltage noise.*

This last statement can be given a heuristic explanation. If there are out-of-phase correlations between current and voltage noise, we can easily make use of these by appropriately choosing our source impedance. However, if there are in-phase correlations between current and voltage noise, we cannot use these simply by tuning the source impedance. We *could* however have used them by implementing feedback in our amplifier. The fact that we have not done this means that these correlations represent a kind of missing information; as a result, we must necessarily miss the quantum limit. In Sec. VII.B, we explicitly give an example of a voltage amplifier which misses the quantum limit due to the presence of in-phase current and voltage fluctuations; we show how this amplifier can be made to reach the quantum limit by adding feedback in Sec. I.

F. Near quantum-limited mesoscopic detectors

Having discussed the origin and precise definition of the quantum limit on the added noise of a linear, phase-preserving amplifier, we now provide a brief review of work examining whether particular detectors are able (in principle) to achieve this ideal limit. We will focus on the "op-amp" mode of operation discussed in Sec. VI.C, where the detector is only weakly coupled to the system producing the signal to be amplified. As we have repeatedly stressed, reaching the quantum limit in this case requires the detector to have "quantum ideal noise", as defined by Eq. (5.16). Heuristically, this corresponds to the general requirement of no wasted information: there should be no other quantity besides the detector output that could be monitored to provide information on the input signal (Clerk *et al.*, 2003). We have already given one simple but relevant example of a detector which reaches the amplifier quantum limit: the parametric cavity detector, discussed extensively in Sec. IV.B. Here, we turn to other more complex detectors.

1. dc SQUID amplifiers

The dc SQUID (superconducting quantum interference device) is a detector based on a superconducting ring having two Josephson junctions. It can in principle be used as a near quantum-limited voltage amplifier or flux-to-voltage amplifier. Theoretically, this was investigated using a quantum Langevin approach (Danilov *et al.*, 1983; Koch *et al.*, 1980), as well as more rigorously by using perturbative techniques (Averin, 2000b) and mappings to quantum impurity problems (Clerk, 2006). Experiments on SQUIDS have also confirmed its potential for near quantum-limited operation. Mück *et al.* (2001) were able to achieve a noise temperature T_N approximately 1.9 times the quantum limited value at an operating frequency of $\omega = 2\pi \times 519$ MHz. Working at lower frequencies appropriate to gravitational wave detection applications, Vinante *et al.* (2001) were able to achieve a T_N approximately 200 times the quantum limited value at a frequency $\omega = 2\pi \times 1.6$ kHz. In practice, it can be difficult to achieve the theoretically-predicted quantum-limited performance due to spurious heating caused by the dissipation in the shunt resistances used in the SQUID.

2. Quantum point contact detectors

A quantum point contact (QPC) is a narrow conducting channel formed in a two-dimensional gas. The current through the constriction is very sensitive to nearby charges, and thus the QPC acts as a charge-to-current amplifier. It has been shown theoretically that the QPC can achieve the amplifier quantum limit , both in the regime where transport is due to tunneling (Gurvitz, 1997), as well as in regimes where the transmission is not small (Aleiner *et al.*, 1997; Clerk *et al.*, 2003; Korotkov and Averin, 2001; Levinson, 1997; Pilgram and Büttiker, 2002). Experimentally, QPCs are in widespread use as detectors of quantum dot qubits. The back-action dephasing of QPC detectors was studied in (Buks *et al.*, 1998; Sprinzak *et al.*, 2000); a good agreement was found with the theoretical prediction, confirming that the QPC has quantum-limited back-action noise.

3. Single-electron transistors and resonant-level detectors

A metallic single-electron transistor (SET) consists of a small metallic island attached via tunnel junctions to larger source and drain electrodes. Because of Coulomb blockade effects, the conductance of a SET is very sensitive to nearby charges, and hence it acts as a sensitive charge-to-current amplifier. Considerable work has investigated whether metallic SETs can approach the quantum limit in various different operating regimes. Theoretically, the performance of a normal-metal SET in the sequential tunneling regime was studied by Devoret and Schoelkopf (2000); Makhlin *et al.* (2000); Shnirman and Schön (1998). In this regime, where transport is via a sequence of energy-conserving tunnel events, one is far from optimizing the quantum noise constraint of Eq. (5.16), and hence one cannot reach the quantum limit (Korotkov, 2001b; Shnirman and Schön, 1998). If one instead chooses to work with a normal-metal SET in the regime where transport is due to cotunneling (a higher-order tunneling process involving a virtual transition), then one can indeed approach the quantum limit (Averin, 2000a; van den Brink, 2002). However, by virtue of being a higher-order process, the related currents and gain factors are small, impinging on the practical utility of this regime of operation. It is worth noting that while most theory on SETs assume a dc voltage bias, to enhance bandwidth, experiments are usually conducted using the rf-SET configuration (Schoelkopf *et al.*, 1998), where the SET changes the damping of a resonant LC circuit. Korotkov and Paalanen (1999) have shown that this mode of operation for a sequential tunneling SET increases the measurement imprecision noise by approximately a factor of 2. The measurement properties of a normal-metal, sequential-tunneling rf-SET (including back-action) were studied experimentally in Turek *et al.* (2005).

Measurement using superconducting SET's has also been studied. Clerk *et al.* (2002) have shown that so-called incoherent Cooper-pair tunneling processes in a superconducting SET can have a noise temperature which is approximately a factor of two larger than the quantum limited value. The measurement properties of superconducting SETs bias at a point of incoherent Cooper-pair tunneling have been probed recently in experiment (Naik *et al.*, 2006; Thalakulam *et al.*, 2004).

The quantum measurement properties of non-interacting resonant level detectors have also been studied theoretically (Averin, 2000b; Clerk and Stone, 2004; Gavish *et al.*, 2006; Mozyrsky *et al.*, 2004). These systems are similar to metallic SET, except that the central island only has a single level (as opposed to a continuous density of states), and Coulomb-blockade effects are typically neglected. These detectors can reach the quantum limit in the regime where the voltage and temperature are smaller than the intrinsic energy broadening of the level due to tunneling. They can also reach the quantum limit in a large-voltage regime that is analogous to the cotunneling regime in a metallic SET (Averin, 2000b; Clerk and Stone, 2004).

G. Back-action evasion and noise-free amplification

Having discussed in detail quantum limits on phase-preserving linear amplifiers (i.e. amplifiers which measure both quadratures of a signal equally well), we now return to the situation discussed at the very start of Sec. VI.A: imagine we wish only to amplify a *single* quadrature of some time-dependent signal. For this case, there need not be any added noise from the measurement. Unlike the case of amplifying both quadratures, Liouville's theorem does not require the existence of any additional degrees of freedom when amplifying a single quadrature: phase space volume can be conserved during amplification simply by contracting the unmeasured quadrature (cf. Eq. 6.2). As no extra degrees of freedom are needed, there need not be any extra noise associated with the amplification process.

Alternatively, single-quadrature detection can take a form similar to a QND measurement, where the back-action does not affect the dynamics of the quantity being measured (Bocko and Onofrio, 1996; Braginsky and Khalili, 1992; Braginsky *et al.*, 1980; Caves, 1982; Caves *et al.*, 1980; Thorne *et al.*, 1978). For concreteness, consider a high-Q harmonic oscillator with position $x(t)$ and resonant frequency Ω. Its motion may be written in terms of quadrature operators defined as in Eq. (4.66):

$$\hat{x}(t) \;=\; \hat{X}_\delta(t)\cos\left(\Omega t+\delta\right) + \hat{Y}_\delta(t)\sin\left(\Omega t+\delta\right) \tag{6.63}$$

Here, $\hat{x}(t)$ is the Heisenberg-picture position operator of the oscillator. The quadrature operators can be written in terms of the (Schrödinger-picture) oscillator creation and destruction operators as:

$$\hat{X}_\delta(t) \;=\; x_{\rm ZPF}\left(\hat{c}e^{i(\Omega t+\delta)} + \hat{c}^\dagger e^{-i(\Omega t+\delta)}\right) \tag{6.64a}$$

$$\hat{Y}_\delta(t) \;=\; -ix_{\rm ZPF}\left(\hat{c}e^{i(\Omega t+\delta)} - \hat{c}^\dagger e^{-i(\Omega t+\delta)}\right) \tag{6.64b}$$

As previously discussed ((c.f. Eq.(4.67)), the two quadrature amplitude operators $\hat{X}_\delta$ and $\hat{Y}_\delta$ are canonically conjugate (c.f. Eq.(4.67)). Making a measurement of one quadrature amplitude, say $\hat{X}_\delta$, will thus invariably lead to back-action disturbance of the other, conjugate quadrature $\hat{Y}_\delta$. However, due to the dynamics of a harmonic oscillator, this disturbance will not affect the measured quadrature at later times. One can already see this from the classical equations of motion. Suppose our oscillator is driven by a time-dependent force $F(t)$ which only has appreciable bandwidth near Ω. We may write this as:

$$F(t) = F_X(t)\cos(\Omega t+\delta) + F_Y(t)\sin(\Omega t+\delta) \tag{6.65}$$

where $F_X(t), F_Y(t)$ are slowly varying compared to Ω. Using the fact that the oscillator has a high-quality factor $Q = \Omega/\gamma$, one can easily find the equations of motion:

$$\frac{d}{dt}X_\delta(t) = -\frac{\gamma}{2}X_\delta(t) - \frac{F_Y(t)}{2m\Omega}, \tag{6.66a}$$

$$\frac{d}{dt}Y_\delta(t) = -\frac{\gamma}{2}Y_\delta(t) + \frac{F_X(t)}{2m\Omega}. \tag{6.66b}$$

Thus, as long as $F_Y(t)$ and $F_X(t)$ are uncorrelated and sufficiently slow, the dynamics of the two quadratures are completely independent; in particular, if Y_δ is subject to a narrow-bandwidth, noisy force, it is of no consequence to the evolution of X_δ. An ideal measurement of X_δ will result in a back-action force having the form in Eq. (6.65) with $F_Y(t) = 0$, implying that $X_\delta(t)$ will be completely unaffected by the measurement.

Not surprisingly, if one can measure and amplify X_δ without any back-action, there need not be any added noise due to the amplification. In such a setup, the only added noise is the measurement-imprecision noise associated with intrinsic fluctuations of the amplifier output. These may be reduced (in principle) to an arbitrarily small value by simply increasing the amplifier gain (e.g. by increasing the detector-system coupling): in an ideal setup, there is no back-action penalty on the measured quadrature associated with this increase.

The above conclusion can lead to what seems like a contradiction. Imagine we use a back-action evading amplifier to make a "perfect" measurement of X_δ (i.e. negligible added noise). We would then have no uncertainty as to the value of this quadrature. Consequently, would expect the quantum state of our oscillator to be a squeezed state, where the uncertainty in X_δ is much smaller than $x_{\rm ZPF}$. However, if there is no back-action acting on X_δ, how is the amplifier able to reduce its uncertainty? This seeming paradox can be fully resolved by considering the conditional aspects of an ideal single quadrature measurement, where one considers the state of the oscillator given a particular measurement history (Clerk *et al.*, 2008; Ruskov *et al.*, 2005).

It is worth stressing that the possibility of amplifying a single quadrature without back-action (and hence, without added noise) relies crucially on our oscillator resembling a perfect harmonic oscillator: the oscillator Q must be large, and non-linearities (which could couple the two quadratures) must be small. In addition, the envelope of the non-vanishing back-action force $F_X(t)$ must have a narrow bandwidth. One should further note that a very high precision measurement of X_δ will produce a very large back action force F_X. If the system is not nearly perfectly harmonic, then the large amplitude imparted to the conjugate quadrature Y_δ will inevitably leak back into X_δ.

Amplifiers or detectors which treat the two signal quadratures differently are known in the quantum optics literature as 'phase sensitive'; we prefer the designation 'phase-non-preserving' since they do not preserve the phase of the original signal. Such amplifiers invariably rely on some internal clock (i.e. an oscillator with a well defined phase) which breaks time-translation invariance and picks out the phase of the quadrature that will be amplified (i.e. the choice of δ used to define the two quadratures in Eq. (6.63)); we will see this explicitly in what follows. This leads to an important caveat: even in a situation where the interesting information is in a single signal quadrature, to benefit from using a phase non-preserving amplifier, we must know in advance the precise phase of this quadrature. If we do not know this phase, we will have either to revert to a phase-preserving amplification scheme (and thus be susceptible to added noise) or we would have to develop a sophisticated and high speed quantum feedback scheme to dynamically adapt the measurement to the correct quadrature in real time (Armen *et al.*, 2002). In what follows, we will make the above ideas concrete by considering a few examples of quantum, phase non-preserving amplifiers.

1. Degenerate parametric amplifier

Perhaps the simplest example of a phase non-preserving amplifier is the degenerate parametric amplifier; the classical version of this system was described at the start of Sec. VI.A (cf. Eq. 6.2). The quantum version is also extremely simple to treat, and has many similarities to the single-mode, phase-preserving amplifier discussed in Sec. VI.B. Similar to that system, in the degenerate parametric amplifier both the amplifier input and output are described by single bosonic modes, having annihilation operators $\hat{a}$ and $\hat{b}$ respectively. This amplifier is operated in the "scattering" mode of operation described in Sec. VI.C: $\hat{a}$ describes the input signal, which is the amplitude of a wave incident on the amplifier, while $\hat{b}$ describes the output signal, the amplitude of a wave leaving the amplifier. The dimensionless quadrature operators corresponding to the input and output (taking, without loss of generality, the phase δ in Eq. (6.63) to be zero) are given by:

$$\begin{aligned}
\hat{x}_{\rm in} &= \frac{1}{\sqrt{2}}\left(\hat{a}^\dagger + \hat{a}\right) \\
\hat{y}_{\rm in} &= \frac{i}{\sqrt{2}}\left(\hat{a}^\dagger - \hat{a}\right) \\
\hat{x}_{\rm out} &= \frac{1}{\sqrt{2}}\left(\hat{b}^\dagger + \hat{b}\right) \\
\hat{y}_{\rm out} &= \frac{i}{\sqrt{2}}\left(\hat{b}^\dagger - \hat{b}\right)
\end{aligned} \tag{6.67}$$

These operators are canonically conjugate, satisfying:

$$[\hat{x}_{\rm in}, \hat{y}_{\rm in}] = [\hat{x}_{\rm out}, \hat{y}_{\rm out}] = i. \tag{6.68}$$

With these definitions, the action of the amplifier is described by the input-output relations (compare against

Eq. (6.6)):

$$\hat{x}_{\rm out} = \sqrt{G}\,\hat{x}_{\rm in} \tag{6.69a}$$

$$\hat{y}_{\rm out} = \frac{1}{\sqrt{G}}\,\hat{y}_{\rm in} \tag{6.69b}$$

These input-output relations are derived in Appendix F. We see that our amplifier clearly treats the two quadratures differently, and hence is a phase-sensitive amplifier: one quadrature is amplified and the other is deamplified in such a way that the commutation relation can be preserved without the necessity of any added noise. Note that the degenerate parametric amplifier relies on having a "pump" mode which has a large amplitude and an almost-definite phase. This pump mode plays the role of a clock; in particular, its phase picks out the quadrature of the signal which is amplified (see Appendix F for more details).

It is important to stress that while the degenerate parametric amplifier is phase-sensitive and has no added noise, it is *not* an example of back-action evasion (see Caves *et al.* (1980), footnote on p. 342). This amplifier is operated in the scattering mode of amplifier operation, a mode where (as discussed extensively in Sec. VI.C) back-action is not at all relevant. Recall that in this mode of operation, the amplifier input is perfectly impedance matched to the signal source, and the input signal is simply the amplitude of an incident wave on the amplifier input. This mode of operation necessarily requires a strong coupling between the input signal and the amplifier input. If one instead tried to weakly couple the degenerate parametric amplifier to a signal source, and operate it in the "op-amp" mode of operation (c.f. Sec. VI.C), one finds that there is indeed a back-action disturbance of the measured quadrature. We have yet another example which demonstrates that one must be very careful to distinguish the "op-amp" and "scattering" mode of amplifier operation.

2. Double-sideband cavity detector

We now turn to a simple but experimentally-relevant detector that is truly back-action evading. We will take as our input signal the position $\hat{x}$ of a mechanical oscillator. The amplifier setup we consider is almost identical to the cavity position detector discussed in Sec. IV.B.3: we again have a single-sided resonant cavity whose frequency depends linearly on the oscillator's position, with the Hamiltonian being given by Eq. (4.22) (with $\hat{z} = \hat{x}/x_{\rm ZPF}$). We showed in Sec. IV.B.3 and Appendix D.3 that by driving the cavity on resonance, it could be used to make a quantum limited position measurement: one can operate it as a phase-preserving amplifier of the mechanical's oscillators position, and achieve the minimum possible amount of added noise. To use the same system to make a back-action free measurement of one oscillator quadrature only, one simply uses a different cavity drive. Instead of driving at the cavity resonance frequency $\omega_{\rm c}$, one drives at the two sidebands associated with the mechanical motion (i.e. at frequencies $\omega_{\rm c} \pm \Omega$, where Ω is as always the frequency of the mechanical resonator). As we will see, such a drive results in an effective interaction which only couples the cavity to one quadrature of the oscillator's motion. This setup was first proposed as a means of back-action evasion in Braginsky *et al.* (1980); further discussion can be found in Braginsky and Khalili (1992); Caves *et al.* (1980), as well as in Clerk *et al.* (2008), which gives a fully quantum treatment and considers conditional aspects of the measurement. In what follows, we sketch the operation of this system following Clerk *et al.* (2008); details are provided in Appendix D.4.

We will start by requiring that our system be in the "good-cavity" limit, where $\omega_{\rm c} \gg \Omega \gg \kappa$ (κ is the damping of the cavity mode); we will also require the mechanical oscillator to have a high Q-factor. In this regime, the two sidebands associated with the mechanical motion at $\omega_{\rm c} \pm \Omega$ are well-separated from the main cavity resonance at $\omega_{\rm c}$. Making a single-quadrature measurement requires that one drives the cavity at equally at the two sideband frequencies. The amplitude of driving field $\bar{b}_{\rm in}$ entering the cavity will be chosen to have the form:

$$\begin{aligned}\bar{b}_{\rm in}(t) &= -\frac{i\sqrt{\dot{N}}}{4}\left(e^{i\delta}e^{-i(\omega_{\rm c}-\Omega)t} - e^{-i\delta}e^{-i(\omega_{\rm c}+\Omega)t}\right) \\ &= \frac{\sqrt{\dot{N}}}{2}\sin(\Omega t+\delta)e^{-i\omega_{\rm c}t}.\end{aligned} \tag{6.70}$$

Here, $\dot{N}$ is the photon number flux associated with the cavity drive (see Appendix D for more details on how to properly include a drive using input-output theory). Such a drive could be produced by taking a signal at the cavity resonance frequency, and amplitude modulating it at the mechanical frequency.

To understand the effect of this drive, note that it sends the cavity both photons with frequency $(\omega_{\rm c} - \Omega)$ and photons with frequency $(\omega_{\rm c} + \Omega)$. The first kind of drive photon can be converted to a cavity photon if a quanta is *absorbed from* the mechanical oscillator; the second kind of drive photon can be converted to a cavity photon if a quanta is *emitted to* the mechanical oscillator. The result is that we can create a cavity photon by either absorbing or emitting a mechanical oscillator quanta. Keeping track that there is a well-defined relative phase of $e^{i2\delta}$ between the two kinds of drive photons, we would expect the double-sideband drive to yield an effective cavity-oscillator interaction of the form:

$$V_{\rm eff} \propto \sqrt{\dot{N}}\left[\hat{a}^\dagger\left(e^{i\delta}\hat{c} + e^{-i\delta}\hat{c}^\dagger\right) + \text{h.c. }\right] \tag{6.71a}$$

$$\propto \sqrt{\dot{N}}(\hat{a}+\hat{a}^\dagger)\hat{X}_\delta \tag{6.71b}$$

This is exactly what is found in a full calculation (see Appendix D.4). Note that we have written the interaction in an interaction picture in which the fast oscillations of the cavity and oscillator operators have been removed. In the second line, we have made use of Eqs. (6.64) to

show that the effective interaction only involves the $\hat{X}_\delta$ oscillator quadrature.

We thus see from Eq. (6.71b) that the cavity is only coupled to the oscillator X_δ quadrature. As shown rigorously in Appendix subapp:CavityPositionDetector, the result is that the system only measures and amplifies this quadrature: the light leaving the cavity has a signature of $\hat{X}_\delta$, but not of $\hat{Y}_\delta$. Further, Eq. (6.71b) implies that the cavity operator $\sqrt{\dot{N}}\left(\hat{a}+\hat{a}^\dagger\right)$ will act as a noisy force on the Y_δ quadrature. While this will cause a back-action heating of Y_δ, it will not affect the measured quadrature X_δ. We thus have a true back-action evading amplifier: the cavity output light lets one measure X_δ free from any back-action effect. Note that in deriving Eq. (6.71a), we have used the fact that the cavity operators have fluctuations in a narrow bandwidth $\sim \kappa \ll \Omega$: the back-action force noise is slow compared to the oscillator frequency. If this were not the case, we could still have a back-action heating of the measured X_δ quadrature. Such effects, arising from a non-zero ratio κ/Ω, are treated in Clerk *et al.* (2008).

Finally, as there is no back-action on the measured X_δ quadrature, the only added noise of the amplification scheme is measurement-imprecision noise (e.g. shot noise in the light leaving the cavity). This added noise can be made arbitrarily small by increasing the gain of the detector by, for example, increasing the strength of the cavity drive $\dot{N}$. In a real system where κ/ω_M is non-zero, the finite-bandwidth of the cavity number fluctuations leads to a small back-action on the X_δ. As a result, one cannot make the added noise arbitrarily small, as too large a cavity drive will heat the measured quadrature. Nonetheless, for a sufficiently small ratio κ/ω_M, one can still beat the standard quantum limit on the added noise (Clerk *et al.*, 2008).

3. Stroboscopic measurements

With sufficiently high bandwidth it should be able to do stroboscopic measurements in sync with the oscillator motion which could allow one to go below the standard quantum limit in one of the quadratures of motion (Braginsky and Khalili, 1992; Caves *et al.*, 1980). To understand this idea, imagine an extreme form of phase sensitive detection in which a Heisenberg microscope makes a strong high-resolution measurement which projects the oscillator onto a state of well defined position X_0 at time $t = 0$:

$$\Psi_{X_0}(t) = \sum_{n=0}^{\infty} a_n e^{-i(n+1/2)\Omega t} \left|n\right\rangle , \qquad (6.72)$$

where the coefficients obey $a_n = \langle n|X_0\rangle$. Because the position is well-defined the momentum is extremely uncertain. (Equivalently the momentum kick delivered by the back action of the microscope makes the oscillator momentum uncertain.) Thus the wave packet quickly spreads out and the position uncertainty becomes large. However because of the special feature that the harmonic oscillator levels are evenly spaced, we can see from Eq. (6.72) that the wave packet reassembles itself precisely once each period of oscillation because $e^{in\Omega t} = 1$ for every integer n. (At half periods, the packet reassembles at position $-X_0$.) Hence stroboscopic measurements made once (or twice) per period will be back action evading and can go below the standard quantum limit. The only limitations will be the finite anharmonicity and damping of the oscillator. Note that the possibility of using mesoscopic electron detectors to perform stroboscopic measurements has recently received attention (Jordan and Büttiker, 2005; Ruskov *et al.*, 2005).

VII. BOSONIC SCATTERING DESCRIPTION OF A TWO-PORT AMPLIFIER

In this section, we return again to the topic of Sec. VI.E, quantum limits on a quantum voltage amplifier. We now discuss the physics in terms of the bosonic voltage amplifier first introduced in Sec. VI.C. Recall that in that subsection, we demonstrated that the standard Haus-Caves derivation of the quantum limit was not directly relevant to the usual weak-coupling "op-amp" mode of amplifier operation, a mode where the input signal is not simply the amplitude of a wave incident on the amplifier. In this section, we will expand upon that discussion, giving an explicit discussion of the differences between the op-amp description of an amplifier presented in Sec. VI.D, and the scattering description often used in the quantum optics literature (Courty *et al.*, 1999; Grassia, 1998). We will see that what one means by "back-action" and "added noise" are not the same in the two descriptions! Further, even though an amplifier may reach the quantum limit when used in the scattering mode (i.e. its added noise is as small as allowed by commutation relations), it can nonetheless fail to achieve the quantum limit when used in the op-amp mode. Finally, the discussion here will also allow us to highlight important aspects of the quantum limit not easily discussed in the more general context of Sec. V.

A. Scattering versus op-amp representations

In the bosonic scattering approach, a generic linear amplifier is modeled as a set of coupled bosonic modes. To make matters concrete, we will consider the specific case of a voltage amplifier with distinct input and output ports, where each port is a semi-infinite transmission line (see Fig. 9). We gave a heuristic description of this system in Sec. VI.C; here, we will investigate its features in more detail and with more rigour.

As discussed in Appendix C and Yurke and Denker (1984), a transmission line can be described as a set of non-interacting bosonic modes. Denoting the input transmission line with an a and the output transmission

line with a b, the current and voltage operators in these lines may be written:

$$\hat{V}_q(t) = \int_0^\infty \frac{d\omega}{2\pi}\left(\hat{V}_q[\omega]e^{-i\omega t} + h.c.\right) \tag{7.1a}$$

$$\hat{I}_q(t) = \sigma_q \int_0^\infty \frac{d\omega}{2\pi}\left(\hat{I}_q[\omega]e^{-i\omega t} + h.c.\right) \tag{7.1b}$$

with

$$\hat{V}_q[\omega] = \sqrt{\frac{\hbar\omega}{2}Z_q}\left(\hat{q}_{in}[\omega] + \hat{q}_{out}[\omega]\right) \tag{7.2a}$$

$$\hat{I}_q[\omega] = \sqrt{\frac{\hbar\omega}{2Z_q}}\left(\hat{q}_{in}[\omega] - \hat{q}_{out}[\omega]\right) \tag{7.2b}$$

Here, q can be equal to a or b, and we have $\sigma_a = 1, \sigma_b = -1$. The operators $\hat{a}_{\rm in}[\omega], \hat{a}_{\rm out}[\omega]$ are canonical bosonic annihilation operators; $\hat{a}_{\rm in}[\omega]$ describes an incoming wave in the input transmission line (i.e. incident on the amplifier) having frequency ω, while $\hat{a}_{\rm out}[\omega]$ describes an outgoing wave with frequency ω. The operators $\hat{b}_{\rm in}[\omega]$ and $\hat{b}_{\rm out}[\omega]$ describe analogous waves in the output transmission line. We can think of $\hat{V}_a$ as the input voltage to our amplifier, and $\hat{V}_b$ as the output voltage. Similarly, $\hat{I}_a$ is the current drawn by the amplifier at the input, and $\hat{I}_b$ the current drawn at the output of the amplifier. Finally, Z_a (Z_b) is the characteristic impedance of the input (output) transmission line. Note that we use a slightly different sign convention than in Yurke and Denker (1984).

Amplification of a signal at a particular frequency ω will in general involve $2N$ bosonic modes in the amplifier. Four of these modes are simply the frequency-ω modes in the input and output lines (i.e. $\hat{a}_{\rm in}[\omega]$,$\hat{a}_{\rm out}[\omega]$,$\hat{b}_{\rm in}[\omega]$ and $\hat{b}_{\rm out}[\omega]$). The remaining $2(N-2)$ modes describe auxiliary degrees of freedom involved in the amplification process; these additional modes could correspond to frequencies different from the signal frequency ω. The auxiliary modes can also be divided into incoming and outgoing modes. It is thus convenient to represent them as additional transmission lines attached to the amplifier; these additional lines could be semi-infinite, or could be terminated by active elements.

1. Scattering representation

In general, our generic two-port bosonic amplifier will be described by a $N \times N$ scattering matrix which determines the relation between the outgoing mode operators and incoming mode operators. The form of this matrix is constrained by the requirement that the output modes obey the usual canonical bosonic commutation relations. It is convenient to express the scattering matrix in a form which *only* involves the input and output lines explicitly:

$$\begin{pmatrix} \hat{a}_{\rm out}[\omega] \\ \hat{b}_{\rm out}[\omega] \end{pmatrix} = \begin{pmatrix} s_{11}[\omega] & s_{12}[\omega] \\ s_{21}[\omega] & s_{22}[\omega] \end{pmatrix}\begin{pmatrix} \hat{a}_{\rm in}[\omega] \\ \hat{b}_{\rm in}[\omega] \end{pmatrix} + \begin{pmatrix} \hat{\mathcal{F}}_a[\omega] \\ \hat{\mathcal{F}}_b[\omega] \end{pmatrix} \tag{7.3}$$

Here $\hat{\mathcal{F}}_a[\omega]$ and $\hat{\mathcal{F}}_b[\omega]$ are each an unspecified linear combination of the auxiliary-line incident mode operators. They thus describe noise in the outgoing modes of the input and output transmission lines which arises from the auxiliary modes involved in the amplification process. Note the similarity between Eq. (7.3) and Eq. (6.7a) for the simple one-port bosonic amplifier considered in Sec. VI.B.

In the quantum optics literature, one typically views Eq. (7.3) as the defining equation of the amplifier; we will call this the scattering representation of our amplifier. The representation is best suited to the scattering mode of amplifier operation described in Sec. VI.C. In this mode of operation, the experimentalist ensures that $\langle\hat{a}_{in}[\omega]\rangle$ is precisely equal to the signal to be amplified, *irrespective* of what is coming out of the amplifier. Similarly, the output signal from the amplifier is the amplitude of the outgoing wave in the output line, $\langle\hat{b}_{\rm out}[\omega]\rangle$. If we focus on $\hat{b}_{\rm out}$, we have precisely the same situation as described in Sec. 6.10, where we presented the Haus-Caves derivation of the quantum limit (c.f. Eq. (6.7a)). It thus follows that in the scattering mode of operation, the matrix element $s_{21}[\omega]$ represents the gain of our amplifier at frequency ω, $|s_{21}[\omega]|^2$ the corresponding "photon number gain", and $\hat{\mathcal{F}}_b$ the added noise operator of the amplifier. The operator $\hat{\mathcal{F}}_a$ represents the back-action noise in the scattering mode of operation; this back-action has no effect on the added noise of the amplifier in the scattering mode.

Similar to Sec. VI.B, one can now apply the standard argument of Haus and Mullen (1962) and Caves (1982) to our amplifier. This argument tells us that since the "out" operators must have the same commutation relations as the "in" operators, the added noise $\hat{\mathcal{F}}_b$ cannot be arbitrarily small in the large gain limit (i.e. $|s_{21}| \gg 1$). Note that this version of the quantum limit on the added noise has nothing to do with back-action. As already discussed, this is perfectly appropriate for the scattering mode of operation, as in this mode, the experimentalist ensures that the signal going into the amplifier is completely independent of whatever is coming out of the amplifier. This mode of operation could be realized in time-dependent experiments, where a pulse is launched at the amplifier. This mode is *not* realized in most weak-coupling amplification experiments, where the signal to be amplified is not identical to an incident wave amplitude.

2. Op-amp representation

In the usual op-amp amplifier mode of operation (described extensively in Sec. V), the input and output signals are not simply incoming/outgoing wave amplitudes; thus, the scattering representation is not an optimal description of our amplifier. The system we are describing here is a voltage amplifier: thus, in the op-amp mode, the experimentalist would ensure that the voltage at the end of the input line ($\hat{V}_a$) is equal to the signal to be amplified, and would read out the voltage at the end of the output transmission line ($\hat{V}_b$) as the output of the amplifier. From Eq. (7.1a), we see that this implies that the amplitude of the wave going into the amplifier, $a_{\rm in}$, will depend on the amplitude of the wave exiting the amplifier, $a_{\rm out}$.

Thus, if we want to use our amplifier as a voltage amplifier, we would like to find a description which is more tailored to our needs than the scattering representation of Eq. (7.3). This can be found by simply re-expressing the scattering matrix relation of Eq. (7.3) in terms of voltages and currents. The result will be what we term the "op amp" representation of our amplifier, a representation which is standard in the discussion of classical amplifiers (see, e.g., Boylestad and Nashelsky (2006)). In this representation, one views $\hat{V}_a$ and $\hat{I}_b$ as inputs to the amplifier: $\hat{V}_a$ is set by whatever we connect to the amplifier input, while $\hat{I}_b$ is set by whatever we connect to the amplifier output. In contrast, the outputs of our amplifier are the voltage in the output line, $\hat{V}_b$, and the current drawn by the amplifier at the input, $\hat{I}_a$. Note that this interpretation of voltages and currents is identical to how we viewed the voltage amplifier in the linear-response/quantum noise treatment of Sec. VI.E.

Using Eqs. (7.1a) and (7.1b), and suppressing frequency labels for clarity, Eq. (7.3) may be written in the form:

$$\begin{pmatrix} \hat{V}_b \\ \hat{I}_a \end{pmatrix} = \begin{pmatrix} \lambda_V & -Z_{\rm out} \\ \frac{1}{Z_{\rm in}} & \lambda_I' \end{pmatrix} \begin{pmatrix} \hat{V}_a \\ \hat{I}_b \end{pmatrix} + \begin{pmatrix} \lambda_V \cdot \hat{\tilde{V}} \\ \hat{\tilde{I}} \end{pmatrix} \quad (7.4)$$

The coefficients in the above matrix are familiar from the discussion of voltage amplifier in Sec. VI.E. $\lambda_V[\omega]$ is the voltage gain of the amplifier, $\lambda_I'[\omega]$ is the reverse current gain of the amplifier, $Z_{\rm out}$ is the output impedance, and $Z_{\rm in}$ is the input impedance. The last term on the RHS of Eq. (7.4) describes the two familiar kinds of amplifier noise. $\hat{\tilde{V}}$ is the usual voltage noise of the amplifier (referred back to the amplifier input), while $\hat{\tilde{I}}$ is the usual current noise of the amplifier. Recall that in this standard description of a voltage amplifier (cf. Sec. VI.E), $\tilde{I}$ represents the back-action of the amplifier: the system producing the input signal responds to these current fluctuations, resulting in an additional fluctuation in the input signal going into the amplifier. Similarly, $\lambda_V \cdot \tilde{V}$ represents the intrinsic output noise of the amplifier: this contribution to the total output noise does not depend on properties of the input signal. Note that we are using a sign convention where a positive $\langle \hat{I}_a \rangle$ indicates a current flowing *into* the amplifier at its input, while a positive $\langle \hat{I}_b \rangle$ indicates a current flowing *out of* the amplifier at its output. Also note that the operators $\hat{V}_a$ and $\hat{I}_b$ on the RHS of Eq. (7.4) will have noise; this noise is entirely due to the systems attached to the input and output of the amplifier, and as such, should not be included in what we call the added noise of the amplifier.

Additional important properties of our amplifier follow immediately from quantities in the op-amp representation. As discussed in Sec. VI.D, the most important measure of gain in our amplifier is the dimensionless power gain. This is the ratio between power dissipated at the output to that dissipated at the input, taking the output current I_B to be $V_B/Z_{\rm out}$:

$$G_P \equiv \frac{(\lambda_V)^2}{4} \frac{Z_{\rm in}}{Z_{\rm out}} \cdot \left(1 + \frac{\lambda_V \lambda_I'}{2} \frac{Z_{\rm in}}{Z_{\rm out}}\right)^{-1} \quad (7.5)$$

Note that for zero reverse gain, this coincides with Eq. (6.58) of Sec. VI.E.

Another important quantity is the loaded input impedance: what is the input impedance of the amplifier in the presence of a load attached to the output? In the presence of reverse current gain $\lambda_I' \neq 0$, the input impedance will depend on the output load. Taking the load impedance to be $Z_{\rm load}$, some simple algebra yields:

$$\frac{1}{Z_{\rm in,loaded}} = \frac{1}{Z_{\rm in}} + \frac{\lambda_I' \lambda_V}{Z_{\rm load} + Z_{\rm out}} \quad (7.6)$$

It is of course undesirable to have an input impedance which depends on the load. Thus, we see yet again that it is undesirable to have appreciable reverse gain in our amplifier (cf. Sec. V.A.2).

3. Converting between representations

Some straightforward algebra now lets us express the op-amp parameters appearing in Eq. (7.4) in terms of the scattering matrix appearing in Eq. (7.3):

$$\lambda_V = 2\sqrt{\frac{Z_b}{Z_a}} \frac{s_{21}}{D} \quad (7.7a)$$

$$\lambda_I' = 2\sqrt{\frac{Z_b}{Z_a}} \frac{s_{12}}{D} \quad (7.7b)$$

$$Z_{\rm out} = Z_b \frac{(1+s_{11})(1+s_{22}) - s_{12}s_{21}}{D} \quad (7.7c)$$

$$\frac{1}{Z_{\rm in}} = \frac{1}{Z_a} \frac{(1-s_{11})(1-s_{22}) - s_{12}s_{21}}{D} \quad (7.7d)$$

where all quantities are evaluated at the same frequency ω, and D is defined as:

$$D = (1+s_{11})(1-s_{22}) + s_{12}s_{21} \quad (7.8)$$

Further, the voltage and current noises in the op-amp representation are simple linear combinations of the

noises $\hat{\mathcal{F}}_a$ and $\hat{\mathcal{F}}_b$ appearing in the scattering representation:

$$\begin{pmatrix} \hat{\hat{V}} \\ Z_a \cdot \hat{\hat{I}} \end{pmatrix} = \sqrt{2\hbar\omega Z_a} \begin{pmatrix} -\frac{1}{2} & \frac{1+s_{11}}{2s_{21}} \\ \frac{s_{22}-1}{D} & -\frac{s_{12}}{D} \end{pmatrix} \begin{pmatrix} \hat{\mathcal{F}}_a \\ \hat{\mathcal{F}}_b \end{pmatrix} \tag{7.9}$$

Again, all quantities above are evaluated at frequency ω.

Eq. (7.9) immediately leads to an important conclusion and caveat: *what one calls the "back-action" and "added noise" in the scattering representation (i.e. $\mathcal{F}_a$ and $\mathcal{F}_b$) are not the same as the "back-action" and "added noise" defined in the usual op-amp representation.* For example, the op-amp back-action $\hat{\hat{I}}$ does not in general coincide with the $\hat{\mathcal{F}}_a$, the back-action in the scattering picture. If we are indeed interested in using our amplifier as a voltage amplifier, we are interested in the total added noise of our amplifier *as defined in the op-amp representation.* As we saw in Sec. VI.E (cf. Eq. (6.43)), this quantity involves both the noises $\hat{\hat{I}}$ and $\hat{\hat{V}}$. We thus see explicitly something already discussed in Sec. VI.C: it is very dangerous to make conclusions about how an amplifier behaves in the op-amp mode of operation based on its properties in the scattering mode of operation. As we will see, even though an amplifier is "ideal" in the scattering mode (i.e. $\mathcal{F}_a$ as small as possible), it can nonetheless fail to reach the quantum limit in the op-amp mode of operation.

In what follows, we will calculate the op-amp noises $\hat{\hat{V}}$ and $\hat{\hat{I}}$ in a minimal bosonic voltage amplifier, and show explicitly how this description is connected to the more general linear-response treatment of Sec. VI.E. However, before proceeding, it is worth noting that Eqs. (7.7a)-(7.7d) are themselves completely consistent with linear-response theory. Using linear-response, one would calculate the op-amp parameters $\lambda_V, \lambda_I', Z_{\rm in}$ and $Z_{\rm out}$ using Kubo formulas (cf. Eqs. (6.56), (6.57) and the discussion following Eq. (6.51)). These in turn would involve correlation functions of $\hat{I}_a$ and $\hat{V}_b$ evaluated at zero coupling to the amplifier input and output. Zero coupling means that there is no input voltage to the amplifier (i.e. a short circuit at the amplifier input, $\hat{V}_a = 0$) and there is nothing at the amplifier output drawing current (i.e. an open circuit at the amplifier output, $\hat{I}_b = 0$). Eq. (7.4) tells us that in this case, $\hat{V}_b$ and $\hat{I}_a$ reduce to (respectively) the noise operators $\lambda_V \hat{\hat{V}}$ and $\hat{\hat{I}}$. Using the fact that the commutators of $\hat{\mathcal{F}}_a$ and $\hat{\mathcal{F}}_b$ are completely determined by the scattering matrix (cf. Eq. (7.3)), we verify explicitly in Appendix J.4 that the Kubo formulas yield the same results for the op-amp gains and impedances as Eqs. (7.7a)-(7.7d) above.

B. Minimal two-port scattering amplifier

1. Scattering versus op-amp quantum limit

In this subsection we demonstrate that an amplifier which is "ideal" and minimally complex when used in the scattering operation mode fails, when used as a voltage op-amp, to have a quantum limited noise temperature. The system we look at is very similar to the amplifier considered by Grassia (1998), though our conclusions are somewhat different than those found there.

In the scattering representation, one might guess that an "ideal" amplifier would be one where there are no reflections of signals at the input and output, and no way for incident signals at the output port to reach the input. In this case, Eq. (7.3) takes the form:

$$\begin{pmatrix} \hat{a}_{\rm out} \\ \hat{b}_{\rm out} \end{pmatrix} = \begin{pmatrix} 0 & 0 \\ \sqrt{G} & 0 \end{pmatrix} \begin{pmatrix} \hat{a}_{\rm in} \\ \hat{b}_{\rm in} \end{pmatrix} + \begin{pmatrix} \hat{\mathcal{F}}_a \\ \hat{\mathcal{F}}_b \end{pmatrix} \tag{7.10}$$

where we have defined $\sqrt{G} \equiv s_{21}$. All quantities above should be evaluated at the same frequency ω; for clarity, we will omit writing the explicit ω dependence of quantities throughout this section.

Turning to the op-amp representation, the above equation implies that our amplifier has no reverse gain, and that the input and output impedances are simply given by the impedances of the input and output transmission lines. From Eqs. (7.7), we have:

$$\lambda_V = 2\sqrt{\frac{Z_b}{Z_a}G} \tag{7.11a}$$

$$\lambda_I' = 0 \tag{7.11b}$$

$$Z_{\rm out} = Z_b \tag{7.11c}$$

$$\frac{1}{Z_{\rm in}} = \frac{1}{Z_a} \tag{7.11d}$$

We immediately see that our amplifier looks less ideal as an op-amp. The input and output impedances are the same as those of the input and output transmission line. However, for an ideal op-amp, we would have liked $Z_{\rm in} \to \infty$ and $Z_{\rm out} \to 0$.

Also of interest are the expressions for the amplifier noises in the op-amp representation:

$$\begin{pmatrix} \hat{\hat{V}} \\ Z_a \cdot \hat{\hat{I}} \end{pmatrix} = -\sqrt{2\hbar\omega Z_a} \begin{pmatrix} \frac{1}{2} & -\frac{1}{2\sqrt{G}} \\ 1 & 0 \end{pmatrix} \begin{pmatrix} \hat{\mathcal{F}}_a \\ \hat{\mathcal{F}}_b \end{pmatrix} \tag{7.12}$$

As $s_{12} = 0$, the back-action noise is the same in both the op-amp and scattering representations: it is determined completely by the noise operator $\hat{\mathcal{F}}_a$. However, the voltage noise (i.e. the intrinsic output noise) involves *both* $\hat{\mathcal{F}}_a$ and $\hat{\mathcal{F}}_b$. We thus have the unavoidable consequence that there will be correlations in $\hat{\hat{I}}$ and $\hat{\hat{V}}$. Note that from basic linear response theory, we know that there must be some correlations between $\hat{\hat{I}}$ and $\hat{\hat{V}}$ if there is to be

gain (i.e. λ_V is given by a Kubo formula involving these operators, cf. Eq. (5.3)).

To make further progress, we note again that commutators of the noise operators $\hat{\mathcal{F}}_a$ and $\hat{\mathcal{F}}_b$ are completely determined by Eq. (7.10) and the requirement that the output operators obey canonical commutation relations. We thus have:

$$\left[\hat{\mathcal{F}}_a, \hat{\mathcal{F}}_a^\dagger\right] = 1 \tag{7.13a}$$

$$\left[\hat{\mathcal{F}}_b, \hat{\mathcal{F}}_b^\dagger\right] = 1 - |G| \tag{7.13b}$$

$$\left[\hat{\mathcal{F}}_a, \hat{\mathcal{F}}_b\right] = 0 \tag{7.13c}$$

$$\left[\hat{\mathcal{F}}_a, \hat{\mathcal{F}}_b^\dagger\right] = 0 \tag{7.13d}$$

We will be interested in the limit of a large power gain, which requires $|G| \gg 1$. A minimal solution to the above equations would be to have the noise operators determined by two independent (i.e. mutually commuting) auxiliary input mode operators u_{in} and $v_{in}^\dagger$:

$$\hat{\mathcal{F}}_a = \hat{u}_{\rm in} \tag{7.14}$$

$$\hat{\mathcal{F}}_b = \sqrt{|G|-1}\,\hat{v}_{\rm in}^\dagger \tag{7.15}$$

Further, to minimize the noise of the amplifier, we take the operating state of the amplifier to be the vacuum for both these modes. With these choices, our amplifier is in exactly the minimal form described by Grassia (1998): an input and output line coupled to a negative resistance box and an auxiliary "cold load" via a four-port circulator (see Fig. 13). The negative resistance box is nothing but the single-mode bosonic amplifier discussed in Sec. VI.B; an explicit realization of this element would be the parametric amplifier discussed in Appendix F. The "cold load" is a semi-infinite transmission line which models dissipation due to a resistor at zero-temperature (i.e. its noise is vacuum noise, cf. Appendix C).

Note that within the scattering picture, one would conclude that our amplifier is ideal: in the large gain limit, the noise added by the amplifier to $\hat{b}_{\rm out}$ corresponds to a single quantum at the input:

$$\frac{\left\langle\left\{\hat{\mathcal{F}}_b\,, \hat{\mathcal{F}}_b^\dagger\right\}\right\rangle}{|G|} = \frac{|G|-1}{|G|}\left\langle\left\{\hat{v}_{\rm in}^\dagger, \hat{v}_{\rm in}\right\}\right\rangle \to 1 \tag{7.16}$$

This however is *not* the quantity which interests us: as we want to use this system as a voltage op-amp, we would like to know if the noise temperature *defined in the op-amp picture* is as small as possible. We are also usually interested in the case of a signal which is weakly coupled to our amplifier; here, weak-coupling means that the input impedance of the amplifier is much larger than the impedance of the signal source (i.e. $Z_{\rm in} \gg Z_{\rm s}$). In this limit, the amplifier only slightly increases the total damping of the signal source.

To address whether we can reach the op-amp quantum limit in the weak-coupling regime, we can make use of the results of the general theory presented in Sec. VI.E. In particular, we need to check whether the quantum noise constraint of Eq. (6.60) is satisfied, as this is a prerequisite for reaching the (weak-coupling) quantum limit. Thus, we need to calculate the *symmetrized* spectral densities of the current and voltage noises, and their cross-correlation. It is easy to confirm from the definitions of Eq. (7.1a) and (7.1b) that these quantities take the form:

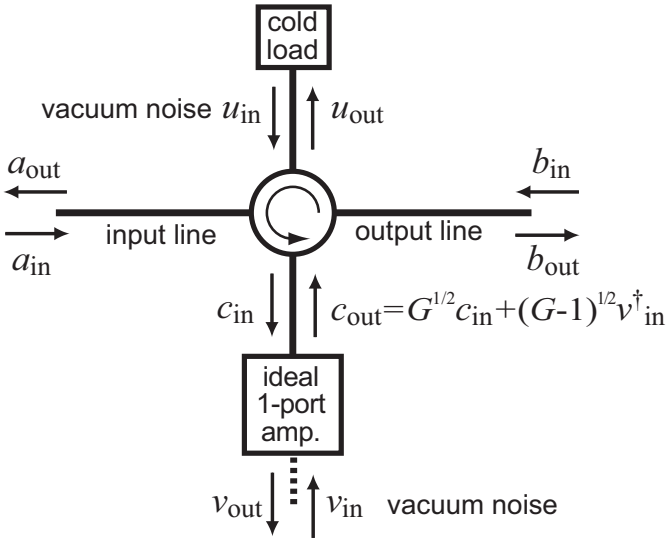

FIG. 13 Schematic of a "minimal" two-port amplifier which reaches the quantum limit in the scattering mode of operation, but misses the quantum limit when used as a weakly-coupled op-amp. See text for further description

$$\bar{S}_{VV}[\omega] = \frac{\left\langle\left\{\hat{\tilde{V}}[\omega], \hat{\tilde{V}}^\dagger(\omega')\right\}\right\rangle}{4\pi\delta(\omega-\omega')} \tag{7.17a}$$

$$\bar{S}_{II}[\omega] = \frac{\left\langle\left\{\hat{\tilde{I}}[\omega], \hat{\tilde{I}}^\dagger(\omega')\right\}\right\rangle}{4\pi\delta(\omega-\omega')} \tag{7.17b}$$

$$\bar{S}_{VI}[\omega] = \frac{\left\langle\left\{\hat{\tilde{V}}[\omega], \hat{\tilde{I}}^\dagger(\omega')\right\}\right\rangle}{4\pi\delta(\omega-\omega')} \tag{7.17c}$$

The expectation values here are over the operating state of the amplifier; we have chosen this state to be the vacuum for the auxiliary mode operators $\hat{u}_{\rm in}$ and $\hat{v}_{\rm in}$ to minimize the noise.

Taking $|s_{21}| \gg 1$, and using Eqs. (7.14) and (7.15), we have

$$\bar{S}_{VV}[\omega] = \frac{\hbar\omega Z_a}{4}\left(\sigma_{uu}+\sigma_{vv}\right) = \frac{\hbar\omega Z_a}{2} \tag{7.18a}$$

$$\bar{S}_{II}[\omega] = \frac{\hbar\omega}{Z_a}\sigma_{uu} = \frac{\hbar\omega}{Z_a} \tag{7.18b}$$

$$\bar{S}_{VI}[\omega] = \frac{\hbar\omega}{2}\sigma_{uu} = \frac{\hbar\omega}{2} \tag{7.18c}$$

where we have defined:

$$\sigma_{ab} \equiv \left\langle \hat{a}\hat{b}^\dagger + \hat{b}^\dagger\hat{a}\right\rangle \tag{7.19}$$

and have used the fact that there cannot be any correlations between the operators u and v in the vacuum state (i.e. $\langle \hat{u}\hat{v}^\dagger \rangle = 0$).

It follows immediately from the above equations that our minimal amplifier does not optimize the quantum noise constraint of Eq. (6.60):

$$\bar{S}_{VV}[\omega]\bar{S}_{II}[\omega] - \left[\text{Im } \bar{S}_{VI}\right]^2 = 2 \times \left(\frac{\hbar\omega}{2}\right)^2. \quad (7.20)$$

The noise product $\bar{S}_{VV}\bar{S}_{II}$ is precisely twice the quantum-limited value. As a result, the general theory of Sec. VI.E tells us *if one couples an input signal weakly to this amplifier (i.e. $Z_{\rm s} \ll Z_{\rm in}$), it is impossible to reach the quantum limit on the added noise.* Thus, while our amplifier is ideal in the scattering mode of operation (cf. Eq. (7.16)), it fails to reach the quantum limit when used in the weak-coupling, op-amp mode of operation. Our amplifier's failure to have "ideal" quantum noise also means that if we tried to use it to do QND qubit detection, the resulting back-action dephasing would be twice as large as the minimum required by quantum mechanics (cf. Sec. V.B).

One might object to the above conclusions based on the classical expression for the minimal noise temperature, Eq. (6.48). Unlike the quantum noise constraint of Eq. (6.60), this equation also involves the real part of $\bar{S}_{VI}$, and is optimized by our "minimal" amplifier. However, this does not mean that one can achieve a noise temperature of $\hbar\omega/2$ at weak coupling! Recall from Sec. VI.E that in the usual process of optimizing the noise temperature, one starts by assuming the weak coupling condition that the source impedance $Z_{\rm s}$ is much smaller than the amplifier input impedance $Z_{\rm in}$. One then finds that to minimize the noise temperature, $|Z_{\rm s}|$ should be tuned to match the noise impedance of the amplifier $Z_{\rm N} \equiv \sqrt{\bar{S}_{VV}/\bar{S}_{II}}$. However, in our minimal bosonic amplifier, it follows from Eqs. (7.18) that $Z_{\rm N} = Z_{\rm in}/\sqrt{2} \sim Z_{\rm in}$: the noise impedance is on the order of the input impedance. Thus, it is *impossible* to match the source impedance to the noise impedance while at the same time satisfying the weak coupling condition $Z_{\rm s} \ll Z_{\rm in}$.

Despite its failings, our amplifier can indeed yield a quantum-limited noise temperature in the op-amp mode of operation *if* we no longer insist on a weak coupling to the input signal. To see this explicitly, imagine we connected our amplifier to a signal source with source impedance Z_s. The total output noise of the amplifier, referred back to the signal source, will now have the form:

$$\hat{\tilde{V}}_{\rm tot} = -\left(\frac{Z_s Z_a}{Z_s + Z_a}\right)\hat{\tilde{I}} + \hat{\tilde{V}} \quad (7.21)$$

Note that this classical-looking equation can be rigorously justified within the full quantum theory if one starts with a full description of the amplifier and the signal source (e.g. a parallel LC oscillator attached in parallel to the amplifier input). Plugging in the expressions for $\hat{\tilde{I}}$ and $\hat{\tilde{V}}$, we find:

$$\begin{aligned}\hat{\tilde{V}}_{\rm tot} &= \sqrt{\frac{\hbar\omega}{2}}\left[\left(\frac{Z_{\rm s}Z_a}{Z_{\rm s}+Z_a}\right)\left(\frac{2}{\sqrt{Z_a}}\hat{u}_{\rm in}\right) - \right. \\ &\qquad \left. \sqrt{Z_a}(\hat{u}_{\rm in} - \hat{v}_{\rm in}^\dagger)\right] \\ &= \sqrt{\frac{\hbar\omega Z_a}{2}}\left[\left(\frac{Z_{\rm s}-Z_a}{Z_{\rm s}+Z_a}\right)\hat{u}_{\rm in} - \hat{v}_{\rm in}^\dagger\right] \quad (7.22)\end{aligned}$$

Thus, if one tunes $Z_{\rm s}$ to $Z_a = Z_{\rm in}$, the mode $\hat{u}_{\rm in}$ does not contribute to the total added noise, and one reaches the quantum limit. Physically speaking, by matching the signal source to the input line, the "back-action" noise described by $\hat{\mathcal{F}}_a = \hat{u}_{\rm in}$ does not feed back into the input of the amplifier. Note that achieving this matching explicitly requires one to be far from weak coupling! Having $Z_s = Z_a$ means that when we attach the amplifier to the signal source, we will dramatically increase the damping of the signal source.

2. Why is the op-amp quantum limit not achieved?

Returning to the more interesting case of a weak amplifier-signal coupling, one might still be puzzled as to why our seemingly ideal amplifier misses the quantum limit. While the mathematics behind Eq. (7.20) is fairly transparent, it is also possible to understand this result heuristically. To that end, note again that the amplifier noise cross-correlation $\bar{S}_{IV}$ does not vanish in the large-gain limit (cf. Eq. (7.18c)). Correlations between the two amplifier noises represent a kind of information, as by making use of them, we can improve the performance of the amplifier. It is easy to take advantage of out-of-phase correlations between $\tilde{I}$ and $\tilde{V}$ (i.e. Im $\bar{S}_{VI}$) by simply tuning the phase of the source impedance (cf. Eq. (6.47)). However, one cannot take advantage of in-phase noise correlations (i.e. Re $\bar{S}_{VI}$) as easily. To take advantage of the information here, one needs to modify the amplifier itself. By feeding back some of the output voltage to the input, one could effectively cancel out some of the back-action current noise $\tilde{I}$ and thus reduce the overall magnitude of $\bar{S}_{II}$. Hence, the unused information in the cross-correlator Re $\bar{S}_{VI}$ represents a kind of wasted information: had we made use of these correlations via a feedback loop, we could have reduced the noise temperature and increased the information provided by our amplifier. The presence of a non-zero Re $\bar{S}_{VI}$ thus corresponds to wasted information, implying that we cannot reach the quantum limit. Recall that within the linear-response approach, we were able to prove rigorously that a large-gain amplifier with ideal quantum noise *must* have Re $\bar{S}_{VI} = 0$ (cf. the discussion following Eq. (6.29)); thus, a non-vanishing Re $\bar{S}_{VI}$ rigorously implies that one cannot be at the quantum limit. In Appendix I, we give

an explicit demonstration of how feedback may be used to utilize these cross-correlations to reach the quantum limit.

Finally, yet another way of seeing that our amplifier does not reach the quantum limit (in the weak coupling regime) is to realize that this system *does not have a well defined effective temperature*. Recall from Sec.VI.E that a system with "ideal" quantum noise (i.e. one that satisfies Eq. (6.60) as an equality) necessarily has the *same* effective temperature at its input and output ports (cf. Eq. (6.27)). Here, that implies the requirement:

$$\frac{|\lambda_V|^2 \cdot \bar{S}_{VV}}{Z_{\rm out}} \;=\; Z_{\rm in}\bar{S}_{II} \equiv 2k_{\rm B}T_{\rm eff} \qquad (7.23)$$

In contrast, our minimal bosonic amplifier has very different input and output effective temperatures:

$$2k_B T_{\rm eff,in} \;=\; Z_{\rm in}\bar{S}_{II} = \frac{\hbar\omega}{2} \qquad (7.24)$$

$$2k_B T_{\rm eff,out} \;=\; \frac{|\lambda_V|^2 \cdot \bar{S}_{VV}}{Z_{\rm out}} = 2|G|\hbar\omega \qquad (7.25)$$

This huge difference in effective temperatures means that it is impossible for the system to possess "ideal" quantum noise, and thus it cannot reach the weak-coupling quantum limit.

While it implies that one is not at the quantum limit, the fact that $T_{\rm eff,in} \ll T_{\rm eff,out}$ can nonetheless be viewed as an asset. From a practical point of view, a large $T_{\rm eff,in}$ can be dangerous. Even though the direct effect of the large $T_{\rm eff,in}$ is offset by an appropriately weak coupling to the amplifier (see Eq. (6.42) and following discussion), this large $T_{\rm eff,in}$ can also heat up other degrees of freedom if they couple strongly to the back-action noise of the amplifier. This can in turn lead to unwanted heating of the input system. As $T_{\rm eff,in}$ is usually constant over a broad range of frequencies, this unwanted heating effect can be quite bad. In the minimal amplifier discussed here, this problem is circumvented by having a small $T_{\rm eff,in}$. The only price that is payed is that the added noise will be $\sqrt{2}$ the quantum limit value. We discuss this issue further in Sec. VIII.

VIII. REACHING THE QUANTUM LIMIT IN PRACTICE

A. Importance of QND measurements

The fact that QND measurements are repeatable is of fundamental practical importance in overcoming detector inefficiencies (Gambetta *et al.*, 2007). A prototypical example is the electron shelving technique (Nagourney *et al.*, 1986; Sauter *et al.*, 1986) used to measure trapped ions. A related technique is used in present implementations of ion-trap based quantum computation. Here the (extremely long-lived) hyperfine state of an ion is read out via state-dependent optical fluorescence. With properly chosen circular polarization of the exciting laser, only one hyperfine state fluoresces and the transition is cycling; that is, after fluorescence the ion almost always returns to the same state it was in prior to absorbing the exciting photon. Hence the measurement is QND. Typical experimental parameters (Wineland *et al.*, 1998) allow the cycling transition to produce $N \sim 10^6$ fluorescence photons. Given the photomultiplier quantum efficiency and typically small solid angle coverage, only a very small number $\bar{n}_d$ will be detected on average. The probability of getting zero detections (ignoring dark counts for simplicity) and hence misidentifying the hyperfine state is $P(0) = e^{-\bar{n}_d}$. Even for a very poor overall detection efficiency of only 10^{-5}, we still have $\bar{n}_d = 10$ and nearly perfect fidelity $F = 1 - P(0) \approx 0.999955$. It is important to note that the total time available for measurement is not limited by the phase coherence time (T_2) of the qubit or by the measurement-induced dephasing (Gambetta *et al.*, 2006; Korotkov, 2001a; Makhlin *et al.*, 2001; Schuster *et al.*, 2005), but rather only by the rate at which the qubit makes real transitions between measurement ($\hat{\sigma}_z$) eigenstates. In a perfect QND measurement there is no measurement-induced state mixing (Makhlin *et al.*, 2001) and the relaxation rate $1/T_1$ is unaffected by the measurement process.

B. Power matching versus noise matching

In Sec. VI, we saw that an important part of reaching the quantum limit on the added noise of an amplifier (when used in the op-amp mode of operation) is to optimize the coupling strength to the amplifier. For a position detector, this condition corresponds to tuning the strength of the back-action damping γ to be much smaller than the intrinsic oscillator damping (c.f. Eq. (6.41)). For a voltage amplifier, this condition corresponds to tuning the impedance of the signal source to be equal to the noise impedance (c.f. Eq. (6.49)), an impedance which is much smaller than the amplifier's input impedance (c.f. Eq. (6.62)).

In this subsection, we make the simple point that optimizing the coupling (i.e. source impedance) to reach the quantum limit *is not* the same as what one would do to optimize the power gain. To understand this, we need to introduce another measure of power gain commonly used in the engineering community, the available power gain $G_{P,\rm avail}$. For simplicity, we will discuss this quantity in the context of a linear voltage amplifier, using the notations of Sec. VI.E; it can be analogously defined for the position detector of Sec.VI.D. $G_{P,\rm avail}$ tells us how much power we are providing to an optimally matched output load relative to the maximum power we *could* in principle have extracted from the source. This is in marked contrast to the power gain G_P, which was calculated using the *actual* power drawn at the amplifier input.

For the available power gain, we first consider $P_{\rm in,avail}$. This is the maximum possible power that could be delivered to the input of the amplifier, assuming we optimized

both the value of the input impedance $Z_{\rm in}$ and the load impedance $Z_{\rm load}$ while keeping $Z_{\rm s}$ fixed. For simplicity, we will take all impedances to be real in our discussion. In general, the power drawn at the input of the amplifier is given by:

$$P_{\rm in} = \frac{v_{\rm in}^2}{Z_{\rm in}} \frac{Z_s Z_{\rm in}}{(Z_s + Z_{\rm in})^2} \tag{8.1}$$

Maximizing this over $Z_{\rm in}$, we obtain the available input power $P_{\rm in,avail}$:

$$P_{\rm in,avail} = \frac{v_{\rm in}^2}{4Z_{\rm s}} \tag{8.2}$$

The maximum occurs for $Z_{\rm in} = Z_{\rm s}$.

The output power supplied to the load is calculated as before, keeping $Z_{\rm in}$ and $Z_{\rm s}$ distinct. One has:

$$\begin{aligned} P_{\rm out} &= \frac{v_{\rm load}^2}{Z_{\rm load}} && (8.3)\\ &= \frac{v_{\rm out}^2}{Z_{\rm load}} \left(\frac{Z_{\rm load}}{Z_{\rm out} + Z_{\rm load}} \right)^2 && (8.4)\\ &= \frac{\lambda^2 v_{\rm in}^2}{Z_{\rm out}} \left(\frac{Z_{\rm in}}{Z_{\rm in} + Z_{\rm s}} \right)^2 \frac{Z_{\rm load}/Z_{\rm out}}{(1 + Z_{\rm load}/Z_{\rm out})^2} && (8.5) \end{aligned}$$

As a function of $Z_{\rm load}$, $P_{\rm out}$ is maximized when $Z_{\rm load} = Z_{\rm out}$:

$$P_{\rm out,max} = \frac{\lambda^2 v_{\rm in}^2}{4Z_{\rm out}} \left(\frac{Z_{\rm in}}{Z_{\rm in} + Z_{\rm s}} \right)^2 \tag{8.6}$$

The available power gain is now defined as:

$$\begin{aligned} G_{P,\rm avail} &\equiv \frac{P_{\rm out,max}}{P_{\rm in,avail}} && (8.7)\\ &= \frac{\lambda^2 Z_{\rm s}}{Z_{\rm out}} \left(\frac{Z_{\rm in}}{Z_{\rm in} + Z_{\rm s}} \right)^2 && (8.8)\\ &= G_P \frac{4Z_{\rm s}/Z_{\rm in}}{(1 + Z_{\rm s}/Z_{\rm in})^2} && (8.9) \end{aligned}$$

We see that $G_{P,\rm avail}$ is strictly less than or equal to the power gain G_P; equality is only achieved when $Z_{\rm s} = Z_{\rm in}$ (i.e. when the source impedance is "power matched" to the input of the amplifier). The general situation where $G_{P,\rm avail} < G_P$ indicates that we are not drawing as much power from the source as we could, and hence the actual power supplied to the load is not as large as it could be.

Consider now a situation where we have achieved the quantum limit on the added noise. This necessarily means that we have "noise matched", i.e. taken $Z_{\rm s}$ to be equal to the noise impedance $Z_{\rm N}$. The available power gain in this case is:

$$G_{P,\rm avail} \simeq \lambda^2 \frac{Z_N}{Z_{\rm out}} \simeq 2\sqrt{G_P} \ll G_P \tag{8.10}$$

We have used Eq. (6.62), which tells us that the noise impedance is smaller than the input impedance by a large factor $1/(2\sqrt{G_P})$. Thus, as reaching the quantum limit requires the use of a source impedance much smaller than $Z_{\rm in}$, it results in a dramatic drop in the available power gain compared to the case where we "power match" (i.e. take $Z_{\rm s} = Z_{\rm in}$). In practice, one must decide whether it is more important to minimize the added noise, or maximize the power provided at the output of the amplifier: one cannot do both at the same time.

IX. CONCLUSIONS

In this review, we have given an introduction to the physics of quantum noise. We have discussed how one can measure quantum noise using quantum spectrum analyzers, as well as how fundamental constraints on quantum noise are directly tied to various quantum limits on measurement and amplification. As already mentioned in the introduction, there are many interesting topics related to quantum noise and quantum circuits that we were not able to cover in this review. In what follows, we give a brief listing of some of these topics, along with relevant review literature.

Quantum noise has long been of interest in mesoscopic physics, even before the recent resurgence inspired by connections to measurement and amplification. In particular, the study of non-equilibrium current fluctuations (i.e. shot noise) of a mesoscopic conductor, and the related full statistics of current fluctuations ("full counting statistics"), have been intensely studied, as they can reveal important insights into quantum transport. Both topics have been covered in a number of recent reviews (Blanter and Büttiker, 2000; Levitov, 2003; Nazarov, 2003). Connections between full counting statistics and quantum measurement have also been explored (Averin and Sukhorukov, 2005; Nazarov and Kindermann, 2003).

There are also several important aspects of weak quantum measurement that we have not been able to discuss in this review. A relatively recent development has been the study of conditional quantum evolution and quantum trajectories. Such studies attempt to understand the evolution of a quantum system in a particular run of an experiment: given a particular measurement record, what is the state of the measured system? Further, can the measurement record contain evidence of quantum jumps of the measured system between different states (e.g. a mechanical resonator jumping from one Fock state to another). Such topics have received substantial attention in the quantum optics and atomic physics community. The topic of quantum jumps and stochastic wavefunction evolution is given a tutorial review in Brun, 2002, while an introduction to conditional quantum evolution and quantum feedback is given in Jacobs and Steck, 2006. These topics have also recently been discussed in the context of condensed matter systems. Studies have examined continuous measurement of a qubit by a quantum point contact (Goan and Milburn, 2001; Goan *et al.*, 2001; Korotkov, 1999, 2001b), as well as the possibility of detect-

ing quantum jumps in the state of a mechanical resonator via QND measurement of its energy (Santamore *et al.*, 2004a,b).

While we have discussed many measurement and amplification schemes, there are several which we did not address. So-called "latching" measurements of the state of a qubit have recently been used to make measurements of the state of a superconducting qubit (Siddiqi *et al.*, 2004). For a sufficiently slow input signal, such latching measurements can also be used as an efficient means of linear amplification, possibly reaching the amplifier quantum limit.

Acknowledgements

This work was supported in part by NSERC, the Canadian Institute for Advanced Research (CIFAR), NSA under ARO contract number W911NF-05-1-0365, the NSF under grants DMR-0653377 and DMR-0603369, the David and Lucile Packard Foundation, the W.M. Keck Foundation and the Alfred P. Sloan Foundation. We acknowledge the support and hospitality of the Aspen Center for Physics where part of this work was carried out. F.M. acknowledges support via DIP and through SFB 631, SFB/TR 12, the Nanosystems Initiative Munich, and the Emmy-Noether program. S. M. G. acknowledges the support of the Centre for Advanced Study at the Norwegian Academy of Science and Letters where part of this work was carried out.

APPENDIX A: The Wiener-Khinchin Theorem

From the definition of the spectral density in Eqs.(2.2-2.3) we have

$$\mathcal{S}_{VV}[\omega] = \frac{1}{T}\int_0^T dt \int_0^T dt'\, e^{i\omega(t-t')}\langle v(t)v(t')\rangle$$
$$= \frac{1}{T}\int_0^T dt \int_{-2B(t)}^{+2B(t)} d\tau\, e^{i\omega\tau}\,\langle v(t+\tau/2)v(t-\tau/2)\rangle \quad \text{(A1)}$$

where

$$\begin{aligned} B\,(t) &= t \text{ if } t < T/2 \\ &= T-t \text{ if } t > T/2. \end{aligned}$$

If T greatly exceeds the noise autocorrelation time $\tau_{\rm c}$ then it is a good approximation to extend the bound $B(t)$ in the second integral to infinity, since the dominant contribution is from small τ. Using time translation invariance gives

$$\begin{aligned} \mathcal{S}_{VV}[\omega] &= \frac{1}{T}\int_0^T dt \int_{-\infty}^{+\infty} d\tau\, e^{i\omega\tau}\,\langle v(\tau)v(0)\rangle \\ &= \int_{-\infty}^{+\infty} d\tau\, e^{i\omega\tau}\,\langle v(\tau)v(0)\rangle\,. \end{aligned} \quad \text{(A2)}$$

This proves the Wiener-Khinchin theorem stated in Eq. (2.4).

A useful application of these ideas is the following. Suppose that we have a noisy signal $V(t) = \bar{V} + \eta(t)$ which we begin monitoring at time $t = 0$. The integrated signal up to time t given by

$$I(T) = \int_0^T dt\, V(t) \quad \text{(A3)}$$

has mean

$$\langle I(T)\rangle = \bar{V}T. \quad \text{(A4)}$$

Provided that the integration time greatly exceeds the autocorrelation time of the noise, $I(T)$ is a sum of a large number of uncorrelated random variables. The central limit theorem tells us in this case that $I(t)$ is gaussian distributed even if the signal itself is not. Hence the probability distribution for I is fully specified by its mean and its variance

$$\langle(\Delta I)^2\rangle = \int_0^T dtdt'\,\langle\eta(t)\eta(t')\rangle. \quad \text{(A5)}$$

From the definition of spectral density above we have the simple result that the variance of the integrated signal grows linearly in time with proportionality constant given by the noise spectral density at zero frequency

$$\langle(\Delta I)^2\rangle = \mathcal{S}_{VV}[0]\,T. \quad \text{(A6)}$$

As a simple application, consider the photon shot noise of a coherent laser beam. The total number of photons detected in time T is

$$N(T) = \int_0^T dt\,\dot{N}(t). \quad \text{(A7)}$$

The photo-detection signal $\dot{N}(t)$ is *not* gaussian, but rather is a *point process*, that is, a sequence of delta functions with random Poisson distributed arrival times and mean photon arrival rate $\overline{\dot{N}}$. Nevertheless at long times the mean number of detected photons

$$\langle N(T)\rangle = \overline{\dot{N}}T \quad \text{(A8)}$$

will be large and the photon number distribution will be gaussian with variance

$$\langle(\Delta N)^2\rangle = S_{\dot{N}\dot{N}}\,T. \quad \text{(A9)}$$

Since we know that for a Poisson process the variance is equal to the mean

$$\langle(\Delta N)^2\rangle = \langle N(T)\rangle, \quad \text{(A10)}$$

it follows that the shot noise power spectral density is

$$S_{\dot{N}\dot{N}}(0) = \overline{\dot{N}}. \quad \text{(A11)}$$

Since the noise is white this result happens to be valid at all frequencies, but the noise is gaussian distributed only at low frequencies.

APPENDIX B: Modes, Transmission Lines and Classical Input/Output Theory

In this appendix we introduce a number of important classical concepts about electromagnetic signals which are essential to understand before moving on to the study of their quantum analogs. A signal at carrier frequency ω can be described in terms of its amplitude and phase or equivalently in terms of its two quadrature amplitudes

$$s(t) = X\cos(\omega t) + Y\sin(\omega t). \tag{B1}$$

We will see in the following that the physical oscillations of this signal in a transmission line are precisely the sinusoidal oscillations of a simple harmonic oscillator. Comparison of Eq. (B1) with Eq. (2.18) shows that we can identify the quadrature amplitude X with the coordinate of this oscillator and thus the quadrature amplitude Y is proportional to the momentum conjugate to X. Quantum mechanically, X and Y become operators $\hat{X}$ and $\hat{Y}$ which do not commute. Thus their quantum fluctuations obey the Heisenberg uncertainty relation.

Ordinarily (e.g., in the absence of squeezing), the phase choice defining the two quadratures is arbitrary and so their vacuum (i.e. zero-point) fluctuations are equal

$$X_{\rm ZPF} = Y_{\rm ZPF}. \tag{B2}$$

Thus the canonical commutation relation becomes

$$[\hat{X},\hat{Y}] = iX^2_{\rm ZPF}. \tag{B3}$$

We will see that the fact that X and Y are canonically conjugate has profound implications both classically and quantum mechanically. In particular, the action of any circuit element (beam splitter, attenuator, amplifier, etc.) must preserve the Poisson bracket (or in the quantum case, the commutator) between the signal quadratures. This places strong constraints on the properties of these circuit elements and in particular, forces every amplifier to add noise to the signal.

1. Transmission lines and classical input-output theory

We begin by considering a coaxial transmission line modeled as a perfectly conducting wire with inductance per unit length of ℓ and capacitance to ground per unit length c as shown in Fig. 14. If the voltage at position x at time t is $V(x,t)$, then the charge density is $q(x,t) = cV(x,t)$. By charge conservation the current I and the charge density are related by the continuity equation

$$\partial_t q + \partial_x I = 0. \tag{B4}$$

The constitutive relation (essentially Newton's law) gives the acceleration of the charges

$$\ell\partial_t I = -\partial_x V. \tag{B5}$$

We can decouple Eqs. (B4) and (B5) by introducing left and right propagating modes

$$V(x,t) = [V^{\rightarrow} + V^{\leftarrow}] \tag{B6}$$

$$I(x,t) = \frac{1}{Z_{\rm c}}[V^{\rightarrow} - V^{\leftarrow}] \tag{B7}$$

where $Z_{\rm c} \equiv \sqrt{\ell/c}$ is called the characteristic impedance of the line. In terms of the left and right propagating modes, Eqs. (B4) and B5 become

$$v_{\rm p}\partial_x V^{\rightarrow} + \partial_t V^{\rightarrow} = 0 \tag{B8}$$

$$v_{\rm p}\partial_x V^{\leftarrow} - \partial_t V^{\leftarrow} = 0 \tag{B9}$$

where $v_{\rm p} \equiv 1/\sqrt{\ell c}$ is the wave phase velocity. These equations have solutions which propagate by uniform translation without changing shape since the line is dispersionless

$$V^{\rightarrow}(x,t) = V_{\rm out}(t - \frac{x}{v_{\rm p}}) \tag{B10}$$

$$V^{\leftarrow}(x,t) = V_{\rm in}(t + \frac{x}{v_{\rm p}}), \tag{B11}$$

where $V_{\rm in}$ and $V_{\rm out}$ are *arbitrary* functions of their arguments. For an infinite transmission line, $V_{\rm out}$ and $V_{\rm in}$ are completely independent. However for the case of a semi-infinite line terminated at $x = 0$ (say) by some system S, these two solutions are not independent, but rather related by the boundary condition imposed by the system. We have

$$V(x=0,t) = [V_{\rm out}(t) + V_{\rm in}(t)] \tag{B12}$$

$$I(x=0,t) = \frac{1}{Z_{\rm c}}[V_{\rm out}(t) - V_{\rm in}(t)], \tag{B13}$$

from which we may derive

$$V_{\rm out}(t) = V_{\rm in}(t) + Z_{\rm c}I(x=0,t). \tag{B14}$$

If the system under study is just an open circuit so that $I(x=0,t) = 0$, then $V_{\rm out} = V_{\rm in}$, meaning that the outgoing wave is simply the result of the incoming wave reflecting from the open circuit termination. In general however, there is an additional outgoing wave radiated by the current I that is injected by the system dynamics into the line. In the absence of an incoming wave we have

$$V(x=0,t) = Z_{\rm c}I(x=0,t), \tag{B15}$$

indicating that the transmission line acts as a simple resistor which, instead of dissipating energy by Joule heating, carries the energy away from the system as propagating waves. The fact that the line can dissipate energy despite containing only purely reactive elements is a consequence of its infinite extent. One must be careful with the order of limits, taking the length to infinity *before* allowing time to go to infinity. In this way the outgoing waves never reach the far end of the transmission line and

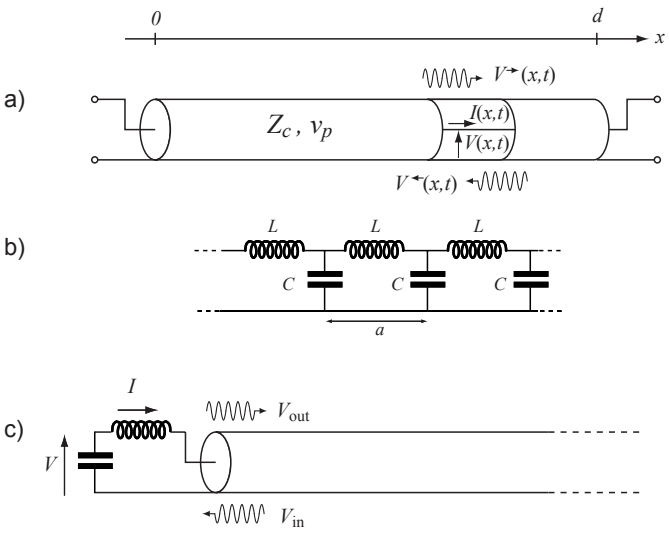

FIG. 14 a) Coaxial transmission line, indicating voltages and currents as defined in the main text. b) Lumped element representation of a transmission line with capacitance per unit length c and inductance per unit length ℓ. c) Discrete LC resonator terminating a transmission line.

reflect back. Since this is a conservative Hamiltonian system, we will be able to quantize these waves and make a quantum theory of resistors (Caldeira and Leggett, 1983) in Appendix C. The net power flow carried to the right by the line is

$$P = \frac{1}{Z_{\rm c}}[V_{\rm out}^2(t) - V_{\rm in}^2(t)]. \tag{B16}$$

The fact that the transmission line presents a dissipative impedance to the system means that it causes damping of the system. It also however opens up the possibility of controlling the system via the input field which partially determines the voltage driving the system. From this point of view it is convenient to eliminate the output field by writing the voltage as

$$V(x=0,t) = 2V_{\rm in}(t) + Z_{\rm c}I(x=0,t). \tag{B17}$$

As we will discuss in more detail below, the first term drives the system and the second damps it. From Eq. (B14) we see that measurement of the outgoing field can be used to determine the current $I(x=0,t)$ injected by the system into the line and hence to infer the system dynamics that results from the input drive field.

As a simple example, consider the system consisting of an LC resonator shown in Fig. (14 c). This can be viewed as a simple harmonic oscillator whose coordinate Q is the charge on the capacitor plate (on the side connected to L_0). The current $I(x=0,t) = \dot{Q}$ plays the role of the velocity of the oscillator. The equation of motion for the oscillator is readily obtained from

$$Q = C_0[-V(x=0^+,t) - L_0\dot{I}(x=0^+,t)]. \tag{B18}$$

Using Eq. (B17) we obtain a harmonic oscillator damped by the transmission line and driven by the incoming waves

$$\ddot{Q} = -\Omega_0^2 Q - \gamma\dot{Q} - \frac{2}{L_0}V_{\rm in}(t), \tag{B19}$$

where the resonant frequency is $\Omega_0^2 \equiv 1/\sqrt{L_0C_0}$. Note that the term $Z_{\rm c}I(x=0,t)$ in Eq. (B17) results in the linear viscous damping rate $\gamma \equiv Z_{\rm c}/L_0$.

If we solve the equation of motion of the oscillator, we can predict the outgoing field. In the present instance of a simple oscillator we have a particular example of the general case where the system responds linearly to the input field. We can characterize any such system by a complex, frequency dependent impedance $Z[\omega]$ defined by

$$Z[\omega] = -\frac{V(x=0,\omega)}{I(x=0,\omega)}. \tag{B20}$$

Note the peculiar minus sign which results from our definition of positive current flowing to the right (out of the system and into the transmission line). Using Eqs. (B12, B13) and Eq. (B20) we have

$$V_{\rm out}[\omega] = r[\omega]V_{\rm in}[\omega], \tag{B21}$$

where the reflection coefficient r is determined by the impedance mismatch between the system and the line and is given by the well known result

$$r[\omega] = \frac{Z[\omega] - Z_{\rm c}}{Z[\omega] + Z_{\rm c}}. \tag{B22}$$

If the system is constructed from purely reactive (i.e. lossless) components, then $Z[\omega]$ is purely imaginary and the reflection coefficient obeys $|r| = 1$ which is consistent with Eq. (B16) and the energy conservation requirement of no net power flow into the lossless system. For example, for the series LC oscillator we have been considering, we have

$$Z[\omega] = \frac{1}{j\omega C_0} + j\omega L_0, \tag{B23}$$

where, to make contact with the usual electrical engineering sign conventions, we have used $j = -i$. If the damping γ of the oscillator induced by coupling it to the transmission line is small, the quality factor of the resonance will be high and we need only consider frequencies near the resonance frequency $\Omega_0 \equiv 1/\sqrt{L_0C_0}$ where the impedance has a zero. In this case we may approximate

$$Z[\omega] \approx \frac{2}{jC_0\Omega_0^2}[\Omega_0 - \omega] = 2jL(\omega - \Omega_0) \tag{B24}$$

which yields for the reflection coefficient

$$r[\omega] = \frac{\omega - \Omega_0 + j\gamma/2}{\omega - \Omega_0 - j\gamma/2} \tag{B25}$$

showing that indeed $|r| = 1$ and that the phase of the reflected signal winds by 2π upon passing through the resonance. [22]

Turning to the more general case where the system also contains lossy elements, one finds that $Z[\omega]$ is no longer purely imaginary, but has a real part satisfying $\mathrm{Re}\, Z[\omega] > 0$. This in turn implies via Eq. (B22) that $|r| < 1$. In the special case of impedance matching $Z[\omega] = Z_c$, all the incident power is dissipated in the system and none is reflected. The other two limits of interest are open circuit termination with $Z = \infty$ for which $r = +1$ and and short circuit termination $Z = 0$ for which $r = -1$.

Finally, if the system also contains an active device which has energy being pumped into it from a separate external source, it may under the right conditions be described by an effective *negative* resistance $\mathrm{Re}\, Z[\omega] < 0$ over a certain frequency range. Eq. (B22) then gives $|r| \geq 1$, implying $|V_{\rm out}| > |V_{\rm in}|$. Our system will thus act like the one-port amplifier discussed in Sec. VI.C: it amplifies signals incident upon it. We will discuss this idea of negative resistance further in Sec. B.4; a physical realization is provided by the two-port reflection parametric amplifier discussed in Appendix F.

2. Lagrangian, Hamiltonian, and wave modes for a transmission line

Prior to moving on to the case of quantum noise it is useful to review the classical statistical mechanics of transmission lines. To do this we need to write down the Lagrangian and then determine the canonical momenta and the Hamiltonian. Very conveniently, the system is simply a large collection of harmonic oscillators (the normal modes) and hence can be readily quantized. This representation of a physical resistor is essentially the one used by Caldeira and Leggett (Caldeira and Leggett, 1983) in their seminal studies of the effects of dissipation on tunneling. The only difference between this model and the vacuum fluctuations in free space is that the relativistic bosons travel in one dimension and do not carry a polarization label. This changes the density of states as a function of frequency, but has no other essential effect.

It is convenient to define a flux variable (Devoret, 1997)

$$\varphi(x,t) \equiv \int_{-\infty}^{t} d\tau\, V(x,\tau), \tag{B26}$$

where $V(x,t) = \partial_t \varphi(x,t)$ is the local voltage on the transmission line at position x and time t. Each segment of the line of length dx has inductance $\ell\, dx$ and the voltage drop along it is $-dx\, \partial_x \partial_t \varphi(x,t)$. The flux through this inductance is thus $-dx\, \partial_x \varphi(x,t)$ and the local value of the current is given by the constitutive equation

$$I(x,t) = -\frac{1}{\ell}\, \partial_x \varphi(x,t). \tag{B27}$$

The Lagrangian for the system is

$$\mathcal{L} = \int_0^\infty dx\, \frac{c}{2} (\partial_t \varphi)^2 - \frac{1}{2\ell}\, (\partial_x \varphi)^2, \tag{B28}$$

The Euler-Lagrange equation for this Lagrangian is simply the wave equation

$$v_{\rm p}^2 \partial_x^2 \varphi - \partial_t^2 \varphi = 0. \tag{B29}$$

The momentum conjugate to $\varphi(x)$ is simply the charge density

$$q(x,t) \equiv \frac{\delta \mathcal{L}}{\delta \partial_t \varphi} = c \partial_t \varphi = c V(x,t) \tag{B30}$$

and so the Hamiltonian is given by

$$H = \int dx\, \left\{ \frac{1}{2c} q^2 + \frac{1}{2\ell} (\partial_x \varphi)^2 \right\}. \tag{B31}$$

We know from our previous results that the charge density consists of left and right moving solutions of arbitrary fixed shape. For example we might have for the right moving case

$$q(t - x/v_{\rm p}) = \alpha_k \cos[k(x - v_{\rm p} t)] + \beta_k \sin[k(x - v_{\rm p} t)]. \tag{B32}$$

A confusing point is that since q is real valued, we see that it necessarily contains both e^{ikx} and e^{-ikx} terms even if it is only right moving. Note however that for $k > 0$ and a right mover, the e^{ikx} is associated with the positive frequency term $e^{-i\omega_k t}$ while the e^{-ikx} term is associated with the negative frequency term $e^{+i\omega_k t}$ where $\omega_k \equiv v_{\rm p}|k|$. For left movers the opposite holds. We can appreciate this better if we define

$$A_k \equiv \frac{1}{\sqrt{L}} \int dx\, e^{-ikx} \left\{ \frac{1}{\sqrt{2c}} q(x,t) - i \sqrt{\frac{k^2}{2\ell}}\, \varphi(x,t) \right\} \tag{B33}$$

where for simplicity we have taken the fields to obey periodic boundary conditions on a length L. Thus we have (in a form which anticipates the full quantum theory)

$$H = \frac{1}{2} \sum_k \left(A_k^* A_k + A_k A_k^* \right). \tag{B34}$$

The classical equation of motion (B29) yields the simple result

$$\partial_t A_k = -i \omega_k A_k. \tag{B35}$$

Thus

$$q(x,t) = \sqrt{\frac{c}{2L}} \sum_k e^{ikx} \left[A_k(0) e^{-i\omega_k t} + A_{-k}^*(0) e^{+i\omega_k t} \right] \tag{B36}$$

$$= \sqrt{\frac{c}{2L}} \sum_k \left[A_k(0) e^{+i(kx - \omega_k t)} + A_k^*(0) e^{-i(kx - \omega_k t)} \right]. \tag{B37}$$

[22] For the case of resonant *transmission* through a symmetric cavity, the phase shift only winds by π.

We see that for $k > 0$ ($k < 0$) the wave is right (left) moving, and that for right movers the e^{ikx} term is associated with positive frequency and the e^{-ikx} term is associated with negative frequency. We will return to this in the quantum case where positive (negative) frequency will refer to the destruction (creation) of a photon. Note that the right and left moving voltages are given by

$$V^{\rightarrow} = \sqrt{\frac{1}{2Lc}} \sum_{k>0} \left[A_k(0) e^{+i(kx-\omega_k t)} + A_k^*(0) e^{-i(kx-\omega_k t)} \right] \tag{B38}$$

$$V^{\leftarrow} = \sqrt{\frac{1}{2Lc}} \sum_{k<0} \left[A_k(0) e^{+i(kx-\omega_k t)} + A_k^*(0) e^{-i(kx-\omega_k t)} \right] \tag{B39}$$

The voltage spectral density for the right moving waves is thus

$$S_{VV}^{\rightarrow}[\omega] = \frac{2\pi}{2Lc} \sum_{k>0} \{ \langle A_k A_k^* \rangle \delta(\omega - \omega_k) + \langle A_k^* A_k \rangle \delta(\omega + \omega_k) \} \tag{B40}$$

The left moving spectral density has the same expression but $k < 0$.

Using Eq. (B16), the above results lead to a net power flow (averaged over one cycle) within a frequency band defined by a pass filter $G[\omega]$ of

$$P = P^{\rightarrow} - P^{\leftarrow} = \frac{v_{\rm p}}{2L} \sum_k \mathrm{sgn}(k) \left[G[\omega_k] \langle A_k A_k^* \rangle + G[-\omega_k] \langle A_k^* A_k \rangle \right]. \tag{B41}$$

3. Classical statistical mechanics of a transmission line

Now that we have the Hamiltonian, we can consider the classical statistical mechanics of a transmission line in thermal equilibrium at temperature T. Since each mode k is a simple harmonic oscillator we have from Eq. (B34) and the equipartition theorem

$$\langle A_k^* A_k \rangle = k_{\rm B} T. \tag{B42}$$

Using this, we see from Eq. (B40) we see that the right moving voltage signal has a simple white noise power spectrum. Using Eq. (B41) we have for the right moving power in a bandwidth B (in Hz rather than radians/sec) the very simple result

$$\begin{aligned} P^{\rightarrow} &= \frac{v_{\rm p}}{2L} \sum_{k>0} \langle G[\omega_k] A_k^* A_k + G[-\omega_k] A_k A_k^* \rangle \\ &= \frac{k_{\rm B} T}{2} \int_{-\infty}^{+\infty} \frac{d\omega}{2\pi} G[\omega] \\ &= k_{\rm B} T B. \end{aligned} \tag{B43}$$

where we have used the fact mentioned in connection with Eq. (2.15) and the discussion of square law detectors that all passive filter functions are symmetric in frequency.

One of the basic laws of statistical mechanics is Kirchhoff's law stating that the ability of a hot object to emit radiation is proportional to its ability to absorb. This follows from very general thermodynamic arguments concerning the thermal equilibrium of an object with its radiation environment and it means that the best possible emitter is the black body. In electrical circuits this principle is simply a form of the fluctuation dissipation theorem which states that the electrical thermal noise produced by a circuit element is proportional to the dissipation it introduces into the circuit. Consider the example of a terminating resistor at the end of a transmission line. If the resistance R is matched to the characteristic impedance $Z_{\rm c}$ of a transmission line, the terminating resistor acts as a black body because it absorbs 100% of the power incident upon it. If the resistor is held at temperature T it will bring the transmission line modes into equilibrium at the same temperature (at least for the case where the transmission line has finite length). The rate at which the equilibrium is established will depend on the impedance mismatch between the resistor and the line, but the final temperature will not.

A good way to understand the fluctuation-dissipation theorem is to represent the resistor R which is terminating the $Z_{\rm c}$ line in terms of a second semi-infinite transmission line of impedance R as shown in Fig. (15). First consider the case when the R line is not yet connected to the $Z_{\rm c}$ line. Then according to Eq. (B22), the open termination at the end of the $Z_{\rm c}$ line has reflectivity $|r|^2 = 1$ so that it does not dissipate any energy. Additionally of course, this termination does not transmit any signals from the R line into the $Z_{\rm c}$. However when the two lines are connected the reflectivity becomes less than unity meaning that incoming signals on the $Z_{\rm c}$ line see

a source of dissipation R which partially absorbs them. The absorbed signals are not turned into heat as in a true resistor but are partially transmitted into the R line which is entirely equivalent. Having opened up this port for energy to escape from the Z_c system, we have also allowed noise energy (thermal or quantum) from the R line to be transmitted into the Z_c line. This is completely equivalent to the effective circuit shown in Fig. (16 a) in which a real resistor has in parallel a random current generator representing thermal noise fluctuations of the electrons in the resistor. This is the essence of the fluctuation dissipation theorem.

In order to make a quantitative analysis in terms of the power flowing in the two lines, voltage is not the best variable to use since we are dealing with more than one value of line impedance. Rather we define incoming and outgoing fields via

$$A_{\rm in} = \frac{1}{\sqrt{Z_c}} V_c^{\leftarrow} \tag{B44}$$

$$A_{\rm out} = \frac{1}{\sqrt{Z_c}} V_c^{\rightarrow} \tag{B45}$$

$$B_{\rm in} = \frac{1}{\sqrt{R}} V_R^{\rightarrow} \tag{B46}$$

$$B_{\rm out} = \frac{1}{\sqrt{R}} V_R^{\leftarrow} \tag{B47}$$

Normalizing by the square root of the impedance allows us to write the power flowing to the right in each line in the simple form

$$P_c = (A_{\rm out})^2 - (A_{\rm in})^2 \tag{B48}$$

$$P_R = (B_{\rm in})^2 - (B_{\rm out})^2 \tag{B49}$$

The out fields are related to the in fields by the s matrix

$$\begin{pmatrix} A_{\rm out} \\ B_{\rm out} \end{pmatrix} = s \begin{pmatrix} A_{\rm in} \\ B_{\rm in} \end{pmatrix} \tag{B50}$$

Requiring continuity of the voltage and current at the interface between the two transmission lines, we can solve for the scattering matrix s:

$$s = \begin{pmatrix} +r & t \\ t & -r \end{pmatrix} \tag{B51}$$

where

$$r = \frac{R - Z_c}{R + Zc} \tag{B52}$$

$$t = \frac{2\sqrt{RZ_c}}{R + Zc}. \tag{B53}$$

Note that $|r|^2 + |t|^2 = 1$ as required by energy conservation and that s is unitary with $\det(s) = -1$. By moving the point at which the phase of the $B_{\rm in}$ and $B_{\rm out}$ fields are determined one-quarter wavelength to the left, we can put s into different standard form

$$s' = \begin{pmatrix} +r & it \\ it & +r \end{pmatrix} \tag{B54}$$

which has $\det(s') = +1$.

FIG. 15 (Color online) Semi-infinite transmission line of impedance Z_c terminated by a resistor R which is represented as a second semi-infinite transmission line.

As mentioned above, the energy absorbed from the Z_c line by the resistor R is not turned into heat as in a true resistor but is is simply transmitted into the R line, which is entirely equivalent. Kirchhoff's law is now easy to understand. The energy absorbed from the Z_c line and the energy transmitted into it by thermal fluctuations in the R line are both proportional to the absorption coefficient

$$A = 1 - |r|^2 = |t|^2 = \frac{4RZ_c}{(R + Z_c)^2}. \tag{B55}$$

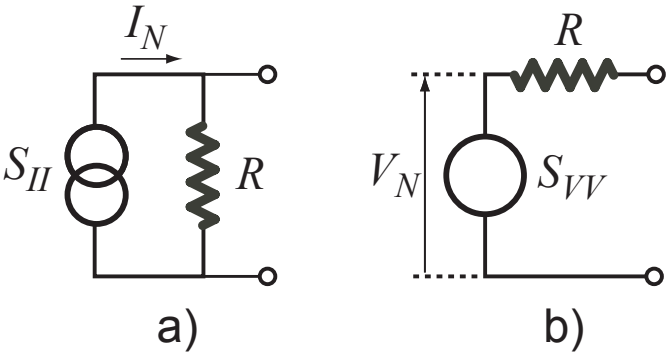

FIG. 16 Equivalent circuits for noisy resistors.

The requirement that the transmission line Z_c come to equilibrium with the resistor allows us to readily compute the spectral density of current fluctuations of the random current source shown in Fig. (16 a). The power dissipated in Z_c by the current source attached to R is

$$P = \int_{-\infty}^{+\infty} \frac{d\omega}{2\pi} S_{II}[\omega] \frac{R^2 Z_c}{(R + Z_c)^2} \tag{B56}$$

For the special case $R = Z_c$ we can equate this to the right moving power $P^{\rightarrow}$ in Eq. (B43) because left moving waves in the Z_c line are not reflected and hence cannot contribute to the right moving power. Requiring $P = P^{\rightarrow}$ yields the classical Nyquist result for the current noise of a resistor

$$\mathcal{S}_{II}[\omega] = \frac{2}{R} k_B T \tag{B57}$$

or in the electrical engineering convention

$$\mathcal{S}_{II}[\omega] + \mathcal{S}_{II}[-\omega] = \frac{4}{R} k_{\rm B} T. \tag{B58}$$

We can derive the equivalent expression for the voltage noise of a resistor (see Fig. 16 b) by considering the voltage noise at the open termination of a semi-infinite transmission line with $Z_{\rm c} = R$. For an open termination $V^{\rightarrow} = V^{\leftarrow}$ so that the voltage at the end is given by

$$V = 2V^{\leftarrow} = 2V^{\rightarrow} \tag{B59}$$

and thus using Eqs. (B40) and (B42) we find

$$\mathcal{S}_{VV} = 4\mathcal{S}^{\rightarrow}_{VV} = 2Rk_{\rm B}T \tag{B60}$$

which is equivalent to Eq. (B57).

4. Amplification with a transmission line and a negative resistance

We close our discussion of transmission lines by further expanding upon the idea mentioned at the end of App. B.1 that one can view a one-port amplifier as a transmission line terminated by an effective negative resistance. The discussion here will be very general: we will explore what can be learned about amplification by simply extending the results we have obtained on transmission lines to the case of an effective negative resistance. Our general discussion will not address the important issues of *how* one achieves an effective negative resistance over some appreciable frequency range: for such questions, one must focus on a specific physical realization, such as the parametric amplifier discussed in Appendix F.

We start by noting that for the case $-Z_{\rm c} < R < 0$ the power gain G is given by

$$G = |r|^2 > 1, \tag{B61}$$

and the s' matrix introduced in Eq. (B54) becomes

$$s' = -\begin{pmatrix} \sqrt{G} & \pm\sqrt{G-1} \\ \pm\sqrt{G-1} & \sqrt{G} \end{pmatrix} \tag{B62}$$

where the sign choice depends on the branch cut chosen in the analytic continuation of the off-diagonal elements. This transformation is clearly no longer unitary (because there is no energy conservation since we are ignoring the work done by the amplifier power supply). Note however that we still have $\det(s') = +1$. It turns out that this naive analytic continuation of the results from positive to negative resistance is not strictly correct. As we will show in the following, we must be more careful than we have been so far in order to insure that the transformation from the in fields to the out fields must be canonical.

In order to understand the canonical nature of the transformation between input and output modes, it is necessary to delve more deeply into the fact that the two quadrature amplitudes of a mode are canonically conjugate. Following the complex amplitudes defined in Eqs. (B44-B47), let us define a vector of real-valued quadrature amplitudes for the incoming and outgoing fields

$$\vec{q}^{\,\rm in} = \begin{pmatrix} X_A^{\rm in} \\ X_B^{\rm in} \\ Y_B^{\rm in} \\ Y_A^{\rm in} \end{pmatrix}, \ \vec{q}^{\,\rm out} = \begin{pmatrix} X_A^{\rm out} \\ X_B^{\rm out} \\ Y_B^{\rm out} \\ Y_A^{\rm out} \end{pmatrix}. \tag{B63}$$

The Poisson brackets amongst the different quadrature amplitudes is given by

$$\{q_i^{\rm in}, q_j^{\rm in}\} \propto J_{ij}, \tag{B64}$$

or equivalently the quantum commutators are

$$[q_i^{\rm in}, q_j^{\rm in}] = iX_{\rm ZPF}^2 J_{ij}, \tag{B65}$$

where

$$J \equiv \begin{pmatrix} 0 & 0 & 0 & +1 \\ 0 & 0 & +1 & 0 \\ 0 & -1 & 0 & 0 \\ -1 & 0 & 0 & 0 \end{pmatrix}. \tag{B66}$$

In order for the transformation to be canonical, the same Poisson bracket or commutator relations must hold for the outgoing field amplitudes

$$[q_i^{\rm out}, q_j^{\rm out}] = iX_{\rm ZPF}^2 J_{ij}. \tag{B67}$$

In the case of a non-linear device these relations would apply to the small fluctuations in the input and output fields around the steady state solution. Assuming a linear device (or linearization around the steady state solution) we can define a 4×4 real-valued scattering matrix $\tilde{s}$ in analogy to the 2×2 complex-valued scattering matrix s in Eq. (B51) which relates the output fields to the input fields

$$q_i^{\rm out} = \tilde{s}_{ij} q_j^{\rm in}. \tag{B68}$$

Eq. (B67) puts a powerful constraint on on the $\tilde{s}$ matrix, namely that it must be symplectic. That is, $\tilde{s}$ and its transpose must obey

$$\tilde{s} J \tilde{s}^{\rm T} = J. \tag{B69}$$

From this it follows that

$$\det \tilde{s} = \pm 1. \tag{B70}$$

This in turn immediately implies Liouville's theorem that Hamiltonian evolution preserves phase space volume (since $\det \tilde{s}$ is the Jacobian of the transformation which propagates the amplitudes forward in time).

Let us further assume that the device is phase preserving, that is that the gain or attenuation is the same for

both quadratures. One form for the $\tilde{s}$ matrix consistent with all of the above requirements is

$$\tilde{s} = \begin{pmatrix} +\cos\theta & \sin\theta & 0 & 0 \\ \sin\theta & -\cos\theta & 0 & 0 \\ 0 & 0 & -\cos\theta & \sin\theta \\ 0 & 0 & \sin\theta & +\cos\theta \end{pmatrix}. \quad \text{(B71)}$$

This simply corresponds to a beam splitter and is the equivalent of Eq. (B51) with $r = \cos\theta$. As mentioned in connection with Eq. (B51), the precise form of the scattering matrix depends on the choice of planes at which the phases of the various input and output waves are measured.

Another allowed form of the scattering matrix is:

$$\tilde{s}' = -\begin{pmatrix} +\cosh\theta & +\sinh\theta & 0 & 0 \\ +\sinh\theta & +\cosh\theta & 0 & 0 \\ 0 & 0 & +\cosh\theta & -\sinh\theta \\ 0 & 0 & -\sinh\theta & +\cosh\theta \end{pmatrix}. \quad \text{(B72)}$$

If one takes $\cosh\theta = \sqrt{G}$, this scattering matrix is essentially the canonically correct formulation of the negative-resistance scattering matrix we tried to write in Eq. (B62). Note that the off-diagonal terms have changed sign for the Y quadrature relative to the naive expression in Eq. (B62) (corresponding to the other possible analytic continuation choice). This is necessary to satisfy the symplecticity condition and hence make the transformation canonical. The scattering matrix $\tilde{s}'$ can describe amplification. Unlike the beam splitter scattering matrix $\tilde{s}$ above, $\tilde{s}'$ is not unitary (even though $\det\tilde{s}' = 1$). Unitarity would correspond to power conservation. Here, power is not conserved, as we are not explicitly tracking the power source supplying our active system.

The form of the negative-resistance amplifier scattering matrix $\tilde{s}'$ confirms many of the general statements we made about phase-preserving amplification in Sec. VI.B. First, note that the requirement of finite gain $G > 1$ and phase preservation makes all the diagonal elements of $\tilde{s}'$ (i.e. $\cosh\theta$) equal. We see that to amplify the A mode, it is impossible to avoid coupling to the B mode (via the $\sinh\theta$ term) because of the requirement of symplecticity. We thus see that it is impossible classically or quantum mechanically to build a linear phase-preserving amplifier whose only effect is to amplify the desired signal. The presence of the $\sinh\theta$ term above means that the output signal is always contaminated by amplified noise from at least one other degree of freedom (in this case the B mode). If the thermal or quantum noise in A and B are equal in magnitude (and uncorrelated), then in the limit of large gain where $\cosh\theta \approx \sinh\theta$, the output noise (referred to the input) will be doubled. This is true for both classical thermal noise and quantum vacuum noise.

The negative resistance model of an amplifier here gives us another way to think about the noise added by an amplifier: crudely speaking, we can view it as being directly analogous to the fluctuation-dissipation theorem simply continued to the case of negative dissipation. Just as dissipation can occur only when we open up a new channel and thus we bring in new fluctuations, so amplification can occur only when there is coupling to an additional channel. Without this it is impossible to satisfy the requirement that the amplifier perform a canonical transformation.

APPENDIX C: Quantum Modes and Noise of a Transmission Line

1. Quantization of a transmission line

Recall from Eq. (B30) and the discussion in Appendix B that the momentum conjugate to the transmission line flux variable $\varphi(x,t)$ is the local charge density $q(x,t)$. Hence in order to quantize the transmission line modes we simply promote these two physical quantities to quantum operators obeying the commutation relation

$$[\hat{q}(x), \hat{\varphi}(x')] = -i\hbar\delta(x - x') \quad \text{(C1)}$$

from which it follows that the mode amplitudes defined in Eq. (B33) become quantum operators obeying

$$[\hat{A}_{k'}, \hat{A}_k^\dagger] = \hbar\omega_k\delta_{kk'} \quad \text{(C2)}$$

and we may identify the usual raising and lowering operators by

$$\hat{A}_k = \sqrt{\hbar\omega_k}\,\hat{b}_k \quad \text{(C3)}$$

where $\hat{b}_k$ destroys a photon in mode k. The quantum form of the Hamiltonian in Eq. (B34) is thus

$$H = \sum_k \hbar\omega_k \left[\hat{b}_k^\dagger\hat{b}_k + \frac{1}{2}\right]. \quad \text{(C4)}$$

For the quantum case the thermal equilibrium expression then becomes

$$\langle\hat{A}_k^\dagger\hat{A}_k\rangle = \hbar\omega_k n_{\rm B}(\hbar\omega_k), \quad \text{(C5)}$$

which reduces to Eq. (B42) in the classical limit $\hbar\omega_k \ll k_{\rm B}T$.

We have seen previously in Eqs. (B6) that the voltage fluctuations on a transmission line can be resolved into right and left moving waves which are functions of a combined space-time argument

$$V(x,t) = V^{\rightarrow}(t - \frac{x}{v_{\rm p}}) + V^{\leftarrow}(t + \frac{x}{v_{\rm p}}). \quad \text{(C6)}$$

Thus in an infinite transmission line, specifying $V^{\rightarrow}$ everywhere in space at $t = 0$ determines its value for all times. Conversely specifying $V^{\rightarrow}$ at $x = 0$ for all times fully specifies the field at all spatial points. In preparation for our study of the quantum version of input-output theory in Appendix D, it is convenient to extend

Eqs. (B38-B39) to the quantum case:

$$\hat{V}^{\rightarrow}(t) = \sqrt{\frac{1}{2Lc}}\sum_{k>0}\sqrt{\hbar\omega_k}\left[\hat{b}_k(t)e^{-i\omega_k t}+h.c.\right] = \int_0^\infty \frac{d\omega}{2\pi}\sqrt{\frac{\hbar\omega Z_c}{2}}\left[\hat{b}^{\rightarrow}[\omega]e^{-i\omega t}+h.c.\right] \quad \text{(C7)}$$

In the second line, we have defined:

$$\hat{b}^{\rightarrow}[\omega] \equiv 2\pi\sqrt{\frac{v_p}{L}}\sum_{k>0}\hat{b}_k\delta(\omega-\omega_k) \quad \text{(C8)}$$

In a similar fashion, we have:

$$\hat{V}^{\leftarrow}(t) = \int_0^\infty \frac{d\omega}{2\pi}\sqrt{\frac{\hbar\omega Z_c}{2}}\left[\hat{b}^{\leftarrow}[\omega]e^{-i\omega t}+h.c.\right] \quad \text{(C9)}$$

$$\hat{b}^{\leftarrow}[\omega] \equiv 2\pi\sqrt{\frac{v_p}{L}}\sum_{k<0}\hat{b}_k\delta(\omega-\omega_k) \quad \text{(C10)}$$

One can easily verify that among the $\hat{b}^{\rightarrow}[\omega], \hat{b}^{\leftarrow}[\omega]$ operators and their conjugates, the only non-zero commutators are given by:

$$\left[\hat{b}^{\rightarrow}[\omega],\left(\hat{b}^{\rightarrow}[\omega']\right)^\dagger\right] = \left[\hat{b}^{\leftarrow}[\omega],\left(\hat{b}^{\leftarrow}[\omega']\right)^\dagger\right] = 2\pi\delta(\omega-\omega') \quad \text{(C11)}$$

We have taken the continuum limit $L\to\infty$ here, allowing us to change sums on k to integrals. We have thus obtained the description of a quantum transmission line in terms of left and right-moving frequency resolved modes, as used in our discussion of amplifiers in Sec. VII (see Eqs. 7.2). Note that if the right-moving modes are further taken to be in thermal equilibrium, one finds (again, in the continuum limit):

$$\langle\hat{b}^{\dagger\rightarrow}[\omega]\hat{b}^{\rightarrow}[\omega']\rangle = 2\pi\delta(\omega-\omega')n_B(\hbar\omega) \quad \text{(C12a)}$$

$$\langle\hat{b}^{\rightarrow}[\omega]\hat{b}^{\dagger\rightarrow}[\omega']\rangle = 2\pi\delta(\omega-\omega')\left[1+n_B(\hbar\omega)\right] \quad \text{(C12b)}$$

We are typically interested in a relatively narrow band of frequencies centered on some characteristic drive or resonance frequency Ω_0. In this case, it is useful to work in the time-domain, in a frame rotating at Ω_0. Fourier transforming [23] Eqs. (C8) and (C10), one finds:

$$\hat{b}^{\rightarrow}(t) = \sqrt{\frac{v_p}{L}}\sum_{k>0}e^{-i(\omega_k-\Omega_0)t}\hat{b}_k(0), \quad \text{(C13a)}$$

$$\hat{b}^{\leftarrow}(t) = \sqrt{\frac{v_p}{L}}\sum_{k<0}e^{-i(\omega_k-\Omega_0)t}\hat{b}_k(0). \quad \text{(C13b)}$$

[23] Here and throughout we use a convention which differs from the one commonly used in quantum optics: $\hat{a}[\omega]=\int_{-\infty}^{+\infty}dt\,e^{+i\omega t}\hat{a}(t)$ and $\hat{a}^\dagger[\omega]=[\hat{a}[-\omega]]^\dagger=\int_{-\infty}^{+\infty}dt\,e^{+i\omega t}\hat{a}^\dagger(t)$.

These represent temporal right and left moving modes. Note that the normalization factors in Eqs. (C13) has been chosen so that the right moving photon flux at $x=0$ and time t is given by

$$\langle\dot{N}\rangle = \langle\hat{b}^{\dagger\rightarrow}(t)\hat{b}^{\rightarrow}(t)\rangle \quad \text{(C14)}$$

In the same rotating frame, and within the approximation that all relevant frequencies are near Ω_0, Eq. (C7) becomes simply:

$$\hat{V}^{\rightarrow}(t) \approx \sqrt{\frac{\hbar\Omega_0 Z_c}{2}}\left[\hat{b}^{\rightarrow}(t)+\hat{b}^{\dagger\rightarrow}(t)\right] \quad \text{(C15)}$$

We have already seen that using classical statistical mechanics, the voltage noise in equilibrium is white. The corresponding analysis of the temporal modes using Eqs. (C13) shows that the quantum commutator obeys

$$[\hat{b}^{\rightarrow}(t),\hat{b}^{\dagger\rightarrow}(t')] = \delta(t-t'). \quad \text{(C16)}$$

In deriving this result, we have converted summations over mode index to integrals over frequency. Further, because (for finite time resolution at least) the integral is dominated by frequencies near $+\Omega_0$ we can, within the Markov (Wigner Weisskopf) approximation, extend the lower limit of frequency integration to minus infinity and thus arrive at a delta function in time. If we further take the right moving modes to be in thermal equilibrium, then we may similarly approximate:

$$\langle\hat{b}^{\dagger\rightarrow}(t')\hat{b}^{\rightarrow}(t)\rangle = n_B(\hbar\Omega_0)\delta(t-t') \quad \text{(C17a)}$$

$$\langle\hat{b}^{\rightarrow}(t)\hat{b}^{\dagger\rightarrow}(t')\rangle = \left[1+n_B(\hbar\Omega_0)\right]\delta(t-t'). \quad \text{(C17b)}$$

Equations (C15) to (C17b) indicate that $\hat{V}^{\rightarrow}(t)$ can be treated as the quantum operator equivalent of white noise; a similar line of reasoning applies *mutatis mutandis* to the left moving modes. We stress that these results rely crucially on our assumption that we are dealing with a relatively narrow band of frequencies in the vicinity of Ω_0; the resulting approximations we have made are known as the Markov approximation. As one can already see from the form of Eqs. (C7,C9), and as will be discussed further, the actual spectral density of vacuum noise on a transmission line is not white, but is linear in frequency. The approximation made in Eq. (C16) treats it as a constant within the narrow band of frequencies of interest. If the range of frequencies of importance is large then the Markov approximation is not applicable.

2. Modes and the windowed Fourier transform

While the delta function correlations can make the quantum noise relatively easy to deal with in both the time and frequency domain, it is sometimes the case that it is easier to deal with a 'smoothed' noise variable. The introduction of an ultraviolet cutoff regulates the mathematical singularities in the noise operators evaluated at

equal times and is physically sensible because every real measurement apparatus has finite time resolution. A second motivation is that real spectrum analyzers output a time varying signal which represents the noise power in a certain frequency interval (the 'resolution bandwidth') averaged over a certain time interval (the inverse 'video bandwidth'). The mathematical tool of choice for dealing with such situations in which time and frequency both appear is the 'windowed Fourier transform'. The windowed transform uses a kernel which is centered on some frequency window and some time interval. By summation over all frequency and time windows it is possible to invert the transformation. The reader is directed to (Mallat, 1999) for the mathematical details.

For our present purposes where we are interested in just a single narrow frequency range centered on Ω_0, a convenient windowed transform kernel for smoothing the quantum noise is simply a box of width Δt representing the finite integration time of our detector. In the frame rotating at Ω_0 we can define

$$\hat{B}_j^{\rightarrow} = \frac{1}{\sqrt{\Delta t}} \int_{t_j}^{t_{j+1}} d\tau \, \hat{b}^{\rightarrow}(\tau) \tag{C18}$$

where $t_j = j(\Delta t)$ denotes the time of arrival of the jth temporal mode at the point $x = 0$. Recall that $\hat{b}^{\rightarrow}$ has a photon flux normalization and so $\hat{B}_j^{\rightarrow}$ is dimensionless. From Eq. (C16) we see that these smoothed operators obey the usual bosonic commutation relations

$$[\hat{B}_j^{\rightarrow}, \hat{B}_k^{\dagger\rightarrow}] = \delta_{jk}. \tag{C19}$$

The state $B_j^{\dagger}|0\rangle$ has a single photon occupying basis mode j, which is centered in frequency space at Ω_0 and in time space on the interval $j\Delta t < t < (j+1)\Delta t$. (That is, this temporal mode passes the point $x = 0$ during the jth time interval.) This basis mode is much like a note in a musical score: it has a certain specified pitch and occurs at a specified time for a specified duration. Just as we can play notes of different frequencies simultaneously, we can define other temporal modes on the same time interval and they will be mutually orthogonal provided the angular frequency spacing is a multiple of $2\pi/\Delta t$. The result is a set of modes $B_{m,p}$ labeled by both a frequency index m and a time index p. p labels the time interval as before, while m labels the angular frequency:

$$\omega_m = \Omega_0 + m\frac{2\pi}{\Delta t} \tag{C20}$$

The result is, as illustrated in Fig. (17), a complete lattice of possible modes tiling the frequency-time phase space, each occupying area 2π corresponding to the time-frequency uncertainty principle.

We can form other modes of arbitrary shapes centered on frequency Ω_0 by means of linear superposition of our basis modes (as long as they are smooth on the time scale Δt). Let us define

$$\Psi = \sum_j \psi_j \hat{B}_j^{\rightarrow}. \tag{C21}$$

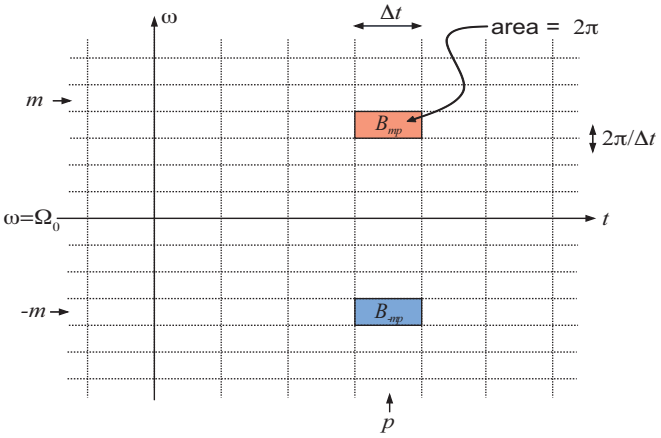

FIG. 17 (Color online) Schematic figure indicating how the various modes defined by the windowed Fourier transform tile the time-frequency plane. Each individual cell corresponds to a different mode, and has an area 2π.

This is also a canonical bosonic mode operator obeying

$$[\Psi, \Psi^{\dagger}] = 1 \tag{C22}$$

provided that the coefficients obey the normalization condition

$$\sum_j |\psi_j|^2 = 1. \tag{C23}$$

We might for example want to describe a mode which is centered at a slightly higher frequency $\Omega_0 + \delta\Omega$ (obeying $(\delta\Omega)(\Delta t) << 1$) and spread out over a large time interval T centered at time T_0. This could be given for example by

$$\psi_j = \mathcal{N} e^{-\frac{(j-T_0/(\Delta t))^2}{2T^2}} e^{-i(\delta\Omega)(\Delta t)j} \tag{C24}$$

where $\mathcal{N}$ is the appropriate normalization constant.

The state having n photons in the mode is simply

$$\frac{1}{\sqrt{n!}} \left(\Psi^{\dagger}\right)^n |0\rangle. \tag{C25}$$

The concept of 'wave function of the photon' is fraught with dangers. In the very special case where we restrict attention solely to the subspace of single photon Fock states, we can usefully think of the amplitudes $\{\psi_j\}$ as the 'wave function of the photon' (Cohen-Tannoudji *et al.*, 1989) since it tells us about the spatial mode which is excited. In the general case however it is essential to keep in mind that the transmission line is a collection of coupled LC oscillators with an infinite number of degrees of freedom. Let us simplify the argument by considering a single LC oscillator. We can perfectly well write a wave function for the system as a function of the coordinate (say the charge q on the capacitor). The ground state wave function $\chi_0(q)$ is a gaussian function of the coordinate. The one photon state created by $\Psi^{\dagger}$ has a wave

function $\chi_1(q) \sim q\chi_0(q)$ proportional to the coordinate times the same gaussian. In the general case χ is a *wave functional* of the charge distribution $q(x)$ over the entire transmission line.

Using Eq. (C17a) we have

$$\langle \hat{B}_j^{\dagger\rightarrow} \hat{B}_k^{\rightarrow} \rangle = n_{\rm B}(\hbar\Omega_0)\delta_{jk} \tag{C26}$$

independent of our choice of the coarse-graining time window Δt. This result allows us to give meaning to the phrase one often hears bandied about in descriptions of amplifiers that 'the noise temperature corresponds to a mode occupancy of X photons'. This simply means that the photon flux *per unit bandwidth* is X. Equivalently the flux in bandwidth B is

$$\overline{\dot{N}} = \frac{X}{\Delta t}(B\Delta t) = XB. \tag{C27}$$

The interpretation of this is that X photons in a temporal mode of duration Δt pass the origin in time Δt. Each mode has bandwidth $\sim \frac{1}{\Delta t}$ and so there are $B\Delta t$ independent temporal modes in bandwidth B all occupying the same time interval Δt. The longer is Δt the longer it takes a given mode to pass the origin, but the more such modes fit into the frequency window.

As an illustration of these ideas, consider the following elementary question: What is the mode occupancy of a laser beam of power P and hence photon flux $\overline{\dot{N}} = \frac{P}{\hbar\Omega_0}$? We cannot answer this without knowing the coherence time or equivalently the bandwidth. The output of a good laser is like that of a radio frequency oscillator–it has essentially no amplitude fluctuations. The frequency is nominally set by the physical properties of the oscillator, but there is nothing to pin the phase which consequently undergoes slow diffusion due to unavoidable noise perturbations. This leads to a finite phase coherence time τ and corresponding frequency spread $1/\tau$ of the laser spectrum. (A laser beam differs from a thermal source that has been filtered to have the same spectrum in that it has smaller amplitude fluctuations.) Thus we expect that the mode occupancy is $X = \overline{\dot{N}}\tau$. A convenient approximate description in terms of temporal modes is to take the window interval to be $\Delta t = \tau$. Within the jth interval we take the phase to be a (random) constant φ_j so that (up to an unimportant normalization constant) we have the coherent state

$$\prod_j e^{\sqrt{X}e^{i\varphi_j}\hat{B}_j^{\dagger\rightarrow}}|0\rangle \tag{C28}$$

which obeys

$$\langle \hat{B}_k^{\rightarrow} \rangle = \sqrt{X}e^{i\varphi_k} \tag{C29}$$

and

$$\langle \hat{B}_k^{\dagger\rightarrow} \hat{B}_k^{\rightarrow} \rangle = X. \tag{C30}$$

3. Quantum noise from a resistor

Let us consider the quantum equivalent to Eq. (B60), $\mathcal{S}_{VV} = 2Rk_{\rm B}T$, for the case of a semi-infinite transmission line with open termination, representing a resistor. From Eq. (B27) we see that the proper boundary condition for the φ field is $\partial_x\varphi(0,t) = \partial_x\varphi(L,t) = 0$. (We have temporarily made the transmission line have a large but finite length L.) The normal mode expansion that satisfies these boundary conditions is

$$\varphi(x,t) = \sqrt{\frac{2}{L}}\sum_{n=1}^{\infty}\varphi_n(t)\cos(k_n x), \tag{C31}$$

where φ_n is the normal coordinate and $k_n \equiv \frac{\pi n}{L}$. Substitution of this form into the Lagrangian and carrying out the spatial integration yields a set of independent harmonic oscillators representing the normal modes.

$$\mathcal{L} = \sum_{n=1}^{\infty}\frac{c}{2}\dot{\varphi}_n^2 - \frac{1}{2\ell}k_n^2\varphi_n^2. \tag{C32}$$

From this we can find the momentum operator $\hat{p}_n$ canonically conjugate to the coordinate operator $\hat{\varphi}_n$ and quantize the system to obtain an expression for the operator representing the voltage at the end of the transmission line in terms of the mode creation and destruction operators

$$\hat{V} = \sum_{n=1}^{\infty}\sqrt{\frac{\hbar\Omega_n}{Lc}}i(\hat{b}_n^\dagger - \hat{b}_n). \tag{C33}$$

The spectral density of voltage fluctuations is then found to be

$$S_{\rm VV}[\omega] = \frac{2\pi}{L}\sum_{n=1}^{\infty}\frac{\hbar\Omega_n}{c}\big\{n_{\rm B}(\hbar\Omega_n)\delta(\omega+\Omega_n) + [n_{\rm B}(\hbar\Omega_n)+1]\delta(\omega-\Omega_n)\big\}, \tag{C34}$$

where $n_{\rm B}(\hbar\omega)$ is the Bose occupancy factor for a photon with energy $\hbar\omega$. Taking the limit $L\to\infty$ and converting the summation to an integral yields

$$S_{\rm VV}(\omega) = 2Z_{\rm c}\hbar|\omega|\big\{n_{\rm B}(\hbar|\omega|)\Theta(-\omega)+[n_{\rm B}(\hbar|\omega|)+1]\Theta(\omega)\big\}, \tag{C35}$$

where Θ is the step function. We see immediately that at zero temperature there is no noise at negative frequencies because energy can not be extracted from zero-point motion. However there remains noise at positive frequencies indicating that the vacuum is capable of absorbing energy from another quantum system. The voltage spectral density at both zero and non-zero temperature is plotted in Fig. (1).

Eq. (C35) for this 'two-sided' spectral density of a resistor can be rewritten in a more compact form

$$S_{\rm VV}[\omega] = \frac{2Z_{\rm c}\hbar\omega}{1-e^{-\hbar\omega/k_{\rm B}T}}, \tag{C36}$$

which reduces to the more familiar expressions in various limits. For example, in the classical limit $k_{\rm B}T \gg \hbar\omega$ the spectral density is equal to the Johnson noise result[24]

$$S_{\rm VV}[\omega] = 2Z_{\rm c}k_{\rm B}T, \tag{C37}$$

in agreement with Eq. (B60). In the quantum limit it reduces to

$$S_{\rm VV}[\omega] = 2Z_{\rm c}\hbar\omega\Theta(\omega). \tag{C38}$$

Again, the step function tells us that the resistor can only absorb energy, not emit it, at zero temperature.

If we use the engineering convention and add the noise at positive and negative frequencies we obtain

$$S_{\rm VV}[\omega] + S_{\rm VV}[-\omega] = 2Z_{\rm c}\hbar\omega\coth\frac{\hbar\omega}{2k_{\rm B}T} \tag{C39}$$

for the symmetric part of the noise, which appears in the quantum fluctuation-dissipation theorem (cf. Eq. (3.33)). The antisymmetric part of the noise is simply

$$S_{\rm VV}[\omega] - S_{\rm VV}[-\omega] = 2Z_{\rm c}\hbar\omega, \tag{C40}$$

yielding

$$\frac{S_{\rm VV}[\omega] - S_{\rm VV}[-\omega]}{S_{\rm VV}[\omega] + S_{\rm VV}[-\omega]} = \tanh\frac{\hbar\omega}{2k_{\rm B}T}. \tag{C41}$$

This quantum treatment can also be applied to any arbitrary dissipative network (Burkhard *et al.*, 2004; Devoret, 1997). If we have a more complex circuit containing capacitors and inductors, then in all of the above expressions, $Z_{\rm c}$ should be replaced by Re $Z[\omega]$ where $Z[\omega]$ is the complex impedance presented by the circuit.

In the above we have explicitly quantized the standing wave modes of a finite length transmission line. We could instead have used the running waves of an infinite line and recognized that, as the in classical treatment in Eq. (B59), the left and right movers are not independent. The open boundary condition at the termination requires $V^{\leftarrow} = V^{\rightarrow}$ and hence $b^{\rightarrow} = b^{\leftarrow}$. We then obtain

$$S_{VV}[\omega] = 4S^{\rightarrow}_{VV}[\omega] \tag{C42}$$

and from the quantum analog of Eq. (B40) we have

$$\begin{aligned} S_{VV}[\omega] &= \frac{4\hbar|\omega|}{2cv_{\rm p}}\left\{\Theta(\omega)(n_{\rm B}+1) + \Theta(-\omega)n_{\rm B}\right\} \\ &= 2Z_c\hbar|\omega|\left\{\Theta(\omega)(n_{\rm B}+1) + \Theta(-\omega)n_{\rm B}\right\} \end{aligned} \tag{C43}$$

in agreement with Eq. (C35).

[24] Note again that in the engineering convention this would be $S_{\rm VV}[\omega] = 4Z_{\rm c}k_{\rm B}T$.

APPENDIX D: Back Action and Input-Output Theory for Driven Damped Cavities

A high Q cavity whose resonance frequency can be parametrically controlled by an external source can act as a very simple quantum amplifier, encoding information about the external source in the phase and amplitude of the output of the driven cavity. For example, in an optical cavity, one of the mirrors could be moveable and the external source could be a force acting on that mirror. This defines the very active field of optomechanics, which also deals with microwave cavities coupled to nanomechanical systems and other related setups (Arcizet *et al.*, 2006; Brown *et al.*, 2007; Gigan *et al.*, 2006; Harris *et al.*, 2007; Höhberger-Metzger and Karrai, 2004; Marquardt *et al.*, 2007, 2006; Meystre *et al.*, 1985; Schliesser *et al.*, 2006; Teufel *et al.*, 2008; Thompson *et al.*, 2008; Wilson-Rae *et al.*, 2007). In the case of a microwave cavity containing a qubit, the state-dependent polarizability of the qubit acts as a source which shifts the frequency of the cavity (Blais *et al.*, 2004; Schuster *et al.*, 2005; Wallraff *et al.*, 2004).

The dephasing of a qubit in a microwave cavity and the fluctuations in the radiation pressure in an optical cavity both depend on the quantum noise in the number of photons inside the cavity. We here use a simple equation of motion method to exactly solve for this quantum noise in the perturbative limit where the dynamics of the qubit or mirror degree of freedom has only a weak back action effect on the cavity.

In the following, we first give a basic discussion of the cavity field noise spectrum, deferring the detailed microscopic derivation to subsequent subsections. We then provide a review of the input-output theory for driven cavities, and employ this theory to analyze the important example of a dispersive position measurement, where we demonstrate how the standard quantum limit can be reached. Finally, we analyze an example where a modified dispersive scheme is used to detect only one quadrature of a harmonic oscillator's motion, such that this quadrature does not feel any back-action.

1. Photon shot noise inside a cavity and back action

Consider a degree of freedom $\hat{z}$ coupled parametrically with strength A to the cavity oscillator

$$\hat{H}_{\rm int} = \hbar\omega_{\rm c}(1 + A\hat{z})\left[\hat{a}^\dagger\hat{a} - \langle\hat{a}^\dagger\hat{a}\rangle\right] \tag{D1}$$

where following Eq. (4.22), we have taken A to be dimensionless, and use $\hat{z}$ to denote the dimensionless system variable that we wish to probe. For example, $\hat{z}$ could represent the dimensionless position of a mechanical oscillator

$$\hat{z} \equiv \frac{\hat{x}}{x_{\rm ZPF}}. \tag{D2}$$

We have subtracted the $\langle\hat{a}^\dagger\hat{a}\rangle$ term so that the mean force on the degree of freedom is zero. To obtain the full

Hamiltonian, we would have to add the cavity damping and driving terms, as well as the Hamiltonian governing the intrinsic dynamics of the system $\hat{z}$. From Eq. (4.29) we know that the back action noise force acting on $\hat{z}$ is proportional to the quantum fluctuations in the number of photons $\hat{n} = \hat{a}^\dagger \hat{a}$ in the cavity,

$$S_{nn}(t) = \langle \hat{a}^\dagger(t)\hat{a}(t)\hat{a}^\dagger(0)\hat{a}(0)\rangle - \langle \hat{a}^\dagger(t)\hat{a}(t)\rangle^2. \quad \text{(D3)}$$

For the case of continuous wave driving at frequency $\omega_{\rm L} = \omega_{\rm c} + \Delta$ detuned by Δ from the resonance, the cavity is in a coherent state $|\psi\rangle$ obeying

$$\hat{a}(t) = e^{-i\omega_{\rm L} t}[\bar{a} + \hat{d}(t)] \quad \text{(D4)}$$

where the first term is the 'classical part' of the mode amplitude $\psi(t) = \bar{a}e^{-i\omega_{\rm L} t}$ determined by the strength of the drive field, the damping of the cavity and the detuning Δ, and d is the quantum part. By definition,

$$\hat{a}|\psi\rangle = \psi|\psi\rangle \quad \text{(D5)}$$

so the coherent state is annihilated by $\hat{d}$:

$$\hat{d}|\psi\rangle = 0. \quad \text{(D6)}$$

That is, in terms of the operator $\hat{d}$, the coherent state looks like the undriven quantum ground state . The displacement transformation in Eq. (D4) is canonical since

$$[\hat{a}, \hat{a}^\dagger] = 1 \;\Rightarrow\; [\hat{d}, \hat{d}^\dagger] = 1. \quad \text{(D7)}$$

Substituting the displacement transformation into Eq. (D3) and using Eq. (D6) yields

$$S_{nn}(t) = \bar{n}\langle \hat{d}(t)\hat{d}^\dagger(0)\rangle, \quad \text{(D8)}$$

where $\bar{n} = |\bar{a}|^2$ is the mean cavity photon number. If we set the cavity energy damping rate to be κ, such that the amplitude damping rate is $\kappa/2$, then the undriven state obeys

$$\langle \hat{d}(t)\hat{d}^\dagger(0)\rangle = e^{+i\Delta t}e^{-\frac{\kappa}{2}|t|}. \quad \text{(D9)}$$

This expression will be justified formally in the subsequent subsection, after introducing input-output theory. We thus arrive at the very simple result

$$S_{nn}(t) = \bar{n}e^{i\Delta t - \frac{\kappa}{2}|t|}. \quad \text{(D10)}$$

The power spectrum of the noise is, via the Wiener-Khinchin theorem (Appendix A), simply the Fourier transform of the autocorrelation function given in Eq. (D10)

$$S_{nn}[\omega] = \int_{-\infty}^{+\infty} dt\, e^{i\omega t} S_{nn}(t) = \bar{n}\frac{\kappa}{(\omega+\Delta)^2 + (\kappa/2)^2}. \quad \text{(D11)}$$

As can be seen in Fig. 18a, for positive detuning $\Delta = \omega_L - \omega_{\rm c} > 0$, i.e. for a drive that is blue-detuned with respect to the cavity, the noise peaks at *negative* ω. This means that the noise tends to pump energy into the degree of freedom $\hat{z}$ (i.e. contribute negative damping). For negative detuning the noise peaks at positive ω corresponding to the cavity absorbing energy from $\hat{z}$. Basically, the interaction with $\hat{z}$ (three wave mixing) tries to Raman scatter the drive photons into the high density of states at the cavity frequency. If this is uphill in energy, then $\hat{z}$ is cooled.

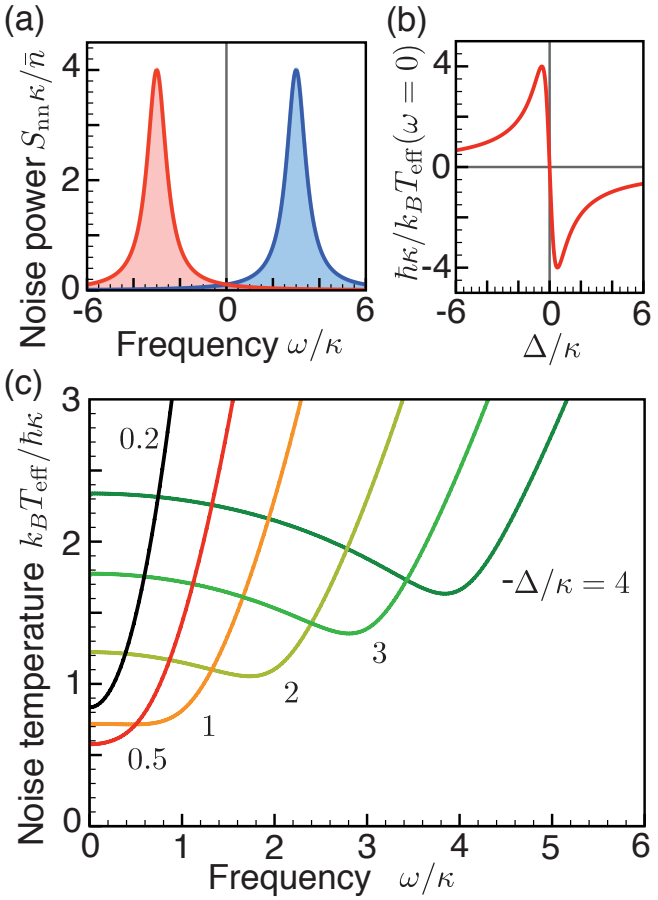

FIG. 18 (Color online) (a) Noise spectrum of the photon number in a driven cavity as a function of frequency when the cavity drive frequency is detuned from the cavity resonance by $\Delta = +3\kappa$ (left peak) and $\Delta = -3\kappa$ (right peak). (b) Effective temperature $T_{\rm eff}$ of the low frequency noise, $\omega \to 0$, as a function of the detuning Δ of the drive from the cavity resonance. (c) Frequency-dependence of the effective noise temperature, for different values of the detuning.

As discussed in Sec. III.B (c.f. Eq. (3.21)), at each frequency ω, we can use detailed balance to assign the noise an effective temperature $T_{\rm eff}[\omega]$:

$$\frac{S_{nn}[\omega]}{S_{nn}[-\omega]} = e^{\hbar\omega/k_B T_{\rm eff}[\omega]} \Leftrightarrow$$
$$k_{\rm B}T_{\rm eff}[\omega] \equiv \frac{\hbar\omega}{\log\left[\frac{S_{nn}[\omega]}{S_{nn}[-\omega]}\right]} \quad \text{(D12)}$$

or equivalently

$$\frac{S_{nn}[\omega]-S_{nn}[-\omega]}{S_{nn}[\omega]+S_{nn}[-\omega]}=\tanh(\beta\hbar\omega/2). \tag{D13}$$

If $\hat{z}$ is the coordinate of a harmonic oscillator of frequency ω (or some non-conserved observable of a qubit with level splitting ω), then that system will acquire a temperature $T_{\rm eff}[\omega]$ in the absence of coupling to any other environment. In particular, if the characteristic oscillation frequency of the system $\hat{z}$ is much smaller than κ, then we have the simple result

$$\begin{aligned}\frac{1}{k_{\rm B}T_{\rm eff}} &= \lim_{\omega\to 0^+}\frac{2}{\hbar\omega}\frac{S_{nn}[\omega]-S_{nn}[-\omega]}{S_{nn}[\omega]+S_{nn}[-\omega]}\\ &= 2\frac{d\ln S_{nn}[\omega]}{d\hbar\omega}\\ &= \frac{1}{\hbar}\frac{-4\Delta}{\Delta^2+(\kappa/2)^2}.\end{aligned} \tag{D14}$$

As can be seen in Fig. 18, the asymmetry in the noise changes sign with detuning, which causes the effective temperature to change sign.

First we discuss the case of a positive $T_{\rm eff}$, where this mechanism can be used to laser cool an oscillating mechanical cantilever, provided $T_{\rm eff}$ is lower than the intrinsic equilibrium temperature of the cantilever. (Arcizet *et al.*, 2006; Brown *et al.*, 2007; Gigan *et al.*, 2006; Harris *et al.*, 2007; Höhberger-Metzger and Karrai, 2004; Marquardt *et al.*, 2007; Schliesser *et al.*, 2006; Thompson *et al.*, 2008; Wilson-Rae *et al.*, 2007). A simple classical argument helps us understand this cooling effect. Suppose that the moveable mirror is at the right hand end of a cavity being driven below the resonance frequency. If the mirror moves to the right, the resonance frequency will fall and the number of photons in the cavity will rise. There will be a time delay however to fill the cavity and so the extra radiation pressure will not be fully effective in doing work on the mirror. During the return part of the oscillation as the mirror moves back to the left, the time delay in emptying the cavity will cause the mirror to have to do extra work against the radiation pressure. At the end of the cycle it ends up having done net positive work on the light field and hence is cooled. The effect can therefore be understood as being due to the introduction of some extra optomechanical damping.

The signs reverse (and $T_{\rm eff}$ becomes negative) if the cavity is driven above resonance, and consequently the cantilever motion is heated up. In the absence of intrinsic mechanical losses, negative values of the effective temperature indicate a dynamical instability of the cantilever (or population inversion in the case of a qubit), where the amplitude of motion grows until it is finally stabilized by nonlinear effects. This can be interpreted as negative damping introduced by the optomechanical coupling and can be used to create parametric amplification of mechanical forces acting on the oscillator.

Finally, we mention that cooling towards the quantum ground state of a mechanical oscillator (where phonon numbers become much less than one), is only possible (Marquardt *et al.*, 2007; Wilson-Rae *et al.*, 2007) in the "far-detuned regime", where $-\Delta=\omega\gg\kappa$ (in contrast to the $\omega\ll\kappa$ regime discussed above).

2. Input-output theory for a driven cavity

The results from the previous section can be more formally and rigorously derived in a full quantum theory of a cavity driven by an external coherent source. The theory relating the drive, the cavity and the outgoing waves radiated by the cavity is known as input-output theory and the classical description was presented in Appendix B. The present quantum discussion closely follows standard references on the subject (Walls and Milburn, 1994; Yurke, 1984; Yurke and Denker, 1984). The crucial feature that distinguishes such an approach from many other treatments of quantum-dissipative systems is the goal of keeping the bath modes instead of tracing them out. This is obviously necessary for the situations we have in mind, where the output field emanating from the cavity contains the information acquired during a measurement of the system coupled to the cavity. As we learned from the classical treatment, we can eliminate the outgoing waves in favor of a damping term for the system. However we can recover the solution for the outgoing modes completely from the solution of the equation of motion of the damped system being driven by the incoming waves.

In order to drive the cavity we must partially open one of its ports which exposes the cavity both to the external drive and to the vacuum noise outside which permits energy in the cavity to leak out into the surrounding bath. We will formally separate the degrees of freedom into internal cavity modes and external bath modes. Strictly speaking, once the port is open, these modes are not distinct and we only have 'the modes of the universe' (Gea-Banacloche *et al.*, 1990a,b; Lang *et al.*, 1973). However for high Q cavities, the distinction is well-defined and we can model the decay of the cavity in terms of a spontaneous emission process in which an internal boson is destroyed and an external bath boson is created. We assume a single-sided cavity as shown in Fig. 3. For a high Q cavity, this physics is accurately captured in the following Hamiltonian

$$\hat{H}=\hat{H}_{\rm sys}+\hat{H}_{\rm bath}+\hat{H}_{\rm int}. \tag{D15}$$

The bath Hamiltonian is

$$\hat{H}_{\rm bath}=\sum_q \hbar\omega_q\hat{b}_q^\dagger\hat{b}_q \tag{D16}$$

where q labels the quantum numbers of the independent harmonic oscillator bath modes obeying

$$[\hat{b}_q,\hat{b}_{q'}^\dagger]=\delta_{q,q'}. \tag{D17}$$

Note that since the bath terminates at the system, there is no translation invariance, the normal modes are standing not running waves, and the quantum numbers q are not necessarily wave vectors.

The coupling Hamiltonian is (within the rotating wave approximation)

$$\hat{H}_{\rm int} = -i\hbar \sum_q \left[f_q \hat{a}^\dagger \hat{b}_q - f_q^* \hat{b}_q^\dagger \hat{a} \right]. \tag{D18}$$

For the moment we will leave the system (cavity) Hamiltonian to be completely general, specifying only that it consists of a single degree of freedom (i.e. we concentrate on only a single resonance of the cavity with frequency $\omega_{\rm c}$) obeying the usual bosonic commutation relation

$$[\hat{a}, \hat{a}^\dagger] = 1. \tag{D19}$$

(N.B. this does not imply that it is a harmonic oscillator. We will consider both linear and non-linear cavities.) Note that the most general linear coupling to the bath modes would include terms of the form $\hat{b}_q^\dagger \hat{a}^\dagger$ and $\hat{b}_q a$ but these are neglected within the rotating wave approximation because in the interaction representation they oscillate at high frequencies and have little effect on the dynamics.

The Heisenberg equation of motion (EOM) for the bath variables is

$$\dot{\hat{b}}_q = \frac{i}{\hbar}[\hat{H}, \hat{b}_q] = -i\omega_{\rm q} \hat{b}_q + f_q^* \hat{a} \tag{D20}$$

We see that this is simply the EOM of a harmonic oscillator driven by a forcing term due to the motion of the cavity degree of freedom. Since this is a linear system, the EOM can be solved exactly. Let $t_0 < t$ be a time in the distant past before any wave packet launched at the cavity has reached it. The solution of Eq. (D20) is

$$\hat{b}_q(t) = e^{-i\omega_{\rm q}(t-t_0)} \hat{b}_q(t_0) + \int_{t_0}^{t} d\tau \, e^{-i\omega_{\rm q}(t-\tau)} f_q^* \, \hat{a}(\tau). \tag{D21}$$

The first term is simply the free evolution of the bath while the second represents the waves radiated by the cavity into the bath.

The EOM for the cavity mode is

$$\dot{\hat{a}} = \frac{i}{\hbar}[\hat{H}_{\rm sys}, \hat{a}] - \sum_q f_q \hat{b}_q. \tag{D22}$$

Substituting Eq. (D21) into the last term above yields

$$\sum_q f_q \hat{b}_q = \sum_q f_q e^{-i\omega_{\rm q}(t-t_0)} \hat{b}_q(t_0)$$
$$+ \sum_q |f_q|^2 \int_{t_0}^{t} d\tau \, e^{-i(\omega_{\rm q}-\omega_{\rm c})(t-\tau)} [e^{+i\omega_{\rm c}(\tau-t)} \hat{a}(\tau)], \tag{D23}$$

where the last term in square brackets is a slowly varying function of τ. To simplify our result, we note that if the cavity system were a simple harmonic oscillator of frequency $\omega_{\rm c}$ then the decay rate from the $n = 1$ single photon excited state to the $n = 0$ ground state would be given by the following Fermi Golden Rule expression

$$\kappa(\omega_{\rm c}) = 2\pi \sum_q |f_q|^2 \delta(\omega_{\rm c} - \omega_{\rm q}). \tag{D24}$$

From this it follows that

$$\int_{-\infty}^{+\infty} \frac{d\nu}{2\pi} \kappa(\omega_{\rm c} + \nu) e^{-i\nu(t-\tau)} = \sum_q |f_q|^2 e^{-i(\omega_{\rm q}-\omega_{\rm c})(t-\tau)}. \tag{D25}$$

We now make the Markov approximation which assumes that $\kappa(\nu) = \kappa$ is a constant over the range of frequencies relevant to the cavity so that Eq. (D25) may be represented as

$$\sum_q |f_q|^2 e^{-i(\omega_{\rm q}-\omega_{\rm c})(t-\tau)} = \kappa \delta(t-\tau). \tag{D26}$$

Using

$$\int_{-\infty}^{x_0} dx \, \delta(x - x_0) = \frac{1}{2} \tag{D27}$$

we obtain for the cavity EOM

$$\dot{\hat{a}} = \frac{i}{\hbar}[\hat{H}_{\rm sys}, \hat{a}] - \frac{\kappa}{2}\hat{a} - \sum_q f_q e^{-i\omega_{\rm q}(t-t_0)} \hat{b}_q(t_0). \tag{D28}$$

The second term came from the part of the bath motion representing the wave radiated by the cavity and, within the Markov approximation, has become a simple linear damping term for the cavity mode. Note the important factor of 2. The amplitude decays at half the rate of the intensity (the energy decay rate κ).

Within the spirit of the Markov approximation it is further convenient to treat $f \equiv \sqrt{|f_q|^2}$ as a constant and define the density of states (also taken to be a constant) by

$$\rho = \sum_q \delta(\omega_{\rm c} - \omega_{\rm q}) \tag{D29}$$

so that the Golden Rule rate becomes

$$\kappa = 2\pi f^2 \rho. \tag{D30}$$

We can now define the so-called 'input mode'

$$\hat{b}_{\rm in}(t) \equiv \frac{1}{\sqrt{2\pi\rho}} \sum_q e^{-i\omega_{\rm q}(t-t_0)} \hat{b}_q(t_0) \, . \tag{D31}$$

For the case of a transmission line treated in Appendix C, this coincides with the field $\hat{b}^{\rightarrow}$ moving towards the cavity [see Eq. (C13a)]. We finally have for the cavity EOM

$$\dot{\hat{a}} = \frac{i}{\hbar}[\hat{H}_{\rm sys}, \hat{a}] - \frac{\kappa}{2}\hat{a} - \sqrt{\kappa}\, \hat{b}_{\rm in}(t). \tag{D32}$$

Note that when a wave packet is launched from the bath towards the cavity, causality prevents it from knowing about the cavity's presence until it reaches the cavity. Hence the input mode evolves freely as if the cavity were not present until the time of the collision at which point it begins to drive the cavity. Since $\hat{b}_{\rm in}(t)$ evolves under the free bath Hamiltonian and acts as the driving term in the cavity EOM, we interpret it physically as the input mode. Eq. (D32) is the quantum analog of the classical equation (B19), for our previous example of an LC-oscillator driven by a transmission line. The latter would also have been first order in time if as in Eq. (B35) we had worked with the complex amplitude A instead of the coordinate Q.

Eq. (D31) for the input mode contains a time label just as in the interaction representation. However it is best interpreted as simply labeling the particular linear combination of the bath modes which is coupled to the system at time t. Some authors even like to think of the bath modes as non-propagating while the cavity flies along the bath (taken to be 1D) at a velocity v. The system then only interacts briefly with the local mode positioned at $x = vt$ before moving an interacting with the next local bath mode. We will elaborate on this view further at the end of this subsection.

The expression for the power $P_{\rm in}$ (energy per time) impinging on the cavity depends on the normalization chosen in our definition of $\hat{b}_{\rm in}$. It can be obtained, for example, by imagining the bath modes $\hat{b}_q$ to live on a one-dimensional waveguide with propagation velocity v and length L (using periodic boundary conditions). In that case we have to sum over all photons to get the average power flowing through a cross-section of the waveguide, $P_{\rm in} = \sum_q \hbar\omega_q (v_p/L) \left\langle \hat{b}_q^\dagger \hat{b}_q \right\rangle$. Inserting the definition for $\hat{b}_{\rm in}$, Eq. (D31), the expression for the input power carried by a monochromatic beam at frequency ω is

$$P_{\rm in}(t) = \hbar\omega \left\langle \hat{b}_{\rm in}^\dagger(t) \hat{b}_{\rm in}(t) \right\rangle \tag{D33}$$

Note that this has the correct dimensions due to our choice of normalization for $\hat{b}_{\rm in}$ (with dimensions $\sqrt{\omega}$). In the general case, an integration over frequencies is needed (as will be discussed further below). An analogous formula holds for the power radiated by the cavity, to be discussed now.

The output mode $\hat{b}_{\rm out}(t)$ is radiated into the bath and evolves freely after the system interacts with $\hat{b}_{\rm in}(t)$. If the cavity did not respond at all, then the output mode would simply be the input mode reflected off the cavity mirror. If the mirror is partially transparent then the output mode will also contain waves radiated by the cavity (which is itself being driven by the input mode partially transmitted into the cavity through the mirror) and hence contains information about the internal dynamics of the cavity. To analyze this output field, let $t_1 > t$ be a time in the distant future after the input field has interacted with the cavity. Then we can write an alternative solution to Eq. (D20) in terms of the final rather than the initial condition of the bath

$$\hat{b}_q(t) = e^{-i\omega_q(t-t_1)} \hat{b}_q(t_1) - \int_t^{t_1} d\tau\, e^{-i\omega_{\rm q}(t-\tau)} f_q^* \hat{a}(\tau). \tag{D34}$$

Note the important minus sign in the second term associated with the fact that the time t is now the lower limit of integration rather than the upper as it was in Eq. (D21).

Defining

$$\hat{b}_{\rm out}(t) \equiv \frac{1}{\sqrt{2\pi\rho}} \sum_q e^{-i\omega_{\rm q}(t-t_1)} \hat{b}_q(t_1), \tag{D35}$$

we see that this is simply the free evolution of the bath modes from the distant future (after they have interacted with the cavity) back to the present, indicating that it is indeed appropriate to interpret this as the outgoing field. Proceeding as before we obtain

$$\dot{\hat{a}} = \frac{i}{\hbar}[\hat{H}_{\rm sys}, \hat{a}] + \frac{\kappa}{2}\hat{a} - \sqrt{\kappa}\, \hat{b}_{\rm out}(t). \tag{D36}$$

Subtracting Eq. (D36) from Eq. (D32) yields

$$\hat{b}_{\rm out}(t) = \hat{b}_{\rm in}(t) + \sqrt{\kappa}\, \hat{a}(t) \tag{D37}$$

which is consistent with our interpretation of the outgoing field as the reflected incoming field plus the field radiated by the cavity out through the partially reflecting mirror.

The above results are valid for any general cavity Hamiltonian. The general procedure is to solve Eq. (D32) for $\hat{a}(t)$ for a given input field, and then solve Eq. (D37) to obtain the output field. For the case of an empty cavity we can make further progress because the cavity mode is a harmonic oscillator

$$\hat{H}_{\rm sys} = \hbar\omega_{\rm c} \hat{a}^\dagger \hat{a}. \tag{D38}$$

In this simple case, the cavity EOM becomes

$$\dot{\hat{a}} = -i\omega_{\rm c}\hat{a} - \frac{\kappa}{2}\hat{a} - \sqrt{\kappa}\, \hat{b}_{\rm in}(t). \tag{D39}$$

Eq. (D39) can be solved by Fourier transformation, yielding

$$\hat{a}[\omega] = -\frac{\sqrt{\kappa}}{i(\omega_{\rm c} - \omega) + \kappa/2}\, \hat{b}_{\rm in}[\omega] \tag{D40}$$

$$= -\sqrt{\kappa}\chi_{\rm c}[\omega - \omega_{\rm c}] \hat{b}_{\rm in}[\omega] \tag{D41}$$

and

$$\hat{b}_{\rm out}[\omega] = \frac{\omega - \omega_{\rm c} - i\kappa/2}{\omega - \omega_{\rm c} + i\kappa/2}\, \hat{b}_{\rm in}[\omega] \tag{D42}$$

which is the result for the reflection coefficient quoted in Eq. (4.23). For brevity, here and in the following, we will sometimes use the susceptibility of the cavity, defined as

$$\chi_{\rm c}[\omega - \omega_{\rm c}] \equiv \frac{1}{-i(\omega - \omega_{\rm c}) + \kappa/2} \tag{D43}$$

For the case of steady driving on resonance where $\omega = \omega_c$, the above equations yield

$$\hat{b}_{\rm out}[\omega] = \frac{\sqrt{\kappa}}{2}\hat{a}[\omega]. \tag{D44}$$

In steady state, the incoming power equals the outgoing power, and both are related to the photon number inside the single-sided cavity by

$$P = \hbar\omega \left\langle \hat{b}^\dagger_{\rm out}(t)\hat{b}_{\rm out}(t)\right\rangle = \hbar\omega\frac{\kappa}{4}\left\langle \hat{a}^\dagger(t)\hat{a}(t)\right\rangle \tag{D45}$$

Note that this does not coincide with the naive expectation, which would be $P = \hbar\omega\kappa\left\langle \hat{a}^\dagger\hat{a}\right\rangle$. The reason for this discrepancy is the the interference between the part of the incoming wave which is promptly reflected from the cavity and the field radiated by the cavity. The naive expression becomes correct after the drive has been switched off (where ignoring the effect of the incoming vacuum noise, we would have $\hat{b}_{\rm out} = \sqrt{\kappa}\hat{a}$). We note in passing that for a driven two-sided cavity with coupling constants κ_L and κ_R (where $\kappa = \kappa_L + \kappa_R$), the incoming power sent into the left port is related to the photon number by

$$P = \hbar\omega\kappa^2/(4\kappa_L)\left\langle \hat{a}^\dagger\hat{a}\right\rangle. \tag{D46}$$

Here for $\kappa_L = \kappa_R$ the interference effect completely eliminates the reflected beam and we have in contrast to Eq. (D45)

$$P = \hbar\omega\frac{\kappa}{2}\left\langle \hat{a}^\dagger\hat{a}\right\rangle. \tag{D47}$$

Eq. (D39) can also be solved in the time domain to obtain

$$\begin{aligned}\hat{a}(t) &= e^{-(i\omega_c+\kappa/2)(t-t_0)}\hat{a}(t_0)\\ &- \sqrt{\kappa}\int_{t_0}^{t} d\tau\, e^{-(i\omega_c+\kappa/2)(t-\tau)}\hat{b}_{\rm in}(\tau).\end{aligned} \tag{D48}$$

If we take the input field to be a coherent drive at frequency $\omega_{\rm L} = \omega_c + \Delta$ so that its amplitude has a classical and a quantum part

$$\hat{b}_{\rm in}(t) = e^{-i\omega_{\rm L}t}[\bar{b}_{\rm in} + \hat{\xi}(t)] \tag{D49}$$

and if we take the limit $t_0 \to \infty$ so that the initial transient in the cavity amplitude has damped out, then the solution of Eq. (D48) has the form postulated in Eq. (D4) with

$$\bar{a} = -\frac{\sqrt{\kappa}}{-i\Delta + \kappa/2}\bar{b}_{\rm in} \tag{D50}$$

and (in the frame rotating at the drive frequency)

$$\hat{d}(t) = -\sqrt{\kappa}\int_{-\infty}^{t} d\tau\, e^{+(i\Delta-\kappa/2)(t-\tau)}\hat{\xi}(\tau). \tag{D51}$$

Even in the absence of any classical drive, the input field delivers vacuum fluctuation noise to the cavity. Notice that from Eqs. (D31, D49)

$$\begin{aligned}[\hat{b}_{\rm in}(t), \hat{b}^\dagger_{\rm in}(t')] &= [\hat{\xi}(t), \hat{\xi}^\dagger(t')]\\ &= \frac{1}{2\pi\rho}\sum_q e^{-i(\omega_q-\omega_{\rm L})(t-t')}\\ &= \delta(t-t'),\end{aligned} \tag{D52}$$

which is similar to Eq. (C16) for a quantum transmission line. This is the operator equivalent of white noise. Using Eq. (D48) in the limit $t_0 \to -\infty$ in Eqs. (D4,D51) yields

$$\begin{aligned}[\hat{a}(t), \hat{a}^\dagger(t)] &= [\hat{d}(t), \hat{d}^\dagger(t)]\\ &= \kappa\int_{-\infty}^{t} d\tau \int_{-\infty}^{t} d\tau'\, e^{-(-i\Delta+\kappa/2)(t-\tau)}\\ &\quad e^{-(+i\Delta+\kappa/2)(t-\tau')}\delta(\tau-\tau')\\ &= 1\end{aligned} \tag{D53}$$

as is required for the cavity bosonic quantum degree of freedom. We can interpret this as saying that the cavity zero-point fluctuations arise from the vacuum noise that enters through the open port. We also now have a simple physical interpretation of the quantum noise in the number of photons in the driven cavity in Eqs. (D3,D8,D11). It is due to the vacuum noise which enters the cavity through the same ports that bring in the classical drive. The interference between the vacuum noise and the classical drive leads to the photon number fluctuations in the cavity.

In thermal equilibrium, $\hat{\xi}$ also contains thermal radiation. If the bath is being probed only over a narrow range of frequencies centered on ω_c (which we have have assumed in making the Markov approximation) then we have to a good approximation (consistent with the above commutation relation)

$$\langle\hat{\xi}^\dagger(t)\hat{\xi}(t')\rangle = N\delta(t-t') \tag{D54}$$

$$\langle\hat{\xi}(t)\hat{\xi}^\dagger(t')\rangle = (N+1)\delta(t-t') \tag{D55}$$

where $N = n_{\rm B}(\hbar\omega_c)$ is the thermal equilibrium occupation number of the mode at the frequency of interest. We can gain a better understanding of Eq. (D54) by Fourier transforming it to obtain the spectral density

$$S[\omega] = \int_{-\infty}^{+\infty} dt\,\langle\hat{\xi}^\dagger(t)\hat{\xi}(t')\rangle e^{i\omega(t-t')} = N. \tag{D56}$$

As mentioned previously, this dimensionless quantity is the spectral density that would be measured by a photomultiplier: it represents the number of thermal photons passing a given point per unit time per unit bandwidth. Equivalently the thermally radiated power in a narrow bandwidth B is

$$P = \hbar\omega NB. \tag{D57}$$

One often hears the confusing statement that the noise added by an amplifier is a certain number N of photons ($N = 20$, say for a good cryogenic HEMT amplifier operating at 5 GHz). This means that the excess output noise (referred back to the input by dividing by the power gain) produces a flux of N photons per second in a 1 Hz bandwidth, or $10^6 N$ photons per second in 1 MHz of bandwidth.

We can gain further insight into input-output theory by using the following picture. The operator $\hat{b}_{\rm in}(t)$ represents the classical drive plus vacuum fluctuations which are just about to arrive at the cavity. We will be able to show that the output field is simply the input field a short while later after it has interacted with the cavity. Let us consider the time evolution over a short time period Δt which is very long compared to the inverse bandwidth of the vacuum noise (i.e., the frequency scale beyond which the vacuum noise cannot be treated as constant due to some property of the environment) but very short compared to the cavity system's slow dynamics. In this circumstance it is useful to introduce the quantum Wiener increment related to Eq. (C18)

$$d\widehat{W} \equiv \int_t^{t+\Delta t} d\tau\, \hat{\xi}(\tau) \tag{D58}$$

which obeys

$$[d\widehat{W}, d\widehat{W}^\dagger] = \Delta t. \tag{D59}$$

In the interaction picture (in a displaced frame in which the classical drive has been removed) the Hamiltonian term that couples the cavity to the quantum noise of the environment is from Eq. (D18)

$$\hat{V} = -i\hbar\sqrt{\kappa}(\hat{a}^\dagger\hat{\xi} - \hat{a}\hat{\xi}^\dagger). \tag{D60}$$

Thus the time evolution operator (in the interaction picture) on the jth short time interval $[t_j, t_j + \Delta t]$ is

$$\hat{U}_j = e^{\sqrt{\kappa}(\hat{a}\, d\widehat{W}^\dagger - \hat{a}^\dagger\, d\widehat{W})} \tag{D61}$$

Using this we can readily evolve the incoming temporal mode forward in time by a small step Δt

$$d\widehat{W}' = \hat{U}^\dagger d\widehat{W}\hat{U} \approx d\widehat{W} + \sqrt{\kappa}\Delta t\, \hat{a}. \tag{D62}$$

Recall that in input-output theory we formally defined the outgoing field as the bath field far in the future propagated back (using the free field time evolution) to the present, which yielded

$$\hat{b}_{\rm out} = \hat{b}_{\rm in} + \sqrt{\kappa}\hat{a}. \tag{D63}$$

Eq. (D62) is completely equivalent to this. Thus we confirm our understanding that the incoming field is the bath temporal mode just before it interacts with the cavity and the outgoing field is the bath temporal mode just after it interacts with the cavity.

This leads to the following picture which is especially useful in the quantum trajectory approach to conditional quantum evolution of a system subject to weak continuous measurement (Gardiner *et al.*, 1992; Walls and Milburn, 1994). On top of the classical drive $\bar{b}_{\rm in}(t)$, the bath supplies to the system a continuous stream of "fresh" harmonic oscillators, each in their ground state (if $T = 0$). Each oscillator with its quantum fluctuation $d\widehat{W}$ interacts briefly for a period Δt with the system and then is disconnected to propagate freely thereafter, never interacting with the system again. Within this picture it is useful to think of the oscillators arrayed in an infinite stationary line and the cavity flying over them at speed $v_{\rm p}$ and touching each one for a time Δt.

3. Quantum limited position measurement using a cavity detector

We will now apply the input-output formalism introduced in the previous section to the important example of a dispersive position measurement, which employs a cavity whose resonance frequency shifts in response to the motion of a harmonic oscillator. This physical system was considered heuristically in Sec. (IV.B.3). Here we will present a rigorous derivation using the (linearized) equations of motion for the coupled cavity and oscillator system.

Let the dimensionless position operator

$$\hat{z} = \frac{1}{x_{\rm ZPF}}\hat{x} = [\hat{c}^\dagger + \hat{c}] \tag{D64}$$

be the coordinate of a harmonic oscillator whose energy is

$$H_{\rm M} = \hbar\omega_{\rm M}\hat{c}^\dagger\hat{c} \tag{D65}$$

and whose position uncertainty in the quantum ground state is $x_{\rm ZPF} = \sqrt{\langle 0|\hat{x}^2|0\rangle}$.

This Hamiltonian could be realized for example by mounting one of the cavity mirrors on a flexible cantilever (see the discussion above).

When the mirror moves, the cavity resonance frequency shifts,

$$\tilde{\omega}_{\rm c} = \omega_{\rm c}[1 + A\hat{z}(t)] \tag{D66}$$

where for a cavity of length L, $A = -x_{\rm ZPF}/L$.

Assuming that the mirror moves slowly enough for the cavity to adiabatically follow its motion (i.e. $\Omega \ll \kappa$), the outgoing light field suffers a phase shift which follows the changes in the mirror position. This phase shift can be detected in the appropriate homodyne set up as discussed in Sec. IV.B, and from this phase shift we can determine the position of the mechanical oscillator. In addition to the actual zero-point fluctuations of the oscillator, our measurement will suffer from shot noise in the homodyne signal and from additional uncertainty due to the back action noise of the measurement acting on the oscillator.

All of these effects will appear naturally in the derivation below.

We begin by considering the optical cavity equation of motion based on Eq. (D32) and the optomechanical coupling Hamiltonian in Eq. (D1). These yield

$$\dot{\hat{a}} = -i\omega_{\rm c}(1 + A\hat{z})\hat{a} - \frac{\kappa}{2}\hat{a} - \sqrt{\kappa}\hat{b}_{\rm in}. \tag{D67}$$

Let the cavity be driven by a laser at a frequency $\omega_{\rm L} = \omega_{\rm c} + \Delta$ detuned from the cavity by Δ. Moving to a frame rotating at $\omega_{\rm L}$ we have

$$\dot{\hat{a}} = +i(\Delta - A\omega_{\rm c}\hat{z})\hat{a} - \frac{\kappa}{2}\hat{a} - \sqrt{\kappa}\hat{b}_{\rm in}. \tag{D68}$$

and we can write the incoming field as a constant plus white noise vacuum fluctuations (again, in the rotating frame)

$$\hat{b}_{\rm in} = \bar{b}_{\rm in} + \hat{\xi} \tag{D69}$$

and similarly for the cavity field following Eq. (D4)

$$\hat{a} = \bar{a} + \hat{d}. \tag{D70}$$

Substituting these expressions into the equation of motion, we find that the constant classical fields obey

$$\bar{a} = -\frac{\sqrt{\kappa}}{\kappa/2 - i\Delta}\bar{b}_{\rm in} \tag{D71}$$

and the new quantum equation of motion is, after neglecting a small term $\hat{d}\hat{z}$:

$$\dot{\hat{d}} = +i\Delta\hat{d} - iA\omega_{\rm c}\bar{a}\hat{z} - \frac{\kappa}{2}\hat{d} - \sqrt{\kappa}\hat{\xi}. \tag{D72}$$

The quantum limit for position measurement will be reached only at zero detuning, so we specialize to the case $\Delta = 0$. We also choose the incoming field amplitude and phase to obey

$$\bar{b}_{\rm in} = -i\sqrt{\dot{\overline{N}}}, \tag{D73}$$

so that

$$\bar{a} = +2i\sqrt{\frac{\dot{\overline{N}}}{\kappa}}, \tag{D74}$$

where $\dot{\overline{N}}$ is the incoming photon number flux. The quantum equation of motion for the cavity then becomes

$$\dot{\hat{d}} = +g\hat{z} - \frac{\kappa}{2}\hat{d} - \sqrt{\kappa}\hat{\xi}, \tag{D75}$$

where the opto-mechanical coupling constant is proportional to the laser drive amplitude

$$g \equiv 2A\omega_{\rm c}\sqrt{\frac{\dot{\overline{N}}}{\kappa}} = A\omega_{\rm c}\sqrt{\bar{n}}. \tag{D76}$$

and

$$\bar{n} = |\bar{a}|^2 = 4\frac{\dot{\overline{N}}}{\kappa} \tag{D77}$$

is the mean cavity photon number. Eq. (D75) is easily solved by Fourier transformation

$$\hat{d}[\omega] = \frac{1}{[\kappa/2 - i\omega]}\left\{g\hat{z}[\omega] - \sqrt{\kappa}\hat{\xi}[\omega]\right\}. \tag{D78}$$

Let us assume that we are in the limit of low mechanical frequency relative to the cavity damping, $\Omega \ll \kappa$, so that the cavity state adiabatically follows the motion of the mechanical oscillator. Then we obtain to a good approximation

$$\hat{d}[\omega] = \frac{2}{\kappa}\left\{g\hat{z}[\omega] - \sqrt{\kappa}\hat{\xi}[\omega]\right\} \tag{D79}$$

$$\hat{d}^\dagger[\omega] = \frac{2}{\kappa}\left\{g\hat{z}[\omega] - \sqrt{\kappa}\hat{\xi}^\dagger[\omega]\right\} \tag{D80}$$

The mechanical oscillator equation of motion which is identical in form to that of the optical cavity

$$\partial_t\hat{c} = -[\frac{\gamma_0}{2} + i\Omega]\hat{c} - \sqrt{\gamma_0}\hat{\eta}(t) + \frac{i}{\hbar}[\hat{H}_{\rm int}, \hat{c}(t)], \tag{D81}$$

where $\hat{H}_{\rm int}$ is the Hamiltonian in Eq. (D1) and $\hat{\eta}$ is the mechanical vacuum noise from the (zero temperature) bath which is causing the mechanical damping at rate γ_0. Using Eq. (D70) and expanding to first order in small fluctuations yields the equation of motion linearized about the steady state solution

$$\partial_t\hat{c} = -[\frac{\gamma_0}{2} + i\Omega]\hat{c} - \sqrt{\gamma_0}\hat{\eta}(t) + 2\frac{g}{\sqrt{\kappa}}[\hat{\xi}(t) - \hat{\xi}^\dagger(t)]. \tag{D82}$$

It is useful to consider an equivalent formulation in which we expand the Hamiltonian in Eq. (D1) to second order in the quantum fluctuations about the classical solution

$$\hat{H}_{\rm int} \approx \hbar\omega_{\rm c}\hat{d}^\dagger\hat{d} + \hat{x}\hat{F}, \tag{D83}$$

where the force (including the coupling A) is (up to a sign)

$$\hat{F} = -i\frac{\hbar g}{x_{\rm ZPF}}[\hat{d} - \hat{d}^\dagger]. \tag{D84}$$

Note that the radiation pressure fluctuations (photon shot noise) inside the cavity provide a forcing term. The state of the field inside the cavity in general depends on the past history of the cantilever position. However for this special case of driving the cavity on resonance, the dependence of the cavity field on the cantilever history is such that the latter drops out of the radiation pressure. To see this explicitly, consider the equation of motion for the force obtained from Eq. (D75)

$$\dot{\hat{F}} = -\frac{\kappa}{2}\hat{F} + i\frac{\hbar g}{x_{\rm ZPF}}\sqrt{\kappa}[\hat{\xi} - \hat{\xi}^\dagger]. \tag{D85}$$

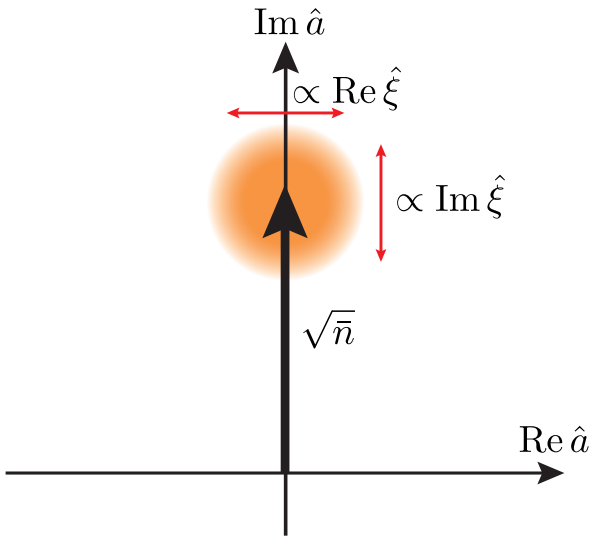

FIG. 19 (Color online) Phasor diagram for the cavity amplitude showing that (for our choice of parameters) the imaginary quadrature of the vacuum noise $\hat{\xi}$ interferes with the classical drive to produce photon number fluctuations while the real quadrature produces phase fluctuations which lead to measurement imprecision. The quantum fluctuations are illustrated in the usual fashion, depicting the Gaussian Wigner density of the coherent state in terms of color intensity.

Within our linearization approximation, the position of the mechanical oscillator has no effect on the radiation pressure (photon number in the cavity), but of course it does affect the *phase* of the cavity field (and hence the outgoing field) which is what we measure in the homodyne detection.

Thus for this special case $\hat{z}$ does not appear on the RHS of either Eq. (D85) or Eq. (D82), which means that there is no optical renormalization of the cantilever frequency ('optical spring') or optical damping of the cantilever. The lack of back-action damping in turn implies that the effective temperature $T_{\rm eff}$ of the cavity detector is infinite (cf. Eq. (3.21)). For this special case of zero detuning the back action force noise is controlled by a single quadrature of the incoming vacuum noise (which interferes with the classical drive to produce photon number fluctuations). This is illustrated in the cavity amplitude phasor diagram of Fig. (19). We see that the vacuum noise quadrature $\hat{\xi}+\hat{\xi}^\dagger$ conjugate to $\hat{F}$ controls the phase noise which determines the measurement imprecision (shot noise in the homodyne signal). This will be discussed further below.

The solution for the cantilever position can again be obtained by Fourier transformation. For frequencies small on the scale of κ the solution of Eq. (D85) is

$$\hat{F}[\omega] = \frac{2i\hbar g}{x_{\rm ZPF}\sqrt{\kappa}}\left\{\hat{\xi}[\omega]-\hat{\xi}^\dagger[\omega]\right\} \tag{D86}$$

and hence the back action force noise spectral density is at low frequencies

$$S_{FF}[\omega] = \frac{4\hbar^2 g^2}{x_{\rm ZPF}^2\kappa} \tag{D87}$$

in agreement with Eq. (4.29).

Introducing a quantity proportional to the cantilever (mechanical) susceptibility (within the rotating wave approximation we are using)

$$\chi_{\rm M}[\omega-\Omega] \equiv \frac{1}{-i(\omega-\Omega)+\frac{\gamma_0}{2}}, \tag{D88}$$

we find from Eq. (D82)

$$\hat{z}[\omega] = \hat{z}_0[\omega] - \frac{i}{\hbar}x_{\rm ZPF}\left\{\chi_{\rm M}[\omega-\Omega]-\chi_{\rm M}[\omega+\Omega]\right\}\hat{F}[\omega], \tag{D89}$$

where the equilibrium fluctuations in position are given by

$$\hat{z}_0[\omega] \equiv -\sqrt{\gamma_0}\left\{\chi_{\rm M}[\omega-\Omega]\hat{\eta}[\omega]+\chi_{\rm M}[\omega+\Omega]\hat{\eta}^\dagger[\omega]\right\}. \tag{D90}$$

We can now obtain the power spectrum S_{zz} describing the total position fluctuations of the cantilever driven by the mechanical vacuum noise plus the radiation pressure shot noise. From Eqs. (D89, D90) we find

$$\begin{aligned}\frac{S_{xx}[\omega]}{x_{\rm ZPF}^2} &= S_{zz}[\omega] \\ &= \gamma_0|\chi[\omega-\Omega]|^2 \\ &\quad + \frac{x_{\rm ZPF}^2}{\hbar^2}\left|\chi_{\rm M}[\omega-\Omega]-\chi_{\rm M}[\omega+\Omega]\right|^2 S_{FF}.\end{aligned} \tag{D91}$$

Note that (assuming high mechanical Q, i.e. $\gamma_0 \ll \Omega$) the equilibrium part has support only at positive frequencies while the back action induced position noise is symmetric in frequency reflecting the effective infinite temperature of the back action noise. Symmetrizing this result with respect to frequency (and using $\gamma_0 \ll \Omega$) we have

$$\bar{S}_{xx}[\omega] \approx \bar{S}^0_{xx}[\omega]\left(1+\frac{\bar{S}^0_{xx}[\Omega]}{\hbar^2}\bar{S}_{FF}\right), \tag{D92}$$

where $\bar{S}^0_{xx}[\omega]$ is the symmetrized spectral density for position fluctuations in the ground state given by Eq. (4.71).

Now that we have obtained the effect of the back action noise on the position fluctuations, we must turn our attention to the imprecision of the measurement due to shot noise in the output. The appropriate homodyne quadrature variable to monitor to be sensitive to the output phase shift caused by position fluctuations is

$$\hat{I} = \hat{b}_{\rm out} + \hat{b}^\dagger_{\rm out}, \tag{D93}$$

which, using the input-output results above, can be written

$$\hat{I} = -(\hat{\xi}+\hat{\xi}^\dagger) + \lambda\hat{x}. \tag{D94}$$

We see that the cavity homodyne detector system acts as a position transducer with gain

$$\lambda = \frac{4g}{x_{\rm ZPF}\sqrt{\kappa}}. \tag{D95}$$

The first term in Eq. (D94) represents the vacuum noise that mixes with the homodyne local oscillator to produce the shot noise in the output. The resulting measurement imprecision (symmetrized) spectral density referred back to the position of the oscillator is

$$\bar{S}^{\rm I}_{xx} = \frac{1}{\lambda^2}. \tag{D96}$$

Comparing this to Eq. (D87) we see that we reach the quantum limit relating the imprecision noise to the back action noise

$$\bar{S}^{\rm I}_{xx}\bar{S}_{FF} = \frac{\hbar^2}{4} \tag{D97}$$

in agreement with Eq. (4.20).

Notice also from Eq. (D94) that the quadrature of the vacuum noise which leads to the measurement imprecision is conjugate to the one which produces the back action force noise as illustrated previously in Fig. (19). We saw in Eq. (2.20) that the two quadratures of motion of a harmonic oscillator in its ground state have no classical (i.e., symmetrized) correlation. Hence the symmetrized cross correlator

$$\bar{S}_{IF}[\omega] = 0 \tag{D98}$$

vanishes. Because there is no correlation between the output imprecision noise and the forces controlling the position fluctuations, the total output noise referred back to the position of the oscillator is simply

$$\begin{aligned} \bar{S}_{xx,\rm tot}[\omega] &= \bar{S}_{xx}[\omega] + \bar{S}^{\rm I}_{xx} \\ &= \bar{S}^0_{xx}[\omega]\left(1 + \frac{\bar{S}^0_{xx}[\Omega]}{\hbar^2}\bar{S}_{FF}\right) + \frac{\hbar^2}{4\bar{S}_{FF}}. \end{aligned} \tag{D99}$$

This expression again clearly illustrates the competition between the back action noise proportional to the drive laser intensity and the measurement imprecision noise which is inversely proportional. We again emphasize that all of the above relations are particular to the case of zero detuning of the cavity drive field from the cavity.

The total output noise at some particular frequency will be a minimum at some optimal drive intensity. The precise optimal value depends on the frequency chosen. Typically this is taken to be the mechanical resonance frequency where we find that the optimal coupling leads to an optimal back action noise

$$\bar{S}_{FF,\rm opt} = \frac{\hbar^2}{2\bar{S}^0_{xx}[\Omega]} = \frac{\hbar^2\gamma_0}{4x^2_{\rm ZPF}}. \tag{D100}$$

This makes sense because the higher the damping the less susceptible the oscillator is to back action forces. At this optimal coupling the total output noise spectral density at frequency Ω referred to the position is simply twice the vacuum value

$$\bar{S}_{xx,\rm tot}[\Omega] = 2\bar{S}^0_{xx}[\Omega], \tag{D101}$$

in agreement with Eq. (4.81). Evaluation of Eq. (D100) at the optimal coupling yields the graph shown in Fig. (7). The background noise floor is due to the frequency independent imprecision noise with value $\frac{1}{2}\bar{S}^0_{xx}[\Omega]$. The peak value at $\omega = \Omega$ rises a factor of three above this background.

We derived the gain λ in Eq. (D95) by direct solution of the equations of motion. With the results we have derived above, it is straightforward to show that the Kubo formula in Eq. (5.3) yields equivalent results. We have already seen that the classical (i.e. symmetrized) correlations between the output signal $\hat{I}$ and the force $\hat{F}$ which couples to the position vanishes. However the Kubo formula evaluates the *quantum* (i.e. antisymmetric) correlations for the uncoupled system ($A = g = 0$). Hence we have

$$\chi_{IF}(t) = -\frac{i}{\hbar}\theta(t)\left\langle\left[-\big(\hat{\xi}(t-\delta t) + \hat{\xi}^\dagger(t-\delta t)\big), \frac{2i\hbar g}{x_{\rm ZPF}\sqrt{\kappa}}\big(\hat{\xi}(0) - \hat{\xi}^\dagger(0)\big)\right]\right\rangle_0, \tag{D102}$$

where δt is a small (positive) time representing the delay between the time when the vacuum noise impinges on the cavity and when the resulting outgoing wave reaches the homodyne detector. (More precisely it also compensates for certain small retardation effects neglected in the limit $\omega \ll \kappa$ used in several places in the above derivations.) Using the fact that the commutator between the two quadratures of the vacuum noise is a delta function, Fourier transformation of the above yields (in the limit $\omega\,\delta t \ll 1$ the desired result

$$\chi_{IF}[\omega] = \lambda. \tag{D103}$$

Similarly we readily find that the small retardation causes the reverse gain to vanish. Hence all our results are consistent with the requirements needed to reach the standard quantum limit.

Thus with this study of the specific case of an oscillator parametrically coupled to a cavity, we have reproduced

all of the key results in Sec. (VI.D) derived from completely general considerations of linear response theory.

4. Back-action free single-quadrature detection

We now provide details on the cavity single-quadrature detection scheme discussed in Sec. VI.G.2. We again consider a high-Q cavity whose resonance frequency is modulated by a high-Q mechanical oscillator with co-ordinate $\hat{x}$ (cf. Eqs. (D1) and (D64)). To use this system for amplification of a single quadrature, we will consider the typical case of a fast cavity ($\omega_c \gg \Omega$), and take the "good cavity" limit, where $\Omega \gg \kappa$. As explained in the main text, the crucial ingredient for single-quadrature detection is to take an amplitude-modulated cavity drive described by the classical input field $\bar{b}_{\rm in}$ given in Eq. (6.70). As before (cf. Eq. (D4)), we may write the cavity annihilation operator $\hat{a}$ as the sum of a classical piece $\bar{a}(t)$ and a quantum piece $\hat{d}$; only $\hat{d}$ is influenced by the mechanical oscillator. $\bar{a}(t)$ is easily found from the classical (noise-free) equations of motion for the isolated cavity; making use of the conditions $\omega_c \gg \Omega \gg \kappa$, we have

$$\bar{a}(t) \simeq \frac{\sqrt{\dot{N}\kappa}}{2\Omega}\cos(\Omega t+\delta)\, e^{-i\omega_c t} \tag{D104}$$

To proceed with our analysis, we work in an interaction picture with respect to the uncoupled cavity and oscillator Hamiltonians. Making standard rotating-wave approximations, the Hamiltonian in the interaction picture takes the simple form corresponding to Eq. (6.71b):

$$\begin{aligned} H_{\rm int} &= \hbar\tilde{A}\left(\hat{d}+\hat{d}^\dagger\right)\left(e^{i\delta}\hat{c}+e^{-i\delta}\hat{c}^\dagger\right) \\ &= \hbar\tilde{A}\left(\hat{d}+\hat{d}^\dagger\right)\frac{\hat{X}_\delta}{x_{\rm ZPF}}, \end{aligned} \tag{D105}$$

where

$$\tilde{A} = A\cdot\omega_c\frac{\sqrt{\dot{N}\kappa}}{4\Omega}, \tag{D106}$$

and in the second line, we have made use of the definition of the quadrature operators $\hat{X}_\delta, \hat{Y}_\delta$ given in Eqs. (6.64). The form of $H_{\rm int}$ was discussed heuristically in the main text in terms of Raman processes where photons are removed from the classical drive $\bar{b}_{\rm in}$ and either up or down converted to the cavity frequency via absorption or emission of a mechanical phonon. Alternatively, we can think of the drive yielding a time-dependent cavity-oscillator coupling which "follows" the X_δ quadrature. Note that we made crucial of use of the good cavity limit ($\kappa \ll \Omega$) to drop terms in $\hat{H}_{int}$ which oscillate at frequencies $\pm 2\Omega$. These terms represent Raman sidebands which are away from the cavity resonance by a distance $\pm 2\Omega$. In the good cavity limit, the density of photon states is negligible so far off resonance and these processes are suppressed.

Similar to Eqs. (D39) and (D81), the Heisenberg equations of motion (in the rotating frame) follow directly from $H_{\rm int}$ and the dissipative terms in the total Hamiltonian:

$$\partial_t\hat{d} = -\frac{\kappa}{2}\hat{d}-\sqrt{\kappa}\hat{\xi}(t)e^{i\omega_c t}-i\tilde{A}\left(e^{i\delta}\hat{c}+e^{-i\delta}\hat{c}^\dagger\right) \tag{D107a}$$

$$\partial_t\hat{c} = -\frac{\gamma_0}{2}\hat{c}-\sqrt{\gamma_0}\hat{\eta}(t)e^{i\Omega t}-ie^{-i\delta}\left[\tilde{A}\left(\hat{d}+\hat{d}^\dagger\right)-f(t)\right] \tag{D107b}$$

As before, $\hat{\xi}(t)$ represents the unavoidable noise in the cavity drive, and $\hat{\eta}(t)$, γ_0 are the noisy force and damping resulting from an equilibrium bath coupled to the mechanical oscillator. Note from Eq. (D107a) that as anticipated, the cavity is only driven by one quadrature of the oscillator's motion. We have also included a driving force $F(t)$ on the mechanical oscillator which has some narrow bandwidth centered on the oscillator frequency; this force is parameterized as:

$$F(t) = \frac{2\hbar}{x_{\rm ZPF}}{\rm Re}\left[f(t)e^{-i\Omega t}e^{-i\delta}\right] \tag{D108}$$

where $f(t)$ is a complex function which is slowly varying on the scale of an oscillator period.

The equations of motion are easily solved upon Fourier transformation, resulting in:

$$\begin{aligned} \hat{X}_\delta[\omega] &= -x_{\rm ZPF}\cdot\chi_M[\omega]\Big[i\left(f^*[-\omega]-f[\omega]\right) \\ &\quad +\sqrt{\gamma_0}\left(e^{i\delta}\hat{\eta}(\omega+\Omega)+e^{-i\delta}\hat{\eta}^\dagger(\omega-\Omega)\right)\Big] \end{aligned} \tag{D109a}$$

$$\begin{aligned} \hat{Y}_\delta[\omega] &= ix_{\rm ZPF}\cdot\chi_M[\omega]\Big[(-i)\left(f[\omega]+f^*[-\omega]\right) \\ &\quad +\sqrt{\gamma_0}\left(e^{i\delta}\hat{\eta}(\omega+\Omega)-e^{-i\delta}\hat{\eta}^\dagger(\omega-\Omega)\right) \\ &\quad -2i\tilde{A}\chi_c[\omega]\sqrt{\kappa}\left(\hat{\xi}(\omega+\omega_c)+\hat{\xi}^\dagger(\omega-\omega_c)\right)\Big] \end{aligned} \tag{D109b}$$

where the cavity and mechanical susceptibilities χ_c, χ_M are defined in Eqs. (D43) and (D88).

As anticipated, the detected quadrature $\hat{X}_\delta$ is *completely* unaffected by the measurement: Eq. (D109a) is identical to what we would have if there were no coupling between the oscillator and the cavity. In contrast, the conjugate quadrature $\hat{Y}_\delta$ experiences an extra stochastic force due to the cavity: this is the measurement back-action.

Turning now to the output field from the cavity $\hat{b}_{\rm out}$, we use the input-output relation Eq. (D37) to find in the *lab* (i.e. non-rotating) frame:

$$\begin{aligned} \hat{b}_{\rm out}[\omega] &= \bar{b}_{\rm out}[\omega]+\left[\frac{-i(\omega-\omega_c)-\kappa/2}{-i(\omega-\omega_c)+\kappa/2}\right]\hat{\xi}[\omega] \\ &\quad -i\frac{\tilde{A}\sqrt{\kappa}}{x_{\rm ZPF}}\chi_c[\omega-\omega_c]\cdot\hat{X}_\delta(\omega-\omega_c) \end{aligned} \tag{D110}$$

The first term on the RHS simply represents the output field from the cavity in the absence of the mechanical oscillator and any fluctuations. It will yield sharp peaks at the two sidebands associated with the drive, $\omega = \omega_c \pm \Omega$. The second term on the RHS of Eq. (D110) represents the reflected noise of the incident cavity drive. This noise will play the role of the "intrinsic ouput noise" of this amplifier.

Finally, the last term on the RHS of Eq. (D110) is the amplified signal: it is simply the amplified quadrature $\hat{X}_\delta$ of the oscillator. This term will result in a peak in the output spectrum at the resonance frequency of the cavity, ω_c. As there is no back-action on the measured $\hat{X}_\delta$ quadrature, the added noise can be made arbitrarily small by simply increasing the drive strength $\dot{N}$ (and hence $\tilde{A}$).

APPENDIX E: Information Theory and Measurement Rate

Suppose that we are measuring the state of a qubit via the phase shift $\pm\theta_0$ from a one-sided cavity. Let $I(t)$ be the homodyne signal integrated up to time t as in Eqs. (4.36-4.37). We would like to understand the relationship between the signal-to-noise ratio defined in Eq. (4.38), and the rate at which information about the state of the qubit is being gained. The probability distribution for I conditioned on the state of the qubit $\sigma = \pm 1$ is

$$p(I|\sigma) = \frac{1}{\sqrt{2\pi S_{\theta\theta} t}} \exp\left[\frac{-(I - \sigma\theta_0 t)^2}{2 S_{\theta\theta} t}\right]. \tag{E1}$$

Based on knowledge of this conditional distribution, we now present two distinct but equivalent approaches to giving an information theoretic basis for the definition of the measurement rate.

1. Method I

Suppose we start with an initial qubit density matrix

$$\rho_0 = \begin{pmatrix} \frac{1}{2} & 0 \\ 0 & \frac{1}{2} \end{pmatrix}. \tag{E2}$$

After measuring for a time t, the new density matrix conditioned on the results of the measurement is

$$\rho_1 = \begin{pmatrix} p_+ & 0 \\ 0 & p_- \end{pmatrix} \tag{E3}$$

where it will be convenient to parameterize the two probabilities by the polarization $m \equiv \mathrm{Tr}(\sigma_z \rho_1)$ by

$$\mathbf{p}_\pm = \frac{1 \pm m}{2}. \tag{E4}$$

The information gained by the measurement is the entropy loss[25] of the qubit

$$\mathcal{I} = \mathrm{Tr}(\rho_1 \ln \rho_1 - \rho_0 \ln \rho_0). \tag{E5}$$

We are interested in the initial rate of gain of information at short times $\theta_0^2 t \ll S_{\theta\theta}$ where m will be small. In this limit we have

$$\mathcal{I} \approx \frac{m^2}{2}. \tag{E6}$$

We must now calculate m conditioned on the measurement result I

$$m_I \equiv \sum_\sigma \sigma p(\sigma|I). \tag{E7}$$

From Bayes theorem we can express this in terms of $p(I|\sigma)$, which is the quantity we know,

$$p(\sigma|I) = \frac{p(I|\sigma)p(\sigma)}{\sum_{\sigma'} p(I|\sigma')p(\sigma')}. \tag{E8}$$

Using Eq. (E1) the polarization is easily evaluated

$$m_I = \tanh\left(\frac{I\theta_0}{S_{\theta\theta}}\right). \tag{E9}$$

The information gain is thus

$$\mathcal{I}_I = \frac{1}{2}\tanh^2\left(\frac{I\theta_0}{S_{\theta\theta}}\right) \approx \frac{I^2}{2}\left(\frac{\theta_0}{S_{\theta\theta}}\right)^2 \tag{E10}$$

where the second equality is only valid for small $|m|$. Ensemble averaging this over all possible measurement results yields the mean information gain at short times

$$\mathcal{I} \approx \frac{1}{2}\frac{\theta_0^2}{S_{\theta\theta}} t \tag{E11}$$

which justifies the definition of the measurement rate given in Eq. (4.39).

2. Method II

An alternative information theoretic derivation is to consider the qubit plus measurement device to be a signaling channel. The two possible inputs to the channel are the two states of the qubit. The output of the channel is the result of the measurement of I. By toggling the qubit state back and forth, one can send information through the signal channel to another party. The channel is noisy because even for a fixed state of the qubit,

[25] It is important to note that we use throughout here the physicist's entropy with the natural logarithm rather than the log base 2 which gives the information in units of bits.

the measured values of the signal I have intrinsic fluctuations. Shannon's noisy channel coding theorem (Cover and Thomas, 1991) tells us the maximum rate at which information can be reliably sent down the channel by toggling the state of the qubit and making measurements of I. It is natural to take this rate as defining the measurement rate for our detector.

The reliable information gain by the receiver on a noisy channel is a quantity known as the 'mutual information' of the communication channel (Clerk *et al.*, 2003; Cover and Thomas, 1991)

$$R = -\int_{-\infty}^{+\infty} dI \left\{ p(I)\ln p(I) - \sum_{\sigma} p(\sigma)\left[p(I|\sigma)\ln p(I|\sigma)\right] \right\} \tag{E12}$$

The first term is the Shannon entropy in the signal I when we do not know the input signal (the value of the qubit). The second term represents the entropy given that we do know the value of the qubit (averaged over the two possible input values). Thus the first term is signal plus noise, the second is just the noise. Subtracting the two gives the net information gain. Expanding this expression for short times yields

$$\begin{aligned} R &= \frac{1}{8}\frac{(\langle I(t)\rangle_+ - \langle I(t)\rangle_-)^2}{S_{\theta\theta}t} \\ &= \frac{\theta_0^2}{2S_{\theta\theta}}t \\ &= \Gamma_{\rm meas}t \end{aligned} \tag{E13}$$

exactly the same result as Eq. (E11). (Here $\langle I(t)\rangle_\sigma$ is the mean value of I given that the qubit is in state σ.)

APPENDIX F: Quantum Parametric Amplifiers

1. Non-degenerate case

a. Gain and added noise

The so-called non-degenerate parametric amplifier is a linear, phase preserving amplifier which can in principle reach the quantum limit (Gordon *et al.*, 1963; Louisell *et al.*, 1961; Mollow and Glauber, 1967a,b). One possible realization (Yurke *et al.*, 1989) is a cavity with three internal resonances that are coupled together by a nonlinear element (such as a Josephson junction) whose symmetry permits three-wave mixing. The three modes are called the pump, idler and signal and their energy level structure illustrated in Fig. 20 obeys

$$\omega_{\rm P} = \omega_{\rm I} + \omega_{\rm S}. \tag{F1}$$

It is important that the system be such that these are the only three modes to which the cavity couples. The system Hamiltonian is then

$$\begin{aligned} \hat{H}_{\rm sys} &= \hbar\left(\omega_{\rm P}\hat{a}_{\rm P}^\dagger\hat{a}_{\rm P} + \omega_{\rm I}\hat{a}_{\rm I}^\dagger\hat{a}_{\rm I} + \omega_{\rm S}\hat{a}_{\rm S}^\dagger\hat{a}_{\rm S}\right) \\ &+ i\hbar\eta\left(\hat{a}_{\rm S}^\dagger\hat{a}_{\rm I}^\dagger\hat{a}_{\rm P} - \hat{a}_{\rm S}\hat{a}_{\rm I}\hat{a}_{\rm P}^\dagger\right). \end{aligned} \tag{F2}$$

We have made the rotating wave approximation in the three-wave mixing term, and without loss of generality, we take the non-linear susceptibility η to be real and positive. The system is driven at the pump frequency and the three wave mixing term permits a single pump photon to split into an idler photon and a signal photon. This process is stimulated by signal photons already present and leads to gain. A typical mode of operation would be the negative resistance reflection mode (Yurke *et al.*, 1989) in which the input signal is reflected from a nonlinear cavity and the reflected beam extracted using a circulator. Since input and output travel on the same line, the input and output impedances of the amplifier are equal.

The non-linear EOMs become tractable if we assume the pump has large amplitude and can be treated classically by making the substitution

$$\hat{a}_{\rm P} = \psi_{\rm P}e^{-i\omega_{\rm P}t} = \psi_{\rm P}e^{-i(\omega_{\rm I}+\omega_{\rm S})t}, \tag{F3}$$

where without loss of generality we take $\psi_{\rm P}$ to be real and positive. We note here the important point that if this approximation is not valid, then our amplifier would in any case not be the linear amplifier which we seek. With this approximation we can hereafter forget about the dynamics of the pump degree of freedom and deal with the reduced system Hamiltonian

$$\begin{aligned} \hat{H}_{\rm sys} &= \hbar\left(\omega_{\rm I}\hat{a}_{\rm I}^\dagger\hat{a}_{\rm I} + \omega_{\rm S}\hat{a}_{\rm S}^\dagger\hat{a}_{\rm S}\right) + i\hbar\lambda \\ &\left(\hat{a}_{\rm S}^\dagger\hat{a}_{\rm I}^\dagger e^{-i(\omega_{\rm I}+\omega_{\rm S})t} - \hat{a}_{\rm S}\hat{a}_{\rm I}e^{+i(\omega_{\rm I}+\omega_{\rm S})t}\right) \end{aligned} \tag{F4}$$

where $\lambda \equiv \eta\psi_{\rm P}$. Transforming to the interaction representation we are left with the following time-independent quadratic Hamiltonian for the system

$$\hat{V}_{\rm sys} = i\hbar\lambda\left(\hat{a}_{\rm S}^\dagger\hat{a}_{\rm I}^\dagger - \hat{a}_{\rm S}\hat{a}_{\rm I}\right) \tag{F5}$$

To get some intuitive understanding of the physics, let us temporarily ignore the damping of the cavity modes due to their coupling to the external baths. We now have a pair of coupled EOMs for the two modes

$$\begin{aligned} \dot{\hat{a}}_{\rm S} &= +\lambda\hat{a}_{\rm I}^\dagger \\ \dot{\hat{a}}_{\rm I}^\dagger &= +\lambda\hat{a}_{\rm S} \end{aligned} \tag{F6}$$

for which the solutions are

$$\begin{aligned} \hat{a}_{\rm S}(t) &= \cosh(\lambda t)\hat{a}_{\rm S}(0) + \sinh(\lambda t)\hat{a}_{\rm I}^\dagger(0) \\ \hat{a}_{\rm I}^\dagger(t) &= \sinh(\lambda t)\,\hat{a}_{\rm S}(0) + \cosh(\lambda t)\,\hat{a}_{\rm I}^\dagger(0) \end{aligned} \tag{F7}$$

We see that the amplitude in the signal channel grows exponentially in time and that the effect of the time evolution is to perform a simple unitary transformation which mixes $\hat{a}_{\rm S}$ with $\hat{a}_{\rm I}^\dagger$ in such a way as to preserve the commutation relations. We now see the close connection with the form found from very general arguments in Eqs. (6.7a-6.12).

With this initial result in hand, we are ready to consider the presence of finite damping, necessary to feed the input signal into the amplifier, which will cut off the exponential growth and give a fixed amplitude gain. Following our standard Markovian approximation for both the idler and signal baths, we obtain in analogy with the previous results the following EOMs in the interaction representation

$$\begin{aligned}\dot{\hat{a}}_{\rm S} &= -\frac{\kappa_{\rm S}}{2}\,\hat{a}_{\rm S} + \lambda \hat{a}_{\rm I}^\dagger - \sqrt{\kappa_{\rm S}}\,\hat{b}_{\rm S,in} \\ \dot{\hat{a}}_{\rm I}^\dagger &= -\frac{\kappa_{\rm I}}{2}\,\hat{a}_{\rm I}^\dagger + \lambda\,\hat{a}_{\rm S} - \sqrt{\kappa_{\rm I}}\,\hat{b}_{\rm I,in}^\dagger \end{aligned} \tag{F8}$$

where $\kappa_{\rm S}$ and $\kappa_{\rm I}$ are the respective damping rates of the cavity signal mode and the idler mode.

Let us fix our attention on signals inside a frequency window $\delta\omega$ centered on $\omega_{\rm S}$ (hence zero frequency in the interaction representation). For simplicity, we will first consider the case where the signal bandwidth $\delta\omega$ is almost infinitely narrow (i.e. much much smaller than the damping rate of the cavity modes). It then suffices to find the steady state solution of these EOMs

$$\hat{a}_{\rm S} = \frac{2\lambda}{\kappa_{\rm S}}\,\hat{a}_{\rm I}^\dagger - \frac{2}{\sqrt{\kappa_{\rm S}}}\,\hat{b}_{\rm S,in} \tag{F9}$$

$$\hat{a}_{\rm I}^\dagger = \frac{2\lambda}{\kappa_{\rm I}}\,\hat{a}_{\rm S} - \frac{2}{\sqrt{\kappa_{\rm I}}}\,\hat{b}_{\rm I,in}^\dagger \tag{F10}$$

from which the output signal is readily computed using Eq. (D37)

$$\hat{b}_{\rm S,out} = \frac{Q^2+1}{Q^2-1}\,\hat{b}_{\rm S,in} + \frac{2Q}{Q^2-1}\,\hat{b}_{\rm I,in}^\dagger \tag{F11}$$

where $Q \equiv \frac{2\lambda}{\sqrt{\kappa_{\rm I}\kappa_{\rm S}}}$ is proportional to the pump amplitude and inversely proportional to the cavity decay rates. We have to require $Q^2 < 1$ to make sure that the parametric amplifier does not settle into self-sustained oscillations, i.e. it works below threshold. Under that condition, we can define the voltage gain $\sqrt{G_0}$ to be

$$-\sqrt{G_0} = (Q^2+1)/(Q^2-1), \tag{F12}$$

such that

$$\hat{b}_{\rm S,out} = -\sqrt{G_0}\,\hat{b}_{\rm S,in} - \sqrt{G_0-1}\,\hat{b}_{\rm I,in}^\dagger \tag{F13}$$

This is precisely of the Haus-Caves form Eq. (6.12) and shows that the non-degenerate parametric amplifier reaches the quantum limit for minimum added noise. In the limit of large gain the output noise (referred to the input) for a vacuum input signal is precisely doubled.

b. Bandwidth-gain tradeoff

The above results neglected the finite bandwidth $\delta\omega$ of the input signal to the amplifier. The gain G_0 given in Eq. (F12) is only the gain at precisely the mean signal frequency $\omega_{\rm S}$; for a finite bandwidth, we also need to understand how the power gain varies as a function of frequency over the entire signal bandwidth. As we will see, a parametric amplifier suffers from the fact that as one increases the overall magnitude of the gain at the center frequency $\omega_{\rm S}$ (e.g. by increasing the pump amplitude), one simultaneously narrows the frequency range over which the gain is appreciable. Heuristically, this is because parametric amplification involves increasing the quality factor of the signal mode resonance. This increase in quality factor leads to amplification, but it also reduces the bandwidth over which $\hat{a}_{\rm S}$ can respond to the input signal $\hat{b}_{\rm S,in}$.

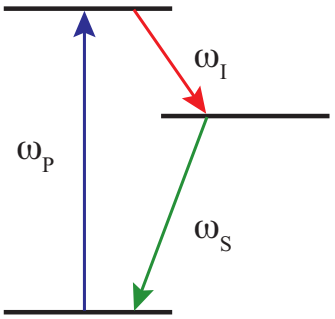

FIG. 20 (Color online) Energy level scheme of the non-degenerate (phase preserving) parametric oscillator.

To deal with a finite signal bandwidth, one simply Fourier transforms Eqs. (F8). The resulting equations are easily solved and substituted into Eq. (D37), resulting in a frequency-dependent generalization of the input-output relation given in Eq. (F13):

$$\hat{b}_{\rm S,out}[\omega] = -g[\omega]\hat{b}_{\rm S,in}[\omega] - g'[\omega]\hat{b}_{\rm I,in}^\dagger[\omega] \tag{F14}$$

Here, $g[\omega]$ is the frequency-dependent voltage gain of the amplifier, and $g'[\omega]$ satisfies $|g'[\omega]|^2 = |g[\omega]|^2 - 1$. In the relevant limit where $G_0 = |g[0]|^2 \gg 1$ (i.e. large gain at the signal frequency), one has to an excellent approximation:

$$g[\omega] = \frac{\sqrt{G_0} - i\left(\frac{\kappa_{\rm S}-\kappa_{\rm I}}{\kappa_{\rm I}+\kappa_{\rm S}}\right)(\omega/D)}{1 - i(\omega/D)}, \tag{F15}$$

with

$$D = \frac{1}{\sqrt{G_0}}\frac{\kappa_{\rm S}\kappa_{\rm I}}{\kappa_{\rm S}+\kappa_{\rm I}}. \tag{F16}$$

As always, we work in an interaction picture where the signal frequency has been shifted to zero. D represents the effective operating bandwidth of the amplifier. Components of the signal with frequencies (in the rotating frame) $|\omega| \ll D$ are strongly amplified, while components with frequencies $|\omega| \gg D$ are not amplified at all, but

can in fact be slightly attenuated. As we already anticipated, the amplification bandwidth D becomes progressively smaller as the pump power and G_0 are increased, with the product $\sqrt{G_0}D$ remaining constant. In a parametric amplifier increasing the gain via increasing the pump strength comes with a price: the effective operating bandwidth is reduced.

c. Effective temperature

Returning to the behaviour of the paramp at the signal frequency, we note that Eq. (F13) implies that even for vacuum input to both the signal and idler ports of the paramp, the output will contain a real photon flux. To quantify this in a simple way, we make use of the temporal modes introduced in our discussion of the windowed Fourier transform (c.f. Eq. (C18)). We thus define the input signal temporal modes as:

$$\hat{B}_{\mathrm{S,in},j} = \frac{1}{\sqrt{\Delta t}} \int_{j\Delta t}^{(j+1)\Delta t} d\tau \hat{b}_{\mathrm{S,in}}(\tau); \tag{F17}$$

the temporal modes $\hat{B}_{\mathrm{S,out},j}$ and $\hat{B}_{\mathrm{I,in},j}$ are defined analogously.

With these definitions, we find that the output mode will have a real occupancy even if the input mode is empty:

$$\begin{aligned} \bar{n}_{\mathrm{S,out}} &= \langle 0|\hat{B}^\dagger_{\mathrm{S,out},j}\hat{B}_{\mathrm{S,out},j}|0\rangle \\ &= G_0\langle 0|\hat{B}^\dagger_{\mathrm{S,in},j}\hat{B}_{\mathrm{S,in},j}|0\rangle + \\ &\quad (G_0-1)\langle 0|\hat{B}_{\mathrm{I,in},j}\hat{B}^\dagger_{\mathrm{I,in},j}|0\rangle \\ &= G_0 - 1. \end{aligned} \tag{F18}$$

The dimensionless mode occupancy $\bar{n}_{\mathrm{S,out}}$ is best thought of as a photon flux per unit bandwidth (c.f. Eq.(C26)). This photon flux is equivalent to the photon flux that would appear in equilibrium at the very high effective temperature (assuming large gain G_0)

$$T_{\mathrm{eff}} \approx \hbar\omega_{\mathrm{S}} G_0. \tag{F19}$$

Thus, as discussed in Sec. VI.D.4, a high gain amplifier must have associated with it a large effective temperature scale. Referring this total output noise back to the input, we have (in the limit $G_0 \gg 1$):

$$\frac{T_{\mathrm{eff}}}{G_0} = \frac{\hbar\omega_{\mathrm{S}}}{2} + \frac{\hbar\omega_{\mathrm{S}}}{2} = \frac{\hbar\omega_{\mathrm{S}}}{2} + T_{\mathrm{N}}. \tag{F20}$$

This corresponds to the half photon of vacuum noise associated with the signal source, plus the added noise of a half photon of our phase preserving amplifier (i.e. the noise temperature T_N is equal to its quantum limited value). Here, the added noise is simply the vacuum noise associated with the idler port.

The above argument is merely suggestive that the output noise looks like an effective temperature. In fact it is possible to show that the photon number distribution is in the output is precisely that of a Bose-Einstein distribution at temperature T_{eff}. From Eq. (F2) we see that the action of the paramp is to destroy a pump photon and create a pair of new photons, one in the signal channel and one in the idler channel. Using the SU(1,1) symmetry of the quadratic hamiltonian in Eq. (F5) it is possible to show that, for vacuum input, the output of the paramp is a so-called 'two-mode squeezed state' of the form (Caves and Schumaker, 1985; Gerry, 1985; Knight and Buzek, 2004)

$$|\Psi_{\mathrm{out}}\rangle = Z^{-1/2} e^{\alpha b^\dagger_{\mathrm{S}} b^\dagger_{\mathrm{I}}} |0\rangle \tag{F21}$$

where α is a constant related to the gain and, to simplify the notation, we have dropped the 'out' labels on the operators. The normalization constant Z can be worked out by expanding the exponential and using

$$(b^\dagger_{\mathrm{S}})^n |0,0\rangle = \sqrt{n!}|n,0\rangle \tag{F22}$$

to obtain

$$|\Psi_{\mathrm{out}}\rangle = Z^{-1/2} \sum_{n=0}^{\infty} \alpha^n |n,n\rangle \tag{F23}$$

and hence

$$Z = \frac{1}{1-|\alpha|^2} \tag{F24}$$

so the state is normalizable only for $|\alpha|^2 < 1$.

Because this output is obtained by unitary evolution from the vacuum input state, the output state is a pure state with zero entropy. In light of this, it is interesting to consider the reduced density matrix obtain by tracing over the idler mode. The pure state density matrix is:

$$\begin{aligned} \rho &= |\Psi_{\mathrm{out}}\rangle \langle \Psi_{\mathrm{out}}| \\ &= \sum_{m,n=0}^{\infty} |n,n\rangle \frac{\alpha^n \alpha^{*m}}{Z} \langle m,m| \end{aligned} \tag{F25}$$

If we now trace over the idler mode we are left with the reduced matrix for the signal channel

$$\begin{aligned} \tilde{\rho}_{\mathrm{S}} &= \mathrm{Tr}_{\mathrm{Idler}}\{\rho\} \\ &= \sum_{n_{\mathrm{S}}=0}^{\infty} |n_{\mathrm{S}}\rangle \frac{|\alpha|^{2n_{\mathrm{S}}}}{Z} \langle n_{\mathrm{S}}| \\ &= \frac{1}{Z} e^{-\beta\hbar\omega_{\mathrm{S}} a^\dagger_{\mathrm{S}} a_{\mathrm{S}}} \end{aligned} \tag{F26}$$

which is a pure thermal equilibrium distribution with effective Boltzmann factor

$$e^{-\beta\hbar\omega_{\mathrm{S}}} = |\alpha|^2 < 1. \tag{F27}$$

The effective temperature can be obtained from the requirement that the signal mode occupancy is $G_0 - 1$

$$\frac{1}{e^{\beta\hbar\omega_{\mathrm{S}}} - 1} = G_0 - 1 \tag{F28}$$

which in the limit of large gain reduces to Eq. (F19).

This appearance of finite entropy in a subsystem even when the full system is in a pure state is a purely quantum effect. Classically the entropy of a composite system is at least as large as the entropy of any of its components. Entanglement among the components allows this lower bound on the entropy to be violated in a quantum system.[26] In this case the two-mode squeezed state has strong entanglement between the signal and idler channels (since their photon numbers are fluctuating identically).

2. Degenerate case

In the degenerate parametric amplifier the idler mode is eliminated, and the non-linearity converts a single pump photon into two signal photons at frequency $\omega_S = \omega_P/2$. This amplifier is not phase preserving (referred to in the literature by the unfortunate name 'phase sensitive'). Rather it amplifies one quadrature of the signal and attenuates the other. As a result, it is not necessary to add extra noise to preserve the commutation relations.

The system Hamiltonian is

$$\begin{aligned}\hat{H}_{\rm sys} &= \hbar\left(\omega_{\rm P}\hat{a}_{\rm P}^\dagger\hat{a}_{\rm P} + \omega_{\rm S}\hat{a}_{\rm S}^\dagger\hat{a}_{\rm S}\right) \\ &+ i\hbar\eta\left(\hat{a}_{\rm S}^\dagger\hat{a}_{\rm S}^\dagger\hat{a}_{\rm P} - \hat{a}_{\rm S}\hat{a}_{\rm S}\hat{a}_{\rm P}^\dagger\right). \end{aligned} \tag{F29}$$

Treating the pump classically as before, the analog of Eq. (F5) is

$$\hat{V}_{\rm sys} = i\hbar\frac{\lambda}{2}\left(\hat{a}_{\rm S}^\dagger\hat{a}_{\rm S}^\dagger - \hat{a}_{\rm S}\hat{a}_{\rm S}\right), \tag{F30}$$

where $\lambda/2 = \eta\psi_P$, and the analog of Eq. (F8) is:

$$\dot{\hat{a}}_{\rm S} = -\frac{\kappa_{\rm S}}{2}\,\hat{a}_{\rm S} + \lambda\hat{a}_{\rm S}^\dagger - \sqrt{\kappa_{\rm S}}\,\hat{b}_{\rm S,in} \tag{F31}$$

It is useful to define two quadrature modes

$$\hat{x}_{\rm S} = \frac{1}{\sqrt{2}}\left(\hat{a}_{\rm S}^\dagger + \hat{a}_{\rm S}\right) \tag{F32}$$

$$\hat{y}_{\rm S} = \frac{i}{\sqrt{2}}\left(\hat{a}_{\rm S}^\dagger - \hat{a}_{\rm S}\right) \tag{F33}$$

which obey $[\hat{x}_{\rm S}, \hat{y}_{\rm S}] = i$. We can define quadrature operators $\hat{X}_{S,\rm in/out}, \hat{Y}_{S,\rm in/out}$ corresponding to the input and output fields in a completely analogous manner.

The steady state solution of Eq. (F31) for the output fields becomes

$$\hat{X}_{\rm S,out} = \sqrt{G}\hat{X}_{\rm S,in} \tag{F34}$$

$$\hat{Y}_{\rm S,out} = \frac{1}{\sqrt{G}}\hat{Y}_{\rm S,in}, \tag{F35}$$

where the number gain G is given by

$$G = \left[\frac{\lambda + \kappa_{\rm S}/2}{\lambda - \kappa_{\rm S}/2}\right]^2. \tag{F36}$$

Thus we see that one quadrature is amplified and the other is correspondingly attenuated. The commutation relation

$$[\hat{X}_{\rm S,out}(t), \hat{Y}_{\rm S,out}(t')] = i\delta(t - t') \tag{F37}$$

is independent of G without the necessity of adding further quantum noise.

APPENDIX G: Number Phase Uncertainty

In this appendix, we briefly review the number-phase uncertainty relation, and from it we derive the relationship between the spectral densities describing the photon number fluctuations and the phase fluctuations. Consider a coherent state labeled by its classical amplitude α

$$|\alpha\rangle = \exp\left\{-\frac{|\alpha|^2}{2}\right\}\exp\{\alpha\hat{a}^\dagger\}|0\rangle. \tag{G1}$$

This is an eigenstate of the destruction operator

$$\hat{a}|\alpha\rangle = \alpha|\alpha\rangle. \tag{G2}$$

It is convenient to make the unitary displacement transformation which maps the coherent state onto a new vacuum state and the destruction operator onto

$$\hat{a} = \alpha + \hat{d} \tag{G3}$$

where d annihilates the new vacuum. Then we have

$$\bar{N} = \langle\hat{N}\rangle = \langle 0|(\alpha^* + \hat{d}^\dagger)(\alpha + \hat{d})|0\rangle = |\alpha|^2, \tag{G4}$$

and

$$(\Delta N)^2 = \langle(\hat{N} - \bar{N})^2\rangle = |\alpha|^2\langle 0|\hat{d}\hat{d}^\dagger|0\rangle = \bar{N}. \tag{G5}$$

Now define the two quadrature amplitudes

$$\hat{X} = \frac{1}{\sqrt{2}}(\hat{a} + \hat{a}^\dagger) \tag{G6}$$

$$\hat{Y} = \frac{i}{\sqrt{2}}(\hat{a}^\dagger - \hat{a}). \tag{G7}$$

Each of these amplitudes can be measured in a homodyne experiment, for example using the Mach-Zehnder interferometer described in Appendix (H). For convenience, let us take α to be real and positive. Then

$$\langle\hat{X}\rangle = \sqrt{2}\alpha \tag{G8}$$

and

$$\langle\hat{Y}\rangle = 0. \tag{G9}$$

[26] This paradox has prompted Charles Bennett to remark that a classical house is at least as dirty as its dirtiest room, but a quantum house can be dirty in every room and still perfectly clean over all.

If the phase of this wave undergoes a small modulation due for example to weak parametric coupling to a qubit then one can estimate the phase by

$$\langle\theta\rangle = \frac{\langle\hat{Y}\rangle}{\langle\hat{X}\rangle}. \tag{G10}$$

The uncertainty will be

$$(\Delta\theta)^2 = \frac{\langle\hat{Y}^2\rangle}{(\langle\hat{X}\rangle)^2} = \frac{\frac{1}{2}\langle 0|\hat{d}\hat{d}^\dagger|0\rangle}{2\bar{N}} = \frac{1}{4\bar{N}}. \tag{G11}$$

Thus using Eq. (G5) we arrive at the fundamental quantum uncertainty relation

$$\Delta\theta\Delta N = \frac{1}{2}. \tag{G12}$$

Using the input-output theory described in Appendix D we can restate the results above in terms of noise spectral densities. Let the amplitude of the field coming in to the homodyne detector be

$$\hat{b}_{\rm in} = \bar{b}_{\rm in} + \hat{\xi}(t) \tag{G13}$$

where $\hat{\xi}(t)$ is the vacuum noise obeying

$$[\hat{\xi}(t), \hat{\xi}^\dagger(t')] = \delta(t-t'). \tag{G14}$$

We are using a flux normalization for the field operators so

$$\overline{\dot{N}} = \langle\hat{b}^\dagger_{\rm in}\hat{b}_{\rm in}\rangle = |\bar{b}_{\rm in}|^2 \tag{G15}$$

and

$$\langle\dot{N}(t)\dot{N}(0)\rangle - \overline{\dot{N}}^2 = \langle 0|(\bar{b}^*_{\rm in} + \hat{\xi}^\dagger(t))(\bar{b}_{\rm in} + \hat{\xi}(t))(\bar{b}^*_{\rm in} + \hat{\xi}^\dagger(0))(\bar{b}_{\rm in} + \hat{\xi}(0))|0\rangle - \left|\bar{b}_{\rm in}\right|^4 = \overline{\dot{N}}\delta(t). \tag{G16}$$

From this it follows that the shot noise spectral density is

$$S_{\dot{N}\dot{N}} = \overline{\dot{N}}. \tag{G17}$$

Similarly the phase can be estimated from the quadrature operator

$$\hat{\theta} = \frac{i(\hat{b}^\dagger_{\rm in} - \hat{b}_{\rm in})}{\langle\hat{b}^\dagger_{\rm in} + \hat{b}_{\rm in}\rangle} = \langle\hat{\theta}\rangle + i\frac{(\hat{\xi}^\dagger - \hat{\xi})}{2\bar{b}_{\rm in}} \tag{G18}$$

which has noise correlator

$$\langle\delta\hat{\theta}(t)\delta\hat{\theta}(0)\rangle = \frac{1}{4\overline{\dot{N}}}\delta(t) \tag{G19}$$

corresponding to the phase imprecision spectral density

$$S_{\theta\theta} = \frac{1}{4\overline{\dot{N}}}. \tag{G20}$$

We thus arrive at the fundamental quantum limit relation

$$\sqrt{S_{\theta\theta}S_{\dot{N}\dot{N}}} = \frac{1}{2}. \tag{G21}$$

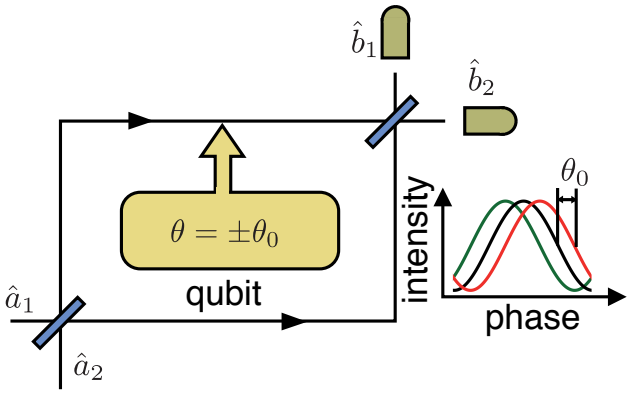

FIG. 21 (Color online) Mach-Zehnder interferometer use as a qubit state detector.

APPENDIX H: Mach Zehnder Interferometer as a Quantum Limited Detector

In this appendix, we examine the properties of a prototypical interferometric detector, the Mach Zehnder interferometer (MZI), see Fig. 21, and ask whether this system can reach the quantum limit. For simplicity, we consider using such an interferometer to do QND measurement of a qubit by having the qubit influence one arm of the interferometer. As follows from the discussion of Sec. IV.B , the conclusions we reach will also apply to the case where the interferometer is used to do position detection of a mechanical oscillator. We show that if one uses a Fock state input, one reaches the quantum limit as long as the second beam splitter is symmetric. In contrast, a coherent state input reaches the quantum limit *only* in the extreme case of an unbalanced interferometer,

where there is a vanishing amplitude in the arm containing the qubit; in the perfectly symmetric case, it misses the quantum limit by a factor of two. We demonstrate that in both the Fock state and coherent state cases, any departure from the quantum limit can be directly tied to unused information available in the *phases* of the output of the interferometer. The differences between the Fock state and coherent state case can be ascribed to the different types of phase information available at the output in each case. Finally, we note that if one were to couple the qubit (or oscillator) to *both* arms of the interferometer, then as long as the second beam-splitter is symmetric, one will reach the quantum limit with a coherent state input; for such a coupling, there is never any wasted phase information.

Note that the standard treatment of measurement with an interferometer (Caves, 1980, 1981) does not explicitly distinguish the Fock state and coherent state cases We show that there are important differences between the two cases. In the case of a Fock state input, one can directly tie the interferometer back-action to the partition noise at the first beam splitter. In contrast, in the coherent state case, there is no partition noise per se; instead, the intrinsic noise in the input state (i.e. an uncertainty in number) serves to constrain the measurement.

1. Basic description of the interferometer

The MZI detector consists of two beam splitters, each of which is described by a 2×2 unitary scattering matrix. The output of the first beam splitter is attached to the input of the second via two "arms"; the phase shift in one of the arms is determined by the state of the qubit we wish to measure. Information on this phase shift can then be determined by looking at the difference between the intensities at MZI's two output ports.

The scattering matrix S of the MZI determines the relation between the annihilation operators describing the MZI input and output ports:

$$\begin{pmatrix} \hat{b}_1 \\ \hat{b}_2 \end{pmatrix} = S \cdot \begin{pmatrix} \hat{a}_1 \\ \hat{a}_2 \end{pmatrix} \tag{H1}$$

where $\hat{a}_1$ and $\hat{a}_2$ are annihilation operators for the two input ports, and $\hat{b}_1$ and $\hat{b}_2$ are annihilation operators for the two output ports. S is given by:

$$S = s_B \cdot s_{\rm arms} \cdot s_A \tag{H2}$$

where s_A, s_B are the scattering matrices of the beam splitters, and $s_{\rm arms}$ is the scattering matrix of the arms. We have:

$$s_A = \begin{pmatrix} \sqrt{1-T_A} & i\sqrt{T_A} \\ i\sqrt{T_A} & \sqrt{1-T_A} \end{pmatrix} \tag{H3}$$

$$s_B = \begin{pmatrix} \sqrt{1-T_B} & i\sqrt{T_B} \\ i\sqrt{T_B} & \sqrt{1-T_B} \end{pmatrix} \tag{H4}$$

$$s_{\rm arms} = \begin{pmatrix} ie^{i\theta} & 0 \\ 0 & 1 \end{pmatrix} \tag{H5}$$

Here, T_A and T_B are real numbers between 0 and 1 which describe the transmission probabilities of the two beam splitters. We have assumed for simplicity that each beam splitter has time-reversal symmetry and parity symmetry (i.e. the symmetry operation which exchanges "1" and "2" ports). $\theta = \pm\theta_0$ is the phase shift provided by the qubit; the factor of i in $s_{\rm arms}$ is chosen to yield a maximum sensitivity to the phase θ_0 in a measurement of the output intensities.

Letting $R_A = 1-T_A$, $R_B = 1-T_B$, it will be convenient to parameterize S as:

$$S = e^{i\eta} \begin{pmatrix} \sqrt{1-\tilde{T}}e^{i\beta} & i\sqrt{\tilde{T}}e^{-i\phi} \\ i\sqrt{\tilde{T}}e^{i\phi} & \sqrt{1-\tilde{T}}e^{-i\beta} \end{pmatrix} \tag{H6}$$

where

$$e^{2i\eta} = ie^{i\theta} \tag{H7}$$

$$\tilde{T} = T_A R_B + T_B R_A - 2\sqrt{T_A R_A T_B R_B}\sin\theta \tag{H8}$$

$\tilde{T}$ determines the intensity at the two output ports, while η, β and ϕ describe the phases of the MZI output. Note that all of these phases depend on θ, although we do not list the explicit dependence here.

In what follows, we will use the scattering matrix to determine the output of the interferometer for different possible input states. For simplicity (and as is standard in the quantum optics literature), we will not describe the input to the interferometer using wavepackets, but rather as extended waves. A more appropriate analysis using wavepackets reaches identical conclusions as the ones we present below.

2. Fock state input

We first consider the case where the input of the MZI is prepared in a state having exactly N photons in input port 1, and zero photons in the input port 2:

$$|\psi_{in}\rangle = |N\rangle_{a_1}|0\rangle_{a_2} \equiv \frac{1}{\sqrt{N!}}\left(\hat{a}_1^\dagger\right)^N|\Omega\rangle \tag{H9}$$

where $|\Omega\rangle$ is the vacuum. Using Eq. (H1) to convert input operators to output operators, and using the binomial theorem, we have:

$$|\psi^{\pm}_{\rm out}\rangle = \frac{1}{\sqrt{N!}}\left(\left[S^{-1}_{\pm}\right]^{*}_{11}\hat{b}^{\dagger}_{1}+\left[S^{-1}_{\pm}\right]^{*}_{12}\hat{b}^{\dagger}_{2}\right)^{N}|\Omega\rangle$$
$$= e^{iN(\eta_{\pm}+\phi_{\pm})}\sum_{m=0}^{N}e^{im(\beta_{\pm}-\phi_{\pm})}\sqrt{\binom{N}{m}}\times\sqrt{(1-\tilde{T}_{\pm})^{m}(i\tilde{T}_{\pm})^{N-m}}|m\rangle_{b1}|N-m\rangle_{b2} \quad \text{(H10)}$$

Here, $\pm$ denotes the two qubit eigenstates, and the two corresponding phase shifts $\theta = \pm\theta_0$. We see that the states $|\psi^{\pm}_{\rm out}\rangle$ yield classical, binomial photon number statistics at the output port; this is the direct result of the partitioning of photons at the two beam splitters, and the resulting noise (i.e. uncertainty in the photon number at one of the output ports) is properly termed "shot noise".

Note that the phase appearing in the sum over m in Eq. (H10), $\lambda_{\pm} = \beta_{\pm} - \phi_{\pm}$, is the *relative* phase difference between the output in port 1 versus port 2. Unlike the global phase of the wavefunction $|\psi_{\rm out}\rangle$, this phase difference is in principle measurable, as the number difference between the two output ports is not fixed. To lowest order in $|\theta|$, $\lambda_{\pm}$ is given by:

$$\lambda_{\pm} = -\arctan\left(\frac{\sqrt{T_A R_A}}{(1-2T_A)\sqrt{T_B R_B}}\right) + \quad \text{(H11)}$$
$$\mp\left(\frac{(1-2T_B)T_A R_A}{(T_A R_B + T_B R_A)\left(1 - T_A R_B + T_B R_A\right)}\right)\theta_0$$

Note that only in the case of a symmetric second beam splitter (i.e. $T_B = R_B = 1/2$) is the phase $\lambda_{\pm}$ independent of the state of the qubit.

a. Measurement rate

The quantity most easily measured at the output of the MZI is $\hat{N}_{\rm diff}$, the difference between the photon numbers at the two outputs: $\hat{N}_{\rm diff} \equiv \hat{b}^{\dagger}_1\hat{b}_1 - \hat{b}^{\dagger}_2\hat{b}_2$. Using the definition of $|\psi^{\pm}_{\rm out}\rangle$ above and taking $|\theta| = \theta_0 \ll 1$ (i.e. a weak measurement), we have:

$$\langle\hat{N}_{\rm diff}\rangle_{\pm} = \tilde{T}_{\pm}N - (1-\tilde{T}_{\pm})N$$
$$\simeq \langle\hat{N}_{\rm diff}\rangle\Big|_{\theta=0} \pm 2N\frac{d\tilde{T}}{d\theta}\theta_0$$
$$= \langle\hat{N}_{\rm diff}\rangle\Big|_{\theta=0} \mp 4N\sqrt{T_A R_A T_B R_B}\theta_0 \quad \text{(H12)}$$

The uncertainty (or noise) in the measured quantity $\hat{N}_{\rm diff}$ in the state $|\psi^{\pm}_{\rm out}\rangle$ is just given by the usual binomial expression; to lowest order in θ it is independent of the qubit state, and is given by:

$$\langle\langle\hat{N}^2_{\rm diff}\rangle\rangle \equiv \langle\hat{N}^2_{\rm diff}\rangle - \langle\hat{N}_{\rm diff}\rangle^2$$
$$= 4\times\left(\tilde{T}_0(1-\tilde{T}_0)\right)N \quad \text{(H13)}$$

where $\tilde{T}_0 = \tilde{T}\Big|_{\theta=0}$.

We can now calculate the measurement rate (see Appendix E) for this setup by asking how long it will take to resolve the difference between the two possible qubit states, i.e. to reach the condition:

$$|\langle N_{\rm diff}\rangle_{+} - \langle N_{\rm diff}\rangle_{-}| \geq 2\sqrt{2}\cdot\sqrt{\langle\langle N^2_{\rm diff}\rangle\rangle} \quad \text{(H14)}$$

The numerical prefactor on the rhs has been chosen to make this definition coincide with our previous definition. In our system, this condition translates into a minimum number of photons that are needed in the input state. We find simply:

$$N \geq N_{\rm meas} = \frac{2\tilde{T}_0(1-\tilde{T}_0)}{\left(\frac{d\tilde{T}}{d\theta}\theta_0\right)^2} \quad \text{(H15)}$$

Note that if one multiplies by eV/h, this expression is identical to the measurement rate of a quantum point-contact detector (Aleiner *et al.*, 1997; Gurvitz, 1997). Also note that for the Fock state input considered here, an equivalent expression for $N_{\rm meas}$ is obtained if one only measures the intensity at one of the output ports. This follows from the fact that the total number of photons is fixed and hence the fluctuations of the two ports are perfectly anticorrelated. Measuring one determines the other.

b. Dephasing rate

Similar to our analysis in Sec. IV.B, we may calculate the measurement induced dephasing of the qubit from the overlap of the two scattering states $|\psi^{\pm}_{\rm out}\rangle$ (cf. Eq. (4.48)); it is this overlap which directly determines how the off-diagonal elements of the qubit's reduced density matrix decay. One generally expects an exponential decay:

$$|\langle\psi^{-}|\psi^{+}\rangle| \propto \exp\left(-N/N_{\varphi}\right) \quad \text{(H16)}$$

where N_{φ} is the number of input photons needed to dephase the qubit (i.e. it is analogous to a dephasing time τ_{φ}).

In our case, we may directly calculate this overlap using Eq. (H10). Letting $\tilde{R} = 1 - \tilde{T}$, we find:

$$|\langle\psi^-|\psi^+\rangle| \;=\; \left|\left(e^{i(\lambda_+-\lambda_-)}\sqrt{\tilde{T}_-\tilde{T}_+}+\sqrt{\tilde{R}_-\tilde{R}_+}\right)^N\right| \tag{H17}$$

Expanding $\lambda, \tilde{T}$ and $\tilde{R}$ in θ, one has:

$$\begin{aligned}|\langle\psi^-|\psi^+\rangle| \;&=\; \left|\left(1+2\tilde{T}\left[i\left(\theta_0\frac{d\lambda}{d\theta}\right)-\left(\theta_0\frac{d\lambda}{d\theta}\right)^2\right]-\left(\theta_0\frac{d\tilde{T}}{d\theta}\right)^2\frac{1}{2\tilde{T}\tilde{R}}+O(\theta_0^4)\right)^N\right| \\ &=\; \exp\left(-N\left[\left(\theta_0\frac{d\tilde{T}}{d\theta}\right)^2\frac{1}{2\tilde{T}\tilde{R}}+2\tilde{T}_0\tilde{R}_0\left(\theta_0\frac{d\lambda}{d\theta}\right)^2\right]+O(\theta_0^4)\right)\end{aligned} \tag{H18}$$

We thus obtain an exponential decay of the overlap as expected, with a dephasing "rate" $1/N_\varphi$ given by:

$$\begin{aligned}\frac{1}{N_\varphi} \;&=\; (\theta_0)^2\left[\left(\frac{d\tilde{T}}{d\theta}\right)^2\frac{1}{2\tilde{T}_0\tilde{R}_0}+2\tilde{T}_0\tilde{R}_0\left(\frac{d\lambda}{d\theta}\right)^2\right] \\ &=\; 2T_1R_1\theta_0^2\end{aligned} \tag{H19}$$

Eq. (H19) for the dephasing rate has the form we would expect from a simple heuristic argument. Each photon traveling down the arm containing the qubit advances the qubit's phase by a *deterministic* amount $2\theta_0$. However, due to the partition noise at the first beam splitter, there is an uncertainty in the number of photons N_{qb} which pass by the qubit, which directly translates into an uncertainty in the qubit's phase ϕ_{qb}:

$$\langle\langle\phi_{qb}^2\rangle\rangle \;=\; (2\theta_0)^2\langle\langle N_{qb}^2\rangle\rangle \tag{H20}$$

$$\;=\; (2\theta_0)^2\left(T_AR_AN\right) \tag{H21}$$

Treating this noise as Gaussian, this implies that the exponential of the qubit's phase decays as:

$$|\langle e^{i\phi_{qb}}\rangle| = \exp\left(-\frac{1}{2}\langle\langle\phi_{qb}^2\rangle\rangle\right) = \exp\left(-2\theta_0^2T_AR_AN\right), \tag{H22}$$

a result which is in exact agreement with Eq. (H19).

Turning to the question of the quantum limit (i.e. does N_φ coincide with $N_{\rm meas}$?), it is more convenient to use the first expression for the dephasing rate, Eq. (H19). As the first term in this equation corresponds exactly to the measurement rate (cf. Eq. (H15)), and the second term is positive definite, we find that $N_\varphi \leq N_{\rm meas}$: *it takes longer to measure than to dephase the qubit, meaning that the MZI detector with a Fock state input generically fails to reach the quantum limit.* As is clear from the calculation, the origin of this failure is the unused or "wasted" information on the qubit's state available in the relative phase λ; this information could be extracted from the output of the MZI via a suitable interference experiment. In fact, the second term in Eq. (H19) is *precisely* the measurement rate associated with trying to determine the qubit state from the relative phase λ. From the number-phase uncertainty relation, we can find the effective uncertainty in the phase λ without specifying a particular measurement scheme; we have to zeroth order in θ:

$$\langle\langle\lambda^2\rangle\rangle = \frac{1}{4\langle\langle\hat{N}_{\rm diff}^2\rangle\rangle} = \frac{1}{4\tilde{T}_0\tilde{R}_0N} \tag{H23}$$

The measurement rate criterion of Eq. (H14) takes the form:

$$2\theta_0\left(\frac{d\lambda}{d\theta}\right) \geq 2\sqrt{2}\sqrt{\langle\langle\lambda^2\rangle\rangle} \tag{H24}$$

Combining equations and solving for the minimal N, we find:

$$N \geq N_{{\rm meas},\lambda} = \left(2\tilde{T}_0\tilde{R}_0\theta_0^2\left(\frac{d\lambda}{d\theta}\right)^2\right)^{-1} \tag{H25}$$

Thus, the second term in Eq. (H19) in indeed $1/N_{{\rm meas},\lambda}$, the measurement rate that would result if we attempted to measure λ.

While the Fock state input fails to reach the quantum limit for a generic choice of parameters, there is an important set of cases where it *does* achieve ideality. It is clear from above that reaching the quantum limit requires there to be no information in the phase λ. Turning to Eq. (H11) for this phase, we see that this necessarily requires that the second beam splitter be completely symmetric: $T_2 = 1/2$. Thus, for a symmetric second beam splitter and a Fock-state input, one reaches the quantum limit irrespective of the asymmetry in the first beam splitter.

As a final comment, note that the structure of Eq. (H19) is identical to that for the measurement induced dephasing rate of a qubit by a quantum point contact detector if one simply multiplies by the inverse timescale eV/h (Gurvitz, 1997).

3. Coherent state input

We now repeat the analysis of the previous section, treating the case where the input of the MZI consists of a coherent state in the input port "1":

$$|\psi_{in}\rangle = |\alpha\rangle_{a1}|0\rangle_{a2} = e^{-|\alpha|^2/2}\exp\left(\alpha\hat{a}_1^\dagger\right)|\Omega\rangle \tag{H26}$$

The magnitude $|\alpha|^2$ corresponds to the average photon number in the input: $|\alpha|^2 = N$.

The output state of the MZI is again given by simply using the scattering matrix S and the transformation rule of Eq. (H1) on Eq. (H26). We find:

$$\begin{aligned}
|\psi_{\text{out}}^{\pm}\rangle &= e^{-|\alpha|^2/2}\exp\left(\alpha\left(\left[S_{\pm}^{-1}\right]_{11}^{*}\hat{b}_1^\dagger + \left[S_{\pm}^{-1}\right]_{12}^{*}\hat{b}_2^\dagger\right)\right)|\Omega\rangle \\
&= e^{-|\alpha|^2/2}\exp\left(\sqrt{\tilde{R}}e^{i(\eta+\beta)}\alpha\cdot\hat{b}_1^\dagger\right)\exp\left(\sqrt{\tilde{T}}e^{i(\eta+\phi)}\alpha\cdot\hat{b}_2^\dagger\right)|\Omega\rangle \\
&= \left|\sqrt{\tilde{R}}e^{i(\eta+\beta)}\alpha\right\rangle_{b1}\left|\sqrt{\tilde{T}}e^{i(\eta+\phi)}\alpha\right\rangle_{b2}
\end{aligned} \tag{H27}$$

There are some immediate differences worth noting from the Fock state case:

- In the coherent state case, the two output ports are not entangled; equivalently, there is no partition noise (i.e. shot noise) in the coherent state case. This follows from the fact that a coherent state incident onto a beam splitter yields two independent coherent states (of diminished amplitude) whose number fluctuations are completely uncorrelated.
- As the total number of photons in the output of the interferometer is not fixed, the *absolute* phase of the the output in each port can in principle be detected

a. Measurement rate

We again take the measured quantity at the output of the MZI to be N_{diff}, the difference in intensities between the two output ports. Unlike the Fock state case, it is important the we use both ports; the measurement rate will be smaller if we only choose to use one.

The average values of the N_{diff} in the two qubit states, $\langle N_{\text{diff}}\rangle_{\pm}$ is again given by Eq. (H12), with $N = |\alpha|^2$. The noise in N_{diff} is however different, as the coherent states have Poissonian statistics as opposed to binomial. One finds to zeroth order in θ_0 that the noise in N_{diff} is identical to that in the input state $|\psi_{\text{in}}\rangle$, and is completely independent of the properties of the beam splitter:

$$\langle\langle\hat{N}_{\text{diff}}^2\rangle\rangle = |\alpha|^2 = N \tag{H28}$$

Thus, unlike the case of the Fock state, the noise in the output does not result from scattering in the MZI (i.e., partitioning of the photons between the two arms by the first beam splitter); rather, it simply reflects the intrinsic noise already present at the input. Note that $\langle\langle\hat{N}_{\text{diff}}^2\rangle\rangle$ in the Fock state case is always less than or equal to that found above.

Using the same criteria as in the previous section (cf. Eq. (H14)), we find that the smallest value of N needed for a measurement is given by:

$$N \geq N_{\text{meas}} = \frac{1}{2\left(\frac{d\tilde{T}}{d\theta}\theta_0\right)^2} \tag{H29}$$

We see that for the same $d\tilde{T}/d\theta$, the measurement rate for the coherent state input is less than or equal to that in the Fock state case– there is more noise in the coherent state case, hence the measurement proceeds more slowly.

b. Measurement induced dephasing

We again wish to calculate the wavefunction overlap in Eq. (H16). Using $|\alpha|^2 = N$, we have simply:

$$|\langle\psi^-|\psi^+\rangle| = \left|\exp\left(-N\left[1-\sqrt{\tilde{R}_-\tilde{R}_+}e^{i(\eta_+-\eta_-)}e^{i(\beta_+-\beta_-)}-\sqrt{\tilde{T}_-\tilde{T}_+}e^{i(\eta_+-\eta_-)}e^{i(\phi_+-\phi_-)}\right]\right)\right| \tag{H30}$$

Expanding terms inside the exponential to order θ_0^2, we find for the dephasing "rate" $1/N_\varphi$:

$$\frac{1}{N_\varphi} = (\theta_0)^2 \left[\left(\frac{d\tilde{T}}{d\theta} \right)^2 \frac{1}{2\tilde{T}\tilde{R}} + 2\tilde{T}_0 \left(\frac{d\lambda_T}{d\theta} \right)^2 + 2\tilde{R}_0 \left(\frac{d\lambda_R}{d\theta} \right)^2 \right] \tag{H31}$$

where the phases λ_R and λ_T are (respectively) the total phases of the output in port 1 and port 2:

$$\lambda_R = \eta + \beta \tag{H32}$$
$$\lambda_T = \eta + \phi \tag{H33}$$

We can evaluate this expression to find the simple result:

$$\frac{1}{N_\varphi} = 2R_A\theta_0^2 \tag{H34}$$

Note that the dephasing rate here is not equal to that in the Fock state case (cf. Eq. (H19)), and thus cannot be interpreted in terms of partition noise at the first beam splitter. This is not surprising– as already discussed, there is no partition noise in the case of a coherent state input. Eq. (H34) can instead be simply interpreted in terms of the number fluctuations of the input state. Heuristically, each photon passing the qubit advances its phase by a deterministic amount $2\theta_0$. Similar to the Fock state case, the uncertainty in the number of photons passing the qubit, N_{qb}, directly translates into a phase uncertainty in the qubit (i.e. dephasing). Unlike the Fock state case, the fluctuations of N_{qb} are not given by partition noise, but simply by Poisson statistics:

$$\langle\langle N_{qb}^2 \rangle\rangle = \langle N_{qb} \rangle = R_A N \tag{H35}$$

This leads to an expression for $|\langle e^{i\phi_{qb}} \rangle|$ which is in exact agreement with Eq. (H34).

Turning now to the question of the quantum limit, it is useful to work with Eq. (H31) for the dephasing rate. Note the close analogy to the corresponding expression for N_φ for the Fock state case, Eq. (H19). The first term describes information available in the modulation of $\tilde{T}$ by the qubit, and corresponds precisely to the measurement rate for the Fock state input (cf. Eq. (H15)). In contrast, the second and third terms are precisely the measurement rates associated with detecting the *phase* at, respectively, the "1" and "2" output ports. One notes directly from Eq. (H31) that in general, $N_{\rm meas} > N_\varphi$: the MZI with a coherent state input does not generically reach the quantum limit. As usual, this is due to wasted information in the detector. Interestingly, even if there is no wasted phase information (i.e $\lambda_T = \lambda_R = 0$), one still does not necessarily reach the quantum limit. This is due to the number uncertainty of the input state: the MZI output corresponds to having effectively averaged over input states with different numbers of photons, a procedure which in general results in a loss of information (see Clerk *et al.* (2003) for a discussion of this point).

For simplicity, consider now the case that was ideal for a Fock state input: an MZI with a symmetric second beam splitter, i.e. $T_B = 1/2$. In this case, $\tilde{T}_0 = 1/2$, and the measurement rate is given by its maximal value:

$$\frac{1}{N_{\rm meas}} = 2T_A R_A (\theta_0)^2 \tag{H36}$$

This is identical to the expression in the Fock state case, even though the origin is different (i.e. partition noise versus intrinsic noise in the input state).

For a symmetric second beam splitter, the three terms in the expression for the dephasing rate reduce to:

$$(\theta_0)^2 \left(\frac{d\tilde{T}}{d\theta} \right)^2 \frac{1}{2\tilde{T}\tilde{R}} = \frac{1}{N_{\rm meas}} \tag{H37}$$
$$2\theta_0^2 \tilde{T}_0 \left(\frac{d\lambda_T}{d\theta} \right)^2 = R_A^2 \theta_0^2 \tag{H38}$$
$$2\theta_0^2 \tilde{R}_0 \left(\frac{d\lambda_R}{d\theta} \right)^2 = R_A^2 \theta_0^2 \tag{H39}$$

Combining these to evaluate Eq. (H31), we find again:

$$\frac{1}{N_\varphi} = \frac{1}{N_{\rm meas}} + 2R_A^2 (\theta_0)^2 = 2R_A\theta_0^2 \tag{H40}$$

This yields an alternate interpretation for Eq. (H34) as a sum of measurement rates. It also demonstrates that *even* with a symmetric second beam splitter, the MZI detector with a coherent state input fails to reach the quantum limit: in general, $N_{\rm meas} > N_\varphi$. In the completely symmetric case, where $T_A = 1/2$ also, the quantum limit is missed by a factor of two. As is clear from the calculation, the reason for this failure is unused information on the state of the qubit available in the *phases* of the two output ports. To approach the quantum limit, one needs to suppress the wasted information in these phases. From Eq. (H39), we see that this requires one to take the limit $R_A \to 0$. In this limit, the amplitude of the wave in the arm containing the qubit is vanishingly small; as a result, the overall measurement rate is also suppressed. Note the sharp difference between the cases of a Fock state input and coherent state input: in the former case, one could reach the quantum limit by simply having $T_A = 1/2$, while in the latter case, one needs to additionally take the limit of a vanishing measurement rate.

4. Symmetric coupling

Our conclusions for the MZI and a coherent state input may seem quite depressing: in order to reach the quantum limit, one must have a highly asymmetric first beam splitter, with the result that the measurement rate is greatly reduced compared to its optimal value. As a final concluding postscript on our discussion of the MZI, we point out that there is another, more practical way to have the MZI with coherent state input reach the quantum limit. Instead of using a highly asymmetric first beam splitter, one can couple the qubit to *both* arms of the interferometer, such that the scattering matrix for the arms is now:

$$s_{\rm arms} \;=\; \begin{pmatrix} ie^{i\theta} & 0 \\ 0 & e^{-i\theta} \end{pmatrix}, \qquad \text{(H41)}$$

where again, $\theta = \pm\theta_0$ depending on the state of the qubit. An analysis identical to that presented above now shows that one reaches the quantum limit for perfectly symmetric beam splitters, meaning that one *also* has an optimal measurement rate. For this coupling, there is no longer any wasted phase information in the output of the interferometer. While this coupling might be difficult to imagine in the qubit case, it can be realized in the case of position detection (see Fig. 21).

APPENDIX I: Using feedback to reach the quantum limit

In Sec. (VII.B), we demonstrated that any two port amplifier whose scattering matrix has $s_{11} = s_{22} = s_{12} = 0$ will fail to reach quantum limit when used as a weakly coupled op-amp; at best, it will miss optimizing the quantum noise constraint of Eq. (6.60) by a factor of two. Reaching the quantum limit thus requires at least one of s_{11}, s_{22} and s_{12} to be non-zero. In this subsection, we demonstrate how this may be done. We show that by introducing a form of negative feedback to the "minimal" amplifier of the previous subsection, one can take advantage of noise correlations to reduce the back-action current noise S_{II} by a factor of two. As a result, one is able to reach the weak-coupling (i.e. op-amp) quantum limit. Note that quantum amplifiers with feedback are also treated in Courty *et al.* (1999); Grassia (1998).

On a heuristic level, we can understand the need for either reflections or reverse gain to reach the quantum limit. A problem with the "minimal" amplifier of the last subsection was that its input impedance was too low in comparison to its noise impedance $Z_{\rm N} \sim Z_a$. From general expression for the input impedance, Eq. (7.7d), we see that having non-zero reverse gain (i.e. $s_{12} \neq 0$) and/or non-zero reflections (i.e. $s_{11} \neq 0$ and/or $s_{22} \neq 0$) could lead to $Z_{\rm in} \gg Z_a$. This is exactly what occurs when feedback is used to reach the quantum limit. Keep in mind that having non-vanishing reverse gain is dangerous: as we discussed earlier, an appreciable non-zero λ_I' can lead to the highly undesirable consequence that the amplifier's input impedance depends on the impedance of the load connected to its output (cf. Eq. (7.6)).

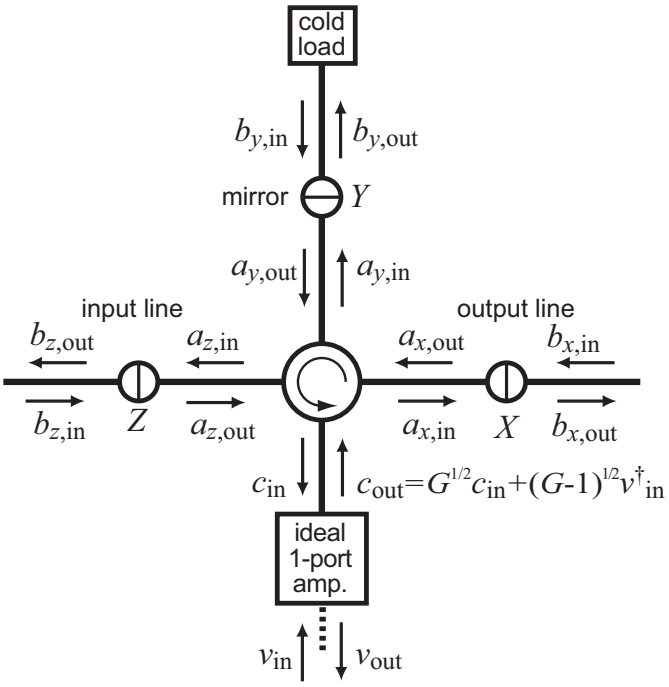

FIG. 22 Schematic of a modified minimal two-port amplifier, where partially reflecting mirrors have been inserted in the input and output transmission lines, as well as in the line leading to the cold load. By tuning the reflection coefficient of the mirror in the cold load arm (mirror Y), we can induce negative feedback which takes advantage of correlations between current and voltage noise. This then allows this system to reach the quantum limit as a weakly coupled voltage op amp. See text for further description

1. Feedback using mirrors

To introduce reverse gain and reflections into the "minimal" two-port bosonic amplifier of the previous subsection, we will insert mirrors in three of the four arms leading from the circulator: the arm going to the input line, the arm going to the output line, and the arm going to the auxiliary "cold load" (Fig. 22). Equivalently, one could imagine that each of these lines is not perfectly impedance matched to the circulator. Each mirror will be described by a 2×2 unitary scattering matrix:

$$\begin{pmatrix} \hat{a}_{j,\rm out} \\ \hat{b}_{j,\rm out} \end{pmatrix} \;=\; U_j \cdot \begin{pmatrix} \hat{b}_{j,\rm in} \\ \hat{a}_{j,\rm in} \end{pmatrix} \qquad \text{(I1)}$$

$$U_j \;=\; \begin{pmatrix} \cos\theta_j & -\sin\theta_j \\ \sin\theta_j & \cos\theta_j \end{pmatrix} \qquad \text{(I2)}$$

Here, the index j can take on three values: $j = z$ for the mirror in the input line, $j = y$ for the mirror in the arm

going to the cold load, and $j = x$ for the mirror in the output line. The mode a_j describes the "internal" mode which exists between the mirror and circulator, while the mode b_j describes the "external" mode on the other side of the mirror. We have taken the U_j to be real for convenience. Note that $\theta_j = 0$ corresponds to the case of no mirror (i.e. perfect transmission).

It is now a straightforward though tedious exercise to construct the scattering matrix for the entire system. From this, one can identify the reduced scattering matrix s appearing in Eq. (7.3), as well as the noise operators $\mathcal{F}_j$. These may then in turn be used to obtain the op-amp description of the amplifier, as well as the commutators of the added noise operators. These latter commutators determine the usual noise spectral densities of the amplifier. Details and intermediate steps of these calculations may be found in Appendix J.5.

As usual, to see if our amplifier can reach the quantum limit when used as a (weakly-coupled) op-amp , we need to see if it optimizes the quantum noise constraint of Eq. (6.60). We consider the optimal situation where both the auxiliary modes of the amplifier ($\hat{u}_{\rm in}$ and $\hat{v}^\dagger_{\rm in}$) are in the vacuum state. The surprising upshot of our analysis (see Appendix J.5) is the following: *if we include a small amount of reflection in the cold load line with the correct phase, then we can reach the quantum limit, irrespective of the mirrors in the input and output lines.* In particular, if $\sin\theta_y = -1/\sqrt{G}$, our amplifier optimizes the quantum noise constraint of Eq. (6.60) in the large gain (i.e. large G) limit, independently of the values of θ_x and θ_y. Note that tuning θ_y to reach the quantum limit does not have a catastrophic impact on other features of our amplifier. One can verify that this tuning only causes the voltage gain λ_V and power gain G_P to decrease by a factor of two compared to their $\theta_y = 0$ values (cf. Eqs. (J55) and (J59)). This choice for θ_y also leads to $Z_{\rm in} \gg Z_a \sim Z_{\rm N}$ (cf. (J57)), in keeping with our general expectations.

Physically, what does this precise tuning of θ_y correspond to? A strong hint is given by the behaviour of the amplifier's cross-correlation noise $\bar{S}_{VI}[\omega]$ (cf. Eq. (J60c)). In general, we find that $\bar{S}_{VI}[\omega]$ is real and non-zero. However, the tuning $\sin\theta_y = -1/\sqrt{G}$ *is exactly what is needed to have* $\bar{S}_{VI}$ *vanish.* Also note from Eq. (J60a) that this special tuning of θ_y decreases the back-action current noise precisely by a factor of two compared to its value at $\theta_y = 0$. A clear physical explanation now emerges. Our original, reflection-free amplifier had correlations between its back-action current noise and output voltage noise (cf. Eq. (7.18c)). By introducing negative feedback of the output voltage to the input current (i.e. via a mirror in the cold-load arm), we are able to use these correlations to decrease the overall magnitude of the current noise (i.e. the voltage fluctuations $\tilde{V}$ partially cancel the original current fluctuations $\tilde{I}$). For an optimal feedback (i.e. optimal choice of θ_y), the current noise is reduced by a half, and the new current noise is not correlated with the output voltage noise. Note that this is indeed negative (as opposed to positive) feedback– it results in a reduction of both the gain and the power gain. To make this explicit, in the next section we will map the amplifier described here onto a standard op-amp with negative voltage feedback.

2. Explicit examples

To obtain a more complete insight, it is useful to go back and consider what the reduced scattering matrix of our system looks like when θ_y has been tuned to reach the quantum limit. From Eq. (J53), it is easy to see that at the quantum limit, the matrix s satisfies:

$$s_{11} = -s_{22} \tag{I3a}$$

$$s_{12} = \frac{1}{G} s_{21} \tag{I3b}$$

The second equation also carries over to the op-amp picture; at the quantum limit, one has:

$$\lambda'_I = \frac{1}{G}\lambda_V \tag{I4}$$

One particularly simple limit is the case where there are no mirrors in the input and output line ($\theta_x = \theta_z = 0$), only a mirror in the cold-load arm. When this mirror is tuned to reach the quantum limit (i.e. $\sin\theta_y = -1/\sqrt{G}$), the scattering matrix takes the simple form:

$$s = \begin{pmatrix} 0 & 1/\sqrt{G} \\ \sqrt{G} & 0 \end{pmatrix} \tag{I5}$$

In this case, the principal effect of the weak mirror in the cold-load line is to introduce a small amount of reverse gain. The amount of this reverse gain is exactly what is needed to have the input impedance diverge (cf. Eq. (7.7d)). It is also what is needed to achieve an optimal, noise-canceling feedback in the amplifier. To see this last point explicitly, we can re-write the amplifier's back-action current noise ($\tilde{I}$) in terms of its original noises $\tilde{I}_0$ and $\tilde{V}_0$ (i.e. what the noise operators would have been in the absence of the mirror). Taking the relevant limit of small reflection (i.e. $\tilde{r} \equiv \sin\theta_y$ goes to zero as $|G| \to \infty$), we find that the modification of the current noise operator is given by:

$$\tilde{I} \simeq \tilde{I}_0 + \frac{2\sqrt{G}\tilde{r}}{1-\sqrt{G}\tilde{r}} \frac{\tilde{V}_0}{Z_a} \tag{I6}$$

As claimed, the presence of a small amount of reflection $\tilde{r} \equiv \sin\theta_y$ in the cold load arm "feeds-back" the original voltage noise of the amplifier $\tilde{V}_0$ into the current. The choice $\tilde{r} = -1/\sqrt{G}$ corresponds to a negative feedback, and optimally makes use of the fact that $\tilde{I}_0$ and $\tilde{V}_0$ are correlated to reduce the overall fluctuations in $\tilde{I}$.

While it is interesting to note that one can reach the quantum limit with no reflections in the input and output arms, this case is not really of practical interest. The

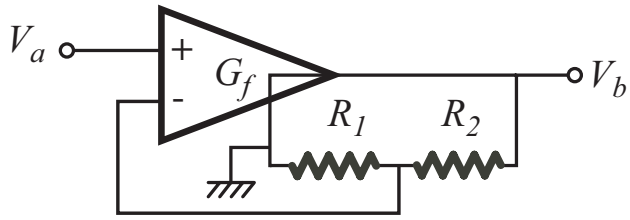

FIG. 23 Schematic of a voltage op-amp with negative feedback.

reverse current gain in this case may be small (i.e. $\lambda_I' \propto 1/\sqrt{G}$), but it is not small enough: one finds that because of the non-zero λ_I', the amplifier's input impedance is strongly reduced in the presence of a load (cf. Eq. (7.6)).

There is a second simple limit we can consider which is more practical. This is the limit where reflections in the input-line mirror and output-line mirror are both strong. Imagine we take $\theta_z = -\theta_x = \pi/2 - \delta/G^{1/8}$. If again we set $\sin\theta_y = -1/\sqrt{G}$ to reach the quantum limit, the scattering matrix now takes the form (neglecting terms which are order $1/\sqrt{G}$):

$$s = \begin{pmatrix} +1 & 0 \\ \frac{\delta^2 G^{1/4}}{2} & -1 \end{pmatrix} \tag{I7}$$

In this case, we see that at the quantum limit, the reflection coefficients s_{11} and s_{22} are exactly what is needed to have the input impedance diverge, while the reverse gain coefficient s_{12} plays no role. For this case of strong reflections in input and output arms, the voltage gain is reduced compared to its zero-reflection value:

$$\lambda_V \to \sqrt{\frac{Z_b}{Z_a}} \left(\frac{\delta}{2}\right)^2 G^{1/4} \tag{I8}$$

The power gain however is independent of θ_x, θ_z, and is still given by $G/2$ when θ_y is tuned to be at the quantum limit.

3. Op-amp with negative voltage feedback

We now show that a conventional op-amp with feedback can be mapped onto the amplifier described in the previous subsection. We will show that tuning the strength of the feedback in the op-amp corresponds to tuning the strength of the mirrors, and that an optimally tuned feedback circuit lets one reach the quantum limit. This is in complete correspondence to the previous subsection, where an optimal tuning of the mirrors also lets one reach the quantum limit.

More precisely, we consider a scattering description of a non-inverting op-amp amplifier having negative voltage feedback. The circuit for this system is shown in Fig. 23. A fraction B of the output voltage of the amplifier is fed back to the negative input terminal of the op-amp. In practice, B is determined by the two resistors R_1 and R_2 used to form a voltage divider at the op-amp output. The op-amp with zero feedback is described by the "ideal" amplifier of Sec. VII.B: at zero feedback, it is described by Eqs. (7.11a)- (7.11d). For simplicity, we consider the relevant case where:

$$Z_b \ll R_1, R_2 \ll Z_a \tag{I9}$$

In this limit, R_1 and R_2 only play a role through the feedback fraction B, which is given by:

$$B = \frac{R_2}{R_1 + R_2} \tag{I10}$$

Letting G_f denote the voltage gain at zero feedback ($B = 0$), an analysis of the circuit equations for our op-amp system yields:

$$\lambda_V = \frac{G_f}{1 + B \cdot G_f} \tag{I11a}$$

$$\lambda_I' = \frac{B}{1 + B \cdot G_f} \tag{I11b}$$

$$Z_{\text{out}} = \frac{Z_b}{1 + B \cdot G_f} \tag{I11c}$$

$$Z_{\text{in}} = (1 + B \cdot G_f) Z_a \tag{I11d}$$

$$G_P = \frac{G_f^2/2}{B \cdot G_f + 2Z_b/Z_a} \tag{I11e}$$

Again, G_f represents the gain of the amplifier in the absence of any feedback, Z_a is the input impedance at zero feedback, and Z_b is the output impedance at zero feedback.

Transforming this into the scattering picture yields a scattering matrix s satisfying:

$$s_{11} = -s_{22} = -\frac{BG_f\,(Z_a - (2 + BG_f)Z_b)}{BG_f Z_a + (2 + BG_f)^2 Z_b} \tag{I12a}$$

$$s_{21} = -\frac{2\sqrt{Z_a Z_b} G_f\,(1 + BG_f)}{BG_f Z_a + (2 + BG_f)^2 Z_b} \tag{I12b}$$

$$s_{12} = \frac{B}{G_f} s_{21} \tag{I12c}$$

Note the connection between these equations and the necessary form of a quantum limited s-matrix found in the previous subsection.

Now, given a scattering matrix, one can always find a minimal representation of the noise operators $\mathcal{F}_a$ and $\mathcal{F}_b$ which have the necessary commutation relations. These are given in general by:

$$\hat{\mathcal{F}}_a = \sqrt{1 - |s_{11}|^2 - |s_{12}|^2 + |l|^2} \cdot \hat{u}_{in} + l \cdot \hat{v}_{in}^\dagger \tag{I13}$$

$$\hat{\mathcal{F}}_b = \sqrt{|s_{21}|^2 + |s_{22}|^2 - 1} \cdot \hat{v}_{in}^\dagger \tag{I14}$$

$$l = \frac{s_{11} s_{21}^* + s_{12} s_{22}^*}{\sqrt{|s_{21}|^2 + |s_{22}|^2 - 1}} \tag{I15}$$

Applying this to the s matrix for our op-amp, and then taking the auxiliary modes $\hat{u}_{\text{in}}$ and $\hat{v}_{\text{in}}^\dagger$ to be in the vacuum state, we can calculate the minimum allowed $\bar{S}_{VV}$

and $\bar{S}_{II}$ for our non-inverting op-amp amplifier. One can then calculate the product $\bar{S}_{VV}\bar{S}_{II}$ and compare against the quantum-limited value ($\bar{S}_{IV}$ is again real). In the case of zero feedback (i.e. $B = 0$), one of course finds that this product is twice as big as the quantum limited value. However, if one takes the large G_f limit while keeping B non-zero but finite, one obtains:

$$\bar{S}_{VV}\bar{S}_{II} \;\rightarrow\; (\hbar\omega)^2\left(1 - \frac{2B}{G_f} + O\left(\frac{1}{G_f}\right)^2\right) \quad \text{(I16)}$$

Thus, for a fixed, non-zero feedback ratio B, it is possible to reach the quantum limit. Note that if B does not tend to zero as G_f tends to infinity, the voltage gain of this amplifier will be finite. The power gain however will be proportional to G_f and will be large. If one wants a large voltage gain, one could set B to go to zero with G_f i.e. $B \propto \frac{1}{\sqrt{G_f}}$. In this case, one will still reach the quantum limit in the large G_f limit, and the voltage gain will also be large (i.e. $\propto \sqrt{G_f}$). Note that in all these limits, the reflection coefficients s_{11} and s_{22} tend to -1 and 1 respectively, while the reverse gain tends to 0. This is in complete analogy to the amplifier with mirrors considered in the previous subsection, in the case where we took the reflections to be strong at the input and at the output (cf. Eq. (I7)). We thus see yet again how the use of feedback allows the system to reach the quantum limit.

APPENDIX J: Additional Technical Details

This appendix provides further details of calculations presented in the main text.

1. Proof of Quantum Noise Constraint

Note first that we may write the symmetrized $\hat{I}$ and $\hat{F}$ noise correlators defined in Eqs. (5.4a) and (5.4b) as sums over transitions between detector energy eigenstates:

$$\bar{S}_{FF}[\omega] \;=\; \pi\hbar\sum_{i,f}\langle i|\hat{\rho}_0|i\rangle\cdot|\langle f|\hat{F}|i\rangle|^2\left[\delta(E_f - E_i + \hbar\omega) + \delta(E_f - E_i - \hbar\omega)\right] \quad \text{(J1)}$$

$$\bar{S}_{II}[\omega] \;=\; \pi\hbar\sum_{i,f}\langle i|\hat{\rho}_0|i\rangle\cdot|\langle f|\hat{I}|i\rangle|^2\left[\delta(E_f - E_i + \hbar\omega) + \delta(E_f - E_i - \hbar\omega)\right] \quad \text{(J2)}$$

Here, $\hat{\rho}_0$ is the stationary density matrix describing the state of the detector, and $|i\rangle$ ($|f\rangle$) is a detector energy eigenstate with energy E_i (E_f). Eq. (J1) expresses the noise at frequency ω as a sum over transitions. Each transition starts with an an initial detector eigenstate $|i\rangle$, occupied with a probability $\langle i|\rho_0|i\rangle$, and ends with a final detector eigenstate $|f\rangle$, where the energy difference between the two states is either $+\hbar\omega$ or $-\hbar\omega$. Further, each transition is weighted by an appropriate matrix element.

To proceed, we fix the frequency $\omega > 0$, and let the index ν label each transition $|i\rangle \rightarrow |f\rangle$ contributing to the noise. More specifically, ν indexes each ordered pair of detector energy eigenstates states $\{|i\rangle, |f\rangle\}$ which satisfy $E_f - E_i \in \pm\hbar[\omega, \omega + d\omega]$ and $\langle i|\rho_0|i\rangle \neq 0$. We can now consider the matrix elements of $\hat{I}$ and $\hat{F}$ which contribute to $\bar{S}_{II}[\omega]$ and $\bar{S}_{FF}[\omega]$ to be complex vectors $\vec{v}$ and $\vec{w}$. Letting δ be any real number, let us define:

$$[\vec{w}]_\nu \;=\; \langle f(\nu)|\hat{F}|i(\nu)\rangle \quad \text{(J3)}$$

$$[\vec{v}]_\nu \;=\; \begin{cases} e^{-i\delta}\langle f(\nu)|\hat{I}|i(\nu)\rangle & \text{if } E_{f(\nu)} - E_{i(\nu)} = +\hbar\omega, \\ e^{i\delta}\langle f(\nu)|\hat{I}|i(\nu)\rangle & \text{if } E_{f(\nu)} - E_{i(\nu)} = -\hbar\omega. \end{cases} \quad \text{(J4)}$$

Introducing an inner product $\langle\cdot,\cdot\rangle_\omega$ via:

$$\langle\vec{a},\vec{b}\rangle_\omega = \pi\sum_\nu\langle i(\nu)|\hat{\rho}_0|i(\nu)\rangle\cdot(a_\nu)^*\,b_\nu, \quad \text{(J5)}$$

we see that the noise correlators $\bar{S}_{II}$ and $\bar{S}_{FF}$ may be written as:

$$\bar{S}_{II}[\omega]d\omega \;=\; \langle\vec{v},\vec{v}\rangle_\omega \quad \text{(J6)}$$

$$\bar{S}_{FF}[\omega]d\omega \;=\; \langle\vec{w},\vec{w}\rangle_\omega \quad \text{(J7)}$$

We may now employ the Cauchy-Schwartz inequality:

$$\langle\vec{v},\vec{v}\rangle_\omega\langle\vec{w},\vec{w}\rangle_\omega \geq |\langle\vec{v},\vec{w}\rangle_\omega|^2 \quad \text{(J8)}$$

A straightforward manipulation shows that the real part of $\langle\vec{v},\vec{w}\rangle_\omega$ is determined by the symmetrized cross-correlator $\bar{S}_{IF}[\omega]$ defined in Eq. (5.4c):

$$\text{Re}\,\langle\vec{v},\vec{w}\rangle_\omega = \text{Re}\,\left[e^{i\delta}\bar{S}_{IF}[\omega]\right]d\omega \quad \text{(J9)}$$

In contrast, the imaginary part of $\langle\vec{v},\vec{w}\rangle_\omega$ is independent of $\bar{S}_{IF}$; instead, it is directly related to the gain λ and reverse gain λ' of the detector:

$$\text{Im}\,\langle\vec{v},\vec{w}\rangle_\omega = \frac{\hbar}{2}\text{Re}\,\left[e^{i\delta}\left(\lambda[\omega] - [\lambda'[\omega]]^*\right)\right]d\omega \quad \text{(J10)}$$

Substituting Eqs. (J10) and (J9) into Eq. (J8), one immediately finds the quantum noise constraint given in Eq. (5.15). Maximizing the RHS of this inequality with respect to the phase δ, one finds that the maximum is achieved for $\delta = \delta_0 = -\arg(\lambda) + \tilde{\delta}_0$ with (we assume the ideal case where $\lambda' = 0$):

$$\tan 2\tilde{\delta}_0 = -\frac{|\bar{S}_{IF}| \sin 2\phi}{|\hbar\lambda/2| + |\bar{S}_{IF}| \cos 2\phi} \tag{J11}$$

where $\phi = \arg(\bar{S}_{IF}\lambda^*)$. At $\delta = \delta_0$, Eq. (5.15) becomes the final noise constraint of Eq. (5.11).

The proof given here also allows one to see what must be done in order to achieve the "ideal" noise condition of Eq. (5.16): one must achieve equality in the Cauchy-Schwartz inequality of Eq. (J8). This requires that the vectors $\vec{v}$ and $\vec{w}$ be proportional to one another; there must exist a complex factor α (having dimensions $[I]/[F]$) such that:

$$\vec{v} = \alpha \cdot \vec{w} \tag{J12}$$

Equivalently, we have that

$$\langle f|I|i\rangle = \begin{cases} e^{i\delta}\alpha\langle f|F|i\rangle & \text{if } E_f - E_i = +\hbar\omega \\ e^{-i\delta}\alpha\langle f|F|i\rangle & \text{if } E_f - E_i = -\hbar\omega. \end{cases} \tag{J13}$$

for *each* pair of initial and final states $|i\rangle$, $|f\rangle$ contributing to $\bar{S}_{FF}[\omega]$ and $\bar{S}_{II}[\omega]$ (cf. Eq. (J1)). Note that this *not* the same as requiring Eq. (J13) to hold for all possible states $|i\rangle$ and $|f\rangle$. This proportionality condition tells us that a detector with ideal noise properties has a tight connection between its input and output ports; in Clerk *et al.* (2003), this condition was directly tied to the idea that there is no "wasted" information in a quantum-limited detector, an idea that we have discussed in Sec. IV.B and Appendix H.

Finally, for a detector with quantum-ideal noise properties, the magnitude of the constant α can be found from Eq. (5.17). The phase of α can also be determined from:

$$\frac{-\text{Im } \alpha}{|\alpha|} = \frac{\hbar|\lambda|/2}{\sqrt{\bar{S}_{II}\bar{S}_{FF}}} \cos\tilde{\delta}_0 \tag{J14}$$

For zero frequency or for a large detector effective temperature, this simplifies to:

$$\frac{-\text{Im } \alpha}{|\alpha|} = \frac{\hbar\lambda/2}{\sqrt{\bar{S}_{II}\bar{S}_{FF}}} \tag{J15}$$

Note importantly that to have a non-vanishing gain and power gain, one needs Im $\alpha \neq 0$. This in turn places a very powerful constraint on a quantum-ideal detectors: *all transitions contributing to the noise must be to final states $|f\rangle$ which are completely unoccupied.* To see this, imagine a transition taking an initial state $|i\rangle = |a\rangle$ to a final state $|f\rangle = |b\rangle$ makes a contribution to the noise. For a quantum-ideal detector, Eq. (J13) will be satisfied:

$$\langle b|\hat{I}|a\rangle = e^{\pm i\delta}\alpha\langle b|\hat{F}|a\rangle \tag{J16}$$

where the plus sign corresponds to $E_b > E_a$, the minus to $E_a > E_b$. If now the final state $|b\rangle$ was also occupied (i.e. $\langle b|\hat{\rho}_0|b\rangle \neq 0$), then the reverse transition $|i = b\rangle \to |f = a\rangle$) would also contribute to the noise. The proportionality condition of Eq. (J13) would now require:

$$\langle a|\hat{I}|b\rangle = e^{\mp i\delta}\alpha\langle a|\hat{F}|b\rangle \tag{J17}$$

As $\hat{I}$ and $\hat{F}$ are both Hermitian operators, and as α must have an imaginary part in order for there to be gain, we have a contradiction: Eq. (J16) and (J17) cannot both be true. It thus follows that the final state of a transition contributing to the noise *must* be unoccupied in order for Eq. (J13) to be satisfied and for the detector to have ideal noise properties. Note that this necessary asymmetry in the occupation of detector energy eigenstates immediately tells us that *a detector or amplifier cannot reach the quantum limit if it is in equilibrium.*

2. Simplifications for a Quantum-Limited Detector

In this appendix, we derive the additional constraints on the property of a detector that arise when it satisfies the quantum noise constraint of Eq. (5.16).

We begin by noting that a necessary condition for satisfying Eq. (5.16) is that the inequality of Eq. (5.15) becomes an *equality* for a particular choice of δ. Thus, assume Eq. (5.15) holds as an equality for our detector for some specific value of δ; further, assume the ideal case of a detector with zero reverse gain, $\lambda' = 0$. Using the proportionality condition between the matrix elements of $\hat{I}$ and $\hat{F}$ (cf. Eq (J13)), the *unsymmetrized I-F* quantum noise correlator $S_{IF}[\omega]$ (cf. Eq. (5.7)) may be written:

$$S_{IF}[\omega] = \begin{cases} e^{-i\delta}\alpha^* S_{FF}[\omega] & \text{if } \omega > 0, \\ e^{i\delta}\alpha^* S_{FF}[\omega] & \text{if } \omega < 0 \end{cases} \tag{J18}$$

In the above equation, $S_{FF}[\omega]$ is the unsymmetrized spectral density of the force noise of the detector (cf. Eq. (3.8)); note that $S_{FF}[\omega]$ is necessarily real and positive.

We may now substitute Eq. (J18) into Eqs. (5.8b)-(5.8a); writing $S_{FF}[\omega]$ in terms of the detector effective temperature T_{eff} (cf. Eq. (3.21)):

$$\frac{\hbar\lambda[\omega]}{2} = -e^{-i\delta}\hbar\left[-\text{Im } \chi_{FF}[\omega]\right] \left[(\text{Im } \alpha)\coth\left(\frac{\hbar\omega}{2k_{\text{B}}T_{\text{eff}}}\right) + i\,(\text{Re } \alpha)\right] \tag{J19}$$

$$\bar{S}_{IF}[\omega] = e^{-i\delta}\hbar\left[-\text{Im } \chi_{FF}[\omega]\right] \left[(\text{Re } \alpha)\coth\left(\frac{\hbar\omega}{2k_{\text{B}}T_{\text{eff}}}\right) - i\,(\text{Im } \alpha)\right] \tag{J20}$$

To proceed, let us write:

$$e^{-i\delta} = \frac{\lambda}{|\lambda|}e^{-i\tilde{\delta}} \tag{J21}$$

The condition that $|\lambda|$ is real yields the condition:

$$\tan\tilde{\delta} = \frac{\text{Re }\alpha}{\text{Im}\alpha}\tanh\left(\frac{\hbar\omega}{2k_{\rm B}T_{\rm eff}}\right) \tag{J22}$$

We now consider the relevant limit of a large detector power gain G_P. G_P is determined by Eq. (6.28); the only way this can become large is if $k_{\rm B}T_{\rm eff}/(\hbar\omega)\to\infty$ while Im α does not tend to zero. We will thus take the large $T_{\rm eff}$ limit in the above equations while keeping both α and the phase of λ fixed. Note that this means the parameter $\tilde{\delta}$ must evolve; it tends to zero in the large $T_{\rm eff}$ limit. In this limit, we thus find for λ and $\bar{S}_{IF}$:

$$\frac{\hbar\lambda[\omega]}{2} = -2e^{-i\delta}k_{\rm B}T_{\rm eff}\gamma[\omega]\,(\text{Im }\alpha)\left[1+O\left[\left(\frac{\hbar\omega}{k_{\rm B}T_{\rm eff}}\right)^2\right]\right] \tag{J23}$$

$$\bar{S}_{IF}[\omega] = 2e^{-i\delta}k_{\rm B}T_{\rm eff}\gamma[\omega]\,(\text{Re }\alpha)\left[1+O\left(\frac{\hbar\omega}{k_{\rm B}T_{\rm eff}}\right)\right] \tag{J24}$$

Thus, in the large power-gain limit (i.e. large $T_{\rm eff}$ limit), the gain λ and the noise cross-correlator $\bar{S}_{IF}$ have the same phase: $\bar{S}_{IF}/\lambda$ is purely real.

3. Derivation of non-equilibrium Langevin equation

In this appendix, we prove that an oscillator weakly coupled to an arbitrary out-of-equilibrium detector is described by the Langevin equation given in Eq. (6.14), an equation which associates an effective temperature and damping kernel to the detector.

We start by defining the oscillator matrix Keldysh green function:

$$\check{G}(t) = \begin{pmatrix} G^K(t) & G^R(t) \\ G^A(t) & 0 \end{pmatrix} \tag{J25}$$

where $G^R(t-t') = -i\theta(t-t')\langle[\hat{x}(t),\hat{x}(t')]\rangle$, $G^A(t-t') = i\theta(t'-t)\langle[\hat{x}(t),\hat{x}(t')]\rangle$, and $G^K(t-t') = -i\langle\{\hat{x}(t),\hat{x}(t')\}\rangle$. At zero coupling to the detector ($A=0$), the oscillator is only coupled to the equilibrium bath, and thus $\check{G}_0$ has the standard equilibrium form:

$$\check{G}_0[\omega] = \frac{\hbar}{m}\begin{pmatrix} -2\text{Im }g_0[\omega]\coth\left(\frac{\hbar\omega}{2k_{\rm B}T_{\rm bath}}\right) & g_0[\omega] \\ g_0[\omega]^* & 0 \end{pmatrix} \tag{J26}$$

where:

$$g_0[\omega] = \frac{1}{\omega^2-\Omega^2+i\omega\gamma_0/m} \tag{J27}$$

and where γ_0 is the intrinsic damping coefficient, and $T_{\rm bath}$ is the bath temperature.

We next treat the effects of the coupling to the detector in perturbation theory. Letting $\check{\Sigma}$ denote the corresponding self-energy, the Dyson equation for $\check{G}$ has the form:

$$\left[\check{G}[\omega]\right]^{-1} = \left[\check{G}_0[\omega]\right]^{-1} - \begin{pmatrix} 0 & \Sigma^A[\omega] \\ \Sigma^R[\omega] & \Sigma^K[\omega] \end{pmatrix} \tag{J28}$$

To lowest order in A, $\check{\Sigma}[\omega]$ is given by:

$$\check{\Sigma}[\omega] = A^2\check{D}[\omega] \tag{J29}$$

$$\equiv \frac{A^2}{\hbar}\int dt\; e^{i\omega t} \begin{pmatrix} 0 & i\theta(-t)\langle[\hat{F}(t),\hat{F}(0)]\rangle \\ -i\theta(t)\langle[\hat{F}(t),\hat{F}(0)]\rangle & -i\langle\{\hat{F}(t),\hat{F}(0)\}\rangle \end{pmatrix} \tag{J30}$$

Using this lowest-order self energy, Eq. (J28) yields:

$$G^R[\omega] = \frac{\hbar}{m(\omega^2-\Omega^2) - A^2\text{Re }D^R[\omega] + i\omega(\gamma_0+\gamma[\omega])} \tag{J31}$$

$$G^A[\omega] = \left[G^R[\omega]\right]^* \tag{J32}$$

$$G^K[\omega] = -2i\text{Im }G^R[\omega]\times \frac{\gamma_0\coth\left(\frac{\hbar\omega}{2k_{\rm B}T_{\rm bath}}\right)+\gamma[\omega]\coth\left(\frac{\hbar\omega}{2k_{\rm B}T_{\rm eff}}\right)}{\gamma_0+\gamma[\omega]} \tag{J33}$$

where $\gamma[\omega]$ is given by Eq. (3.25), and $T_{\rm eff}[\omega]$ is defined by Eq. (3.21). The main effect of the real part of the retarded $\hat{F}$ Green function $D^R[\omega]$ in Eq. (J31) is to renormalize the oscillator frequency Ω and mass m; we simply incorporate these shifts into the definition of Ω and m in what follows.

If $T_{\rm eff}[\omega]$ is frequency independent, then Eqs. (J31) - (J33) for $\check{G}$ corresponds exactly to an oscillator coupled to two equilibrium baths with damping kernels γ_0 and $\gamma[\omega]$. The correspondence to the Langevin equation Eq. (6.14) is then immediate. In the more general case where $T_{\rm eff}[\omega]$ has a frequency dependence, the correlators $G^R[\omega]$ and $G^K[\omega]$ are in exact correspondence to what is found from the Langevin equation Eq. (6.14): $G^K[\omega]$ corresponds to symmetrized noise calculated from Eq. (6.14), while $G^R[\omega]$ corresponds to the response coefficient of the oscillator calculated from Eq. (6.14). This again proves the validity of using the Langevin equation Eq. (6.14) to calculate the oscillator noise in the presence of the detector to lowest order in A.

4. Linear-Response Formulas for a Two-Port Bosonic Amplifier

In this appendix, we use the standard linear-response Kubo formulas of Sec. VI.E to derive expressions for the voltage gain λ_V, reverse current gain λ_I', input impedance Z_{in} and output impedance Z_{out} of a two-port

bosonic voltage amplifier (cf. Sec. VII). We recover the same expressions for these quantities obtained in Sec. VII from the scattering approach. We stress throughout this appendix the important role played by the causal structure of the scattering matrix describing the amplifier.

In applying the general linear response formulas, we must bear in mind that these expressions should be applied to the *uncoupled* detector, i.e. nothing attached to the detector input or output. In our two-port bosonic voltage amplifier, this means that we should have a short circuit at the amplifier input (i.e. no input voltage, $V_a = 0$), and we should have open circuit at the output (i.e. $I_b = 0$, no load at the output drawing current). These two conditions define the uncoupled amplifier. Using the definitions of the voltage and current operators (cf. Eqs. (7.2a) and (7.2b)), they take the form:

$$\hat{a}_{\rm in}[\omega] = -\hat{a}_{\rm out}[\omega] \tag{J34a}$$

$$\hat{b}_{\rm in}[\omega] = \hat{b}_{\rm out}[\omega] \tag{J34b}$$

The scattering matrix equation Eq. (7.3) then allows us to solve for $\hat{a}_{in}$ and $\hat{a}_{out}$ in terms of the added noise operators $\hat{\mathcal{F}}_a$ and $\hat{\mathcal{F}}_b$.

$$\hat{a}_{\rm in}[\omega] = -\frac{1-s_{22}}{D}\hat{\mathcal{F}}_a[\omega] - \frac{s_{12}}{D}\hat{\mathcal{F}}_b[\omega] \tag{J35a}$$

$$\hat{b}_{\rm in}[\omega] = -\frac{s_{21}}{D}\hat{\mathcal{F}}_a[\omega] + \frac{1+s_{11}}{D}\hat{\mathcal{F}}_b[\omega] \tag{J35b}$$

where D is given in Eq. (7.8), and we have omitted writing the frequency dependence of the scattering matrix. Further, as we have already remarked, the commutators of the added noise operators is completely determined by the scattering matrix and the constraint that output operators have canonical commutation relations. The non-vanishing commutators are thus given by:

$$\left[\hat{\mathcal{F}}_a[\omega], \hat{\mathcal{F}}_a^\dagger(\omega')\right] = 2\pi\delta(\omega-\omega')\left(1-|s_{11}|^2-|s_{12}|^2\right) \tag{J36a}$$

$$\left[\hat{\mathcal{F}}_b[\omega], \hat{\mathcal{F}}_b^\dagger(\omega')\right] = 2\pi\delta(\omega-\omega')\left(1-|s_{21}|^2-|s_{22}|^2\right) \tag{J36b}$$

$$\left[\hat{\mathcal{F}}_a[\omega], \hat{\mathcal{F}}_b^\dagger(\omega')\right] = -2\pi\delta(\omega-\omega')\left(s_{11}s_{21}^* + s_{12}s_{22}^*\right) \tag{J36c}$$

The above equations, used in conjunction with Eqs. (7.2a) and (7.2b), provide us with all all the information needed to calculate commutators between current and voltage operators. It is these commutators which enter into the linear-response Kubo formulas. As we will see, our calculation will crucially rely on the fact that the scattering description obeys causality: disturbances at the input of our system must take some time before they propagate to the output. Causality manifests itself in the energy dependence of the scattering matrix: as a function of energy, it is an analytic function in the upper half complex plane.

a. Input and output impedances

Eq. (6.56) is the linear response Kubo formula for the input impedance of a voltage amplifier. Recall that the input operator $\hat{Q}$ for a voltage amplifier is related to the input current operator $\hat{I}_a$ via $-d\hat{Q}/dt = \hat{I}_a$ (cf. Eq. (6.55)). The Kubo formula for the input impedance may thus be re-written in the more familiar form:

$$Y_{\rm in,Kubo}[\omega] \equiv \frac{i}{\omega}\left(-\frac{i}{\hbar}\int_0^\infty dt\langle[\hat{I}_a(t),\hat{I}_a(0)]\rangle e^{i\omega t}\right) \tag{J37}$$

where $Y_{\rm in}[\omega] = 1/Z_{\rm in}[\omega]$,

Using the defining equation for $\hat{I}_a$ (Eq. (7.1b)) and Eq. (J34a) (which describes an uncoupled amplifier), we obtain:

$$Y_{\rm in,Kubo}[\omega] = \frac{2}{Z_a}\int_0^\infty dt e^{i\omega t}\int_0^\infty \frac{d\omega'}{2\pi}\frac{\omega'}{\omega}\Lambda_{aa}(\omega')\left(e^{-i\omega' t}-e^{i\omega' t}\right) \tag{J38}$$

where we have defined the real function $\Lambda_{aa}[\omega]$ for $\omega > 0$ via:

$$\left[\hat{a}_{\rm in}[\omega], \hat{a}_{\rm in}^\dagger(\omega')\right] = 2\pi\delta(\omega-\omega')\Lambda_{aa}[\omega] \tag{J39}$$

It will be convenient to also define $\Lambda_{aa}[\omega]$ for $\omega < 0$ via $\Lambda_{aa}[\omega] = \Lambda_{aa}[-\omega]$. Eq. (J38) may then be written as:

$$\begin{aligned} Y_{\rm in,Kubo}[\omega] &= \frac{2}{Z_a}\int_0^\infty dt\int_{-\infty}^\infty \frac{d\omega'}{2\pi}\frac{\omega'}{\omega}\Lambda_{aa}(\omega')e^{i(\omega-\omega')t} \\ &= \frac{\Lambda_{aa}[\omega]}{Z_a} + \frac{i}{\pi\omega}\mathcal{P}\int_{-\infty}^\infty d\omega'\frac{\omega'\Lambda_{aa}(\omega')/Z_a}{\omega-\omega'} \end{aligned} \tag{J40}$$

Next, by making use of Eq. (J35a) and Eqs. (J36) for the commutators of the added noise operators, we can explicitly evaluate the commutator in Eq. (J39) to calculate $\Lambda_{aa}[\omega]$. Comparing the result against the result Eq. (7.7d) of the scattering calculation, we find:

$$\frac{\Lambda_{aa}[\omega]}{Z_a} = \text{Re } Y_{\rm in,scatt}[\omega] \tag{J41}$$

where $Y_{\rm in,scatt}[\omega]$ is the input admittance of the amplifier obtained from the scattering approach. Returning to Eq. (J40), we may now use the fact that $Y_{in,scatt}[\omega]$ is an analytic function in the upper half plane to simplify the second term on the RHS, as this term is simply a Kramers-Kronig integral:

$$\begin{aligned} &\frac{1}{\pi\omega}\mathcal{P}\int_{-\infty}^\infty d\omega'\frac{\omega'\Lambda_{aa}(\omega')/Z_a}{\omega-\omega'} \\ &= \frac{1}{\pi\omega}\mathcal{P}\int_{-\infty}^\infty d\omega'\frac{\omega'\text{Re } Y_{\rm in,scatt}(\omega')}{\omega-\omega'} \\ &= \text{Im } Y_{\rm in,scatt}[\omega] \end{aligned} \tag{J42}$$

It thus follows from Eq. (J40) that input impedance calculated from the Kubo formula is equal to what we found previously using the scattering approach.

The calculation for the output impedance proceeds in the same fashion, starting from the Kubo formula given in Eq. (6.57). As the steps are completely analogous to the above calculation, we do not present it here. One again recovers Eq. (7.7c), as found previously within the scattering approach.

b. Voltage gain and reverse current gain

Within linear response theory, the voltage gain of the amplifier (λ_V) is determined by the commutator between the "input operator" $\hat{Q}$ and $\hat{V}_b$ (cf. Eq. (5.3); recall that $\hat{Q}$ is defined by $d\hat{Q}/dt = -\hat{I}_a$. Similarly, the reverse current gain (λ'_I) is determined by the commutator between $\hat{I}_a$ and $\hat{\Phi}$, where $\hat{\Phi}$ is defined via $d\hat{\Phi}/dt = -\hat{V}_b$ (cf. Eq. (5.6)). Similar to the calculation of the input impedance, to properly evaluate the Kubo formulas for the gains, we must make use of the causal structure of the scattering matrix describing our amplifier.

Using the defining equations of the current and voltage operators (cf. Eqs. (7.1a) and (7.1b)), as well as Eqs. (J34a) and (J34b) which describe the uncoupled amplifier, the Kubo formulas for the voltage gain and reverse current gain become:

$$\lambda_{V,\mathrm{Kubo}}[\omega] = 4\sqrt{\frac{Z_b}{Z_a}} \times \int_0^\infty dt\; e^{i\omega t}\mathrm{Re}\left[\int_0^\infty \frac{d\omega'}{2\pi}\Lambda_{ba}(\omega')e^{-i\omega' t}\right] \tag{J43}$$

$$\lambda'_{I,\mathrm{Kubo}}[\omega] = -4\sqrt{\frac{Z_b}{Z_a}} \times \int_0^\infty dt\; e^{i\omega t}\mathrm{Re}\left[\int_0^\infty \frac{d\omega'}{2\pi}\Lambda_{ba}(\omega')e^{i\omega' t}\right] \tag{J44}$$

where we define the complex function $\Lambda_{ba}[\omega]$ for $\omega > 0$ via:

$$\left[\hat{b}_{in}[\omega], \hat{a}^\dagger_{in}(\omega')\right] \equiv (2\pi\delta(\omega-\omega'))\,\Lambda_{ba}[\omega] \tag{J45}$$

We can explicitly evaluate $\Lambda_{ba}[\omega]$ by using Eqs. (J35a)-(J36) to evaluate the commutator above. Comparing the result against the scattering approach expressions for the gain and reverse gain (cf. Eqs. (7.7a) and (7.7b)), one finds:

$$\Lambda_{ba}[\omega] = \lambda_{V,\mathrm{scatt}}[\omega] - \left[\lambda'_{I,\mathrm{scatt}}[\omega]\right]^* \tag{J46}$$

Note crucially that the two terms above have different analytic properties: the first is analytic in the upper half plane, while the second is analytic in the lower half plane. This follows directly from the fact that the scattering matrix is causal.

At this stage, we can proceed much as we did in the calculation of the input impedance. Defining $\Lambda_{ba}[\omega]$ for $\omega < 0$ via $\Lambda_{ba}[-\omega] = \Lambda^*_{ba}[\omega]$, we can re-write Eqs. (J43) and (J44) in terms of principle part integrals.

$$\begin{aligned}\lambda_{V,\mathrm{Kubo}}[\omega] &= \frac{Z_b}{Z_a}\left(\Lambda_{ba}[\omega] + \frac{i}{\pi}\mathcal{P}\int_{-\infty}^{\infty} d\omega' \frac{\Lambda_{ba}(\omega')}{\omega-\omega'}\right)\\ \lambda'_{I,\mathrm{Kubo}}[\omega] &= -\frac{Z_b}{Z_a}\left(\Lambda_{ba}[\omega] + \frac{i}{\pi}\mathcal{P}\int_{-\infty}^{\infty} d\omega' \frac{\Lambda_{ba}(\omega')}{\omega+\omega'}\right)\end{aligned} \tag{J47}$$

Using the analytic properties of the two terms in Eq. (J46) for $\Lambda_{ba}[\omega]$, we can evaluate the principal part integrals above as Kramers-Kronig relations. One then finds that the Kubo formula expressions for the voltage and current gain coincide precisely with those obtained from the scattering approach.

While the above is completely general, it is useful to go through a simpler, more specific case where the role of causality is more transparent. Imagine that all the energy dependence in the scattering in our amplifier arises from the fact that there are small transmission line "stubs" of length a attached to both the input and output of the amplifier (these stubs are matched to the input and output lines). Because of these stubs, a wavepacket incident on the amplifier will take a time $\tau = 2a/v$ to be either reflected or transmitted, where v is the characteristic velocity of the transmission line. This situation is described by a scattering matrix which has the form:

$$s[\omega] = e^{2i\omega a/v}\cdot\bar{s} \tag{J48}$$

where $\bar{s}$ is frequency-independent and real. To further simplify things, let us assume that $\bar{s}_{11} = \bar{s}_{22} = \bar{s}_{12} = 0$. Eqs. (J46) then simplifies to

$$\Lambda_{ba}[\omega] = \;=\; s_{21}[\omega] = \bar{s}_{21}e^{i\omega\tau} \tag{J49}$$

where the propagation time $\tau = 2a/v$ We then have:

$$\lambda_V[\omega_0] = 2\sqrt{\frac{Z_b}{Z_a}}\bar{s}_{21}\int_0^\infty dt\; e^{i\omega_0 t}\delta(t-\tau) \tag{J50}$$

$$\lambda_I[\omega_0] = -2\sqrt{\frac{Z_b}{Z_a}}\bar{s}_{21}\int_0^\infty dt\; e^{i\omega_0 t}\delta(t+\tau) \tag{J51}$$

If we now do the time integrals and then take the limit $\tau \to 0^+$, we recover the results of the scattering approach (cf. Eqs. (7.7a) and (7.7b)); in particular, $\lambda_I = 0$. Note that if we had set $\tau = 0$ from the outset of the calculation, we would have found that both λ_V and λ_I are non-zero!

5. Details for Two-port Bosonic Voltage Amplifier with Feedback

In this appendix, we provide more details on the calculations for the bosonic-amplifier-plus-mirrors system discussed in Sec. I. Given that the scattering matrix for each of the three mirrors is given by Eq. (I2), and that we know the reduced scattering matrix for the mirror-free

system (cf. Eq. (7.10)), we can find the reduced scattering matrix and noise operators for the system with mirrors. One finds that the reduced scattering matrix s is now given by:

$$s = \frac{1}{M} \times \begin{pmatrix} \sin\theta_z + \sqrt{G}\sin\theta_x\sin\theta_y & -\cos\theta_x\cos\theta_z\sin\theta_y \\ \sqrt{G}\cos\theta_x\cos\theta_z & \sin\theta_x + \sqrt{G}\sin\theta_y\sin\theta_z \end{pmatrix} \tag{J52}$$

where the denominator M describes multiple reflection processes:

$$M = 1 + \sqrt{G}\sin\theta_x\sin\theta_z\sin\theta_y \tag{J53}$$

Further, the noise operators are given by:

$$\begin{pmatrix} \mathcal{F}_a \\ \mathcal{F}_b \end{pmatrix} = \frac{1}{M} \begin{pmatrix} \cos\theta_y\cos\theta_z & \sqrt{G-1}\cos\theta_z\sin\theta_x\sin\theta_y \\ -\sqrt{G}\cos\theta_x\cos\theta_y\sin\theta_z & \sqrt{G-1}\cos\theta_x \end{pmatrix} \begin{pmatrix} u_{in} \\ v_{in}^\dagger \end{pmatrix} \tag{J54}$$

The next step is to convert the above into the op-amp representation, and find the gains and impedances of the amplifier, along with the voltage and current noises. The voltage gain is given by:

$$\lambda_V = \sqrt{\frac{Z_B}{Z_A}} \frac{2\sqrt{G}}{1-\sqrt{G}\sin\theta_y} \cdot \frac{1+\sin\theta_x}{\cos\theta_x} \frac{1-\sin\theta_z}{\cos\theta_z} \tag{J55}$$

while the reverse gain is related to the voltage gain by the simple relation:

$$\lambda_I' = -\frac{\sin\theta_y}{\sqrt{G}}\lambda_V \tag{J56}$$

The input impedance is determined by the amount of reflection in the input line and in the line going to the cold load:

$$Z_{\rm in} = Z_a \frac{1-\sqrt{G}\sin\theta_y}{1+\sqrt{G}\sin\theta_y} \cdot \frac{1+\sin\theta_z}{1-\sin\theta_z} \tag{J57}$$

Similarly, the output impedance only depends on the amount of reflection in the output line and the in the cold-load line:

$$Z_{\rm out} = Z_b \frac{1+\sqrt{G}\sin\theta_y}{1-\sqrt{G}\sin\theta_y} \cdot \frac{1+\sin\theta_x}{1-\sin\theta_x} \tag{J58}$$

Note that as $\sin\theta_y$ tends to $-1/\sqrt{G}$, both the input admittance and output impedance tend to zero.

Given that we now know the op-amp parameters of our amplifier, we can use Eq. (7.5) to calculate the amplifier's power gain G_P. Amazingly, we find that the power gain is completely independent of the mirrors in the input and output lines:

$$G_P = \frac{G}{1+G\sin^2\theta_y} \tag{J59}$$

Note that at the special value $\sin\theta_y = -1\sqrt{G}$ (which allows one to reach the quantum limit), the power gain is reduced by a factor of two compared to the reflection free case (i.e. $\theta_y = 0$).

Turning to the noise spectral densities, we assume the optimal situation where both the auxiliary modes $\hat{u}_{in}$ and $\hat{v}_{in}^\dagger$ are in the vacuum state. We then find that both $\hat{\tilde{I}}$ and $\hat{\tilde{V}}$ are independent of the amount of reflection in the output line (e.g. θ_x):

$$\bar{S}_{II} = \frac{2\hbar\omega}{Z_a}\left[\frac{1-\sin\theta_z}{1+\sin\theta_z}\right] \times \left(\frac{G\sin^2\theta_y + \cos(2\theta_y)}{\left(\sqrt{G}\sin\theta_y - 1\right)^2}\right) \tag{J60a}$$

$$\bar{S}_{VV} = \hbar\omega Z_a\left[\frac{1+\sin\theta_z}{1-\sin\theta_z}\right] \times \left(\frac{3+\cos(2\theta_y)}{4} - \frac{1}{2G}\right) \tag{J60b}$$

$$\bar{S}_{VI} = \frac{\sqrt{G}(1-1/G)\sin\theta_y + \cos^2\theta_y}{1-\sqrt{G}\sin\theta_y} \tag{J60c}$$

As could be expected, introducing reflections in the input line (i.e. $\theta_z \neq 0$) has the opposite effect on $\bar{S}_{II}$ versus $\bar{S}_{VV}$: if one is enhanced, the other is suppressed.

It thus follows that the product of noise spectral densities appearing in the quantum noise constraint of Eq. (6.60) is given by (taking the large-G limit):

$$\frac{\bar{S}_{II}\bar{S}_{VV}}{(\hbar\omega)^2} = \left(2-\sin^2\theta_y\right) \cdot \frac{1+G\sin^2\theta_y}{\left(1-\sqrt{G}\sin\theta_y\right)^2} \tag{J61}$$

Note that somewhat amazingly, this product (and hence the amplifier noise temperature) is completely independent of the mirrors in the input and output arms (i.e. θ_z and θ_x). This is a result of both $\bar{S}_{VV}$ and $\bar{S}_{II}$ having no dependence on the output mirror (θ_x), and their having opposite dependencies on the input mirror (θ_z). Also note that Eq. (J61) does indeed reduce to the result of

the last subsection: if $\theta_y = 0$ (i.e. no reflections in the line going to the cold load), the product $\bar{S}_{II}\bar{S}_{VV}$ is equal to precisely twice the quantum limit value of $(\hbar\omega)^2$. For $\sin(\theta_y) = -1/\sqrt{G}$, the RHS above reduces to one, implying that we reach the quantum limit for this tuning of the mirror in the cold-load arm.

References

Abramovici, A., W. Althouse, R. Drever, Y. Gursel, S. Kawamura, F. Raab, D. Shoemaker, L. Sievers, R. Spero, K. Thorne, R. Vogt, R. Weiss, *et al.*, 1992, Science **256**, 325.

Aguado, R., and L. P. Kouwenhoven, 2000, Phys. Rev. Lett. **84**, 1986.

Aleiner, I. L., N. S. Wingreen, and Y. Meir, 1997, Phys. Rev. Lett. **79**, 3740.

Allahverdyan, A. E., R. Balian, and T. M. Nieuwenhuizen, 2001, Phys. Rev. A **64**, 032108.

Arcizet, O., P.-F. Cohadon, T. Briant, M. Pinard, and A. Hedimann, 2006, Nature **444**, 71.

Armen, M. A., J. K. Au, J. K. Stockton, A. C. Doherty, and H. Mabuchi, 2002, Phys. Rev. Lett. **89**, 133602.

Averin, D., 2003, in *Quantum Noise in Mesoscopic Systems*, edited by Y. Nazarov (Kluwer, Amsterdam), pp. 205–228.

Averin, D. V., 2000a, cond-mat/0010052v1 .

Averin, D. V., 2000b, Fortschr. Phys. **48**, 1055.

Averin, D. V., and E. V. Sukhorukov, 2005, Phys. Rev. Lett. **95**, 126803.

Berestetskii, V. B., E. M. Lifshitz, and L. P. Pitaevskii, 1982, *Quantum Electrodynamics (2nd Edition)*, volume 4 of *Course of Theoretical Physics* (Butterworth-Heinemann, Oxford).

Billangeon, P. M., F. Pierre, H. Bouchiat, and R. Deblock, 2006, Phys. Rev. Lett. **96**, 136804.

Blais, A., R.-S. Huang, A. Wallraff, S. M. Girvin, and R. J. Schoelkopf, 2004, Phys. Rev. A **69**, 062320.

Blanter, Y. M., and M. Büttiker, 2000, Phys. Rep. **336**, 1.

Blencowe, M. P., and E. Buks, 2007, Phys. Rev. B **76**, 014511.

Bocko, M. F., and R. Onofrio, 1996, Rev. Mod. Phys. **68**, 755.

Bohm, D., 1989, *Quantum Theory* (Dover, New York).

Boylestad, R., and L. Nashelsky, 2006, *Electronic Devices and Circuit Theory* (Prentice Hall, New Jersey), 9 edition.

Braginsky, V. B., and F. Y. Khalili, 1992, *Quantum Measurement* (Cambridge University Press, Cambridge).

Braginsky, V. B., and F. Y. Khalili, 1996, Rev. Mod. Phys. **68**, 1.

Braginsky, V. B., Y. I. Vorontsov, and K. P. Thorne, 1980, Science **209**, 547.

van den Brink, A. M., 2002, Europhys. Lett. **58**, 562.

Brown, K. R., J. Britton, R. J. Epstein, J. Chiaverini, D. Leibfried, and D. J. Wineland, 2007, Phys. Rev. Lett. **99**, 137205.

Brun, T. A., 2002, Am. J. Phys. **70**, 719.

Buks, E., R. Schuster, M. Heiblum, D. Mahalu, and V. Umansky, 1998, Nature (London) **391**, 871.

Burkhard, G., R. H. Koch, and D. P. DiVincenzo, 2004, Phys. Rev. B **69**, 064503.

Caldeira, A., and A. Leggett, 1983, Ann. Phys. (NY) **149**, 374.

Callen, H. B., and T. A. Welton, 1951, Phys. Rev. **83**, 34.

Caves, C. M., 1980, Phys. Rev. Lett. **45**, 75.

Caves, C. M., 1981, Phys. Rev. D **23**, 1693.

Caves, C. M., 1982, Phys. Rev. D **26**, 1817.

Caves, C. M., and B. L. Schumaker, 1985, Phys. Rev. A **31**, 3068.

Caves, C. M., K. S. Thorne, R. W. P. Drever, V. D. Sandberg, and M. Zimmermann, 1980, Rev. Mod. Phys. **52**, 341.

Cleland, A. N., J. S. Aldridge, D. C. Driscoll, and A. C. Gossard, 2002, Appl. Phys. Lett. **81**, 1699.

Clerk, A. A., 2004, Phys. Rev. B **70**, 245306.

Clerk, A. A., 2006, Phys. Rev. Lett. **96**, 056801.

Clerk, A. A., and S. M. Girvin, 2004, Phys. Rev. B **70**, 121303.

Clerk, A. A., S. M. Girvin, A. K. Nguyen, and A. D. Stone, 2002, Phys. Rev. Lett. **89**, 176804.

Clerk, A. A., S. M. Girvin, and A. D. Stone, 2003, Phys. Rev. B **67**, 165324.

Clerk, A. A., F. Marquardt, and K. Jacobs, 2008, New J. Phys. **10**, 095010.

Clerk, A. A., and A. D. Stone, 2004, Phys. Rev. B **69**, 245303.

Cohen-Tannoudji, C., J. Dupont-Roc, and G. Grynberg, 1989, *Photons and Atoms - Introduction to Quantum Electrodynamics* (Wiley, New York).

Corbitt, T., Y. Chen, E. Innerhofer, H. Muller-Ebhardt, D. Ottaway, H. Rehbein, D. Sigg, S. Whitcomb, C. Wipf, and N. Mavalvala, 2007, Phys. Rev. Lett **98**, 150802.

Courty, J. M., F. Grassia, and S. Reynaud, 1999, Europhys. Lett. **46**, 31.

Cover, T., and J. Thomas, 1991, *Elements of Information Theory* (Wiley, New York).

Lupaşcu, A., C. J. M. Verwijs, R. N. Schouten, C. J. P. M. Harmans, and J. E. Mooij, 2004, Phys. Rev. Lett. **93**, 177006.

Danilov, V. V., K. K. Likharev, and A. B. Zorin, 1983, IEEE Trans. Magn. **19**, 572.

Deblock, R., E. Onac, L. Gurevich, and L. P. Kouwenhoven, 2003, Science **301**, 203.

Devoret, M., 1997, in *Quantum Fluctuations (Les Houches Session LXIII)* (Elsevier, Amsterdam), pp. 351–86.

Devoret, M. H., and R. J. Schoelkopf, 2000, Nature (London) **406**, 1039.

Doherty, A. C., S. Habib, K. Jacobs, H. Mabuchi, and S. M. Tan, 2000, Phys. Rev. A **62**, 012105.

Duty, T., G. Johansson, K. Bladh, D. Gunnarsson, C. Wilson, and P. Delsing, 2005, Phys. Rev. Lett. **95**, 206807.

Etaki, S., M. Poot, I. Mahboob, K. Onomitsu, H. Yamaguchi, and H. S. J. V. der Zant, 2008, Nature Phys. **4**, 785.

Flowers-Jacobs, N. E., D. R. Schmidt, and K. W. Lehnert, 2007, Phys. Rev. Lett **98**, 096804.

Gambetta, J., A. Blais, D. I. Schuster, A. Wallraff, and R. J. Schoelkopf, 2006, Phys. Rev. A **74**, 042318.

Gambetta, J., W. A. Braff, A. Wallraff, S. M. Girvin, and R. J. Schoelkopf, 2007, Phys. Rev. A **76**, 012325.

Gardiner, C. W., A. S. Parkins, and P. Zoller, 1992, Phys. Rev. A **46**, 4363.

Gardiner, C. W., and P. Zoller, 2000, *Quantum Noise* (Springer, Berlin).

Gavish, U., Y. Levinson, and Y. Imry, 2000, Phys. Rev. B (R) **62**, 10637.

Gavish, U., B. Yurke, and Y. Imry, 2004, Phys. Rev. Lett. **93**, 250601.

Gavish, U., B. Yurke, and Y. Imry, 2006, Phys. Rev. Lett. **96**, 133602.

Gea-Banacloche, J., N. Lu, L. M. Pedrotti, S. Prasad, M. O. Scully, and K. Wodkiewicz, 1990a, Phys. Rev. A **41**, 369.

Gea-Banacloche, J., N. Lu, L. M. Pedrotti, S. Prasad, M. O.

Scully, and K. Wodkiewicz, 1990b, Phys. Rev. A **41**, 381.
Geremia, J., J. K. Stockton, and H. Mabuchi, 2004, Science **304**, 270.
Gerry, C. S., 1985, Phys. Rev. A **31**, 2721.
Gigan, S., H. Böhm, M. Paternostro, F. Blaser, J. B. Hertzberg, K. C. Schwab, D. Bauerle, M. Aspelmeyer, and A. Zeilinger, 2006, Nature **444**, 67.
Glauber, R. J., 2006, Rev. Mod. Phys. **78**, 1267.
Goan, H.-S., and G. J. Milburn, 2001, Phys. Rev. B **64**, 235307.
Goan, H. S., G. J. Milburn, H. M. Wiseman, and B. H. Sun, 2001, Phys. Rev. B **63**, 125326.
Gordon, J. P., W. H. Louisell, and L. R. Walker, 1963, Phys. Rev. **129**, 481.
Gottfried, K., 1966, *Quantum Mechanics, Volume I: Fundamentals* (W. A. Benjamin, Inc.).
Grassia, F., 1998, *Fluctuations quantiques et thermiques dans les transducteurs electromecaniques*, Ph.D. thesis, Universite Pierre et Marie Curie.
Gurvitz, S. A., 1997, Phys. Rev. B **56**, 15215.
Gustavsson, S., M. Studer, R. Leturcq, T. Ihn, K. Ensslin, D. C. Driscoll, and A. C. Gossard, 2007, Phys. Rev. Lett. **99**, 206804.
Haroche, S., and J.-M. Raimond, 2006, *Exploring the Quantum Atoms, Cavities, and Photons* (Oxford University Press, Oxford).
Harris, J. G. E., B. M. Zwickl, and A. M. Jayich, 2007, Review of Scientific Instruments **78**, 013107.
Haus, H. A., 2000, *Electromagnetic Noise and Quantum Optical Measurements* (Springer, New York).
Haus, H. A., and J. A. Mullen, 1962, Phys. Rev. **128**, 2407.
Heffner, H., 1962, Proc. IRE **50**, 1604.
Höhberger-Metzger, C., and K. Karrai, 2004, Nature **432**, 1002.
Il'ichev, E., N. Oukhanski, A. Izmalkov, T. Wagner, M. Grajcar, H.-G. Meyer, A. Y. Smirnov, A. Maassen van den Brink, M. H. S. Amin, and A. M. Zagoskin, 2003, Phys. Rev. Lett. **91**, 097906.
Izmalkov, A., M. Grajcar, E. Il'ichev, T. Wagner, H.-G. Meyer, A. Y. Smirnov, M. H. S. Amin, A. M. van den Brink, and A. M. Zagoskin, 2004, Phys. Rev. Lett. **93**, 037003.
Jacobs, K., and D. A. Steck, 2006, Contemporary Physics **47**, 279.
Jordan, A. N., and M. Büttiker, 2005, Phys. Rev. B **71**, 125333.
Jordan, A. N., and A. N. Korotkov, 2006, Phys. Rev. B **74**, 085307.
Kleckner, D., and D. Bouwmeester, 2006, Nature **444**, 75.
Knight, P. L., and V. Buzek, 2004, in *Quantum Squeezing*, edited by P. D. Drummond and Z. Ficek (Springer, Berlin), pp. 3–32.
Knobel, R. G., and A. N. Cleland, 2003, Nature (London) **424**, 291.
Koch, R. H., D. J. van Harlingen, and J. Clarke, 1980, Appl. Phys. Lett. **38**, 380.
Korotkov, A. N., 1999, Phys. Rev. B **60**, 5737.
Korotkov, A. N., 2001a, Phys. Rev. B **63**, 085312.
Korotkov, A. N., 2001b, Phys. Rev. B **63**, 115403.
Korotkov, A. N., and D. V. Averin, 2001, Phys. Rev. B **64**, 165310.
Korotkov, A. N., and M. A. Paalanen, 1999, Appl. Phys. Lett. **74**, 4052.
LaHaye, M. D., O. Buu, B. Camarota, and K. C. Schwab, 2004, Science **304**, 74.
Lang, R., M. O. Scully, and J. Willis E. Lamb, 1973, Phys. Rev. A **7**, 1788.
Lesovik, G. B., and R. Loosen, 1997, JETP Lett. **65**, 295.
Levinson, Y., 1997, Europhys. Lett. **39**, 299.
Levitov, L. S., 2003, in *Quantum Noise in Mesoscopic Systems*, edited by Y. Nazarov (Kluwer, Amsterdam), pp. 373–396.
Louisell, W. H., A. Yariv, and A. E. Siegman, 1961, Phys. Rev. **124**, 1646.
Lupaşcu, A., C. J. P. M. Harmans, and J. E. Mooij, 2005, Phys. Rev. B. **71**, 184506.
Makhlin, Y., G. Schön, and A. Shnirman, 2000, Phys. Rev. Lett. **85**, 4578.
Makhlin, Y., G. Schon, and A. Shnirman, 2001, Rev. Mod. Phys. **73**, 357.
Mallat, S., 1999, *A Wavelet Tour of Signal Processing* (Academic, San Diego).
Marquardt, F., J. P. Chen, A. A. Clerk, and S. M. Girvin, 2007, Phys. Rev. Lett. **99**, 093902.
Marquardt, F., J. G. E. Harris, and S. M. Girvin, 2006, Phys. Rev. Lett. **96**, 103901.
Meystre, P., E. M. Wright, J. D. McCullen, and E. Vignes, 1985, J. Opt. Soc. Am. B **2**, 1830.
Mollow, B. R., and R. J. Glauber, 1967a, Phys. Rev. **160**, 1076.
Mollow, B. R., and R. J. Glauber, 1967b, Phys. Rev. **160**, 1097.
Mozyrsky, D., I. Martin, and M. B. Hastings, 2004, Phys. Rev. Lett. **92**, 018303.
Mück, M., J. B. Kycia, and J. Clarke, 2001, Appl. Phys. Lett. **78**, 967.
Nagourney, W., J. Sandberg, and H. Dehmelt, 1986, Phys. Rev. Lett. **56**, 2797.
Naik, A., O. Buu, M. D. LaHaye, A. D. Armour, A. A. Clerk, M. P. Blencowe, and K. C. Schwab, 2006, Nature (London) **443**, 193.
Nazarov, Y. V. (ed.), 2003, *Quantum Noise in Mesoscopic Systems* (Kluwer, Amsterdam).
Nazarov, Y. V., and M. Kindermann, 2003, Eur. Phys. J. B **35**, 413.
von Neumann, J., 1932, Mathematische Grundlagen der Quantenmechanik (Springer, Berlin).
Nogues, G., A. Rauschenbeutel, S. Osnaghi, M. Brune, J. M. Raimond, and S. Haroche, 1999, Nature (London) **400**, 239.
Onac, E., F. Balestro, L. H. W. van Beveren, U. Hartmann, Y. V. Nazarov, and L. P. Kouwenhoven, 2006a, Phys. Rev. Lett. **96**, 176601.
Onac, E., F. Balestro, B. Trauzettel, C. F. J. Lodewijk, and L. P. Kouwenhoven, 2006b, Phys. Rev. Lett. **96**, 026803.
Peres, A., 1993, *Quantum Theory: Concepts and Methods* (Kluwer, Dorderecht).
Pilgram, S., and M. Büttiker, 2002, Phys. Rev. Lett. **89**, 200401.
Poggio, M., M. P. Jura, C. L. Degen, M. A. Topinka, H. J. Mamin, D. Goldhaber-Gordon, and D. Rugar, 2008, Nature Phys. **4**, 635.
Raimond, J. M., M. Brune, and S. Haroche, 2001, Rev. Mod. Phys. **73**, 565.
Regal, C. A., J. D. Teufel, and K. W. Lehnert, 2008, Nature Phys. **4**, 555.
Rugar, D., R. Budakian, H. J. Mamin, and B. W. Chui, 2004, Nature (London) **430**, 329.
Ruskov, R., and A. N. Korotkov, 2002, Phys. Rev. B **66**,

041401.
Ruskov, R., K. Schwab, and A. N. Korotkov, 2005, Phys. Rev. B **71**, 235407.
Santamore, D. H., A. C. Doherty, and M. C. Cross, 2004a, Phys. Rev. B **70**, 144301.
Santamore, D. H., H.-S. Goan, G. J. Milburn, and M. L. Roukes, 2004b, Phys. Rev. A **70**, 052105.
Sauter, T., W. Neuhauser, R. Blatt, and P. E. Toschek, 1986, Phys. Rev. Lett. **57**, 1696.
Schliesser, A., P. Del'Haye, N. Nooshi, K. J. Vahala, and T. J. Kippenberg, 2006, Phys. Rev. Lett. **97**, 243905.
Schliesser, A., R. Rivière, G. Anetsberger, O. Arcizet, and T. J. Kippenberg, 2008, Nature Phys. **4**, 415.
Schoelkopf, R. J., P. J. Burke, A. A. Kozhevnikov, D. E. Prober, and M. J. Rooks, 1997, Phys. Rev. Lett. **78**, 3370.
Schoelkopf, R. J., A. A. Clerk, S. M. Girvin, K. W. Lehnert, and M. H. Devoret, 2003, in *Quantum Noise in Mesoscopic Systems*, edited by Y. Nazarov (Kluwer, Amsterdam), pp. 175–203.
Schoelkopf, R. J., P. Wahlgren, A. A. Kozhevnikov, P. Delsing, and D. E. Prober, 1998, Science **280**, 1238.
Schuster, D., A. Houck, J. Schreier, A. Wallraff, J. Gambetta, A. Blais, L. Frunzio, B. Johnson, M. Devoret, S. Girvin, and R. Schoelkopf, 2007, Nature **445**, 515.
Schuster, D. I., A. Wallraff, A. Blais, L. Frunzio, R.-S. Huang, J. Majer, S. M. Girvin, and R. J. Schoelkopf, 2005, Phys. Rev. Lett. **94**, 123602.
Shnirman, A., and G. Schön, 1998, Phys. Rev. B **57**, 15400.
Siddiqi, I., R. Vijay, F. Pierre, C. M. Wilson, M. Metcalfe, C. Rigetti, L. Frunzio, and M. H. Devoret, 2004, Phys. Rev. Lett. **93**, 207002.
Sillanpää, M. A., T. Lehtinen, A. Paila, Y. Makhlin, L. Roschier, and P. J. Hakonen, 2005, Phys. Rev. Lett. **95**, 206806.
Sprinzak, D., E. Buks, M. Heiblum, and H. Shtrikman, 2000, Phys. Rev. Lett. **84**, 5820.
Stern, A., Y. Aharonov, and Y. Imry, 1990, Phys. Rev. A **41**, 3436.
Teufel, J. D., C. A. Regal, and K. W. Lehnert, 2008, New J. Phys. **10**, 095002.
Thalakulam, M., Z. Ji, and A. J. Rimberg, 2004, Phys. Rev. Lett. **93**, 066804.
Thompson, J. D., B. M. Zwickl, A. M. Jayich, F. Marquardt, S. M. Girvin, and J. G. E. Harris, 2008, Nature (London) **452**, 06715.
Thorne, K. S., R. W. P. Drever, C. M. Caves, M. Zimmermann, and V. D. Sandberg, 1978, Phys. Rev. Lett. **40**, 667.
Tittonen, I., G. Breitenbach, T. Kalkbrenner, T. Muller, R. Conradt, S. Schiller, E. Steinsland, N. Blanc, and N. F. de Rooij, 1999, Phys. Rev. A **59**, 1038.
Turek, B. A., K. W. Lehnert, A. Clerk, D. Gunnarsson, K. Bladh, P. Delsing, and R. J. Schoelkopf, 2005, Phys. Rev. B **71**, 193304.
Vinante, A., R. Mezzena, G. A. Prodi, S. Vitale, M. Cerdonio, P. Falferi, and M. Bonaldi, 2001, Appl. Phys. Lett. **79**, 2597.
Wallraff, A., D. I. Schuster, A. Blais, L. Frunzio, R.-S. Huang, J. Majer, S. Kumar, S. M. Girvin, and R. J. Schoelkopf, 2004, Nature (London) **431**, 162.
Walls, D. F., and G. J. Milburn, 1994, *Quantum Optics* (Springer, Berlin).
Weiss, U., 1999, *Quantum Dissipative Systems (Second Edition)* (World Scientific, Singapore).
Wheeler, J. A., and W. H. Zurek, 1984, *Quantum Theory and Measurement* (Princeton University Press, Princeton).
Wigner, E. P., 1955, Phys. Rev. **98**, 145.
Wilson-Rae, I., N. Nooshi, W. Zwerger, and T. J. Kippenberg, 2007, Phys. Rev. Lett. **99**, 093901.
Wineland, D. J., C. Monroe, W. M. Itano, D. Leibfried, B. King, and D. M. Meekhof, 1998, J. Res. NIST **103**, 259.
Yurke, B., 1984, Phys. Rev. A **29**, 408.
Yurke, B., L. R. Corruccini, P. G. Kaminsky, L. W. Rupp, A. D. Smith, A. H. Silver, R. W. Simon, and E. A. Whittaker, 1989, Phys. Rev. A **39**, 2519.
Yurke, B., and J. S. Denker, 1984, Phys. Rev. A **29**, 1419.